THE ROLE OF OCEAN-BASED NEGATIVE EMISSION TECHNOLOGIES FOR CLIMATE MITIGATION

EDITED BY: David Peter Keller, Lennart Thomas Bach, Kerryn Brent and Wilfried Rickels

PUBLISHED IN: Frontiers in Climate and Frontiers for Young Minds

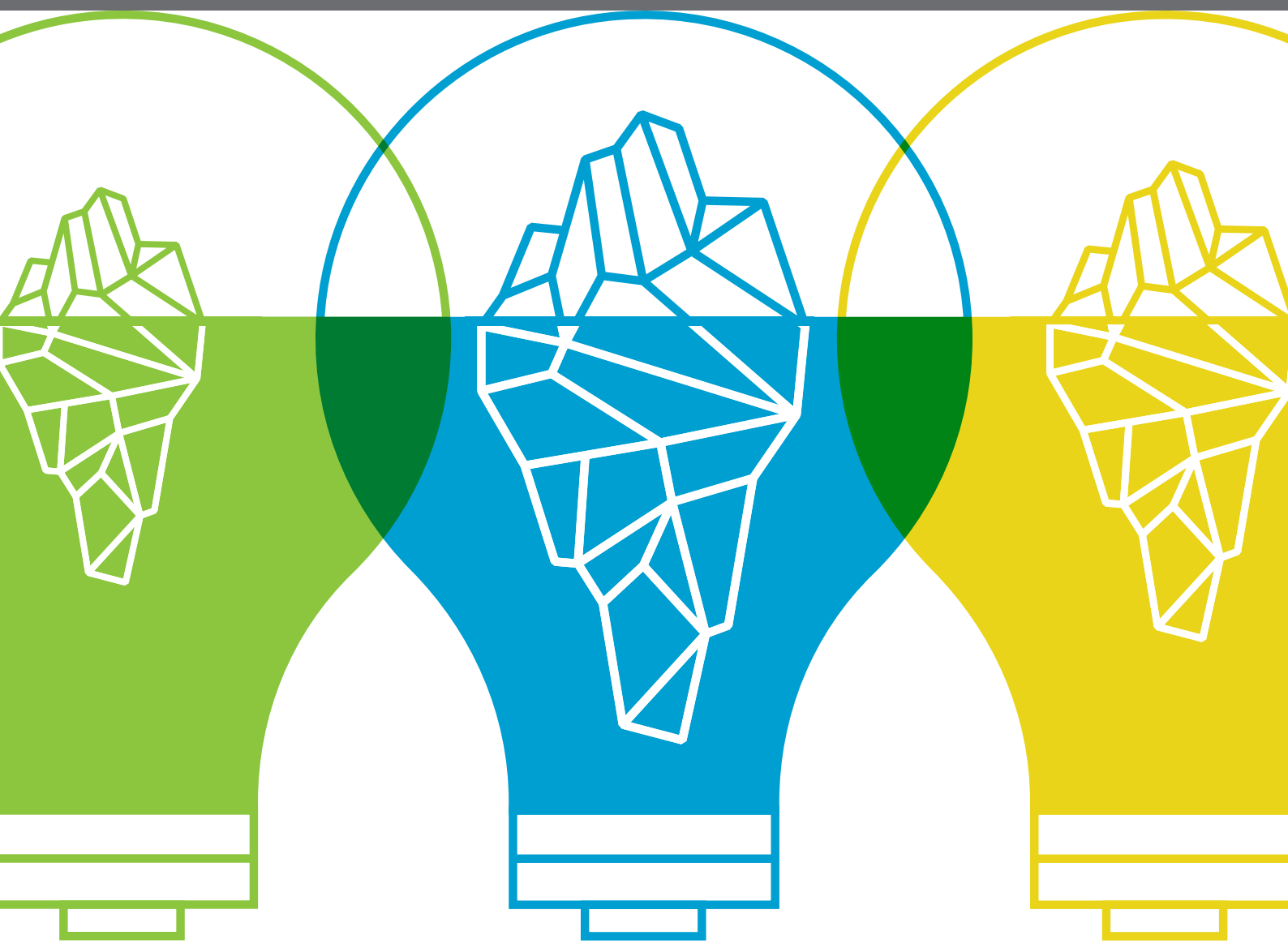

frontiers Research Topics

frontiers

ISSN 1664-8714
ISBN 978-2-88971-550-3
DOI 10.3389/978-2-88971-550-3

About Frontiers

Frontiers is more than just an open-access publisher of scholarly articles: it is a pioneering approach to the world of academia, radically improving the way scholarly research is managed. The grand vision of Frontiers is a world where all people have an equal opportunity to seek, share and generate knowledge. Frontiers provides immediate and permanent online open access to all its publications, but this alone is not enough to realize our grand goals.

Frontiers Journal Series

The Frontiers Journal Series is a multi-tier and interdisciplinary set of open-access, online journals, promising a paradigm shift from the current review, selection and dissemination processes in academic publishing. All Frontiers journals are driven by researchers for researchers; therefore, they constitute a service to the scholarly community. At the same time, the Frontiers Journal Series operates on a revolutionary invention, the tiered publishing system, initially addressing specific communities of scholars, and gradually climbing up to broader public understanding, thus serving the interests of the lay society, too.

Dedication to Quality

Each Frontiers article is a landmark of the highest quality, thanks to genuinely collaborative interactions between authors and review editors, who include some of the world's best academicians. Research must be certified by peers before entering a stream of knowledge that may eventually reach the public - and shape society; therefore, Frontiers only applies the most rigorous and unbiased reviews.
Frontiers revolutionizes research publishing by freely delivering the most outstanding research, evaluated with no bias from both the academic and social point of view. By applying the most advanced information technologies, Frontiers is catapulting scholarly publishing into a new generation.

What are Frontiers Research Topics?

Frontiers Research Topics are very popular trademarks of the Frontiers Journals Series: they are collections of at least ten articles, all centered on a particular subject. With their unique mix of varied contributions from Original Research to Review Articles, Frontiers Research Topics unify the most influential researchers, the latest key findings and historical advances in a hot research area! Find out more on how to host your own Frontiers Research Topic or contribute to one as an author by contacting the Frontiers Editorial Office: frontiersin.org/about/contact

THE ROLE OF OCEAN-BASED NEGATIVE EMISSION TECHNOLOGIES FOR CLIMATE MITIGATION

Topic Editors:
David Peter Keller, GEOMAR Helmholtz Center for Ocean Research Kiel, Helmholtz Association of German Research Centres (HZ), Germany
Lennart Thomas Bach, University of Tasmania, Australia
Kerryn Brent, University of Adelaide, Australia
Wilfried Rickels, Christian Albrechts University Kiel, Germany

Citation: Keller, D. P., Bach, L. T., Brent, K., Rickels, W., eds. (2022). The Role of Ocean-based Negative Emission Technologies for Climate Mitigation. Lausanne: Frontiers Media SA. doi: 10.3389/978-2-88971-550-3

Table of Contents

frontiers in Climate

EDITORIAL
published: 16 August 2021
doi: 10.3389/fclim.2021.743816

Editorial: The Role of Ocean-Based Negative Emission Technologies for Climate Mitigation

David P. Keller[1]*, *Kerryn Brent*[2], *Lennart T. Bach*[3] and *Wilfried Rickels*[4]

[1] GEOMAR Helmholtz Centre for Ocean Research Kiel, Kiel, Germany, [2] Adelaide Law School, University of Adelaide, Adelaide, SA, Australia, [3] Institute for Marine and Antarctic Studies, University of Tasmania, Hobart, TAS, Australia, [4] Kiel Institute for the World Economy, Kiel, Germany

Keywords: negative emission technologies, carbon dioxide removal (CDR), ocean-based carbon dioxide removal, ocean-based NETs, climate mitigation

Editorial on the Research Topic

The Role of Ocean-Based Negative Emission Technologies for Climate Mitigation

OPEN ACCESS

Edited and reviewed by:
Phil Renforth,
Heriot-Watt University,
United Kingdom

***Correspondence:**
David P. Keller
dkeller@geomar.de

Specialty section:
This article was submitted to Negative Emission Technologies, a section of the journal Frontiers in Climate

Received: *19 July 2021*
Accepted: *26 July 2021*
Published: *16 August 2021*

Citation:
Keller DP, Brent K, Bach LT and Rickels W (2021) Editorial: The Role of Ocean-Based Negative Emission Technologies for Climate Mitigation. Front. Clim. 3:743816. doi: 10.3389/fclim.2021.743816

Mitigating climate change is a massive challenge. Atmospheric carbon dioxide removal (CDR) with negative emission technologies (NETs) is now widely considered a necessary additional action since traditional mitigation measures, such as limiting the use of fossil fuels, have had limited success (Intergovernmental Panel on Climate Change, 2018, United Nations Environment Programme, 2020). Until now, the majority of NETs research and development has focused on land-based options such as bioenergy with carbon capture and storage (BECCS). However, ocean-based NETs can potentially also play a significant CDR role.

Like their terrestrial counterparts, ocean-based NETs seek to accelerate the uptake of atmospheric CO_2 by enhancing natural sinks or by engineering the removal and storage of CO_2. Currently there are too many knowledge gaps to fully assess the potential, effectiveness, efficiency, risks and co-benefits, and economic costs of most approaches. Key elements to facilitate responsible R&D are also lacking, including governance and public acceptance (GESAMP, 2019). The purpose of this topic is to examine ocean-based NETs and the challenges associated with them from a multidisciplinary perspective.

Gattuso et al. introduce an assessment framework for ocean-based NETs in which different criteria are used to group different technologies into three policy clusters: (i) Decisive, (ii) Low Regret, and (iii) Concept Stage. They apply the assessment framework to marine BECCS, restoring and increasing coastal vegetation, enhancing open-ocean productivity, and enhancing weathering and alkalinization, comparing these ocean NETs to other (ocean-based) measures. According to their assessment, restoring and increasing coastal vegetation would be a "Low Regret" measure while the other measures are still in the "Concept Stage." Preliminary application of the framework suggests that ocean-based NETs should be scaled up by prioritizing the implementation of Decisive and Low Regret measures, and urgently improving knowledge on Concept Stage measures.

Cox et al. discuss the importance of public perceptions, decision-making, and the role of discourse for the assessment of ocean-based NETs. They argue that ocean-based NETs will generally face greater public acceptability challenges than terrestrial NETs. In this context, they utilize public acceptability studies on Ocean Iron Fertilization, the only thoroughly investigated open ocean NET, to ask whether further research into iron fertilization is necessary because it is unlikely to ever receive social license. The question added by the Editors is: Will less well-understood methods such as Ocean Alkalinity Enhancement (OAE) follow Iron Fertilization into an "acceptability crises" once more data is available?

Bertram and Merk shed further light on this issue. They identify several key determinants of public acceptability. Ocean-based NETs which appear more "natural" are likely to have a higher degree of acceptability than "engineered" proposals. Proposals that can be contained tend to be more acceptable than those perceived as uncontrollable. Bertram and Merk note that such perceptions could result in ocean-based NETs with limited sequestration capacity being privileged over proposals with far greater capacity. They argue that we need to identify who will be affected and to what degree across the entire process-chain of ocean-based NETs to better understand how public perceptions may affect the feasibility of these proposals.

Several articles focused on OAE as a means of chemical CDR, since this approach has a high theoretical potential (Renforth and Henderson, 2017). By examining the long-term dynamics of adding a constant amount of olivine to a carbon cycle model, which includes sediment and weathering feedbacks, Köhler shows how long it would take for OAE to remove most anthropogenic CO_2 in a high emission climate change scenario. This study also shows that the sequestration efficiency of ocean alkalinization has its maximum during the anthropogenic CO_2 emission peak and that altered marine chemistry reverses (after 1–2 kyr) the trend from sedimentary $CaCO_3$ dissolution to a restrengthened accumulation of $CaCO_3$ in the sediments.

How OAE might be achieved in practice is the focus of a study by Caserini et al. that investigates the potential of using existing shipping activities and capacities to add lime, $Ca(OH)_2$, to the ocean. They estimate that the maximum potential discharge of lime from all active vessels worldwide is between 1.7 and 4.0 Gt/year. For the Mediterranean Sea potential discharge of about 186 Mt/year is estimated.

Butenschön et al. use a high resolution (∼6 km), physical-biogeochemical model of the Mediterranean Sea to investigate the efficacy and biogeochemical side effects of adding alkalinity along current shipping routes during a moderate emission scenario (RCP 4.5). They find that with a strategic deployment scenario ocean acidification can be stopped and stabilized, while still allowing for efficient CDR.

In a more global context, Burt et al. use an Ocean carbon cycle model to show that the efficacy of OAE varies substantially across different ocean regions over a timescale of 75 years. Within the regions they tested, they found the highest efficacies of OAE when applied in a narrow circumpolar band in the Southern Ocean at (∼55°S), while lowest efficacies were observed in the sub-polar North Atlantic. They explain the variable efficacies with regional differences in (i) physical water mass transport and (ii) the ability of the seawater carbonate system to absorb additional CO_2 per amount of alkalinity added to the ocean.

This strong focus on OAE is complemented in a *Frontiers for Young Minds* article by Woodall et al. on enhanced mineral weathering. This article is pitched at school-aged readers, and explains the need for NETs and the potential ways in which carbon mineralization can contribute, including via the ocean. In doing so, it seeks to enhance public understanding and awareness of NETs and inspire the next generation of researchers.

In summary, the articles in this Research Topic add critical knowledge to the small, but rapidly growing body of research on ocean-based NETs. These contributions will be of particular value to guide future work as the field begins to transition from mostly theoretical perspectives to applied research and development of promising NETs. As part of this transition, inter- and trans-disciplinary research will become increasingly important to tackle the multi-dimensional challenges associated with ocean-based NETs. For some NETs this transition is yet to commence, as critical disciplinary knowledge gaps remain. However, for proposals like OAE this transition has begun in earnest, necessitating greater inter-/trans-disciplinary engagement from academia, government organizations and civil society.

AUTHOR CONTRIBUTIONS

DPK wrote the introduction and conclusion sections, as well as paragraphs for each article in the topic that he edited. KB, LTB, and WR wrote paragraphs for each article in the topic that they edited. All authors worked together to edit and improve the final text of the whole article.

ACKNOWLEDGMENTS

DPK and WR acknowledge funding from the European Union's Horizon 2020 Research and Innovation Program under grant 869357 (project OceanNETs: Ocean-based Negative Emission Technologies—analyzing the feasibility, risks, and co-benefits of ocean-based negative emission technologies for stabilizing the climate). LTB acknowledges funding from the Australian Research Council under the Future Fellowship grant FT200100846 (Enhanced Weathering—a sustainable tool for CO_2 removal?).

REFERENCES

GESAMP (2019). *High Level Review of a Wide Range of Proposed Marine Geoengineering Techniques*, eds P. W. Boyd and C. M. G. Vivian. IMO/FAO/UNESCO-IOC/UNIDO/WMO/IAEA/UN/UN Environment/UNDP/ISA Joint Group of Experts on the Scientific Aspects of Marine Environmental Protection. Rep. Stud. GESAMP No. 98, 144 p.

Intergovernmental Panel on Climate Change (2018). *Global Warming of 1.5°C. An IPCC Special Report on the Impacts of Global Warming of 1.5°C Above Pre-Industrial Levels and Related Global Greenhouse Gas Emission Pathways, in the Context of Strengthening the Global Response to the Threat of Climate Change*.

Renforth, P., and Henderson, G. (2017). Assessing ocean alkalinity for carbon sequestration. *Rev. Geophys*. 55, 636–674. doi: 10.1002/2016RG000533

United Nations Environment Programme (2020). *Emissions Gap Report 2020*. Nairobi.

Conflict of Interest: The authors declare that the research was conducted in the absence of any commercial or financial relationships that could be construed as a potential conflict of interest.

frontiers in Climate

ORIGINAL RESEARCH
published: 09 December 2020
doi: 10.3389/fclim.2020.575744

Anthropogenic CO_2 of High Emission Scenario Compensated After 3500 Years of Ocean Alkalinization With an Annually Constant Dissolution of 5 Pg of Olivine

*Peter Köhler**

Alfred-Wegener-Institut Helmholtz-Zentrum für Polar-und Meeresforschung (AWI), Bremerhaven, Germany

The CO_2 removal model inter-comparison (CDRMIP) has been established to approximate the usefulness of climate mitigation by some well-defined negative emission technologies. I here analyze ocean alkalinization in a high CO_2 world (emission scenario SSP5-85-EXT++ and CDR-ocean-alk within CDRMIP) for the next millennia using a revised version of the carbon cycle model BICYCLE, whose long-term feedbacks are calculated for the next 1 million years. The applied model version not only captures atmosphere, ocean, and a constant marine and terrestrial biosphere, but also represents solid Earth processes, such as deep ocean $CaCO_3$ accumulation and dissolution, volcanic CO_2 outgassing, and continental weathering. In the applied negative emission experiment, 0.14 Pmol/yr of alkalinity—comparable to the dissolution of 5 Pg of olivine per year—is entering the surface ocean starting in year 2020 for either 50 or 5000 years. I find that the cumulative emissions of 6,740 PgC emitted until year 2350 lead to a peak atmospheric CO_2 concentration of nearly 2,400 ppm in year 2326, which is reduced by only 200 ppm by the alkalinization experiment. Atmospheric CO_2 is brought down to 400 or 300 ppm after 2730 or 3480 years of alkalinization, respectively. Such low CO_2 concentrations are reached without ocean alkalinization only after several hundreds of thousands of years, when the feedbacks from weathering and sediments bring the part of the anthropogenic emissions that stays in the atmosphere (the so-called airborne fraction) below 4%. The efficiency of carbon sequestration by this alkalinization approach peaks at 9.7 PgC per Pmol of alkalinity added during times of maximum anthropogenic CO_2 emissions and slowly declines to half this value 2000 years later due to the non-linear marine chemistry response and ocean-sediment processes. In other words, ocean alkalinization sequesters carbon only as long as the added alkalinity stays in the ocean. To understand the basic model behavior, I analytically explain why in the simulation results a linear relationship in the transient climate response (TCR) to cumulative emissions is found for low emissions (similarly as for more complex climate models), which evolves for high emissions to a non-linear relation.

Keywords: carbon cycle, CDRMIP, negative emissions, geoengineering, ocean, future, box model, transient climate response to cumulative carbon emissions

OPEN ACCESS

Edited by:
David Peter Keller, GEOMAR Helmholtz Center for Ocean Research Kiel, Germany

Reviewed by:
Jerry Tjiputra, Norwegian Research Institute (NORCE), Norway
Wolfgang Koeve, GEOMAR Helmholtz Center for Ocean Research Kiel, Germany

***Correspondence:**
Peter Köhler
Peter.Koehler@awi.de

Specialty section:
This article was submitted to Negative Emission Technologies, a section of the journal Frontiers in Climate

Received: *24 June 2020*
Accepted: *27 August 2020*
Published: *09 December 2020*

Citation:
Köhler P (2020) Anthropogenic CO_2 of High Emission Scenario Compensated After 3500 Years of Ocean Alkalinization With an Annually Constant Dissolution of 5 Pg of Olivine. Front. Clim. 2:575744. doi: 10.3389/fclim.2020.575744

1. INTRODUCTION

Most approaches for negative CO_2 emissions, especially when based on oceanic processes, are still future technologies. This implies, that we do not know in detail how efficient different approaches might work in reality. Furthermore, unknown are also difficulties we need to overcome during potential implementations, and how we minimize in detail unwanted side effects (e.g., Keller et al., 2014; Committee on Geoengineering Climate, 2015; The Royal Society, 2018). For an approximation of the intended climate mitigation, however, some simulation protocols have been established within the *carbon dioxide removal model intercomparison project (CDRMIP)*, part of CMIP6 (Keller et al., 2018), to allow intermodel comparisons. Within the suite of proposed CDR experiments exists the "ocean alkalinization in a high CO_2 world" scenario (CDR-ocean-alk). While most recent studies on negative emission technologies—and most contributions to CDRMIP—focus on centennial time scales (e.g., Keller et al., 2014; González and Ilyina, 2016; Lenton et al., 2018; Beerling et al., 2020), I here concentrate on long-term effects (thousands to millions of years) by analyzing simulations of CDR-ocean-alk performed with only one simple model, the carbon cycle box model BICYCLE.

The long-term fate of fossil fuel emissions have been investigated in details with models of different complexities. Models differ in detail how the different feedbacks amplify or dampen the anthropogenic emissions (e.g., Archer et al., 2009). However, the common understanding can be summarized as follows:

- An anthropogenic-induced CO_2 anomaly in the atmosphere is in pulse experiments after a century (a millennium) reduced to $<$50% (to $\sim$20%) (Joos et al., 2013) due to the CO_2 uptake by the ocean and the vegetation, the later mainly due to the CO_2 fertilization (e.g., Haverd et al., 2020).
- The positive temperature feedback (the fossil fuel-induced global warming) leads to a warming of the surface ocean and via a then lower solubility of CO_2 in water (Henry's law) to a rise in atmospheric CO_2 (Weiss, 1974).
- The carbonate compensation (e.g., Archer et al., 1997) working on multi-millennial time scales is a negative feedback, also called sediment feedback. It implies that the anthropogenic CO_2 entering the ocean reduces the deep ocean carbonate ion concentration, consequently dissolving $CaCO_3$ due to calcite and aragonite undersaturation, leading to a rise in marine alkalinity and dissolved inorganic carbon (DIC) in the ocean. These changes in the carbonate chemistry allow an enhanced oceanic uptake of CO_2 from the atmosphere, roughly reducing the airborne fraction of anthropogenic CO_2 by a factor two down to $\sim$10%.
- On even longer time scales, high atmospheric CO_2 concentration leads via the negative weathering feedback to a further lowering of the CO_2 anomaly (e.g., Colbourn et al., 2015).

These airborne fractions given above are only rough estimates, since results are highly model dependent and also to some extend a function of the amount of emitted fossil fuels (Archer et al., 2009; Joos et al., 2013). They are typically calculated from pulse-response experiments, in which a well-defined amount of carbon (e.g., 100, 1,000, or 5,000 PgC) is injected in the atmosphere in 1 year or so, while already simulations considering the temporal evolution of the historic anthropogenic CO_2 emissions lead to a slightly different response of the carbon cycle (Jones et al., 2013). A nice overview of the time scales of the different processes reducing anthropogenic-induced CO_2 in the atmosphere is given in Lord et al. (2016).

The results presented here make use of the achieved understanding of these processes and feedbacks and focus on how long-term alkalinization might mitigate the impact of high CO_2 emissions. To set this into context to results obtained with more complex models, a good understanding of control simulations without alkalinization is necessary. I will therefore also analyze the implemented temperature, weathering, and sediment feedbacks embedded in the BICYCLE model, and derive an analytical understanding of the TCR to cumulative emissions within the applied model.

2. MATERIALS AND METHODS

Following the protocol described in Keller et al. (2018), I simulated the CDRMIP scenarios using the carbon cycle model BICYCLE. In the following, the chosen model is first briefly described before the experimental setup is explained in detail.

2.1. The Carbon Cycle Box Model BICYCLE

The BICYCLE carbon cycle box model (Köhler et al., 2005) is used here (**Figure 1**). The model consists of a globally average atmosphere (A), a ten boxes ocean (O) with five surface boxes distinguishing non-polar areas from polar areas in an Atlantic and Indo-Pacific basin. The other five boxes contain the intermediate and the deep ocean. A terrestrial biosphere (B) is able to mimic the growth of either C_3 or C_4 grasses, woody, and non-woody parts of trees and litter/soil with different turnover times. In BICYCLE, the concentration of carbon (as DIC in the ocean, as CO_2 in the atmosphere, as organic carbon in the biosphere) are traced. Furthermore, in the ocean alkalinity, PO_4^{3-} as macro-nutrient and O_2 are represented. From the two variables DIC and alkalinity, which fully define the marine carbonate system, other variables (CO_2, HCO_3^-, CO_3^{2-}, and pH) are calculated (Zeebe and Wolf-Gladrow, 2001) with updates of the dissociation constants pK_1 and pK_2 (Prieto and Millero, 2002). The ocean–atmosphere gas exchange is a function of temperature via the solubility of CO_2 and piston velocity (2.5 and 7.5×10^5 m s^{-1} for low and high latitudes, respectively). The net gas exchange, which in this anthropogenic setting is similar to the oceanic carbon uptake, is the difference between an atmosphere–ocean and an ocean–atmosphere CO_2 flux, each depending on the partial pressure of CO_2 in either one of the five surface ocean boxes or the atmosphere. The average gas exchange coefficient (0.051 mol m^{-2} yr^{-1} μatm^{-1}) is of the same order as in carbon isotope studies (Heimann and Maier-Reimer, 1996) and leads to pre-industrial (PI) gross fluxes of CO_2 between ocean surface and atmosphere and vice versa of about 60 PgC yr^{-1}. PI marine export production of organic

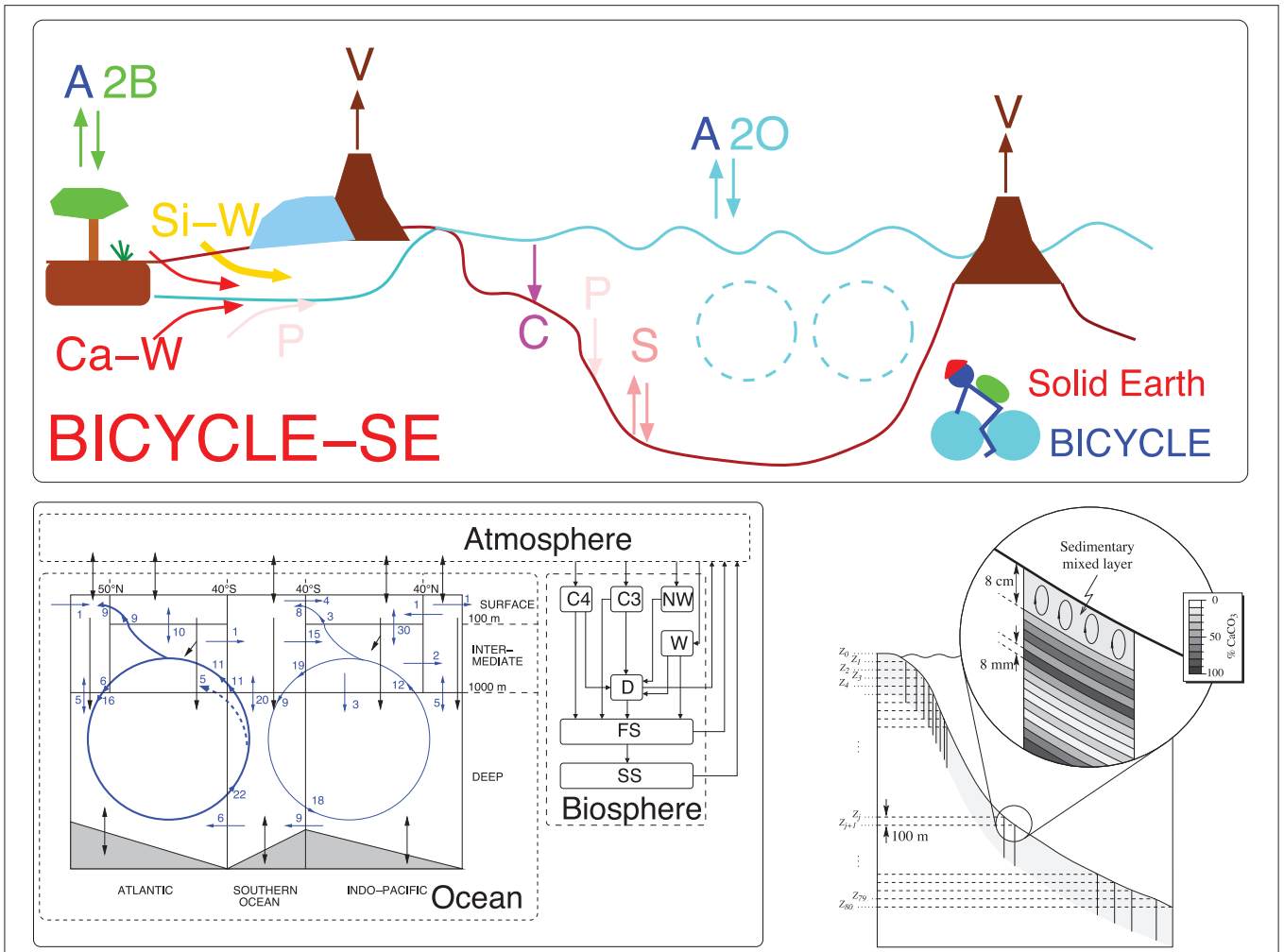

FIGURE 1 | Sketch of the BICYCLE model. Top: Model version including solid Earth fluxes (BICYCLE-SE) explained in detail in Köhler and Munhoven (2020). V: Outgassing of CO_2 from volcanoes on land potentially and temporally overlain by land ice and from hot spot island volcanoes (and mid ocean ridges, not shown) on paleo-time scales influenced by a changing sea level, but kept constant for the future scenarios investigated here; C: shallow water carbonate deposition due to coral reef growth; Si-W: silicate weathering; and Ca-W: carbonate weathering with different sources of C, but both delivering HCO_3^--ions into the ocean; P: PO_4^{3-} riverine input and sedimentary burial; S: $CaCO_3$ sedimentation and dissolution. A2B: atmosphere-biosphere exchange of CO_2; A2O: atmosphere-ocean exchange of CO_2. The cyan-colored broken circles mimic the two overturning cell in the Atlantic and Indo-Pacific Ocean. The model versions without solid Earth processes have been restricted to the fluxes A2O, A2B, and some simplified representation of carbonate compensation between ocean and sediment. Bottom left: Details of subsystem AOB (adopted from Köhler et al., 2010a) with the fixed prescribed pre-industrial water fluxes in the ocean (blue, numbers given in Sv). Black arrows denote carbon fluxes. Boxes in the land biosphere: C4, C_4 ground vegetation; C3, C_3 ground vegetation; NW, non-woody parts of trees; W, woody parts of trees; D, detritus; FS, fast decomposing soil; SS, slow decomposing soil. Bottom right: A conceptual sketch of the sediment module, the figure is taken from Munhoven (1997).

carbon at 100 m water depth is prescribed and kept fixed at 10 PgC/year with a rain ratio of organic C/$CaCO_3$ of 10:1. This keeps the marine biosphere as fixed at PI conditions as the terrestrial biosphere. Export production depends via the applied elemental (redfield) ratios of C:N:P:O2 = 123:17:1:–165 (Körtzinger et al., 2001) on available macro-nutrients (here PO_4^{3-}) and is realized first in the equatorial regions, and filled up to the prescribed numbers in polar regions thereafter. These numbers have been taken from full general circulation models (GCMs) that have been validated with field data (e.g., Schlitzer, 2000; Sarmiento et al., 2002). Other physical boundary conditions have been taken from the literature: for example, ocean circulation is prescribed from WOCE (Ganachaud and Wunsch, 2000), the distribution of temperature, salinity (both necessary for the calculation of the marine carbonate system), and the various tracers have been initialized from the World Ocean Atlas. The model performance has also been validated by the simulated distribution of the carbon isotopes ^{13}C and ^{14}C. Until recently, the carbonate compensation [sediment (S) feedback] is approximated in the model with a response function that brings anomalies in the deep ocean carbonate ion concentration time-delayed back to initial values. This approach has been shown to reasonably well operate on glacial/interglacial time scales (Köhler and Fischer, 2006).

The model has now been extended to cover solid Earth (SE) processes Köhler and Munhoven (2020), in detail volcanic CO_2 outgassing, the riverine input of HCO_3^- from silicate and carbonate weathering, the $CaCO_3$ sink of coral reef growth, and deep ocean $CaCO_3$ accumulation and dissolution. Briefly, a newly implemented process-based sediment model captures early diagenesis in an 8 cm sedimentary mixed layer, under which numerous historical layers are implemented, from which $CaCO_3$ might dissolve once the sedimentary mixed layer is thinned out. In each of the three ocean basins (Atlantic, Southern Ocean, and Indo-Pacific), the pressure-dependent carbonate system is calculated for every 100 m water depth and depending on the over- or undersaturation of the CO_3^{2-}-ion, $CaCO_3$ is either accumulated or dissolved. Implementation and realization of the sedimentary processes directly follows Munhoven and François (1996) and Munhoven (1997). Results with the simplified sedimentary response function and with the new full process-based sediment are in reasonable agreement [see Köhler and Munhoven (2020)], but for such massive perturbations as the proposed anthropogenic emissions both differ in detail, as will be discussed here. Volcanic CO_2 outgassing for PI conditions and the future is kept constant at $9 \cdot 10^{12}$ mol C/yr. Hard shells in coral reefs grow as function of sea level and Ω, the saturation state of $CaCO_3$ (Munhoven and François, 1996) leading to a sink of carbonate of $\sim 4 \cdot 10^{12}$ mol/yr in PI times. Riverine input of silicate and carbonate weathering, partly consuming atmospheric CO_2, are first kept constant at $12 \cdot 10^{12}$ mol/yr HCO_3^- each. However, CO_2-dependent weathering (W) fluxes W_X are alternatively implemented as described in Zeebe (2012), with $W_X = W_0(CO_2/CO_{2,0})^{n_X}$, $n_{Si} = 0.2$, and $n_{Ca} = 0.4$, W_0 the CO_2 independent weathering fluxes mentioned above, and $CO_{2,0}$ the PI CO_2 concentration. This approach leads to a rise in silicate (carbonate) weathering by 50% (130%) for CO_2 being $8\times CO_{2,0}$ (= 2,224 ppm) reached here. These model setups are labeled AOSEW and AOSE for the new model including process-based sediments with and without CO_2-dependent weathering, respectively.

In the following, results with four main setups will be discussed: the setup AOSEW and AOSE, which have been explained in the previous paragraph, in which the atmosphere–ocean is coupled to SE processes. Furthermore, I also use, for an understanding of the role of the sediments, the previous setups consisting of atmosphere–ocean with simplified (label AOS) and without (label AO) sediment feedback. The latter two setups correspond to model version 2.2 as applied in Köhler et al. (2010a) on the late Pleistocene and to some different CDR experiments with focus on C isotopes (Köhler, 2016). None of the labels include "B" (biosphere), since previous experiments (Köhler et al., 2015) have shown that the terrestrial biosphere is too simplistic to simulate meaningful results for a high CO_2 world. BICYCLE's results largely differ from more complex vegetation models, probably due to an unrealistically high CO_2 fertilization effect. I therefore apply the model here with a terrestrial biosphere that stays constant at PI level.

The model calculates only changes in the carbon cycle as response to changing climatic boundary conditions; it thus does not contain the physical part of the climate system. For the future emission scenarios considered here, only changes in temperature as consequence of changing atmospheric CO_2 are implemented, all other environmental conditions stay constant at their pre-industrial values.

The radiative forcing of changes in CO_2 on temperature is calculated as follows: The global temperature change ΔT (relevant for the atmosphere–ocean gas exchange) connected with a change in atmospheric CO_2 is calculated using the transient climate sensitivity (TCS) for CO_2 doubling, which has been obtained from more sophisticated climate models, and which has been recalculated to TCS = 2 K by a data-based approach (Storelvmo et al., 2016). In detail, I calculate

$$\Delta T = \mathrm{TCS} \cdot \frac{\Delta R_{CO_2}}{\Delta R_{2\times CO_2}} \tag{1}$$

with

$$\Delta R_{CO_2} = 5.35 \frac{\mathrm{W}}{\mathrm{m}^2} \cdot \ln\left(\frac{CO_2}{278\ \mathrm{ppm}}\right) \tag{2}$$

(Myhre et al., 1998). Changes in sea surface temperature (SST) are assumed to instantaneously follow ΔT, and changing SST then influences the CO_2 solubility in the ocean via Henry's law.

Heat penetration into the deep ocean is not simulated, but implicitly considered by calculating surface temperature changes out of a relatively small TCS, and not out of the larger equilibrium climate sensitivity (ECS). Thus, deep ocean temperature stays constant. However, tests have shown that deep ocean temperature is not important for the simulated atmospheric CO_2 concentration. Furthermore, this approach implicates that TCS, TCR (ΔT at time of $2\times$ CO_2 in a +1%/yr CO_2 rise scenario), and ECS (long-term ΔT due to $2\times$ CO_2) are identical. This implies that CO_2 and temperature change simultaneously, and the effect of a delayed warming for earlier emissions, as typically seen in GCMs, is not shown. For example, in the GISS-GCM only 60% of a CO_2-induced warming is realized in the first century, and about 90% after one millennia (Hansen et al., 2011). I acknowledge that this is a bold simplification, but I will discuss how the TCR to cumulative emissions (TCRE) is compared with output from CMIP5 model for the twenty-first century. The simulated temperature change is thus comparable with GCMs on a century-time scale but underestimates warming by up to a factor of two on longer time scales.

2.2. Simulation Scenarios: High CO_2 Emissions and Ocean Alkalinization

The model is spun up for 5000 years. Since PI in Keller et al. (2018) is defined as 1850 CE (100 BP), this implies that the spin ups start at 3150 BCE (5100 BP). Plotted results include only the last 100 years of the spinup, so starting at 1750 CE.

Simulations within the proposed CDR-ocean-alk experiment (including the spin up) are performed in emission driven mode, thus not prescribed CO_2, but model-internal calculated atmospheric CO_2 will be given in the following, circumventing slight disagreements between CO_2 at PI in different sources [CDRMIP protocol (284.7 ppm in Keller et al., 2018), the CMIP6

suggested value (284.3 ppm in Meinshausen et al., 2017), and the spline through the CO_2 data (286.1 ppm in Köhler et al., 2017)].

The applied fossil fuel emissions follow an extension of the Shared Socioeconomic Pathway (SSP) SSP5-85-EXT++ (Riahi et al., 2017). Since long-term emissions have not been available in 2018, when simulations have been performed, they have been compiled as follows. CO_2 emissions for SSP5-85-EXT should agree with Figure 5 in O'Neill et al. (2016). My CO_2 historical emissions (fossil fuel (+ industry) and land use change) until 2005 CE are as compiled for RCP8.5 in Meinshausen et al. (2011). For 2006–2100 CE fossil fuel (+ industry), CO_2 emissions are taken from https://esgf-node.llnl.gov/projects/input4mips/ as prescribed for CMIP6 (Hoesly et al., 2018), but CO_2 emissions from land use change (2006–2015 CE) is used as published in Houghton and Nassikas (2017), one of two bookkeeping models in Le Quéré et al. (2018). The extension of the emissions for years 2100–2300 CE is built from scratch following the description in O'Neill et al. (2016). Note that 2250–2300 CE should have emissions "of just below 10 PgC/yr." Here, I take 9.5 PgC/yr. Following a discussion with the coordinator of CDRMIP (Keller, personal communication), emissions are extended from 2300 CE with a linear reduction reaching zero emissions in year 2350 CE and stay zero thereafter. The simulations are extended by at least 5000 years (and up to ∼1 million years) in the future. The annual emissions peak in year 2090 CE at 35.6 PgC/yr and the total cumulative CO_2 emissions of this scenario add up to 6740 PgC (**Figure 2A**). This emission scenario SSP5-85-EXT++ without alkalinization is my control run (CTRL).

In addition to the CTRL, two different ocean alkalinization scenarios are applied. In ALK1 0.14 Pmol/yr, alkalinity is put into the surface ocean from year 2020 CE onward until the end of the simulation in year 7020 CE. From this alkalinization, 50% is put in each of the two 100 m deep equatorial surface ocean boxes ranging from 40°S to 50°N in the Atlantic and to 40°N in the Pacific. This approach follows the CDRMIP protocol putting the alkalinization in surface waters free of sea ice. Furthermore, it has been shown that a large amount of material, which needs to dissolve for such an alkalinity input, might due to the temperature-dependent kinetics sink undissolved into the abyss, when applied in polar waters (Köhler et al., 2013). In ALK2, this alkalinity input stops after 50 years in 2070 CE. Adding 0.14 Pmol/yr alkalinity is equivalent to adding 5.19 Pg/yr of an alkalizing agent like $Ca(OH)_2$ or 4.92 Pg/yr of forsterite (Mg_2SiO_4), a form of olivine. When assuming a theoretically possible net instant dissolution reaction, every mole of the added $Ca(OH)_2$ or Mg_2SiO_4 would sequester 2 or 4 mol of CO_2, respectively (Ilyina et al., 2013; Köhler et al., 2013). However, this back-of-the-envelope approximation ignores changes in sequestration efficiency due to the non-linear marine carbonate chemistry response as will be discussed in detail in the Results section.

These three scenarios (CTRL, ALK1, ALK2) are simulated in the different model setups described in section 2.1. An overview of all scenarios and setups used here is compiled in **Table 1**.

3. RESULTS

Simulated CO_2 depends on the specific setup and varies between 261 and 276 ppm in year 1750 CE, rising to 437–456 ppm in year 2019 CE, thus faster than the historical reconstructed rise from 277 to 410 ppm in the same time window (**Figure 2B**). This difference in the historical CO_2 evolution can be understood by the missing terrestrial carbon sink, which nowadays sequestrates about one-fourth to one-third of the anthropogenic emissions (Friedlingstein et al., 2019).

In all investigated scenarios, the anthropogenic CO_2 emissions in the twenty-first century largely dominate the global carbon cycle. Initial differences of the carbon cycle in the different model versions after spin-up are quickly dwarfed by the proposed emissions in the SSP5-85-EXT++ scenario, which is more than triple from the present-day (2020) fluxes of ∼10 PgC/yr within the next 70 years. Atmospheric CO_2 concentration peaks nearly independently of model version with 2,400 ppm in years 2326, only 24 years before the final fade out of any fossil fuel emissions. If alkalinization is applied (ALK1), the CO_2 peak is smaller by 200 ppm than without those sequestration efforts (**Figure 2B**).

While the long-term evolution of CO_2 in the CTRL runs largely depend on the sediment and weathering feedbacks, having values in year 7000 between 965 and 1,600 ppm, the resulting atmospheric CO_2 during sustained alkalinization (ALK1) obtained with different model versions is more in agreement. Here, atmospheric CO_2 falls below its pre-industrial value—implying the complete neutralization of all anthropogenic emissions—between the years 5500 and 6100.

The long-term atmospheric CO_2 in the control simulations depends on the setup (**Figure 2B**), since in AO only the oceanic carbon uptake is reducing CO_2, while in AOS the carbonate compensation mimicking the dissolution of $CaCO_3$ allows a further CO_2 reduction. Furthermore, in AOSEW a different $CaCO_3$ dissolution scheme together with a small contribution of <110 ppm from CO_2-dependent enhanced weathering fluxes (**Figure 2C**) reduces CO_2 to even lower levels. Simulated atmospheric CO_2 in the alkalinization experiment ALK1 is more setup independent than for the CTRL runs (**Figure 2B**). This implies that the details of CO_2 sequestration largely differ in the different setup (**Figure 2C**), for example, varying from sequestrated 800 ppm in AOSEW to 1,400 ppm in AO. It also shows that the CO_2 sequestration potential for high emission scenarios obtained with carbon cycle models without sediment modules is overestimated after roughly a millennium. However, already on multi-centennial time scales the simulated marine carbonate chemistry (e.g., pH, ocean alkalinity, **Figure 3**) is influenced by the dissolution of sediments, a process which is missing in setups without sediment/ocean interaction.

Coral reef growth (included in AOSEW) is a sink for alkalinity and a source of CO_2. However, the impact of its variability on the carbon cycle is negligible. In both CTRL and ALK1, the reef growth declines by three orders of magnitude in the first half of the future simulation. During ocean alkalinization, Ω and a potential coral reef growth would rise again, the latter to $10 \cdot 10^{12}$ mol/yr after 3000 years. Thus, in comparison to pre-industrial conditions, an initial CO_2 gain caused by reduced coral

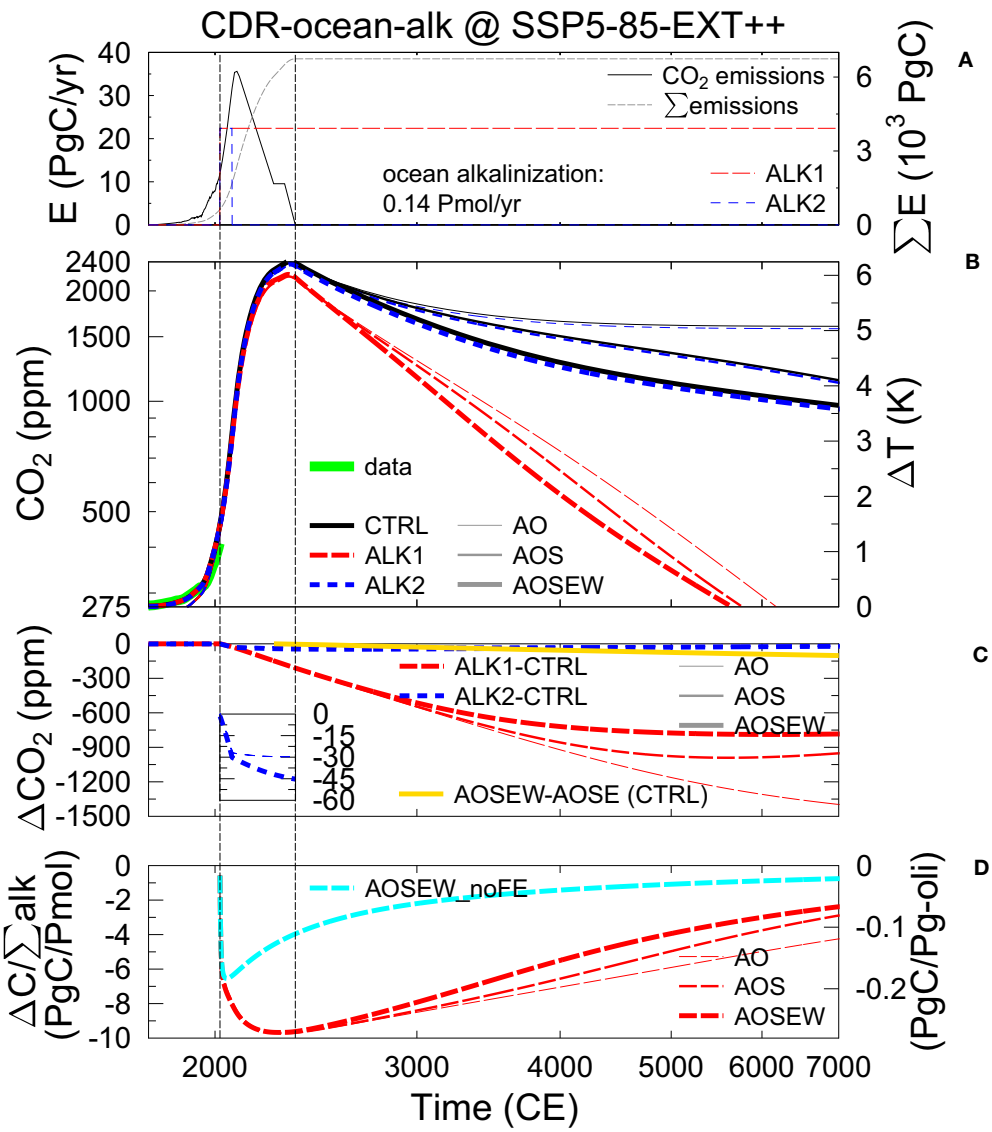

FIGURE 2 | (A) CO_2 emissions of the control run SSP5-85-EXT++ (annual and cumulative emissions E and left and right y-axis, respectively). Timing of ocean alkalinization of 0.14 Pmol/yr in scenarios ALK1 and ALK2 sketched in red and blues lines, respectively (no y-axis). **(B)** Resulting atmospheric CO_2 (left y-axis on log scale) and global temperature change ΔT with respect to pre-industrial (right y-axis) including a spline through compiled CO_2 data (Köhler et al., 2017), extending years 2016–2019 CE with online available data from NOAA. **(C)** Anomaly in atmospheric CO_2 with respect to a CTRL with alkalinization in scenarios ALK1 and ALK2. Zoom-in shows otherwise hardly detectable changes in atmospheric CO_2 due to ALK2 (results for AO and AOS are not distinguishable). Additionally the contribution of the CO_2-dependent weathering in the CTRL runs is shown. **(D)** Efficiency of ocean alkalinization (ratio of C extracted from the atmosphere over accumulated alkalinization) in ALK1. On the right y-axis, the efficiency is transferred in PgC/Pg of olivine assuming a molar mass of 140 g/mol corresponding to the iron-free version of olivine called forsterite (Mg_2SiO_4). Additionally, efficiency is shown for a scenario without future emissions (AOSEW_noFE). In **(B,C,D)**, results from three different setups are plotted: atmosphere-ocean only (AO), atmosphere-ocean including a sedimentary response function (AOS), or atmosphere-ocean in a solid Earth setup including CO_2-dependent weathering (AOSEW), having the terrestrial biosphere always fixed at pre-industrial levels. Vertical lines are at 2020 CE (onset of alkalinization) and 2350 CE (emissions back to 0). Note, that the x-axes are on log scale.

reef growth of <20 ppm is compensated by a similarly large CO_2 loss later on. However, this ignores the potential that corals get extinct due to a prolonged fall of Ω below critical values. If so their contribution as $CaCO_3$ sink might not reach initial values again even if chemical conditions no longer dissolve their $CaCO_3$-based skeletons.

In all setups, the efficiency of the ocean alkalinization has its maximum with 9.7 PgC oceanic carbon uptake per Pmol alkalinity input after 200 years during times of maximum anthropogenic emission, after which the efficiency slowly decreases to 2–4 PgC/Pmol (**Figure 2D**). These values correspond to 0.27 and 0.05–0.1 PgC per Pg of olivine,

TABLE 1 | Compilation of simulated scenarios and setups.

Setup	Scenarios			Description
	CTRL	ALK1	ALK2	
AO	x	x	x	Atmosphere-ocean only
AOS	x	x	x	AO + sedimentary response function
AOSE	x	–	–	AO + solid Earth processes: process-based sediments, volcanism, constant weathering, corals
AOSEW	x	x	x	AOSE + CO_2-dependent weathering
AOSEW_noT	x	x	–	AOSEW without temperature changes (feedback analysis)
AOSEW_noFE	x	x	–	AOSEW no emissions in years 2020 CE and later (efficiency analysis)

CTRL: high emission scenario SSP5-85-EXT++. ALK1: CTRL + 0.14 Pmol/yr ocean alkalinization starting in year 2020 CE. ALK2: same as ALK1, but stopping ocean alkalinization in year 2070 CE. x: simulation under this combination of setup and scenario performed (–: not performed).

respectively, if alkalinization is realized by the dissolution of forsterite. A reduction in efficiency of 20% when increasing the amount CO_2 sequestered by olivine dissolution from 1 to 20 PgC has been proposed based on calculations of the marine carbonate system, but ignoring ocean-sediment interaction and the importance of changes in the anthropogenic CO_2 emissions (Köhler et al., 2010b). I therefore test the influence of the prescribed rise in anthropogenic emissions on the calculated efficiency by an additional ocean alkalinization experiment without future CO_2 emissions (AOSEW_noFE). I indeed find after a 2–3 decades for equilibration (and increasing efficiency) a decrease in efficiency from its peak value of 6.5 PgC/Pmol alkalinity input, clearly different from the evolution of the sequestration efficiency that includes the proposed rise in CO_2 emissions (**Figure 2D**). I find a larger reduction in CO_2 sequestration efficiency in setups with sediments compared to AO-only setups, which is caused by a decline of the artificially added alkalinity (or its residence time) in the ocean (**Figure 3D**). In detail, on the long run the additional alkalinity leads to a deepening of the calcite saturation horizons (CSHs) and the lysocline transition zones (**Figure 4**), and finally to a rise of $CaCO_3$ accumulation in the sediments, which extracts alkalinity from the ocean and thus reduces the carbon sequestration efficiency.

In the scenario ALK2 containing 50 years of alkalinization, only a very small amount of carbon is sequestered (**Figures 2A–C**). Following back-of-the-envelope calculations for olivine (Köhler et al., 2010b), in this scenario about 250 Pg of olivine should lead to a reduction in CO_2 of ∼30 ppm, a difference that is indeed realized around the CO_2 peak in the 2320s years, but then contributes only to a relative reduction in CO_2 of 1–2%. However, after several thousand years the long-term sequestration in ALK2 is reduced to 10–20 ppm in setups with sediment feedback. This long-term change in CO_2 sequestration shows that ocean alkalinization is not a permanent artificial CO_2 sink, but depends in detail on how alkalinity is preserved in the ocean.

Surface ocean pH is back to its pre-industrial values of 8.1–8.2 between years 5000 and 6000 in ALK1 and results agree between different model setups similarly as when all anthropogenic emissions have been neutralized (**Figure 3A**). The pH minima of ∼7.3–7.4 mirror the peaks in atmospheric CO_2. pH in CTRL and ALK2 are similarly setup dependent as atmospheric CO_2.

The effect of the sediment feedback is easily illustrated, when plotting the sum of carbon contained in both the atmosphere and the ocean (**Figure 3B**). While in setups without sediments this number can only increase due to anthropogenic emissions, it might additionally be modified by the dissolution or accumulation of $CaCO_3$ in the sediments. In the SE setup (AOSEW), some small contributions from volcanic CO_2 outgassing, CO_2-dependent weathering, and shallow water deposition of $CaCO_3$ in corals might also play a role, but these fluxes are on the order of $<$ 30 Tmol/yr each, and over the simulated 5000 years about two orders of magnitude smaller than the cumulative CO_2 emission, and therefore negligible. However, what mainly happens in setups with interactive sediments is $CaCO_3$ dissolution (colored areas in **Figure 3B**), which is reduced when ocean alkalinization is applied. The artificial input of alkalinity does not prevent the $CaCO_3$ dissolution in sediments. In my modeling approach, about 2.3 EgC are dissolved from the sediments in CTRL, and nearly half of it during the first 1000 years after the end of the anthropogenic emissions. This dissolution during the first millennium hardly changes during ocean alkalinization. However, later on $CaCO_3$ accumulation in the sediment is again possible, having in year 7000 CE again a nearly similar amount of carbon in the combined ocean–atmosphere system as at the end of the emissions. The amount of dissolvable $CaCO_3$ depends on the initial sedimentary inventory, which has been generated after 800 kyr of simulations. The 8 cm thick sedimentary mixed layer contains globally integrated ∼ 700 PgC, but there are up to 500 historical sediment layers of 8 mm each underneath, which might also dissolved, once the sedimentary mixed layer is sufficiently thinned out. Similar as other parts of the model, the process-based sediment module is simpler than in full GCMs leading to larger dissolvable $CaCO_3$ than in other studies. For example, Archer et al. (1998) suggest that only 1.6 EgC of sedimentary $CaCO_3$ can be dissolved. This implies that the neutralization of anthropogenic emissions by sediment dissolution—the sediment feedback—might be slightly overestimated in this study.

A closer look on the sediment–ocean interaction gives the following details: In the water column, the rise in the CSH close to the ocean surface accompanied by a drop in CO_3^{2-}-ion concentration is clearly seen in the Atlantic and the Indo-Pacific for both CTRL and ALK1 (**Figures 4A–F**). Note that for technical reasons related to the implementation of sea level change in BICYCLE, the CSH cannot rise above 200 m water depth. The sedimentary response to this vertical rise in the CSH is by several thousands of years delayed and follows as an upward shift of the lysocline transient zone of partially dissolved sediments

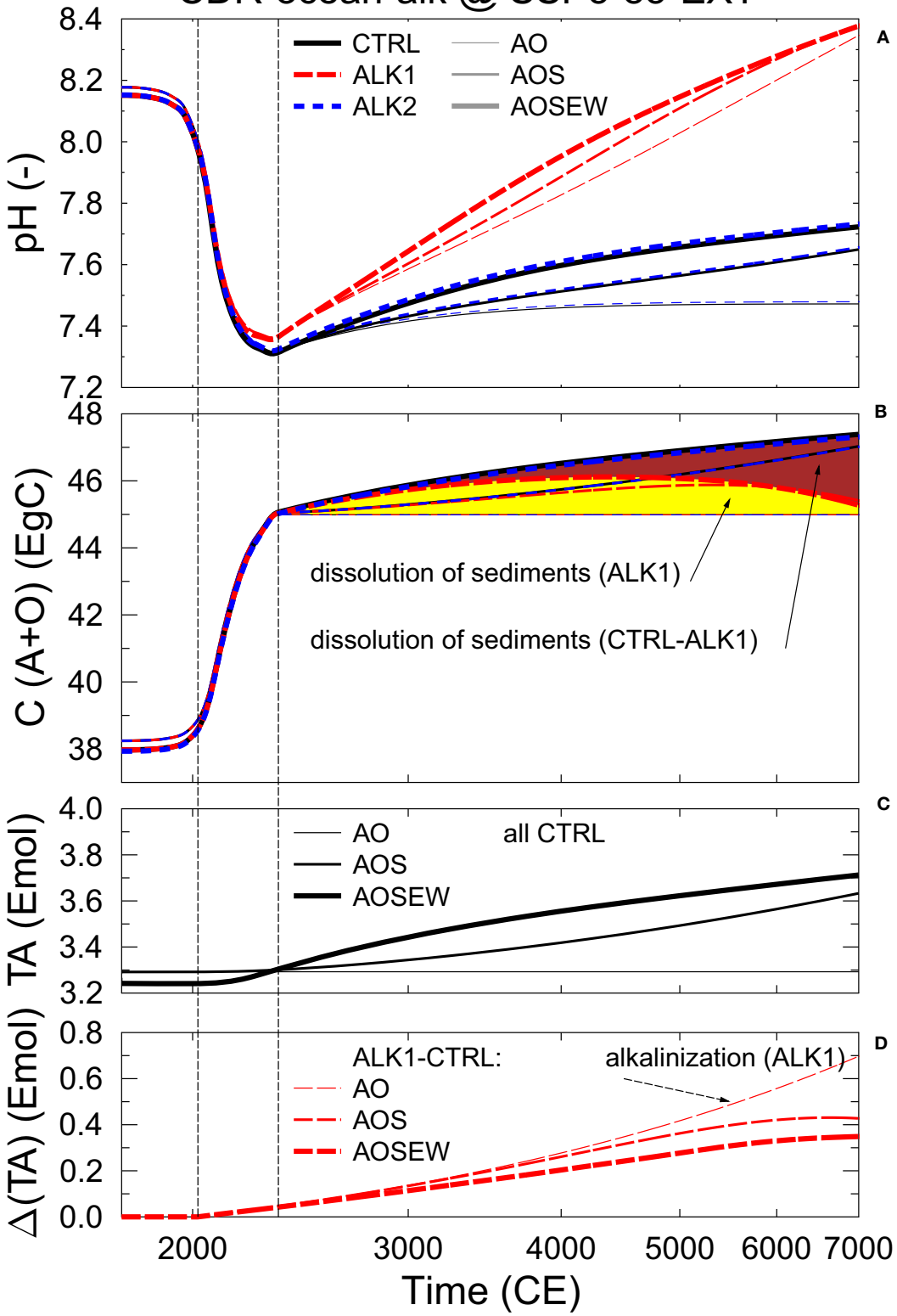

FIGURE 3 | (A) Volume-weighted mean pH of all surface ocean boxes. **(B)** C content of atmosphere (A) and ocean (O), marking the additional C released from the dissolution of $CaCO_3$ in the sediments due to the carbonate compensation feedback. Legend in **(A)** is also used in **(B)**. **(C)** Total alkalinity for different CTRL runs. **(D)** Changes in total alkalinity for ALK1 in different setups. Vertical lines are at 2020 CE (onset of alkalinization) and 2350 CE (emissions back to 0). Note log x-axis. Units of Eg or Emol correspond to 10^{18} g or mol.

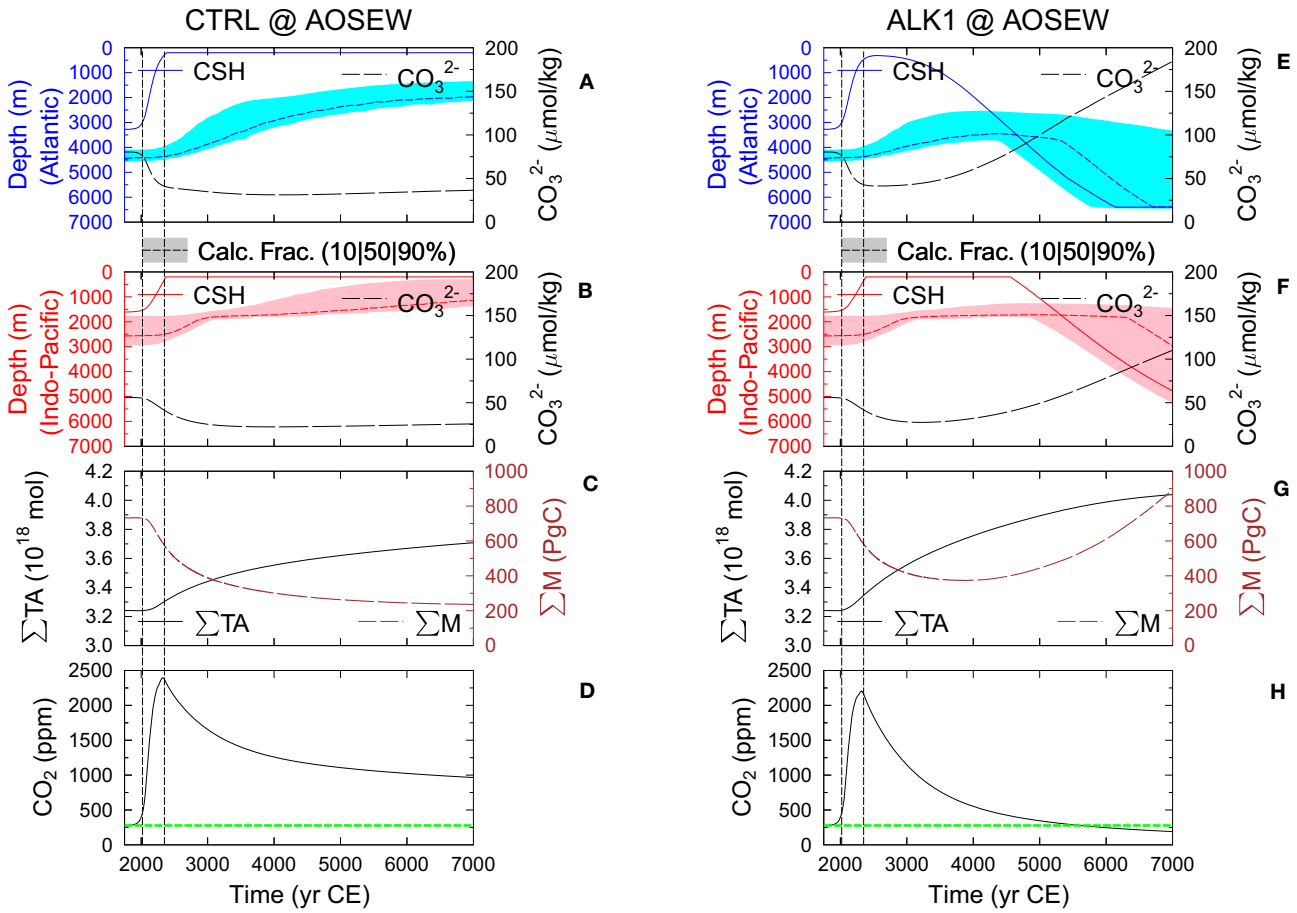

FIGURE 4 | Details for CTRL (left) and ALK1 (right) in AOSEW setup. Calcite saturation depth (CSH), carbonate fraction (shaded area covers depths from 10% (lower bound) to 90% (upper bound) with 50% as short broken line in-between) in sedimentary mixed layers, and CO_3^{2-}-ion concentration in the equatorial ocean of the **(A,E)** Atlantic or **(B,F)** Indo-Pacific. **(C,G)** Sum of total alkalinity in the ocean (∑TA) and global amount of $CaCO_3$ integrated over all sedimentary mixed layer (∑M). **(D,H)** Atmospheric CO_2, and green horizontal line marks the pre-industrial concentration of 278 ppm. Vertical lines are at 2020 CE (onset of alkalinization) and 2350 CE (emissions back to 0).

(**Figures 4A,B**), implying especially a dissolution of $CaCO_3$ from the sediments in water depths in which this transition zone has moved to a shallower depth. The amount of $CaCO_3$ in the sedimentary mixed layer gradually declines in CTRL from 700 to slightly more than 200 PgC (**Figure 4C**). The fact that this number has not been reduced to zero indicates that after 5000 simulated years historical layers are still included into the sedimentary mixed layer and then also potentially dissolved. This process slows down over time due to the increasing fraction of non-$CaCO_3$ material (clay), which is on the long run included in the sedimentary mixed layer, effectively limiting the amount of dissolved $CaCO_3$ (e.g., see also Archer et al., 1998). Ocean alkalinization is able to reverse these trends bringing CSH and CO_3^{2-}-ion concentration back to initial values and even beyond if alkalinity input is sustained until the end of the simulation time (**Figures 4E,F**). The water depth in which the lysocline transition zone is found deepens and widens having in the end a several kilometer deep band in which the fraction of $CaCO_3$ in the sedimentary mixed layer decreases from 90% (upper bound) to 10% (lower bound). Especially the lower bound is found in deeper waters than before, indicating that ocean alkalinization would allow $CaCO_3$ accumulation in the sediments at water depths at which in pre-industrial times a complete dissolution of $CaCO_3$ would have occurred (**Figures 4E,F**). In ALK1, the total amount of $CaCO_3$ in the sedimentary mixed layer increases again after passing its minimum of 400 PgC around year 4000 CE (**Figure 4G**).

The total alkalinity in the ocean is, similarly as the total amount of carbon in the AO subsystem, depending on the consideration of the sediment feedback (**Figure 3C**), since, as already explained, the anthropogenic carbon penetrating the deep ocean partly dissolves the sediment. Therefore, the alkalinization experiments change alkalinity differently (**Figure 3D**): in setups with interactive sediments, further alkalinity input changes the deep ocean–sediment exchange fluxes due to vertical shifts in the CSH toward deeper water, allowing later in the simulation an increase in sedimentary $CaCO_3$ accumulation. The loss of $CaCO_3$ from the ocean to

the sediment is a sink for oceanic alkalinity, therefore reducing total alkalinity in comparison to setups without sedimentary responses (AO).

The strength of the temperature, sediment, and weathering feedbacks can be approximated by plotting differences obtained with setups with the relevant processes being switched on or off (**Figure 5**). I obtained the strength of the feedbacks by calculating differences from the same standard runs obtained with the setup AOSEW. In detail, the temperature feedback is based on Δ_T = AOSEW – AOSEW_noT, in which the latter is a special case in which temperature is kept constant; the weathering feedback is derived from Δ_W = AOSEW – AOSE; the sediment feedback from Δ_S = AOSEW – AO – Δ_W. I find that the positive temperature feedback adds about 150 ppm of CO_2 to the atmosphere, which also persists for several millennia. In other words, carbon cycles with and without temperature feedback do not instantaneously agree with each other once the anthropogenic emissions drop back to zero, since the changes in CO_2 solubility introduced by temperature have in the mean time penetrated into the deep ocean. The negative feedbacks reduce CO_2 by 520 (sediment) and 110 (weathering) ppm over the next 5000 years in the CTRL run. In ALK1, all feedbacks are back to zero after 5000 years, since all anthropogenic emissions have been sequestrated after 3500–4100 years, and existing carbon cycle realizations were slowly merging toward each other, thus marginalizing any differences. Assuming a higher climate sensitivity, for example, more in agreement with its values for equilibrium conditions of 2.6–3.9 K (the 66% probability range in the most recent review of Sherwood et al., 2020) would lead to higher CO_2 concentrations of 30–100 ppm and therefore to a higher temperature feedback. Such higher numbers are probably expectable in the long run (millennium scale), but should be an overestimation for the next centuries, since the full climate response to CO_2 takes 1–2 kyrs (Hansen et al., 2011).

The strength of the feedbacks in the CTRL simulations without alkalinization is comparable to feedbacks in other models. For example, CO_2 anomalies after 10 kyr in a 5000 PgC carbon pulse experiment have been +50 to +400 ppm (climate), −70 to −220 ppm (weathering), and −200 to −550 ppm (sediment) in the in the Long-Term MIP with 5–7 more complex climate models (Archer et al., 2009). The vegetation feedback neglected here is usually a negative feedback reducing CO_2 even further. However, the strength of this feedback is typically reduced over time, potentially also switching to a positive feedback. Paleo studies (Retallack and Conde, 2020) indicate that atmospheric CO_2 concentrations above 1,500 ppm might be toxic to the biosphere, making the vegetation response in a high CO_2 world a rather unknown variable. Furthermore, in Long-Term MIP a climate feedback, not a temperature feedback, is calculated, since in applied models any change in the radiative forcing does not only change temperature as in my box model here, but also other climatic processes. Most importantly for the carbon cycle—and missing here—is a potential reduction or even shutdown of the Atlantic meridional ocean circulation (e.g., Liu et al., 2017), since this would alter the transport of tracers between the surface and the deep ocean, and thus alter the marine carbon pumps. Additionally, permafrost thaw in a high emission world will most likely lead to additional CO_2 (and CH_4) fluxes to the atmosphere not accounted for here and in most other models (e.g., Burke et al., 2018).

The temporal response of the carbon cycle to the anthropogenic emissions is often analyzed as the "airborne fraction" $f = \Delta C_A / \sum E$, which describes the ratio of the difference in atmospheric carbon content ΔC_A over cumulative emissions $\sum E$ (**Figure 6**). Once f is brought back to zero, all anthropogenic emissions have been extracted from the atmosphere and CO_2 has reached pre-industrial concentration again. This fraction reaches 0.7 during peak emission times and is gradually reduced depending on implemented processes. Without interactive sediments it stays above 0.4. The sediment feedback reduces f to 0.1 after 20–40 kyr. Interestingly, both setup with simplified sedimentary response function and process-based sediment reach nearly identical end points, but differ only on their ways toward them. Here, the effect of the response function (AOS) is slower than the process-based sediment (AOSE) until year 9000, while the response function reduces atmospheric CO_2 faster thereafter. This implies that at first sediment dissolution might occur faster than approximated with the response function, while later on this process is slowed down, probably due to the limited amount of available $CaCO_3$, which can be dissolved. The weathering feedback reduces CO_2 during the whole simulation time, but was especially necessary to gradually bring the airborne fraction from 0.1 down to zero (atmospheric CO_2 back to pre-industrial values) on a million years time scale, in agreement with others (e.g., Colbourn et al., 2013). The effect of the alkalinization is an acceleration of the reduction of f toward zero. Airborne fractions f discussed above differ from the numbers given in the introduction due to the difference in the amount and temporal evolution of the anthropogenic emissions.

4. DISCUSSION

In the following discussion I will first (section 4.1) focus on the general model response including an analytical view on the TCR to cumulative emissions (TCRE) to obtain an in-depth understanding of the underlying emission scenarios. TCREs is not central to the ocean alkalinization experiments but gives an understanding for the consequences of the implemented climate sensitivity in the model and sets the box model results in relation to more complex approaches. In the second part, I will then discuss the alkalinization experiments (section 4.2).

4.1. General Model Response to Anthropogenic Emissions Including TCRE

Although the BICYCLE model is focusing on the carbon cycle and has only a very limited implementation of climate change, it is useful to compare the resulting temperature change with output of more complex models. For this effort, TCRE is plotted together with previous simulations of RCP emission scenarios (Köhler, 2016) and CMIP5 contributions (**Figure 7**).

CMIP5 results (IPCC, 2013) are here restricted to idealized scenarios with CO_2 emissions only, in detail to those with 1%/yr

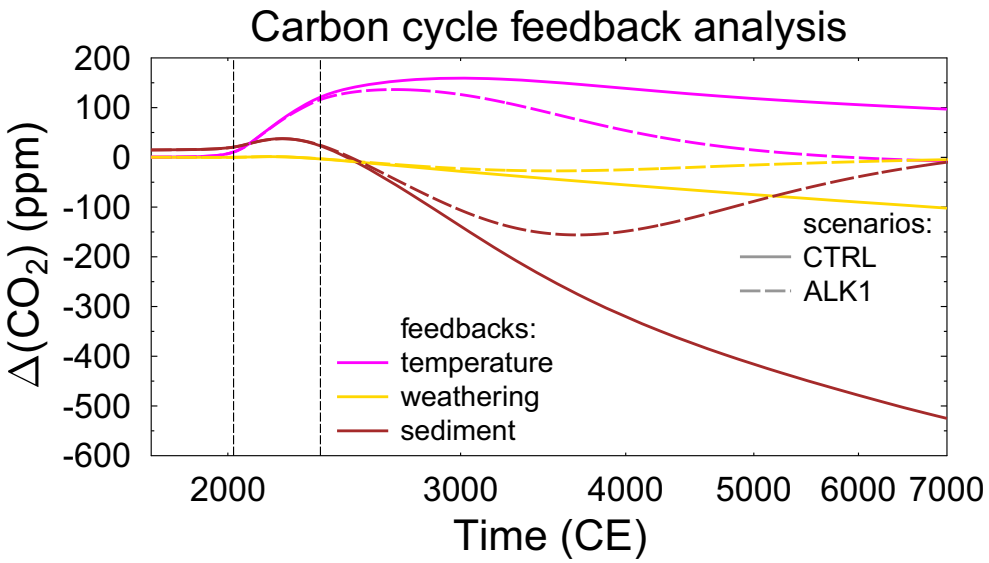

FIGURE 5 | Feedback analysis of the contribution of the positive temperature feedback, and the negative weathering and sediment feedback on the CTRL run and alkalinization scenario ALK1. Vertical lines are at 2020 CE (onset of alkalinization) and 2350 CE (emissions back to 0). Note log x-axis.

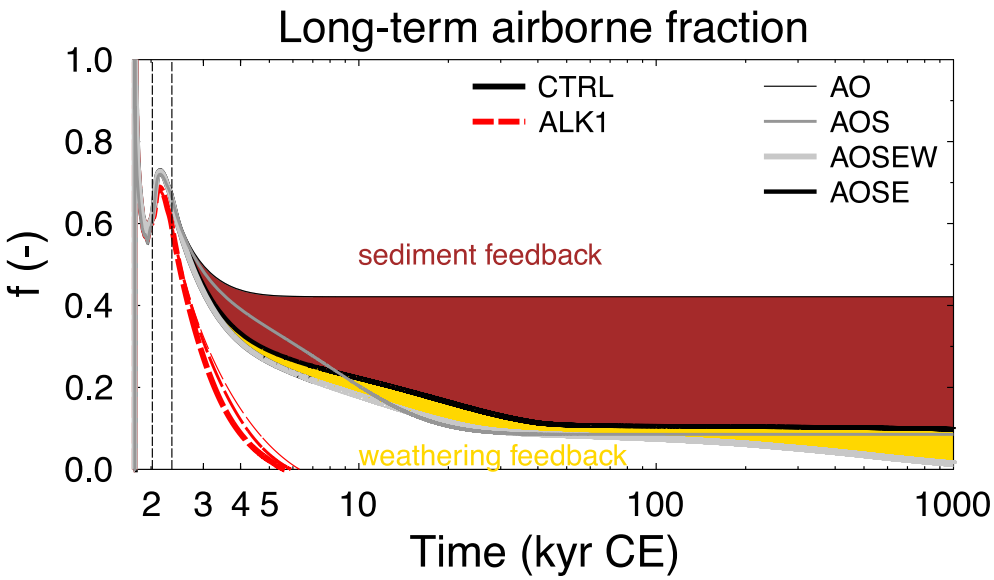

FIGURE 6 | Airborne fraction *f* of anthropogenic emissions for different model versions for up to 1,000 kyr CE (=1 Myr CE) in the CTRL run and alkalinization scenario ALK1. The color-coded areas show the CO_2 sequestration related to weathering and sediment feedback. Vertical lines are at 2020 CE (onset of alkalinization) and 2350 CE (emissions back to 0). Note log x-axis.

rise in CO_2. This approach neglects global warming connected with anthropogenic emissions of CH_4, N_2O, or any aerosol effects, which are also ignored in BICYCLE, and thus allowing a meaningful comparison. For cumulative emissions of 2,500 Pg C, the spread in the simulated global warming ΔT in the CMIP5 output ranges from 2.2 to 5.5 K. BICYCLE results are very well in the middle of the uncertainty range spanned by simulation results of the Earth system models (ESM) contributing to CMIP5, but show especially for higher cumulative emissions a clear non-linear relationship between ΔT and $\sum$E, the so-called TCRE. The drop in ΔT from $>$ 6 K to $<$ 0.5 K for constant $\sum$E in our SSP5-85-EXT++ simulation reflects the sequestration of anthropogenic CO_2 first by marine uptake, followed by the sediment and the weathering feedbacks.

More complex models find a near linear trend for TCRE (e.g., Allen et al., 2009; Goodwin et al., 2015; Frölicher, 2016;

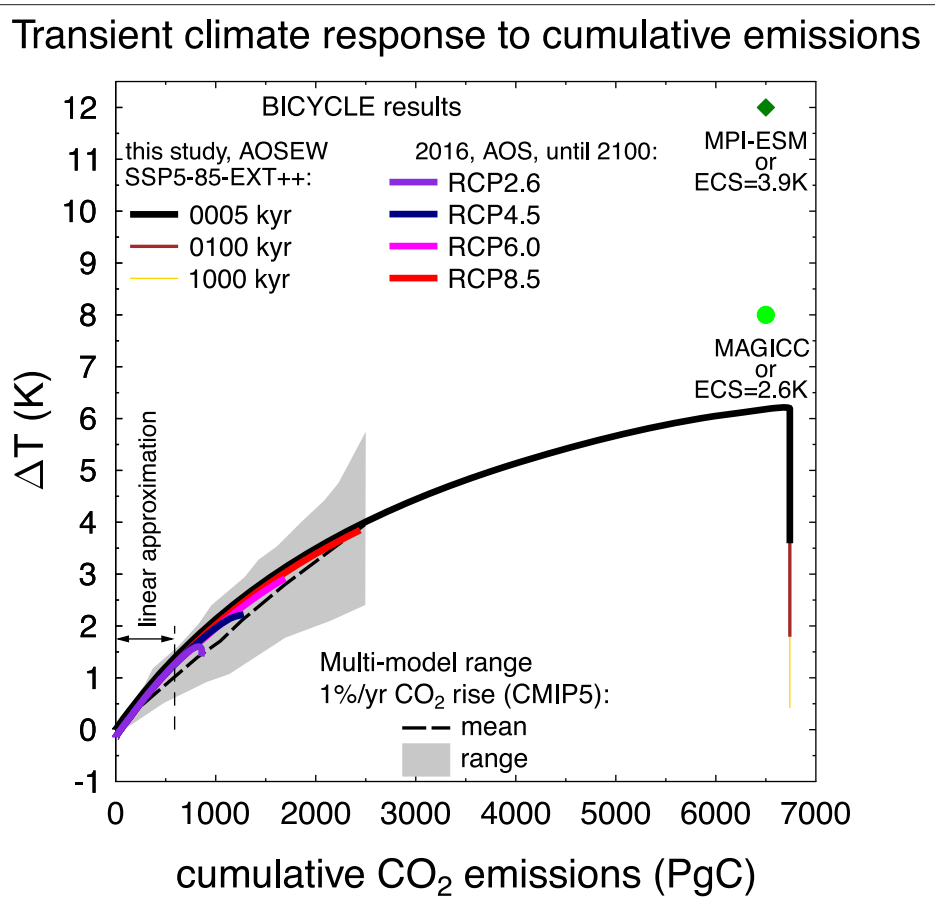

FIGURE 7 | Global mean surface temperature increase as a function of cumulative net global CO_2 emissions, known as transient climate response to cumulative emissions (TCRE) for results from BICYCLE and other models. From this study, results for CTRL (emissions following scenario SSP5-85-EXT++) in model version AOSEW for 5, 100, and 1,000 kyr are shown. In addition, four different RCP emission scenarios (BICYCLE, model version AOS) from Köhler (2016) are included. The 2016 results show changes from the beginning of the emissions (year 1765) until year 2100. For the BICYCLE results I directly calculate ΔT from CO_2 using a transient climate response of 2 K as given in the methods. For comparison the multi-model mean and range simulated by CMIP5 models, forced by a CO_2 increase of 1% per year is given by the broken black line and gray area (after Figure SPM 10 of IPCC, 2013). These simulations exhibit lower warming than those driven by RCPs within CMIP5, which include additional non-CO_2 forcing and therefore lead to higher temperature changes. For the CMIP5 results, ΔT until the year 2100 is calculated relative to the 1861–1880, and CO_2 emissions relative to 1870. I also included the discussed warmings obtained with an ECS of 2.6 or 3.9 K, identical to the simulations for SSP5-85-EXT CO_2 emissions (6500 PgC) obtained with the simple climate model MAGICC (O'Neill et al., 2016) and MPI-ESM (Kleinen, personal communication). The range with cumulative emissions <590 PgC approximated by a linear relationship in the TCRE in the analysis is also marked.

MacDougall, 2016, 2017; Tokarska et al., 2016; Seshadri, 2017; Williams et al., 2017; Katavouta et al., 2018; Rogelj et al., 2019). This relationship compresses the anthropogenic impact on climate into one relationship and one figure, which make the man-made global warming rather easy to grasp and to communicate. Therefore, such a figure has also been included in the last assessment report of the IPCC [Figure 10 in the Summary for Policy Makers (IPCC, 2013)]. Here, I will elaborate why simulation results with a carbon cycle box model also show this behavior by analytically analyzing why and when the ratio of global temperature change over cumulative net CO_2 emissions should be constant.

The relation between CO_2 and ΔT in BICYCLE has already been described in the methods section with Equations (1) and (2) for $\Delta T = f(\Delta R_{CO_2})$ and $\Delta R_{CO_2} = f(CO_2)$, respectively.

The CO_2-dependent term in the natural logarithmic function in Equation (2) can be rewritten as

$$\frac{CO_2}{278\ \text{ppm}} = \frac{C_A}{C_A^0} = \frac{C_A^0 + \Delta C_A}{C_A^0} = 1 + \frac{\Delta C_A}{C_A^0} = 1 + \frac{\Delta C_A}{589\ \text{PgC}} \quad (3)$$

with C_A: CO_2 content in the atmosphere, C_A^0: baseline CO_2 content in the atmosphere (278 ppm or 589 PgC using the well-known correlation of 1 ppm = 2.12 PgC), ΔC_A: the change in atmospheric CO_2 from the baseline. Using as approximation the first term of the Taylor series for the natural logarithmic

$$\ln(1+x) = \sum_{n=1}^{\infty} \frac{(-1)^{n+1}}{n} x^n = x - \frac{x^2}{2} + \frac{x^3}{3} - \ldots, \quad (4)$$

which converges for $x \in (-1, +1]$ (or here for $\Delta C_A \leq 589$ PgC) I find

$$\Delta T = \mathrm{TCS} \cdot \frac{\Delta R_{\mathrm{CO_2}}}{\Delta R_{2\times \mathrm{CO_2}}} \quad (5)$$

$$= \frac{\mathrm{TCS} \cdot 5.35 \frac{\mathrm{W}}{\mathrm{m^2}}}{\Delta R_{2\times \mathrm{CO_2}}} \cdot \ln\left(1 + \frac{\Delta C_A}{589\ \mathrm{PgC}}\right) \quad (6)$$

$$\Delta T \approx \gamma \cdot \Delta C_A \quad (7)$$

$$\text{with } \gamma = \frac{2\ \mathrm{K} \cdot 5.35 \frac{\mathrm{W}}{\mathrm{m^2}}}{3.71 \frac{\mathrm{W}}{\mathrm{m^2}} \cdot 589\ \mathrm{PgC}} = 4.9 \cdot 10^{-3} \frac{\mathrm{K}}{\mathrm{PgC}}. \quad (8)$$

Neglecting changes in the terrestrial carbon storage (as done in those simulations with BICYCLE), the cumulative net emissions, $\sum E$, can be expressed as follows:

$$\sum E = \Delta C_A + \Delta C_O \quad (9)$$

with ΔC_O: the oceanic uptake of anthropogenic CO_2 emissions. Using

$$\Delta C_A = f \cdot (\sum E) \quad (10)$$

$$\Delta C_O = (1 - f) \cdot (\sum E) \quad (11)$$

with f being the airborne fraction. The net emissions can also be expressed as

$$\sum E = \frac{\Delta C_A}{f}. \quad (12)$$

Following our analysis above (Equations 7 and 12), the relationship between global surface temperature change, ΔT, and the cumulative net emissions, $\sum E$, can be expressed as

$$\frac{\Delta T}{\sum E} = \gamma \cdot f, \quad (13)$$

which is for $\sum E < 590$ PgC to the first order a linear relation (constant slope), since $f \sim 0.6$ and changes only very little during the first centuries of the anthropogenic emissions.

Thus, TCRE, is a function of the airborne fraction. In our model results, they are roughly pathway independent until the mid-21st century, when they start to diverge (see Köhler, 2016). This implies that TCRE is not completely pathway independent but depends on the airborne fraction, which depends on the anthropogenic emission strength (e.g., Joos et al., 2013; Lord et al., 2016).

The non-linear character of the TCRE relationship in our results, especially for $\sum E > 589$ PgC, is directly obtained, if the approximation of Equation (7) with the Taylor series is not performed, or if a longer simulation time is analyzed, in which f gradually declines toward lower values. The equations for an explanation of TCRE become more complicated if the oceanic heat uptake is not considered implicitly via TCR, but explicitly (MacDougall, 2017). Models, which have ocean heat uptake implemented, typically also calculate proposed changes in ocean circulation and subsequent oceanic CO_2 uptake. They obtain for high cumulative emissions larger temperatures than the box model used here, and are thus more in line with a linear relationship in TCRE generally found for complex climate models. The long-term temperature response can be approximated if I assume an ECS of 2.6–3.9 according to Sherwood et al. (2020) instead of the TCR of 2 K used here. This would lead to a long-term ΔT for the full cumulative emissions of 8–12 K (instead of ∼6 K seen in **Figure 7**), more in agreement with SSP5-85-EXT-based warming of 8 K obtained with the simple climate model MAGICC (O'Neill et al., 2016) or of 12 K simulated with the MPI-ESM (Kleinen, personal communication).

4.2. Alkalinization

The performed alkalinization in CDR-ocean-alk leaves the question open which mineral should be dissolved to reduce CO_2. It is therefore also not possible to address if and how marine biology might be largely altered, since it is not clear which nutrients, in addition to alkalinity, might be added to the ocean. In a simulation experiment in which the dissolution of olivine has been implemented (Hauck et al., 2016) large shifts in the phytoplankton community due to silicic acid and iron input accompanying the olivine dissolution have been found. In experiments, in which 1-mol-% of the olivine contains bioavailable iron, the relative contributions to the total CO_2 sequestration by olivine dissolution have been 57% via alkalinity input, 37% via iron fertilization, and 6% via silicic acid input. The part of the CDR caused by ocean fertilization (iron, silicic acid) is not permanent, while the CO_2 sequestered by alkalinization would be stored in the ocean as long as alkalinity is not removed from the system (Hauck et al., 2016).

The amount of material necessary for a complete sequestration of all anthropogenic emissions is huge. An atmospheric CO_2 concentration of 400, 350, 300, or even 280 ppm is reached only after 2730, 3060, 3480, or 3710 years of a constant alkalinization of 0.14 Pmol/yr, respectively. If olivine is used for this effort, 13.4–18.2 Eg of this silicate rock needs to be mined, grinded, and transported to suitable places, preferable to tropical waters that allow fast mineral dissolution (Köhler et al., 2013). For any application of ocean alkalinization, its sequestration efficiency maximum around peak CO_2 emissions needs to be considered. The time spans until complete neutralization are difficult to grasp, since they contain more than 100 generations of mankind. It clearly illustrates that, if this process might help for CO_2 sequestration, it certainly is not enough to rely on only ocean alkalinization of the suggested magnitude. It needs more efforts to bring atmospheric CO_2 down faster. Preferably, the high emission world underlying our simulations here is not the one mankind has to deal with. However future emissions might look like most likely a suite of different approaches is needed to fully counteract the amplitude of the anthropogenic emissions. For example, they might follow a multi-wedge approach, in which various different mechanisms are simultaneously applied for an efficient and

manageable neutralization of anthropogenic CO_2 emissions in the foreseeable future (Pacala and Socolow, 2004; Davis et al., 2013).

5. CONCLUSIONS

I here described long-term effects of ocean alkalinization in a high emission world using a simple carbon cycle box model with fixed marine and terrestrial biology and unchanged ocean circulation. The assumed cumulative CO_2 emissions of 6,740 PgC would by oceanic processes and sediment and weathering feedbacks be naturally extracted from the atmosphere on time scales of $10^5 - 10^6$ years. Ocean alkalinization of the proposed strength—equal to an annually constant dissolution of 5 Pg of olivine—would shorten this neutralization time of anthropogenic emissions to ∼3500 years. The carbon sequestration efficiency of ocean alkalinization has its maximum during the anthropogenic CO_2 emission peak and shortly thereafter at 9.7 PgC per Pmol of alkalinization (or 0.27 PgC/Pg of olivine) slowly declining to half of this value two millennia later. The alkalinization partly compensates the natural occurring fossil fuel neutralization by $CaCO_3$ dissolution from ocean sediments. The thus altered marine chemistry reverses after 1–2 kyr the trend from sedimentary $CaCO_3$ dissolution to a restrengthened accumulation of $CaCO_3$ in the sediments. Ocean alkalinization extracts anthropogenic CO_2 from the atmosphere only as long as the added alkalinity stays in the ocean, which can due to ongoing $CaCO_3$ accumulation in the sediments not be guaranteed for 100% of the artificially added alkalinity.

DATA AVAILABILITY STATEMENT

The datasets generated and analyzed for this study can be found in the PANGAEA data base (https://doi.org/10.1594/PANGAEA.921107).

AUTHOR CONTRIBUTIONS

PK was the sole developer of the applied model BICYCLE, followed the conceptional design of the CDRMIP scenario CDR-ocean-alk, performed all the simulations, analyzed the results, and wrote the paper.

FUNDING

PK was institutional funded by AWI via the Helmholtz research program PACES-II.

ACKNOWLEDGMENTS

I thank Guy Munhoven for providing model code, part of **Figure 1**, and discussions on the sediment model over the years. I thank the coordinators of the CDRMIP for their work in getting this effort going, and Thomas Kleinen for sharing his unpublished results with me.

REFERENCES

Allen, M. R., Frame, D. J., Huntingford, C., Jones, C. D., Lowe, J. A., Meinshausen, M., et al. (2009). Warming caused by cumulative carbon emissions towards the trillionth tonne. *Nature* 458, 1163–1166. doi: 10.1038/nature08019

Archer, D., Eby, M., Brovkin, V., Ridgwell, A., Cao, L., Mikolajewicz, U., et al. (2009). Atmospheric lifetime of fossil fuel carbon dioxide. *Annu. Rev. Earth Planet. Sci.* 37, 117–134. doi: 10.1146/annurev.earth.031208.100206

Archer, D., Kheshgi, H., and Maier-Reimer, E. (1997). Multiple time scales for neutralization of fossil fuel CO_2. *Geophys. Res. Lett.* 24, 405–408. doi: 10.1029/97GL00168

Archer, D., Kheshgi, H., and Maier-Reimer, E. (1998). Dynamics of fossil fuel neutralization by marine $CaCO_3$. *Glob. Biogeochem. Cycles* 12, 259–276. doi: 10.1029/98GB00744

Beerling, D. J., Kantzas, E. P., Lomas, M. R., Wade, P., Eufrasio, R. M., Renforth, P., et al. (2020). Potential for large-scale CO_2 removal via enhanced rock weathering with croplands. *Nature* 583, 242–248. doi: 10.1038/s41586-020-2448-9

Burke, E. J., Chadburn, S. E., Huntingford, C., and Jones, C. D. (2018). CO_2 loss by permafrost thawing implies additional emissions reductions to limit warming to 1.5 or 2°C. *Environ. Res. Lett.* 13:024024. doi: 10.1088/1748-9326/aaa138

Colbourn, G., Ridgwell, A., and Lenton, T. M. (2013). The Rock geochemical model (RokGeM) v0.9. *Geosci. Model Dev.* 6, 1543–1573. doi: 10.5194/gmd-6-1543-2013

Colbourn, G., Ridgwell, A., and Lenton, T. M. (2015). The time scale of the silicate weathering negative feedback on atmospheric CO_2. *Glob. Biogeochem. Cycles* 29, 583–596. doi: 10.1002/2014GB005054

Committee on Geoengineering Climate (2015). *Climate Intervention: Carbon Dioxide Removal and Reliable Sequestration*. Washington, DC: National Academic Press.

Davis, S. J., Cao, L., Caldeira, K., and Hoffert, M. I. (2013). Rethinking wedges. *Environ. Res. Lett.* 8:011001. doi: 10.1088/1748-9326/8/1/011001

Friedlingstein, P., Jones, M. W., O'Sullivan, M., Andrew, R. M., Hauck, J., Peters, G. P., et al. (2019). Global carbon budget 2019. *Earth Syst. Sci. Data* 11, 1783–1838. doi: 10.5194/essd-11-1783-2019

Frölicher, T. L. (2016). Climate response: strong warming at high emissions. *Nat. Clim. Change* 6, 823–824. doi: 10.1038/nclimate3053

Ganachaud, A., and Wunsch, C. (2000). Improved estimates of global ocean circulation, heat transport and mixing from hydrographic data. *Nature* 408, 453–457. doi: 10.1038/35044048

González, M. F., and Ilyina, T. (2016). Impacts of artificial ocean alkalinization on the carbon cycle and climate in Earth system simulations. *Geophys. Res. Lett.* 43, 6493–6502. doi: 10.1002/2016GL068576

Goodwin, P., Williams, R. G., and Ridgwell, A. (2015). Sensitivity of climate to cumulative carbon emissions due to compensation of ocean heat and carbon uptake. *Nat. Geosci.* 8, 29–34. doi: 10.1038/ngeo2304

Hansen, J., Sato, M., Kharecha, P., and von Schuckmann, K. (2011). Earth's energy imbalance and implications. *Atmos. Chem. Phys.* 11, 13421–13449. doi: 10.5194/acp-11-13421-2011

Hauck, J., Köhler, P., Wolf-Gladrow, D. A., and Völker, C. (2016). Iron fertilisation and century-scale effects of open ocean dissolution of olivine in a simulated CO_2 removal experiment. *Environ. Res. Lett.* 11:024007. doi: 10.1088/1748-9326/11/2/024007

Haverd, V., Smith, B., Canadell, J. G., Cuntz, M., Mikaloff-Fletcher, S., Farquhar, G., et al. (2020). Higher than expected CO_2 fertilization inferred from leaf to global observations. *Glob. Change Biol.* 26, 2390–2402. doi: 10.1111/gcb.14950

Heimann, M., and Maier-Reimer, E. (1996). On the relations between the oceanic uptake of CO_2 and its carbon isotopes. *Glob. Biogeochem. Cycles* 10, 89–110. doi: 10.1029/95GB03191

Hoesly, R. M., Smith, S. J., Feng, L., Klimont, Z., Janssens-Maenhout, G., Pitkanen, T., et al. (2018). Historical (1750–2014) anthropogenic emissions of reactive gases and aerosols from the community emissions data system (CEDS). *Geosci. Model Dev.* 11, 369–408. doi: 10.5194/gmd-11-369-2018

Houghton, R. A., and Nassikas, A. A. (2017). Global and regional fluxes of carbon from land use and land cover change 1850–2015. *Glob. Biogeochem. Cycles* 31, 456–472. doi: 10.1002/2016GB005546

Ilyina, T., Wolf-Gladrow, D., Munhoven, G., and Heinze, C. (2013). Assessing the potential of calcium-based artificial ocean alkalinization to mitigate rising atmospheric CO_2 and ocean acidification. *Geophys. Res. Lett.* 40, 5909–5914. doi: 10.1002/2013GL057981

IPCC (2013). "Summary for policymakers," in *Climate Change 2013: The Physical Science Basis. Contribution of Working Group I to the Fifth Assessment Report of the Intergovernmental Panel on Climate Change*, eds T. Stocker, D. Qin, G.-K. Plattner, M. Tignor, S. Allen, J. Boschung, et al. (Cambridge; New York, NY: Cambridge University Press), 3–29. doi: 10.1017/CBO9781107415324.004

Jones, C., Robertson, E., Arora, V., Friedlingstein, P., Shevliakova, E., Bopp, L., et al. (2013). Twenty-first-century compatible CO_2 emissions and airborne fraction simulated by CMIP5 earth system models under four representative concentration pathways. *J. Clim.* 26, 4398–4413. doi: 10.1175/JCLI-D-12-00554.1

Joos, F., Roth, R., Fuglestvedt, J. S., Peters, G. P., Enting, I. G., von Bloh, W., et al. (2013). Carbon dioxide and climate impulse response functions for the computation of greenhouse gas metrics: a multi-model analysis. *Atmos. Chem. Phys.* 13, 2793–2825. doi: 10.5194/acp-13-2793-2013

Katavouta, A., Williams, R. G., Goodwin, P., and Roussenov, V. (2018). Reconciling atmospheric and oceanic views of the transient climate response to emissions. *Geophys. Res. Lett.* 45, 6205–6214. doi: 10.1029/2018GL077849

Keller, D. P., Feng, E. Y., and Oschlies, A. (2014). Potential climate engineering effectiveness and side effects during a high carbon dioxide-emission scenario. *Nat. Commun.* 5:3304. doi: 10.1038/ncomms4304

Keller, D. P., Lenton, A., Scott, V., Vaughan, N. E., Bauer, N., Ji, D., et al. (2018). The carbon dioxide removal model intercomparison project (CDRMIP): rationale and experimental protocol for CMIP6. *Geosci. Model Dev.* 11, 1133–1160. doi: 10.5194/gmd-11-1133-2018

Köhler, P. (2016). Using the Suess effect on the stable carbon isotope to distinguish the future from the past in radiocarbon. *Environ. Res. Lett.* 11:124016. doi: 10.1088/1748-9326/11/12/124016

Köhler, P., Abrams, J. F., Völker, C., Hauck, J., and Wolf-Gladrow, D. A. (2013). Geoengineering impact of open ocean dissolution of olivine on atmospheric CO_2, surface ocean pH and marine biology. *Environ. Res. Lett.* 8:014009. doi: 10.1088/1748-9326/8/1/014009

Köhler, P., and Fischer, H. (2006). Simulating low frequency changes in atmospheric CO_2 during the last 740,000 years. *Clim. Past* 2, 57–78. doi: 10.5194/cp-2-57-2006

Köhler, P., Fischer, H., Munhoven, G., and Zeebe, R. E. (2005). Quantitative interpretation of atmospheric carbon records over the last glacial termination. *Glob. Biogeochem. Cycles* 19:GB4020. doi: 10.1029/2004GB002345

Köhler, P., Fischer, H., and Schmitt, J. (2010a). Atmospheric $\delta^{13}CO_2$ and its relation to pCO_2 and deep ocean $\delta^{13}C$ during the late Pleistocene. *Paleoceanography* 25:PA1213. doi: 10.1029/2008PA001703

Köhler, P., Hartmann, J., and Wolf-Gladrow, D. A. (2010b). Geoengineering potential of artificially enhanced silicate weathering of olivine. *Proc. Natl. Acad. Sci. U.S.A.* 107, 20228–20233. doi: 10.1073/pnas.1000545107

Köhler, P., Hauck, J., Völker, C., and Wolf-Gladrow, D. (2015). Interactive comment on *A simple model of the anthropogenically forced CO_2 cycle* by W. Weber et al. *Earth Syst. Dyn. Discuss.* 6:C813. Available online at: http://www.earth-syst-dynam-discuss.net/6/C813/2015/esdd-6-C813-2015.pdf

Köhler, P., and Munhoven, G. (2020). Late Pleistocene carbon cycle revisited by considering solid Earth processes. *Paleoceanogr. Paleoclimatol.* e2020PA004020. doi: 10.1029/2020PA004020. [Epub ahead of print].

Köhler, P., Nehrbass-Ahles, C., Schmitt, J., Stocker, T. F., and Fischer, H. (2017). A 156 kyr smoothed history of the atmospheric greenhouse gases CO_2, CH_4, and N_2O and their radiative forcing. *Earth Syst. Sci. Data* 9, 363–387. doi: 10.5194/essd-9-363-2017

Körtzinger, A., Hedges, J. I., and Quay, P. D. (2001). Redfield ratios revisited: removing the biasing effect of anthropogenic CO_2. *Limnol. Oceanogr.* 46, 946–970. doi: 10.4319/lo.2001.46.4.0964

Le Quéré, C., Andrew, R. M., Friedlingstein, P., Sitch, S., Hauck, J., Pongratz, J., et al. (2018). Global carbon budget 2018. *Earth Syst. Sci. Data* 10, 2141–2194. doi: 10.5194/essd-10-2141-2018

Lenton, A., Matear, R. J., Keller, D. P., Scott, V., and Vaughan, N. E. (2018). Assessing carbon dioxide removal through global and regional ocean alkalinization under high and low emission pathways. *Earth Syst. Dyn.* 9, 339–357. doi: 10.5194/esd-9-339-2018

Liu, W., Xie, S.-P., Liu, Z., and Zhu, J. (2017). Overlooked possibility of a collapsed Atlantic Meridional Overturning Circulation in warming climate. *Sci. Adv.* 3:e1601666. doi: 10.1126/sciadv.1601666

Lord, N. S., Ridgwell, A., Thorne, M. C., and Lunt, D. J. (2016). An impulse response function for the long tail of excess atmospheric CO_2 in an earth system model. *Glob. Biogeochem. Cycles* 30, 2–17. doi: 10.1002/2014GB005074

MacDougall, A. H. (2016). The transient response to cumulative CO_2 emissions: a review. *Curr. Clim. Change Rep.* 2, 39–47. doi: 10.1007/s40641-015-0030-6

MacDougall, A. H. (2017). The oceanic origin of path-independent carbon budgets. *Sci. Rep.* 7:10373. doi: 10.1038/s41598-017-10557-x

Meinshausen, M., Smith, S., Calvin, K., Daniel, J., Kainuma, M., Lamarque, J.-F., et al. (2011). The RCP greenhouse gas concentrations and their extensions from 1765 to 2300. *Clim. Change* 109, 213–241. doi: 10.1007/s10584-011-0156-z

Meinshausen, M., Vogel, E., Nauels, A., Lorbacher, K., Meinshausen, N., Etheridge, D., et al. (2017). Historical greenhouse gas concentrations for climate modelling (CMIP6). *Geosci. Model Dev.* 10, 2057–2116. doi: 10.5194/gmd-10-2057-2017

Munhoven, G. (1997). *Modelling glacial-interglacial atmospheric CO_2 variations: the role of continental weathering* (Ph.D. thesis), Université de Liège, Liège, Belgium. Available online at: http://hdl.handle.net/2268/161314

Munhoven, G., and François, L. M. (1996). Glacial-interglacial variability of atmospheric CO_2 due to changing continental silicate rock weathering: a model study. *J. Geophys. Res.* 101, 21423–21437. doi: 10.1029/96JD01842

Myhre, G., Highwood, E. J., Shine, K. P., and Stordal, F. (1998). New estimates of radiative forcing due to well mixed greenhouse gases. *Geophys. Res. Lett.* 25, 2715–2718. doi: 10.1029/98GL01908

O'Neill, B. C., Tebaldi, C., van Vuuren, D. P., Eyring, V., Friedlingstein, P., Hurtt, G., et al. (2016). The scenario model intercomparison project (ScenarioMIP) for CMIP6. *Geosci. Model Dev.* 9, 3461–3482. doi: 10.5194/gmd-9-3461-2016

Pacala, S., and Socolow, R. (2004). Stabilization wedges: solving the climate problem for the next 50 years with current technologies. *Science* 305, 968–972. doi: 10.1126/science.1100103

Prieto, F. J. M., and Millero, F. J. (2002). The values of pK_1 + pK_2 for the dissolution of carbonic acid in seawater. *Geochim. Cosmochim. Acta* 66, 2529–2540. doi: 10.1016/S0016-7037(02)00855-4

Retallack, G. J., and Conde, G. D. (2020). Deep time perspective on rising atmospheric CO_2. *Glob. Planet. Change* 189:103177. doi: 10.1016/j.gloplacha.2020.103177

Riahi, K., van Vuuren, D. P., Kriegler, E., Edmonds, J., O'Neill, B. C., Fujimori, S., et al. (2017). The shared socioeconomic pathways and their energy, land use, and greenhouse gas emissions implications: an overview. *Glob. Environ. Change* 42, 153–168. doi: 10.1016/j.gloenvcha.2016.05.009

Rogelj, J., Forster, P. M., Kriegler, E., Smith, C. J., and Séférian, R. (2019). Estimating and tracking the remaining carbon budget for stringent climate targets. *Nature* 571, 335–342. doi: 10.1038/s41586-019-1368-z

Sarmiento, J. L., Dunne, J., Gnanadesikan, A., Key, R. M., Matsumoto, K., and Slater, R. (2002). A new estimate of the $CaCO_3$ to organic carbon export ratio. *Glob. Biogeochem. Cycles* 16:1107. doi: 10.1029/2002GB001919

Schlitzer, R. (2000). "Applying the adjoint method for biogeochemical modelling: export of particulate organic matter in the world ocean," in *Inverse Methods in Global Biogeochemical Cycles, Vol. 114 of Geophysical Monographs*, eds P. Kasibhatla, M. Heimann, P. Rayner, N. Mahowald, R. G. Prinn, and D. E. Hartley (Washington, DC: AGU), 107–124. doi: 10.1029/GM114p0107

Seshadri, A. K. (2017). Origin of path independence between cumulative CO_2 emissions and global warming. *Clim. Dyn.* 49, 3383–3401. doi: 10.1007/s00382-016-3519-3

Sherwood, S., Webb, M. J., Annan, J. D., Armour, K. C., Forster, P. M., Hargreaves, J. C., et al. (2020). An assessment of Earth's climate sensitivity using multiple lines of evidence. *Rev. Geophys.* 58:e2019RG000678. doi: 10.1029/2019RG000678

Storelvmo, T., Leirvik, T., Lohmann, U., Phillips, P. C. B., and Wild, M. (2016). Disentangling greenhouse warming and aerosol cooling to reveal Earth's climate sensitivity. *Nat. Geosci.* 9, 286–289. doi: 10.1038/ngeo2670

The Royal Society (2018). *Greenhouse Gas Removal*. London: The Royal Society. Available online at: http://royalsociety.org/greenhouse-gas-removal

Tokarska, K. B., Gillett, N. P., Weaver, A. J., Arora, V. K., and Eby, M. (2016). The climate response to five trillion tonnes of carbon. *Nat. Clim. Change* 6, 851–855. doi: 10.1038/nclimate3036

Weiss, R. F. (1974). Carbon dioxide in water and seawater: the solubility of a non-ideal gas. *Mar. Chem.* 2, 203–215. doi: 10.1016/0304-4203(74)90015-2

Williams, R. G., Roussenov, V., Goodwin, P., Resplandy, L., and Bopp, L. (2017). Sensitivity of global warming to carbon emissions: effects of heat and carbon uptake in a suite of earth system models. *J. Clim.* 30, 9343–9363. doi: 10.1175/JCLI-D-16-0468.1

Zeebe, R. E. (2012). LOSCAR: Long-term Ocean-atmosphere-Sediment CArbon cycle Reservoir Model v2.0.4. *Geosci. Model Dev.* 5, 149–166. doi: 10.5194/gmd-5-149-2012

Zeebe, R. E., and Wolf-Gladrow, D. A. (2001). *CO_2 in Seawater: Equilibrium, Kinetics, Isotopes, Vol. 65 of Elsevier Oceanography Book Series*. Amsterdam: Elsevier Science Publishing.

Conflict of Interest: The author declares that the research was conducted in the absence of any commercial or financial relationships that could be construed as a potential conflict of interest.

frontiers in Climate

PERSPECTIVE
published: 21 December 2020
doi: 10.3389/fclim.2020.594194

Public Perceptions of Ocean-Based Carbon Dioxide Removal: The Nature-Engineering Divide?

*Christine Bertram and Christine Merk**

Research Center Global Commons and Climate Policy, Kiel Insitute for the World Economy, Kiel, Germany

Public acceptability is a standard element on the list of potential constraints on research and deployment of ocean-based carbon dioxide removal (CDR). We outline past work on the public perceptions and acceptability of ocean-based CDR among laypersons covering the main developments over the past 15 years. We compare and synthesize insights from two distinct strands of literature – one on climate engineering approaches and the other on coastal ecosystem management or blue carbon approaches. We also draw conclusions from studies on land-based CDR for emerging ocean-based approaches. Main determinants of perceptions identified in the past are controllability, environmental impacts, containment, permanence of carbon storage, risks and benefits for the local population as well as to which degree an approach is perceived as natural or engineered. We highlight how these aspects may influence perceptions and acceptability of ocean-based CDR approaches which have not yet been on the agenda of perceptions research. Even though ocean-based CDR approaches cannot be neatly divided into categories, the public's tendency to favor approaches perceived more as natural over approaches perceived more as engineering could result in a dilemma between approaches with possibly high carbon sequestration potential but low levels of acceptability and approaches with possibly low sequestration potential but high levels of acceptability. To effectively work toward achieving net-zero carbon emissions by mid-century, however, we need to bridge the gap between natural and engineering-type approaches, also in research, to come up with a broad portfolio of CDR options to complement classic mitigation and adaptation measures.

Keywords: public perception, ocean-based carbon dioxide removal (CDR), climate engineering, nature-based solution, blue carbon, acceptance, negative emission technology, naturalness

OPEN ACCESS

Edited by:
Kerryn Brent,
University of Adelaide, Australia

Reviewed by:
Emily Margaret Cox,
Cardiff University, United Kingdom
Jesse L. Reynolds,
University of California, Los Angeles, United States

***Correspondence:**
Christine Merk
christine.merk@ifw-kiel.de

Specialty section:
This article was submitted to Negative Emission Technologies, a section of the journal Frontiers in Climate

Received: *12 August 2020*
Accepted: *30 November 2020*
Published: *21 December 2020*

Citation:
Bertram C and Merk C (2020) Public Perceptions of Ocean-Based Carbon Dioxide Removal: The Nature-Engineering Divide? Front. Clim. 2:594194. doi: 10.3389/fclim.2020.594194

INTRODUCTION

Intentionally removing carbon dioxide from the atmosphere will be important to achieve net-zero emissions by mid-century and to limit global warming to 1.5°C by 2100. However, the climate change mitigation pathways that include negative emissions via carbon dioxide removal (CDR) are still largely restricted to the land-based approaches afforestation and bioenergy with carbon capture and storage (IPCC, 2018). Relying on the large-scale deployment of these approaches, for example as monoculture plantations, would exacerbate land-use competition, nitrogen pollution, and biodiversity loss (Smith et al., 2019). Portfolios of many different approaches would thus

increase the feasibility and sustainability of CDR as trade-offs and side-effects vary between methods and scale matters (IPCC, 2018; Smith et al., 2019). As the ocean is the largest natural carbon sink, ideas to (artificially) enhance carbon uptake and storage via ocean iron fertilization or direct injection of CO_2 into the deep ocean have already been discussed in the 1990s and early 2000s (GESAMP, 2019). These approaches have often been categorized as geoengineering or climate engineering. More recently, the potential of blue carbon or coastal ecosystem management, i.e., the conservation and restoration of mangroves, salt marshes and seagrass meadows, for carbon sequestration and thus for combating climate change has been put on the political as well the research agenda (Hoegh-Guldberg et al., 2019a,b). These approaches are often categorized as nature-based solutions.

Public acceptability ranks highly on the list of potential constraints on CDR deployment (Fuss et al., 2014; IPCC, 2018; GESAMP, 2019; Rickels et al., 2019). In an expert survey, earth system modelers and integrated assessment modelers perceived political and public acceptability on average as the strongest constraint on the feasibility of ocean iron fertilization, alkalinity enhancement, and artificial upwelling followed by cost effectiveness. In contrast, they only saw it as a weak constraint on blue carbon management (Rickels et al., 2019). This assessment of the role of public acceptability might partly be fueled by past protests against research projects such as LOHAFEX on ocean iron fertilization in the Southern Ocean (Schiermeier, 2009a,b) and SPICE on stratospheric aerosol injection in the UK (Pidgeon et al., 2013), proposals for CO_2-injection off the coast of Hawaii and Norway (Gewin, 2002; Giles, 2002; Figueiredo et al., 2003; Scott, 2006) or the ocean fertilization project by the Haida Salmon Restoration Corporation in international waters off the Canadian west coast (Tollefson, 2017; Gannon and Hulme, 2018).

Our perspective summarizes the research on the perceptions and acceptability of ocean-based CDR options among laypersons covering the main developments over the past 15 years. We compare and synthesize the insights from two distinct strands of literature – one on approaches often labeled as climate engineering and the other on blue carbon management often labeled as a nature-based solution. The main determinants of acceptability of CDR options we identify are the perception of benefits and risks for the local population, environmental impacts, permanence of carbon storage, controllability, containment and naturalness. We argue that ocean-based approaches that include a release of materials into the ocean are less accepted than land-based approaches as their impact is not contained but can potentially spread out through the ocean constituting a global common. Diverging interests between local and global populations should be addressed by political actors via the installation of trustworthy institutions and well-designed management schemes. There is a rift in the acceptability between approaches that are perceived as natural, i.e., blue carbon management, and approaches that are perceived as climate engineering that is also driven by their perceived naturalness. We argue that this could result in a polarization between ocean-based CDR approaches with high carbon sequestration potential but a low level of acceptability and ocean-based CDR approaches with a low sequestration potential but a high level of acceptability, severely limiting the available options for portfolios of CDR approaches. However, this divide should be bridged to achieve net-zero.

LITERATURE REVIEW

In this perspective, we focus on public perceptions of ocean-based CDR approaches drawing on studies directly covering specific approaches (e.g., iron fertilization and mangrove conservation and restoration) and comparable approaches for which very few or no specific studies exist yet (e.g., enhanced weathering on land for ocean alkalinization; mangroves for seagrass; see **Table 1**).

We identify two perspectives on perceptions of ocean-based CDR that are rooted in different interdisciplinary research communities. One perspective is centered on the goal of carbon removal looking at methods like iron fertilization and alkalinity enhancement which tend to be categorized as climate engineering and have mainly been explored in global earth system models (Keller et al., 2018). Perceptions studies in this context have looked at CDR from a *global commons perspective* in the sense that participants mainly assessed the options based on their impact on global atmospheric CO_2-concentrations and environmental impacts on the oceans. *Local perspectives* of directly affected populations are missing—with the exception of the case study on the Haida Salmon Restoration Project (Gannon and Hulme, 2018)—as it remains very hypothetical who would be directly affected by the deployment of these CDR options.

The other perspective centers on ecosystem services (ES) and local field studies of blue carbon management and has only recently started to incorporate carbon uptake. CDR options such as blue carbon management are categorized as nature-based solutions (Hoegh-Guldberg et al., 2019a). The large body of literature on the perceptions and attitudes toward coastal blue carbon management takes an exclusively *local perspective* and analyses the perceptions and attitudes of the directly affected local population. The *global commons perspective* is not present in these studies with the exception of relatively recent ones (e.g., Arumugam et al., 2020).

Public Perceptions of Climate-Engineering Type Approaches

There are only a few studies on the public perceptions of ocean-based CDR options that come from the climate engineering context, namely a few large-N surveys that include ocean fertilization or alkalinitiy enhancement (Ipsos MORI, 2010; Leiserowitz et al., 2010; Jobin and Siegrist, 2020) and several small-N studies on the perception of direct ocean injection or ocean iron fertilization (Palmgren et al., 2004; Itaoka et al., 2009; Bostrom et al., 2012; Amelung and Funke, 2015; Gannon and Hulme, 2018; Shrum et al., 2020). The approaches that have not yet received a lot of attention in natural science research, such as artificial down- or upwelling, biomass dumping or ocean alkalinity enhancement, have not yet been covered by perceptions research either (see **Table 1**).

TABLE 1 | Overview of public perceptions research on ocean-based CDR approaches and other relevant studies.

	General description	Studies on the perceptions of the approach, comparable approaches or components of the approach
Direct injection or dissolution	Inject liquid CO_2 directly into the mid/deep ocean or the seabed. The dissolved inorganic carbon (DIC) will remain isolated from the atmosphere for centuries or longer depending on ocean circulation/ventilation at the location of injection.[b]	Palmgren et al. (2004), Itaoka et al. (2009)
Ocean fertilization	Add micronutrients like iron or macronutrients like nitrogen and phosphorus to increase phytoplankton growth (CO_2 fixation) and ocean carbon storage via the biological pump (the transport of this fixed carbon into the deep ocean).[a]	Ipsos MORI (2010), Leiserowitz et al. (2010), Bostrom et al. (2012), Amelung and Funke (2015), Gannon and Hulme (2018), Jobin and Siegrist (2020), Shrum et al. (2020)
Ocean alkalinization	Increase the alkalinity of the upper ocean to chemically increase the carbon storage capacity of seawater and thus, also increase CO_2 uptake.[a]	Ipsos MORI (2010) *Enhanced weathering on land:* Wright et al. (2014), Carlisle et al. (2020), Cox et al. (2020), Shrum et al. (2020)
Artificial upwelling or downwelling	Use pipes or other methods to pump nutrient rich deep ocean water to the surface where it has a fertilizing effect (upwelling)[a]; pump down surface waters saturated in CO_2 into the ocean interior to enhance the solubility pump of carbon (downwelling).[b]	–
Direct CO_2 removal from seawater with CCS	Remove DIC from the ocean and transport it to sites for long-term storage as for other CCS-schemes. The subsequent return to equilibrium between the ocean and the atmosphere will involve absorption of CO_2 from the atmosphere.[b]	*Only studies on CCS, for a recent overview see* Paluszny et al. (2020)
Terrestrial biomass dumping	Sink bales of crop residues in the deep oceans or off the deltas of major rivers.[b]	–
Marine biomass for biochar or bioenergy	Use marine biomass to fuel biomass energy with CCS (BECCS) on land or use such biomass to produce biochar as a soil additive.[c]	*Only studies on Bioenergy with CCS, for a recent overview see* Thomas et al. (2018)
Blue carbon management	Conserve and restore coastal ecosystems such as mangroves, salt marshes, and seagrass meadows to maintain or enhance carbon storage in biomass and soils.[d]	*No studies on seagrass* *Mangroves:* e.g., Rönnbäck et al. (2007), Badola et al. (2012), Roy (2016); *salt marshes:* e.g., Liski et al. (2019) and Curado et al. (2014)

a Description taken from Keller et al. (2018).
b Description based on GESAMP (2019).
c Description based on Gattuso et al. (2018).
d Description based on Hoegh-Guldberg et al. (2019a).

Direct injection of CO_2 was evaluated very negatively compared to technologies that lower emissions such as energy from renewable sources or energy efficiency increases (Palmgren et al., 2004). Direct injection and dissolution were also perceived less favorably compared to geological storage, i.e., CCS (Palmgren et al., 2004; Itaoka et al., 2009). Participants in focus groups perceived deep-ocean injection as harmful for the marine environment and its permanence as uncertain, thus, they evaluated it unfavorably (Gough et al., 2002). Respondents with stronger pro-environmental attitudes, such as the perception of nature as being fragile or the rejection of anthropocentrism, perceived deep-ocean injection more negatively (Palmgren et al., 2004).

For ocean fertilization, studies in the US show that 64% of Americans did not believe or did not know whether it would actually help against climate change (Leiserowitz et al., 2010). It is perceived more negatively compared to any land-based CDR such as afforestation or direct air capture (Ipsos MORI, 2010; Jobin and Siegrist, 2020). In comparative studies, the perceptions of ocean fertilization are similar to the perceptions of stratospheric aerosol injection: the level of support is low (Ipsos MORI, 2010; Jobin and Siegrist, 2020) and the perceived risks are high (Amelung and Funke, 2015).

In an early study (Bostrom et al., 2012), ocean fertilization—unlike afforestation—was not perceived as a natural solution but as an engineering solution, falling into the same category as stratospheric aerosol injection and nuclear energy. Approaches in the engineering category were favored by respondents that believed more strongly in the controllability of climate change, saw a moral responsibility to fight climate change, and were more likely to believe that climate change was not caused by carbon emissions but by volcanic eruptions (Bostrom et al., 2012).

Thus, the general finding that CDR options are perceived more positively compared to solar radiation management approaches like stratospheric aerosol injection (Wright et al., 2014; Carlisle et al., 2020) has so far not been confirmed for ocean fertilization and ocean dilution approaches; and it might not hold for ocean alkalinization either.

In the only study on ocean alkalinity enhancement so far, the majority of participants in a public dialogue in the UK were not supportive of the idea (Ipsos MORI, 2010). In focus groups on the perceptions of enhanced weathering on land, participants rejected it especially because of the environmental impacts they perceived downstream for the oceans and related to the necessary large-scale mining (Cox et al., 2020) – both factors also pertain to ocean alkalinization. Comparing further the application of onshore and offshore options, we find only small differences for geological CO_2-storage. Studies showed either a small positive effect for offshore storage (Itaoka et al., 2009; Schumann et al., 2014) or no substantial difference (Gough et al., 2002; Upham and Roberts, 2011). There is thus little support for the notion that ocean-based methods might be perceived more positively just because they are farther away. In contrast, the importance of the link between enhanced weathering and the oceans implies that the preservation of the marine environment is a very salient issue.

Local Perceptions of the Restoration and Conservation of Blue Carbon Ecosystems

There is a large literature on the attitudes and perceptions of local communities and other stakeholders toward mangrove management mostly based on surveys (e.g., Badola et al., 2012), semi-structured interviews (e.g., López-Medellín et al., 2011), and, more recently, the Q-methodology (Hugé et al., 2016; Vande Velde et al., 2019; Arumugam et al., 2020). Also for salt marshes, there is a quite substantial body of literature on attitudes toward conservation and restoration of salt marshes, again mostly using surveys and/or semi-structured interviews with the local public.

In studies on mangroves, the multifaceted interaction between people's dependence on the ecosystem and their attitudes toward and preferences for ecosystem conservation and restoration becomes obvious. Here, we can only sketch the most important interlinkages, for a much deeper discussion of the complex social-ecological interactions surrounding mangrove conversion, conservation, and restoration see e.g., Srivastava and Mehta (2017). Most notably, people value in particular the ES that are directly relevant for sustaining their livelihoods such as the provision of timber, fuelwood, tannin, honey, beeswax, fodder, and thatch (e.g., Roy, 2016). People that rely on non-extractive uses of mangrove forests highly value ES such as storm protection and the provision of nursery habitats and are often more in favor of mangrove conservation and restoration (Stone et al., 2008; López-Medellín et al., 2011; Badola et al., 2012). In contrast, people that rely more on extractive uses would more often object to a total closure for the protection of mangrove forests, a trend which is enforced if potential disservices from mangrove forests are considered (e.g., Badola et al., 2012; Roy, 2016).

Attitudes toward mangrove conservation and restoration also vary with the socio-demographic background of the respondents, i.e., gender (Rönnbäck et al., 2007; Badola et al., 2012), education level, awareness of mangrove loss and provided ES (Badola et al., 2012; Rahman and Asmawi, 2016; Roy, 2016). In this context, a higher level of education seems to be related to a higher awareness of conservation issues (Badola et al., 2012). Moreover, there is some recent evidence that the socio-cultural background also influences attitudes toward mangrove conservation and restoration with urban populations focusing more strongly on recreational ES (Vande Velde et al., 2019). However, differences in perceptions can also be explained by the degree to which a community feels attached and connected to nature, with communities living in close contact to nature highly valuing conservation (Queiroz et al., 2017). Another important factor influencing acceptability of conservation is the way in which management is implemented and benefit sharing schemes are designed (Ha et al., 2012).

For salt marshes, similar but varying factors have been found to influence attitudes and perceptions. For example, possibilities for public access particularly increase the likelihood of accepting restoration or conservation measures. Moreover, socio-demographics influence perceptions with, for example, women and higher-income individuals favoring conservation over restoration (Bauer et al., 2004). Visual aspects such as bright coloring of plants and higher diversity of tones of color but also the reduction of visible garbage positively influence perceptions (Casagrande, 1997; Curado et al., 2014). Similarly, more education about and higher awareness of the ecological functions increase acceptance (Ibrahim et al., 2012), while expected economic losses from proposed policy measures can lead to lower acceptance levels (Liski et al., 2019).

There is, however, much less literature on attitudes and perceptions toward the conservation and restoration of seagrass meadows, and seagrass is often not considered in coastal management decisions (Grech et al., 2012; Nordlund et al., 2014). Nordlund et al. (2018) gathered the impression from expert workshop that the public seems to be mostly unaware of seagrasses in general and the ES they provide in particular. Jefferson et al. (2014) underscore this by finding that the ecologically most valuable species, including three plant species, were considered least interesting in a survey on public perceptions of coastal ecosystems in the UK, reflecting the low appeal of plants compared to animals (Wandersee and Schussler, 2001).

THE IMPLICATIONS OF PUBLIC ACCEPTABILITY FOR THE FEASIBILITY OF OCEAN-BASED CDR APPROACHES

The two strands of perceptions research on CDR options have so far almost exclusively either taken a *global commons perspective* for climate-engineering type approaches or a *local perspective* for blue carbon approaches. Bringing in the missing perspective will

add further complexity to the issue: the global interest to preserve or expand areas for blue carbon ecosystems to increase carbon uptake or deploy, for example, alkalinity enhancement might clash with the perceptions and needs of the local population that socially and economically depends on the coastal ecosystems. We know that blue carbon management can be attractive for the *local* population, if the people, directly or indirectly, benefit from the conservation and/or restoration of coastal ecosystems and their basic needs are not threatened. Public opposition to blue carbon approaches could, for example, occur when there are local conflicts around the use of land and resources for mangrove forests and salt marshes (e.g., Myatt et al., 2003; West, 2010). Furthermore, there is no clear case as to whether opposition predominantly comes from local or global actors – such as non-local population, (inter)national NGOs or experts. For example, the development of CCS in Germany faced strong local opposition (Dütschke, 2011). The Haida Salmon Restoration Project evoked polarized views among locals, support from non-locals with business interests and opposition from (inter-)national NGOs and researchers (Gannon and Hulme, 2018).

There is, however, one overarching factor that is indispensable for broad acceptance, both on the local and on the global level: trust in institutions and governance will be crucial for the acceptability of research from the *global perspective* like it is from the *local perspective*. Local support can be strengthened if the management regime is well designed and trust in local institutions and the provision of compensations is high (e.g., Stone et al., 2008; Badola et al., 2012; Roy, 2016; Liski et al., 2019). For CCS, it has also been shown that trust in institutions influences perceptions positively (L'Orange Seigo et al., 2014; Braun et al., 2018; Paluszny et al., 2020).

The distinction between *local* and *global* is not just a matter of geographic closeness and direct affectedness but also of (perceived) containment and control of environmental impacts. Participants in deliberative workshops listed controllability of climate engineering approaches as an important factor for their assessment (Ipsos MORI, 2010; Pidgeon et al., 2013). Thus, one factor of concern about ocean fertilization in the context of the Haida Salmon Restoration Project was the lack of control when materials are released into the ocean which is perceived as a dynamic and interconnected system. The study participants that loaded high on that factor in the Q-sort acknowledged the need to act against climate change but would have preferred contained climate engineering approaches. Afforestation or direct air capture, where no materials are released into the wider environment, would count as such approaches, while alkalinity enhancement would not (referred to as encapsulation in Royal Society, 2009). For blue carbon approaches, these considerations would imply that the conservation and restoration of coastal ecosystems can be expected to have a high level of acceptability from a *global commons perspective* as is the case for afforestation on land (Ipsos MORI, 2010; Braun et al., 2018; Jobin and Siegrist, 2020).

The distinction between *global* and *local* gets a little more blurred if we widen the scope and look at perceptions of climate engineering options research carried out in non-Western contexts with groups of people that are already experiencing negative impacts of climate change. For example, Gannon and Hulme (2018) reported a sense of urgency to take actions against climate change and threats to the marine environment that mobilized parts of the Haida community to support the ocean fertilization project. At the same time, members of the local First Nations community felt the experiment was a morally wrong intervention into nature and felt powerless against decisions of "global people" (Gannon and Hulme, 2018, p. 12). Similar ambiguity was reported by Carr and Yung (2018) who found that populations vulnerable to climate change would accept climate engineering due to the severe impacts of climate change they are already experiencing. This acceptability, however, was characterized as being "both deeply reluctant and highly conditional." Similar to findings in Winickoff et al. (2015), participants interviewed by Carr and Yung (2018) feared that climate engineering was employed as a quick fix by the Western countries without addressing the real causes of climate change. Strengthening commitments to existing efforts to reduce greenhouse gas emissions by the Western countries was thus one major condition for acceptability. In the context of blue carbon management, the increasing awareness of climate change and the potential of coastal ecosystems to contribute to carbon sequestration could induce even stronger preferences for the conservation of these ecosystems to halt further losses among the local population (Tuan et al., 2014; Arumugam et al., 2020).

In addition to the factors described already, perceived naturalness of CDR options influences acceptability. In particular, labeling CDR options as natural increases acceptability and attaches the meaning of nature as pure, permanent and balanced if left alone, while unnatural bears the connotation of immoral and dangerous (Hansen, 2006). For blue carbon management, local people's attachment and connectedness to nature can be observed to influence perceptions of conservation favorably (Queiroz et al., 2017). For land-based CDR approaches, there is an implicit hierarchy in perceptions where seemingly more natural solutions are prioritized over approaches that are perceived as engineering (Merk et al., 2019). Bio-energy with CCS and enhanced weathering are perceived less favorably compared to biochar or afforestation (Merk et al., 2019; Wolske et al., 2019; Carlisle et al., 2020; Cox et al., 2020). Study participants that perceived approaches as unnatural or as tampering with nature evaluated them more negatively (Corner et al., 2013; Wolske et al., 2019).

However, the categorization of approaches into nature-based solutions and climate engineering seems somewhat arbitrary. Bellamy and Osaka (2020) used ocean alkalinization as an example to show that the concept of nature-based CDR is not a definite characteristic of any method but is rather constructed: the process enhances a natural process in the otherwise (relatively) untouched natural marine environment. What is considered natural depends on time, geography, and culture. Naturalness is thus socially constructed. Corner and Pidgeon (2014) showed that framing direct air capture as artificial trees compared to presenting them in a very technical way resulted in more positive views. Framing something as natural or unnatural can thus be a powerful tool in any public debate

to steer the desirability of approaches (Demeritt, 2002; Hansen, 2006; Bellamy and Osaka, 2020) even though all options require human action or intervention and are neither fully natural nor unnatural (Bellamy and Osaka, 2020).

WHAT THE FUTURE MIGHT BRING FOR OCEAN-BASED CDR

It is yet somewhat unclear what the actual carbon removal potential of scaled up deployment of any of the ocean-based CDR options would be. Based on modeling studies (Ilyina et al., 2013; Keller et al., 2014), a recent comprehensive review found that ocean alkalinization applied at the global scale is the CDR method that stands out as having by far the highest potential to increase ocean carbon uptake with practically permanent storage but potentially substantial environmental side-effects (Gattuso et al., 2018). Compared to this theoretically high potential, the sequestration potential of conserving and restoring coastal ecosystems on a global scale is limited even though it would also be permanent if the ecosystems were sufficiently protected. However, Gattuso et al. (2018) rate the carbon sequestration potential of conserving and restoring coastal ecosystems as comparable to that of ocean fertilization carried out at the global scale, but the carbon taken up by the ocean via ocean fertilization would outgas back to the atmosphere over decades to centuries.

The insights from perceptions research presented in this perspective in combination with insights from Gattuso et al. (2018) highlight one important aspect related to the implementation of CDR measures and the goal of reaching net-zero CO_2 emissions by mid-century: there is no silver bullet for reaching net-zero by 2050 in the sense that we will probably not be able to find the one measure that has a high carbon sequestration potential, high levels of perceived naturalness and low environmental side effects. While nature-based solutions with potentially higher levels of acceptance can contribute to a portfolio of measures counteracting climate change, other measures with potentially lower acceptance and/or larger detrimental environmental side effects will likely still be needed to reach international climate goals. This in particular holds since ecosystem restoration, particularly for seagrass ecosystems or open ocean ecosystems, is still in its infancy (Franke et al., 2020) even though conservation of coastal ecosystems and restoration of mangroves are well-established practices. Moreover, coastal ecosystems are themselves under threat due to anthropogenic pressures arising e.g., from eutrophication and climate change (Macreadie et al., 2019; Lovelock and Reef, 2020). A deepening polarization between climate engineering approaches and nature-based solutions could lead to "ideologically-motivated pushback" (Colvin et al., 2020, p. 28) against certain CDR options independently of actual risks and benefits. An upfront exclusion of many ocean-based approaches would severely hamper the feasibility of balanced CDR portfolios.

Summing up, public perceptions will likely play a big role for the feasibility of research and eventual deployment of ocean-based CDR. Important determinants will be to which degree they are perceived as natural, controllable, permanent, and beneficial both for local communities and not directly affected publics. The challenge for future (perceptions) research will be to specify more precisely who is affected by the deployment of CDR in what ways and to which degree people would actually feel affected. This will be crucial to identify potential constraints on the implementation of CDR options from the *global commons perspective* and the *local perspective* on risks and side effects. Depending on the approach, the benefits and side-effects are local and global, on land, at the coast, or in the open ocean. A good example are the impacts of large-scale mining efforts that would be necessary for alkalinity enhancement. Thus, perceptions along the entire process-chain of not just one approach but a portfolio of land- and ocean-based approaches will have to be disentangled.

DATA AVAILABILITY STATEMENT

The original contributions presented in the study are included in the article/supplementary material, further inquiries can be directed to the corresponding author/s.

AUTHOR CONTRIBUTIONS

CM had the initial idea and especially wrote the parts on climate engineering approaches. CB and CM contributed equally to developing the concept and writing the text. CB especially wrote the parts on coastal blue carbon approaches. All authors contributed to the article and approved the submitted version.

FUNDING

CM acknowledges funding from the European Union's Horizon 2020 research and innovation programme under grant agreement No 869357. CB acknowledges funding from Kiel Marine Science (KMS) - Centre for Interdisciplinary Marine Science at Kiel University (G1912 Economic assessments of coastal blue carbon ecosystems - ECOBLUE). CB further acknowledges funding for the research project SeaStore (Diversity Enhancement Through Seagrass Restoration) from the German Federal Ministry of Education and Research under grant agreement number 03F0859E. The publication of this article was funded by the Open Access Fund of the Leibniz Association.

REFERENCES

Amelung, D., and Funke, J. (2015). Laypeople's risky decisions in the climate change context: climate engineering as a risk-defusing strategy? *Hum. Ecol. Risk Asses. Int. J.* 21, 533–559. doi: 10.1080/10807039.2014.932203

Arumugam, M., Niyomugabo, R., Dahdouh-Guebas, F., and Hugé, J. (2020). The perceptions of stakeholders on current management of mangroves in the Sine-Saloum Delta, Senegal. *Estuar. Coast. Shelf Sci.* 247:106751. doi: 10.1016/j.ecss.2020.106751

Badola, R., Barthwal, S., and Hussain, S. A. (2012). Attitudes of local communities towards conservation of mangrove forests: A case study from the east coast of India. *Estuar. Coast. Shelf Sci.* 96, 188–196. doi: 10.1016/j.ecss.2011.11.016

Bauer, D. M., Cyr, N. E., and Swallow, S. K. (2004). Public preferences for compensatory mitigation of salt marsh losses: a contingent choice of alternatives. *Conserv. Biol.* 18, 401–411. doi: 10.1111/j.1523-1739.2004.00367.x

Bellamy, R., and Osaka, S. (2020). Unnatural climate solutions? *Nat. Clim. Change* 10, 98–99. doi: 10.1038/s41558-019-0661-z

Bostrom, A., O'Connor, R. E., Böhm, G., Hanss, D., Bodi, O., Ekström, F., et al. (2012). Causal thinking and support for climate change policies: international survey findings. *Glob. Environ. Change* 22, 210–222. doi: 10.1016/j.gloenvcha.2011.09.012

Braun, C., Merk, C., Pönitzsch, G., Rehdanz, K., and Schmidt, U. (2018). Public perception of climate engineering and carbon capture and storage in Germany: survey evidence. *Clim. Policy* 18, 471–484. doi: 10.1080/14693062.2017.1304888

Carlisle, D. P., Feetham, P. M., Wright, M. J., and Teagle, D. A. H. (2020). The public remain uninformed and wary of climate engineering. *Clim. Change* 160, 303–322. doi: 10.1007/s10584-020-02706-5

Carr, W. A., and Yung, L. (2018). Perceptions of climate engineering in the South Pacific, Sub-Saharan Africa, and North American Arctic. *Clim. Change* 147, 119–132. doi: 10.1007/s10584-018-2138-x

Casagrande, D. G. (1997). *Restoration of an Urban Salt Marsh: An Interdisciplinary Approach. Bulletin Series No. 100.* New Haven, CT: Yale School of Forestry & Environmental Studies.

Colvin, R. M., Kemp, L., Talberg, A., Castella, C., de, Downie, C., Friel, S., et al. (2020). Learning from the climate change debate to avoid polarisation on negative emissions. *Environ. Commun.* 14, 23–35. doi: 10.1080/17524032.2019.1630463

Corner, A., Parkhill, K., Pidgeon, N. F., and Vaughan, N. E. (2013). Messing with nature? Exploring public perceptions of geoengineering in the UK. *Glob. Environ. Change* 23, 938–947. doi: 10.1016/j.gloenvcha.2013.06.002

Corner, A., and Pidgeon, N. F. (2014). Like artificial trees? The effect of framing by natural analogy on public perceptions of geoengineering. *Clim. Change* 130, 425–438. doi: 10.1007/s10584-014-1148-6

Cox, E., Spence, E., and Pidgeon, N. (2020). Public perceptions of carbon dioxide removal in the United States and the United Kingdom. *Nat. Clim. Change* 10, 1–6. doi: 10.1038/s41558-020-0823-z

Curado, G., Manzano-Arrondo, V., Figueroa, E., and Castillo, j. (2014). Public perceptions and uses of natural and restored salt marshes. *Landsc. Res.* 39, 668–679. doi: 10.1080/01426397.2013.772960

Demeritt, D. (2002). What is the 'social construction of nature'? A typology and sympathetic critique. *Prog. Hum. Geogr.* 26, 767–790. doi: 10.1191/0309132502ph402oa

Dütschke, E. (2011). What drives local public acceptance–comparing two cases from Germany: 10th international conference on greenhouse gas control technologies. *Energy Proc.* 4, 6234–6240. doi: 10.1016/j.egypro.2011.02.636

Figueiredo, M. A., de, Reiner, D. M., and Herzog, H. J. (2003). "Ocean carbon sequestration: a case study in public and institutional perceptions," in *Greenhouse Gas Control Technologies - 6th International Conference,* eds J. Gale and Y. Kaya (Oxford: Pergamon), 799–804.

Franke, A., Blenckner, T., Duarte, C. M., Ott, K., Fleming, L. E., Antia, A., et al. (2020). Operationalizing ocean health: toward integrated research on ocean health and recovery to achieve ocean sustainability. *One Earth* 2, 557–565. doi: 10.1016/j.oneear.2020.05.013

Fuss, S., Canadell, J. G., Peters, G. P., Tavoni, M., Andrew, R. M., Ciais, P., et al. (2014). Betting on negative emissions. *Nat. Clim. Change* 4, 850–853. doi: 10.1038/nclimate2392

Gannon, K. E., and Hulme, M. (2018). Geoengineering at the "Edge of the World": exploring perceptions of ocean fertilisation through the Haida Salmon Restoration Corporation. *Geogr. Environ.* 5:e00054. doi: 10.1002/geo2.54

Gattuso, J.-P., Magnan, A. K., Bopp, L., Cheung, W. W. L., Duarte, C. M., Hinkel, J., et al. (2018). Ocean solutions to address climate change and its effects on marine ecosystems. *Front. Mar. Sci.* 5:337. doi: 10.3389/fmars.2018.00337

GESAMP (2019). *High Level Review of a Wide Range of Proposed Marine Geoengineering Techniques: GESAMP Working Group 41.* London: GESAMP.

Gewin, V. (2002). Ocean carbon study to quit Hawaii. *Nature* 417:888. doi: 10.1038/417888b

Giles, J. (2002). Norway sinks ocean carbon study. *Nature* 419:6. doi: 10.1038/419006b

Gough, C., Taylor, I., and Shackley, S. (2002). Burying carbon under the sea: an initial exploration of public opinions. *Energy Environ.* 13, 883–900. doi: 10.1260/095830502762231331

Grech, A., Chartrand-Miller, K., Erftemeijer, P., Fonseca, M., McKenzie, L., Rasheed, M., et al. (2012). A comparison of threats, vulnerabilities and management approaches in global seagrass bioregions. *Environ. Res. Lett.* 7:24006. doi: 10.1088/1748-9326/7/2/024006

Ha, T. T. T., van Dijk, H., and Bush, S. R. (2012). Mangrove conservation or shrimp farmer's livelihood? The devolution of forest management and benefit sharing in the Mekong Delta, Vietnam. *Ocean Coast. Manag.* 69, 185–193. doi: 10.1016/j.ocecoaman.2012.07.034

Hansen, A. (2006). Tampering with nature: 'nature' and the 'natural' in media coverage of genetics and biotechnology. *Media Cult. Soc.* 28, 811–834. doi: 10.1177/0163443706067026

Hoegh-Guldberg, O., Chopin, T., Gaines, S., Haugan, P., Hemer, M., Howard, J., et al. (2019a). *The Ocean as a Solution to Climate Change: Five Opportunities for Action*. Washington, DC: World Resources Institute. Available online at: http://www.oceanpanel.org/climate (accessed December 8, 2020).

Hoegh-Guldberg, O., Northrop, E., and Lubchenco, J. (2019b). The ocean is key to achieving climate and societal goals. *Science* 365, 1372–1374. doi: 10.1126/science.aaz4390

Hugé, J., Vande Velde, K., Benitez-Capistros, F., Japay, J. H., Satyanarayana, B., Nazrin Ishak, M., et al. (2016). Mapping discourses using Q methodology in Matang Mangrove Forest, Malaysia. *J. Environ. Manag.* 183, 988–997. doi: 10.1016/j.jenvman.2016.09.046

Ibrahim, I., Aminudin, N., Young, M. A., and Yahya, S. A. I. (2012). Education for wetlands: public perception in Malaysia. *Proc. Soc. Behav. Sci.* 42, 159–165. doi: 10.1016/j.sbspro.2012.04.177

Ilyina, T., Wolf-Gladrow, D., Munhoven, G., and Heinze, C. (2013). Assessing the potential of calcium-based artificial ocean alkalinization to mitigate rising atmospheric CO_2 and ocean acidification. *Geophys. Res. Lett.* 40, 5909–5914. doi: 10.1002/2013GL057981

IPCC (2018). "Summary for policymakers," in *Global Warming of 1.5°C: An IPCC Special Report on the Impacts of Global Warming of 1.5°C Above Pre-industrial Levels and Related Global Greenhouse Gas Emission Pathways, in the Context of Strengthening the Global Response to the Threat of Climate Change, Sustainable Development, and Efforts to Eradicate Poverty,* eds V. Masson-Delmotte, P. Zhai, H. -O. Pörtner, D. Roberts, J. Skea, and P. R. Shukla. (Geneva: Intergovernmental Panel on Climate Change).

Ipsos MORI (2010). *Experiment Earth? Report on a Public Dialogue on Geoengineering.* Available online at: http://www.nerc.ac.uk/about/whatwedo/engage/engagement/geoengineering/geoengineering-dialogue-final-report/ (accessed December 8, 2020).

Itaoka, K., Okuda, Y., Saito, A., and Akai, M. (2009). Influential information and factors for social acceptance of CCS: The 2nd round survey of public opinion in Japan: greenhouse gas control technologies 9 proceedings of the 9th international conference on greenhouse gas control technologies (GHGT-9), 16–20 November 2008, Washington DC, USA. *Energy Proc.* 1, 4803–4810. doi: 10.1016/j.egypro.2009.02.307

Jefferson, R. L., Bailey, I., Laffoley, D., d., Richards, J. P., and Attrill, M. J. (2014). Public perceptions of the UK marine environment. *Mar. Policy* 43, 327–337. doi: 10.1016/j.marpol.2013.07.004

Jobin, M., and Siegrist, M. (2020). Support for the deployment of climate engineering: a comparison of ten different technologies. *Risk Anal.* 40, 1058–1078. doi: 10.1111/risa.13462

Keller, D. P., Feng, E. Y., and Oschlies, A. (2014). Potential climate engineering effectiveness and side effects during a high carbon dioxide-emission scenario. *Nat. Commun.* 5:3304. doi: 10.1038/ncomms4304

Keller, D. P., Lenton, A., Littleton, E. W., Oschlies, A., Scott, V., and Vaughan, N. E. (2018). The effects of carbon dioxide removal on the carbon cycle. *Curr. Clim. Change Rep.* 4, 250–265. doi: 10.1007/s40641-018-0104-3

Leiserowitz, A., Smith, N., and Marlon, J. (2010). *Americans' Knowledge of Climate Change.* New Haven, CT: Yale Project on Climate Change Communication.

Retrieved from Q237. New technologies can solve global warming, without individuals having to make big changes in their lives.

Liski, A. H., Ambros, P., Metzger, M. J., Nicholas, K. A., Wilson, A. M. W., and Krause, T. (2019). Governance and stakeholder perspectives of managed re-alignment: Adapting to sea level rise in the Inner Forth estuary, Scotland. *Reg. Environ. Change* 19, 2231–2243. doi: 10.1007/s10113-019-01505-8

López-Medellín, X., Castillo, A., and Ezcurra, E. (2011). Contrasting perspectives on mangroves in arid Northwestern Mexico: implications for integrated coastal management. *Ocean Coast. Manag.* 54, 318–329. doi: 10.1016/j.ocecoaman.2010.12.012

L'Orange Seigo, S., Dohle, S., and Siegrist, M. (2014). Public perception of carbon capture and storage (CCS): a review. *Renew. Sust. Energy Rev.* 38, 848–863. doi: 10.1016/j.rser.2014.07.017

Lovelock, C. E., and Reef, R. (2020). Variable impacts of climate change on blue carbon. *One Earth* 3, 195–211. doi: 10.1016/j.oneear.2020.07.010

Macreadie, P. I., Anton, A., Raven, J. A., Beaumont, N., Connolly, R. M., Friess, D. A., et al. (2019). The future of blue carbon science. *Nat. Commun.* 10:3998. doi: 10.1038/s41467-019-11693-w

Merk, C., Klaus, G., Pohlers, J., Ernst, A., Ott, K., and Rehdanz, K. (2019). Public perceptions of climate engineering: Laypersons' acceptance at different levels of knowledge and intensities of deliberation. *GAIA* 28, 348–355. doi: 10.14512/gaia.28.4.6

Myatt, L. B., Scrimshaw, M. D., and Lester, J. N. (2003). Public perceptions and attitudes towards an established managed realignment scheme: Orplands, Essex, UK. *J. Environ. Manag.* 68, 173–181. doi: 10.1016/S0301-4797(03)00065-3

Nordlund, L. M., Jackson, E. L., Nakaoka, M., Samper-Villarreal, J., Beca-Carretero, P., and Creed, J. C. (2018). Seagrass ecosystem services – What's next? *Mar. Pollut. Bull.* 134, 145–151. doi: 10.1016/j.marpolbul.2017.09.014

Nordlund, L. M., La Torre-Castro, M., de, Erlandsson, J., Conand, C., Muthiga, N., Jiddawi, N., et al. (2014). Intertidal zone management in the Western Indian Ocean: assessing current status and future possibilities using expert opinions. *Ambio* 43, 1006–1019. doi: 10.1007/s13280-013-0465-8

Palmgren, C. R., Morgan, M. G., Bruine de Bruin, W., and Keith, D. W. (2004). Initial public perceptions of deep geological and oceanic disposal of carbon dioxide. *Environ. Sci. Technol.* 38, 6441–6450. doi: 10.1021/es040400c

Paluszny, A., Graham, C. C., Daniels, K. A., Tsaparli, V., Xenias, D., Salimzadeh, S., et al. W. (2020). Caprock integrity and public perception studies of carbon storage in depleted hydrocarbon reservoirs. *Int. J. Greenh. Gas Control* 98:103057. doi: 10.1016/j.ijggc.2020.103057

Pidgeon, N. F., Parkhill, K., Corner, A., and Vaughan, N. E. (2013). Deliberating stratospheric aerosols for climate geoengineering and the SPICE project. *Nat. Clim. Change* 3, 451–457. doi: 10.1038/nclimate1807

Queiroz, L., d,. S., Rossi, S., Calvet-Mir, L., Ruiz-Mallén, I., García-Betorz, S., et al. (2017). Neglected ecosystem services: highlighting the socio-cultural perception of mangroves in decision-making processes. *Ecosyst. Serv.* 26, 137–145. doi: 10.1016/j.ecoser.2017.06.013

Rahman, M. A. A., and Asmawi, M. Z. (2016). Local residents' Awareness towards the issue of mangrove degradation in Kuala Selangor, Malaysia. *Proc. Soc. Behav. Sci.* 222, 659–667. doi: 10.1016/j.sbspro.2016.05.222

Rickels, W., Merk, C., Reith, F., Keller, D., and Oschlies, A. (2019). (Mis)conceptions about modelling of negative emissions technologies. *Environ. Res. Lett.* 14:104004. doi: 10.1088/1748-9326/ab3ab4

Rönnbäck, P., Crona, B., and Ingwall, L. (2007). The return of ecosystem goods and services in replanted mangrove forests: Perspectives from local communities in Kenya. *Environ. Conserv.* 34, 313–324. doi: 10.1017/S0376892907004225

Roy, A. K. D. (2016). Local community attitudes towards mangrove forest conservation: lessons from Bangladesh. *Mar. Policy* 74, 186–194. doi: 10.1016/j.marpol.2016.09.021

Royal Society (2009). *Geoengineering the Climate: Science, Governance and Uncertainty*: Royal Society. Available online at: http://eprints.soton.ac.uk/156647/1/Geoengineering_the_climate.pdf (accessed December 8, 2020).

Schiermeier, Q. (2009a). *Ocean Fertilization Experiment Draws Fire: Indo-German Research Cruise Sets Sail Despite Criticism*. Available online at: https://www.nature.com/news/2009/090109/full/news.2009.13.html (accessed December 8, 2020).

Schiermeier, Q. (2009b). *Ocean Fertilization Experiment Suspended: German Science Ministry Demands Environmental Assessment Before Nutrient Dumping Can Begin*. Available online at: https://www.nature.com/news/2009/090114/full/news.2009.26.html (accessed December 8, 2020).

Schumann, D., Duetschke, E., and Pietzner, K. (2014). Public perception of CO_2 offshore storage in germany: regional differences and determinants. *Energy Proc.* 63, 7096–7112. doi: 10.1016/j.egypro.2014.11.744

Scott, K. N. (2006). The day after tomorrow: ocean CO_2 sequestration and the future of climate change. *Georget. Int. Environ. Law Rev.* 18, 57–108.

Shrum, T. R., Markowitz, E., Buck, H., Gregory, R., van der Linden, S., Attari, S. Z., et al. (2020). Behavioural frameworks to understand public perceptions of and risk response to carbon dioxide removal. *Interface Focus* 10:20200002. doi: 10.1098/rsfs.2020.0002

Smith, P., Adams, J., Beerling, D. J., Beringer, T., Calvin, K. V., Fuss, S., et al. (2019). Land-management options for greenhouse gas removal and their impacts on ecosystem services and the sustainable development goals. *Annu. Rev. Environ. Resour.* 44, 255–286. doi: 10.1146/annurev-environ-101718-033129

Srivastava, S., and Mehta, L. (2017). *The Social Life of Mangroves: Resource Complexes and Contestations on the Industrial Coastline of Kutch, India (STEPS Working Paper No. 99)*. STEPS Centre: Brighton.

Stone, K., Bhat, M., Bhatta, R., and Mathews, A. (2008). Factors influencing community participation in mangroves restoration: a contingent valuation analysis. *Ocean Coast. Manag.* 51, 476–484. doi: 10.1016/j.ocecoaman.2008.02.001

Thomas, G., Pidgeon, N., and Roberts, E. (2018). Ambivalence, naturalness and normality in public perceptions of carbon capture and storage in biomass, fossil energy, and industrial applications in the United Kingdom. *Energy Res. Soc. Sci.* 46, 1–9. doi: 10.1016/j.erss.2018.06.007

Tollefson, J. (2017). Plankton-boosting project in Chile sparks controversy: Canadian foundation says its planned ocean-fertilization experiment could help fisheries. *Nature* 545, 393–394. doi: 10.1038/545393a

Tuan, T. H., My, N. H. D., Le Anh, T. Q., and van Toan, N. (2014). Using contingent valuation method to estimate the WTP for mangrove restoration under the context of climate change: a case study of Thi Nai lagoon, Quy Nhon city, Vietnam. *Ocean Coast. Manag.* 95, 198–212. doi: 10.1016/j.ocecoaman.2014.04.008

Upham, P., and Roberts, T. (2011). Public perceptions of CCS in context: results of NearCO2 focus groups in the UK, Belgium, the Netherlands, Germany, Spain and Poland: 10th International Conference on Greenhouse Gas Control Technologies. *Energy Proc.* 4, 6338–6344. doi: 10.1016/j.egypro.2011.02.650

Vande Velde, K., Hugé, J., Friess, D. A., Koedam, N., and Dahdouh-Guebas, F. (2019). Stakeholder discourses on urban mangrove conservation and management. *Ocean Coast. Manag.* 178:104810. doi: 10.1016/j.ocecoaman.2019.05.012

Wandersee, J. H., and Schussler, E. E. (2001). Toward a theory of plant blindness. *Plant Sci. Bull.* 47, 2–9. doi: 10.1111/cobi.12738

West, R. J. (2010). Rehabilitation of seagrass and mangrove sites-successes and failures in NSW. *Wetlands Aust.* 14, 13–19. doi: 10.31646/wa.173

Winickoff, D. E., Flegal, J. A., and Asrat, A. (2015). Engaging the global south on climate engineering research. *Nat. Clim. Change* 5, 627–634. doi: 10.1038/nclimate2632

Wolske, K. S., Raimi, K. T., Campbell-Arvai, V., and Hart, P. S. (2019). Public support for carbon dioxide removal strategies: the role of tampering with nature perceptions. *Clim. Change* 152, 345–361. doi: 10.1007/s10584-019-02375-z

Wright, M. J., Teagle, D. A. H., and Feetham, P. M. (2014). A quantitative evaluation of the public response to climate engineering. *Nat. Clim. Change* 4, 106–110. doi: 10.1038/nclimate2087

Conflict of Interest: The authors declare that the research was conducted in the absence of any commercial or financial relationships that could be construed as a potential conflict of interest.

frontiers in Climate

POLICY BRIEF
published: 25 January 2021
doi: 10.3389/fclim.2020.575716

The Potential for Ocean-Based Climate Action: Negative Emissions Technologies and Beyond

Jean-Pierre Gattuso[1,2,3]*, *Phillip Williamson*[4], *Carlos M. Duarte*[5] and *Alexandre K. Magnan*[2,6]

[1] Sorbonne University, CNRS, Laboratoire d'Océanographie de Villefranche, Villefranche-sur-Mer, France, [2] Institute for Sustainable Development and International Relations, Sciences Po, Paris, France, [3] Monaco Association on Ocean Acidification, Prince Albert II of Monaco Foundation, Monaco, Monaco, [4] School of Environmental Sciences, University of East Anglia, Norwich, United Kingdom, [5] King Abdullah University of Science and Technology (KAUST), Red Sea Research Center (RSRC), Thuwal, Saudi Arabia, [6] UMR LIENSs 7266, Université de La Rochelle-CNRS, La Rochelle, France

The effectiveness, feasibility, duration of effects, co-benefits, disbenefits, cost effectiveness and governability of four ocean-based negative emissions technologies (NETs) are assessed in comparison to eight other ocean-based measures. Their role in revising UNFCCC Parties' future Nationally Determined Contributions is discussed in the broad context of ocean-based actions for both mitigation and ecological adaptation. All measures are clustered in three policy-relevant categories (Decisive, Low Regret, Concept Stage). None of the ocean-based NETs assessed are identified as Decisive at this stage. One is Low Regret (*Restoring and increasing coastal vegetation*), and three are at Concept Stage, one with low to moderate potential disbenefits (*Marine bioenergy with carbon capture and storage*) and two with potentially high disbenefits (*Enhancing open-ocean productivity* and *Enhancing weathering and alkalinization*). Ocean-based NETs are uncertain but potentially highly effective. They have high priority for research and development.

Keywords: ocean-based solutions, blue carbon, carbon capture and storage, ocean fertilization, ocean alkalinization, climate action

OPEN ACCESS

Edited by:
Wilfried Rickels, Christian Albrechts University Kiel, Germany

Reviewed by:
Greg H. Rau, University of California, Santa Cruz, United States
Christine Bertram, Christian Albrechts University Kiel, Germany

***Correspondence:**
Jean-Pierre Gattuso
gattuso@obs-vlfr.fr

Specialty section:
This article was submitted to Negative Emission Technologies, a section of the journal Frontiers in Climate

Received: *24 June 2020*
Accepted: *23 December 2020*
Published: *25 January 2021*

Citation:
Gattuso J-P, Williamson P, Duarte CM and Magnan AK (2021) The Potential for Ocean-Based Climate Action: Negative Emissions Technologies and Beyond. Front. Clim. 2:575716. doi: 10.3389/fclim.2020.575716

1. INTRODUCTION

Implementing the Paris Agreement is a formidable challenge. In pathways limiting global warming to 1.5°C with no or limited overshoot as well as in pathways with a higher overshoot, CO_2 emissions are reduced to net zero globally around 2050 (IPCC, 2018). This would require far-reaching and unprecedented transitions in all sectors, and also large-scale use of negative emissions technologies (NETs), that is removal of greenhouse gases from the atmosphere by deliberate human activities.Yet the trade-offs for food production and nature conservation limit carbon dioxide removal by most land-based approaches (Boysen et al., 2017).

In that context, it is timely to assess the opportunities offered by the ocean to reduce the causes and also the consequences of climate change, globally and locally. Recent papers and reports have reviewed several potential measures (Gattuso et al., 2018; National Academies of Sciences Engineering and Medicine, 2018; Because the Ocean, 2019; GESAMP, 2019; Hoegh-Guldberg et al., 2019). Countries have so far only made limited use of ocean-related measures for tackling climate change and its impacts through their Nationally Determined Contributions (NDC) under the Paris

Agreement (Gallo et al., 2017). Among the 161 initial NDCs submitted in 2014–2015, 70% mentioned marine issues, most frequently as components of adaptation action or in regard to climate impacts. Just over a third (59) also included ocean-related mitigation measures. The only ocean-based negative emission approach specifically mentioned is the conservation and restoration of coastal blue carbon ecosystems (i.e., mangroves, saltmarshes, and seagrasses). The 5-year revisions of NDCs that need to be made before the re-scheduled COP26 in 2021 (26th Conference of the Parties of the United Nations Framework Convention on Climate Change, UNFCCC), offer an opportunity to adopt more ocean-inclusive mitigation and adaptation strategies.

Here we assess four ocean-based NETs involving carbon dioxide removal (*Marine bioenergy with carbon capture and storage*, *Restoring and increasing coastal vegetation*, *Enhancing open-ocean productivity*, *Enhancing weathering and alkalinization*) and put them in the broader context of ocean-based measures to support climate policies, especially greenhouse gas mitigation and ecological adaptation. These carbon dioxide removal pathways are the most documented in the literature. Other pathways are not evaluated here and it is likely that new methods or hybrids between the methods presented here will emerge. Building on recently published material (Gattuso et al., 2018), this Policy Brief brings two innovations. It assesses marine-biomass-fueled bioenergy with carbon capture and storage (*Marine BECCS*) and goes a step further by grouping these NETs and a wide range of other options into policy clusters with the aim of guiding decisions on priority areas of action.

2. OCEAN NEGATIVE EMISSIONS TECHNOLOGIES

Gattuso et al. (2018) published a comprehensive expert assessment of ocean-based measures to reduce climate change and its impacts based on a review of 862 publications and expert judgment. Here we focus on NETs and consider eight criteria: (1) effectiveness to increase net carbon uptake, (2) effectiveness to reduce ocean warming, ocean acidification, and sea level rise; (3) feasibility, covering both technological readiness and lead time until full potential effectiveness; (4) duration of effects; (5) cost effectiveness; (6) co-benefits; (7) disbenefits and (8) governability from an international perspective. **Figure 1** summarizes the assessment. Full information is available in the Supplementary Material of Gattuso et al. (2018) and in **Supplementary Material** (SM3).

2.1. Marine Bioenergy With Carbon Capture and Storage

Considering the area, water and nutrient requirements leads to the tentative conclusion that macroalgae (seaweed) based BECCS could be a better long-term option than woody biomass energy crops, because achievable productivity is higher, freshwater demands are eliminated, and nutrient demands may be lower if efficient recycling systems can be developed (Lenton, 2014). Here we do not consider hybrid bioenergy with carbon capture and storage approaches to focus on marine-biomass-fueled BECCS. The latter is expected to involve three overarching steps: increasing carbon uptake by macroalgal aquaculture; converting the biomass to biofuel; and deploying carbon capture (at power stations) and long-term geological storage. Capron et al. (2020) review recent progress by US researchers in using macroalgae for biofuel.

The effectiveness of *Marine BECCS* to increase carbon uptake is scored high. Its effectiveness to moderate ocean climate drivers is also scored high given the close relationship between CO_2 and ocean warming, acidification and sea level rise.

However, feasibility is considered low because components of this approach have not all been demonstrated at scale and may require a decade or more of research and development to prove capacity, cost effectiveness and safety. Cost effectiveness (based on a single estimate) is high, at 26 US$ per t CO_2 removed for marine biomass fueled BECCS.

Climate-relevant alternatives to using macroalgae for BECCS would be to develop methods for deep water disposal of the additional biomass generated through macroalgal aquaculture (Williamson et al., 2021) and the manufacturing of long-lived products, such as plastic, that displace products generating emissions, thereby avoiding emissions, or enhancing soil fertility while contributing to carbon sequestration through use as biochar.

2.2. Restoring and Increasing Coastal Vegetation

Restoring and increasing coastal vegetation ("blue carbon" ecosystems) aims at enhancing CO_2 uptake and avoiding further emissions. Here we look at the implementation of this measure at the global scale, by restoring a high proportion of the human-degraded salt marsh, mangrove and seagrass habitats of the planet.

Conservation and restoration of blue carbon ecosystems support and enhance CO_2 sequestration, whilst also reducing emissions associated with habitat degradation and loss (McLeod et al., 2011; Pendleton et al., 2012; Duarte et al., 2013; Marbà et al., 2015; Howard et al., 2017; Hamilton and Friess, 2018). The theoretical effectiveness of such measures at the global scale is limited by the maximum area that can be occupied by these habitats, with their maximum global carbon burial estimated to be 234 Tg C per year for salt marshes, mangroves, and seagrasses combined (McLeod et al., 2011). Assuming that historic losses of blue carbon ecosystems (50% for mangroves since the 1940s, 29% for seagrass since 1879, 25% for salt marshes since the 1800s; Waycott et al., 2009; McLeod et al., 2011) are rapidly reversed through restoration, the maximum cumulative carbon burial would be 26 Pg C until 2100, equivalent to about 2.5 years of current anthropogenic emissions. This is a theoretical upper estimate because of likely constraints on implementation. The effectiveness to increase carbon uptake is therefore scored very low, noting also that increased methane (CH_4) emissions may fully or partly negate the climatic benefits of CO_2 removal (Al-Haj and Fulweiler, 2020; Rosentreter and Williamson, 2020). Carbonate formation or dissolution in blue carbon habitats will

also affect the capacity of these habitats to remove atmospheric carbon; although dissolution may dominate, thereby increasing removal (Saderne et al., 2019), these processes have not yet been explored sufficiently to provide global estimates.

Like carbon uptake, the effectiveness to moderate warming, acidification and sea level rise is limited by the maximum area possibly occupied by these habitats, hence it is scored very low. Feasibility is high as blue carbon approaches are well tested and deployed around the world (Howard et al., 2014) but the full delivery of the benefits at their maximum global capacity will require years to decades to be achieved. Protection of blue carbon habitats must be multi-decadal in order to be effective, and successful restoration also requires a long term commitment (e.g., Duarte et al., 2013; Marbà et al., 2015; Reynolds et al., 2016)—with the assumption that future temperature increases can be kept below 2°C (under higher warming, blue carbon ecosystems are at risk, and their stored carbon is likely to be lost; Bindoff et al., 2019). The duration of the effect is scored permanent, with those provisos. At median costs of 240, 30,000, and 7,800 US$ per t CO_2, respectively for mangroves, salt marsh and seagrass habitats, the cost effectiveness (for climate mitigation) is collectively scored very low (Siikamaki et al., 2012; Bayraktarov et al., 2016; Narayan et al., 2016), recognizing that there are large differences in restoration costs between the three ecosystems (and at the local level), and that the cost effectiveness of restoration for the delivery of other ecosystem services could nevertheless be very high.

2.3. Enhancing Open-Ocean Productivity

Enhancing open-ocean productivity (hereafter *Fertilization*) is based on nutrients addition directly or indirectly to increase CO_2 drawdown by phytoplankton. Such methods may appear technologically feasible, as it has been shown for iron/macronutrient addition, as well as for artificial upwellings (Pan et al., 2016).

For iron addition, modeling studies show a maximum effect on atmospheric CO_2 of 15–45 ppmv in 2100 (Zeebe and Archer, 2005; Aumont and Bopp, 2006; Keller et al., 2014). Ocean fertilization with macro-nutrients (N, P) has a higher theoretical potential of 1.5 PgC yr-1 (Harrison, 2017), about 50 times more than the maximum simulated effects of Southern Ocean iron fertilization (Oschlies et al., 2010); however, very large quantities of macronutrients are needed and the proposed scaling of this technique seems unrealistic (Williamson and Bodle, 2016). For artificial upwelling (upward pumping of nutrient-rich deep waters), the intended carbon removal by increased productivity (Lovelock and Rapley, 2007) may be matched by the undesirable release of CO_2 from the deeper water (Shepherd et al., 2007; Dutreuil et al., 2009; Yool et al., 2009). The potential impact of artificial upwellings on nitrogen fixation, and hence on natural carbon sequestration is controversial (Fennel, 2008; Karl and Letelier, 2008). Some modeling studies indicate that net CO_2 drawdown is theoretically possible if upwelling rates are increased in appropriate locations in 2100 for RCP8.5. Because of the many associated uncertainties, the overall effectiveness of *Fertilization* to increase carbon uptake is scored low.

Fertilization has no direct effect on sea level rise nor on ocean warming hence its effectiveness to reduce those drivers is low. Acidification could be ameliorated in the short term in the upper ocean (by CO_2 removal), but enhanced in the long term in the ocean interior (by CO_2 release); the overall effectiveness is considered to be low. Effects would happen through increased carbon uptake but there is limited scope for enhanced ocean productivity and increased carbon uptake due to biological and physical-chemical constraints (Williamson and Bodle, 2016). Mesoscale variability in the strength of different processes responsible for long-term carbon removal (Boyd and Vivian, 2019) make carbon accounting highly uncertain. Furthermore, once *Fertilization* is started, it would need to be done continuously; if not, a large part of the sequestered carbon will be returned to the atmosphere on decadal timescales (e.g., Aumont and Bopp, 2006). Ocean *Fertilization* is considered to have negative consequences for 8 Sustainable Development Goals (SDGs), and a combination of both positive and negative consequences for 7 SDGs (Honegger et al., 2020). The cost of iron fertilization has been estimated at 22–119 and 457 US$ per t CO_2 sequestered (Harrison, 2013). There are lower cost estimates for *Fertilization* using macronutrients, at around US$ 20 per t CO_2 (Jones, 2014), but scalability is questionable and monitoring costs are excluded. The median of all estimates is 230 US$ per t CO_2, indicating very low cost effectiveness.

2.4. Enhancing Weathering and Alkalinization

Enhancing weathering and alkalinization (hereafter *Alkalinization*) is the addition of natural or man-made alkalinity (ground carbonate or silicate rocks, such as olivine or basalt), to enhance CO_2 removal and/or carbon storage. Adding huge amounts of alkalinity globally could, in theory, substantially mitigate atmospheric CO_2 without elevating biogeochemical properties significantly beyond naturally occurring levels (Ilyina et al., 2013; Keller et al., 2014).

Since the carbon uptake capacity of this approach is very high, without a determined limit (Ciais et al., 2013), its effectiveness to reduce ocean warming and acidification is also very high, with impacts on sea level via surface air temperature (Gonzalez and Ilyina, 2016). Regional *Alkalinization* could be effective in protecting coral reefs against acidification (but not warming; Feng et al., 2016). There is technological readiness to add alkalinity to the ocean, at least at small scales. What is needed is research and testing to acquire adequate knowledge about the environmental co-benefits and disbenefits. Feasibility is also impeded by lack of infrastructure to mine or produce, process and distribute alkalinity at large scales. Feasibility is therefore scored very low.

A unit of alkalinity added would sequester CO_2 essentially permanently, hence the duration of the effect is scored very high. Some of the inorganic carbon could precipitate as $CaCO_3$, releasing CO_2 and reducing the carbon storage and alkalinity co-benefits afforded. The addition of alkalinity would probably have to be continued for decades to centuries

(or longer) to have a substantial impact on atmospheric CO_2 (Keller et al., 2014).

The cost of various ocean alkalinity carbon storage technologies is largely speculative at this stage. Renforth et al. (2013) indicated a range of 72–159 US$ per t CO_2 taken up. This range reflects the extraction, calcination, hydration, and surface ocean dispersion costs at a global scale (including transportation). In the case of direct addition of alkaline minerals to the ocean (i.e., without calcination), the cost is estimated to be 20–50 US$ per t CO_2 (Harvey, 2008; Köhler et al., 2013; Renforth and Henderson, 2017). Overall, at 10–190 US$ per t CO_2, the cost effectiveness is moderate.

3. POLICY-RELEVANCE OF NEGATIVE EMISSION TECHNOLOGIES

Understanding the policy relevance of NETs requires putting them into a broader context of global and/or local climate action. Here we consider 12 ocean-related measures to enhance both global mitigation and local coastal ecological adaptation[1] (**Figure 2**). These options can be clustered into three overarching policy-relevant clusters (Decisive, Low Regret, Concept Stage) that are defined in **Figure 2A** according to their state of implementation, effectiveness to reduce climate-related ocean drivers globally, effectiveness to reduce impacts/risks locally, and potential co-benefits and disbenefits (i.e., associated adverse impacts and other undesirable consequences, including opportunity costs).

3.1. Cluster 1

The only ocean-based Decisive measure that we have identified addresses the causes of climate change: *Marine renewable energy*. It includes energy from offshore winds, tides, waves, ocean currents as well as thermal gradients. This action has the

[1]Societal adaptation measures such as infrastructure-based or community-based adaptation, risk reduction policies improvement, and the relocation of people, assets and economic activities are not included.

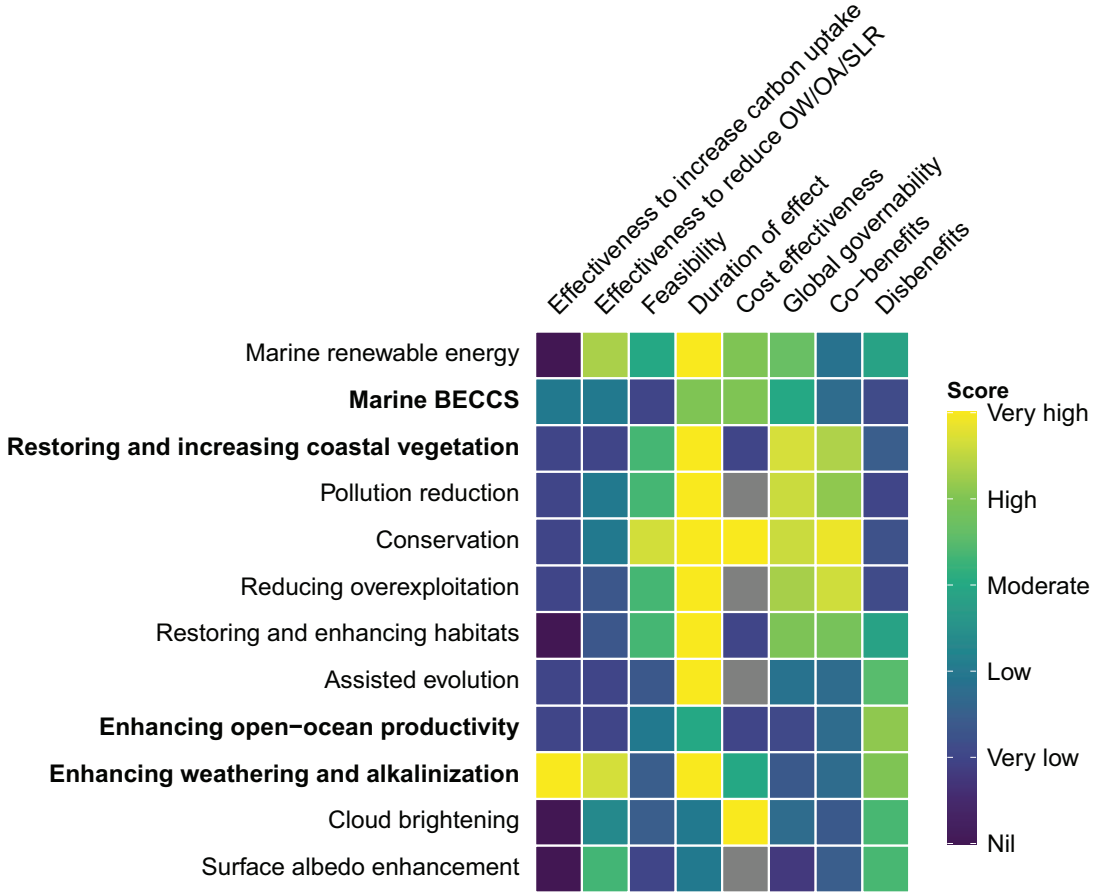

FIGURE 1 | Assessment of ocean negative emissions approaches (in bold) compared with other ocean-based measures. Based on Gattuso et al. (2018), except for marine BECCS (see SM3 in **Supplementary Material**), with the following changes: Vegetation and Alkalinization are only considered at global scale except the co-benefits and disbenefits which are considered at local scale. Two criteria are newly defined by combining criteria assessed earlier. Feasibility is the mean of Technological readiness and Lead time until full potential effectiveness. Effectiveness to reduce OW/OA/SLR (ocean warming, ocean acidification and sea level rise) is the mean of the effectiveness to Moderate warming, Moderate acidification and Moderate sea level rise. Gray tiles indicate criteria not assessed for the corresponding measure. Further information on the measures and criteria are available in **Supplementary Material** (SM1 and SM2).

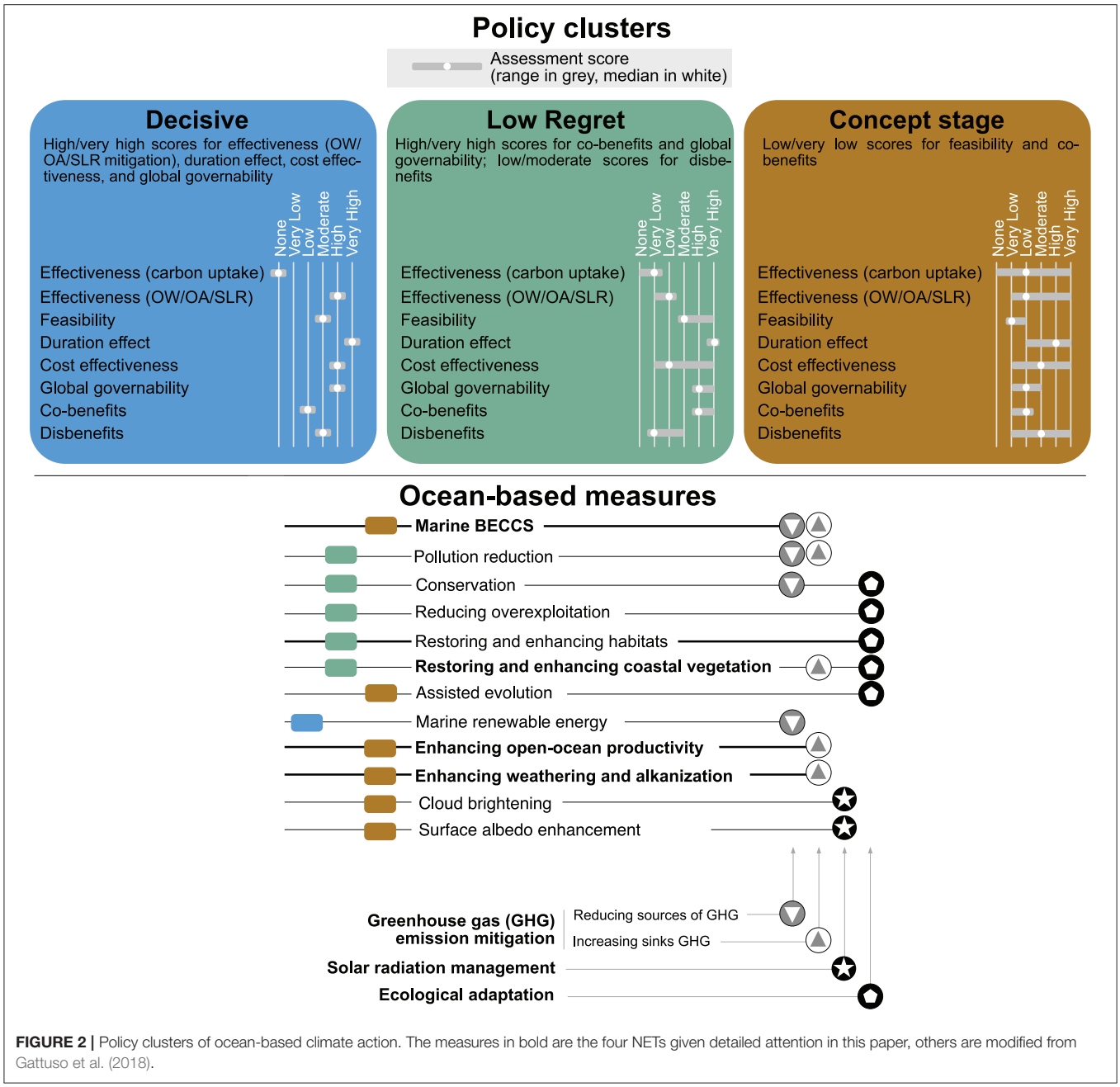

FIGURE 2 | Policy clusters of ocean-based climate action. The measures in bold are the four NETs given detailed attention in this paper, others are modified from Gattuso et al. (2018).

theoretical potential to meet all global electricity requirements, although requiring massive infrastructure development. Whilst some local adverse impacts are inevitable, these can be minimized.

3.2. Cluster 2

Low Regret measures provide both climatic and non-climatic benefits, with few disbenefits. For example, *Conservation* measures can protect carbon-rich coastal ecosystems from direct human disturbance and loss, and play an important role in limiting local climate impacts. Similarly, *Restoring and enhancing coastal vegetation* supports ecological adaptation whilst providing storm protection, contributing to food security, and enhancing biodiversity. It can also increase carbon uptake (i.e., addressing the causes of climate change), at levels that may be locally and/or nationally significant. Nevertheless, because of the limited total area for restoring such blue carbon ecosystems and also associated methane emissions, this action can only make a very small contribution to climate mitigation at the global scale (IPCC, 2019; Al-Haj and Fulweiler, 2020).

Pollution reduction in coastal waters removes contaminants and excess nutrients that impair ecosystem function, thereby supporting ecosystem-based adaptation. Reducing atmospheric pollution from shipping can also, to a limited degree, address the causes of climate change. However, Low Regret measures are not cost-free, requiring well-informed planning and effective coordination over a wide range of spatial and temporal scales.

3.3. Cluster 3

Concept Stage measures are illustrated by the NET *Marine BECCS*, and some forms of *Assisted evolution* (alterations to species and genetics). The former would use cultivated macroalgae (or possibly microalgae) as the biomass source for bioenergy. Such measures have potential but their feasibility and cost-effectiveness for climatic benefits have yet to be demonstrated. Several measures have potentially high disbenefits, as identified for *Fertilization*, *Alkalinization* and the sunlight reflection techniques of marine *Cloud brightening* and *Surface albedo enhancement* (e.g., covering the ocean surface with reflective foam). Whilst all these approaches have a very large theoretical potential to address climate change globally, only *Fertilization* has been investigated through field experiments (although not carried out for climate mitigation purposes), with limited success. Much more attention needs to be given to their governance and public acceptability before they can be considered for implementation as climate policy responses. This agrees with and extends the conclusion of Boyd and Vivian (2019) for marine geoengineering.

The effectiveness of measures such as *Assisted evolution* to support ecological adaptation critically depends on the environmental and societal contexts of their implementation. For example, while some *Assisted evolution* tools could have local benefits, others such as the spread of genetically alien populations have serious risks.

3.4. Global Governability

The global governability of NETs refers in this study to the potential capability of the international community (both nation states and international non-state actors) to implement them, managing associated conflicts and harnessing mutual benefits, It is therefore a key dimension to be considered when discussing the potential role of NETs within a broader range of climate actions. In our assessment, global governability is considered moderate to very high for more than half of the measures considered (**Figure 1**), but low to very low for *Fertilization* and *Alkalinization* as well as for *Assisted evolution* and the two SRM options (*Cloud brightening*, *Surface Albedo enhancement*). *Marine BECCS* score is moderate: although this measure could have high co-benefits and could be implemented at modest scale without having to rely on international cooperation, wider scale implementation could raise serious national and international complications, hence potentially requiring new governing arrangements and accounting, monitoring, and verification entities. *Alkalinization* and *Fertilization* score very low, but for different reasons: concerns regarding their potential adverse environmental impacts result in low public acceptability, reflected in political rejection of such methods (and legal constraints) by the London Convention/London Protocol[2], the UN Convention on Biological Diversity, and other bodies. These findings align with recent conclusions that "marine geoengineering" challenges the ability of the international law system, as it stands now, to govern the implementation of these ideas (McGee et al., 2018).

4. CONCLUSION AND ACTIONABLE RECOMMENDATIONS

Other than by eliminating nearly all anthropogenic greenhouse gas emissions, there is no single measure to dramatically accelerate progress in achieving the net zero target of the Paris Agreement. Nevertheless, opportunities exist for all coastal countries to implement a wide range of ocean-based climate actions, including negative emission approaches. Guidelines and actionable recommendations are required to address the urgency of climate action. Marine geoengineering techniques (e.g., Boyd and Vivian, 2019) and other ocean-based measures need to be assessed and ranked (e.g., Gattuso et al., 2018). Here we build on previous assessments to provide a first attempt to define policy-relevant clusters for climate action, both global mitigation and local ecological adaptation.

None of the four ocean-based NETs assessed are Decisive, one is Low Regret (*Restoring and increasing coastal vegetation*), and three are at Concept Stage with either low to moderate potential disbenefits (*Marine bioenergy with carbon capture and storage*) or with high potential disbenefits (*Enhancing open-ocean productivity* and *Enhancing weathering and alkalinization*). The next iteration of more ambitious NDCs should scale up ocean-based climate action by prioritizing the implementation of Decisive and Low Regret measures, and urgently improving knowledge on Concept Stage measures. Decisive and Low Regret measures are both key priorities for implementation because, on the one hand, the full implementation of Decisive measures will not completely eliminate coastal risks while, on the other hand, the effectiveness and security of Low Regret conservation/nature-based solutions are being put at risk by increasing climate change and rising sea level. Concept Stage measures require further scientific investigations because the full implementation of proven measures runs the risk of falling short of providing enough cost effective NETs capacity.

Balancing ocean-based measures also calls for securing robust national-to-local enabling conditions and enhanced international support for climate action. This is important because the majority of ocean-inclusive NDCs are conditional on external financing and support. They were discussed at COP25, referred to the "Blue COP," and could be, with nature-based solutions, one of the priority concerns for COP26 and the subsequent Global Stocktake in 2023. Enhancing the enabling conditions can be achieved by (i) strengthening the formal recognition of the

[2] As regulated by the London Protocol, with an amendment prohibiting such action unless constituting legitimate scientific research authorized under permit. That amendment has not yet legally entered force.

ocean-climate nexus and the ocean as a provider of solutions for climate change, and (ii) facilitating the UNFCCC Party delegations' understanding of the role of ocean-related measures and how to include them in the next generation of NDCs.

AUTHOR CONTRIBUTIONS

All authors contributed the ideas. J-PG wrote the first draft which was then finalized by all authors.

FUNDING

The Ocean Solutions Initiative was financially supported by the Prince Albert II of Monaco Foundation, the Veolia Foundation, the IAEA Ocean Acidification International Coordination Centre, the French Facility for Global Environment, and the STORISK project (French National Research Agency, ANR-15-CE03-0003). The ANR programme Investissements d'avenir (ANR-10-LABX-14-01) provides support to Iddri.

ACKNOWLEDGMENTS

Thanks are due to the coauthors of the papers by Gattuso et al. (2018) and Gattuso et al. (2019). This work is a product of The Ocean Solutions Initiative (http://bit.ly/2xJ3EV6) and the STORISK project (https://bit.ly/2YMhfZX). Comments from L. Kapsenberg and three reviewers have significantly improved an earlier version of this paper.

SUPPLEMENTARY MATERIAL

The Supplementary Material for this article can be found online at: https://www.frontiersin.org/articles/10.3389/fclim.2020.575716/full#supplementary-material

REFERENCES

Al-Haj, A., and Fulweiler, R. (2020). A synthesis of methane emissions from shallow vegetated coastal ecosystems. *Glob. Change Biol.* 26, 2988–3005. doi: 10.1111/gcb.15046

Aumont, O., and Bopp, L. (2006). Globalizing results from ocean *in situ* iron fertilization studies. *Glob. Biogeochem. Cycles* 20:GB2017. doi: 10.1029/2005GB002591

Bayraktarov, E., Saunders, M., Abdullah, S., Mills, M., Beher, J., Possingham, H., et al. (2016). The cost and feasibility of marine coastal restoration. *Ecol. Appl.* 26, 1055–1074. doi: 10.1890/15-1077

Because the Ocean (2019). *Ocean for Climate*. Because the Ocean. Available online at: https://www.becausetheocean.org/wp-content/uploads/2019/10/Ocean_for_Climate_Because_the_Ocean.pdf

Bindoff, N., Cheung, W., Kairo, J., Aristegui, J., Guinder, V., Hallberg, R., et al. (2019). "Changing ocean, marine ecosystems, and dependent communities," in *Special Report on Ocean and Cryosphere in a Changing Climate*, H. O. Portner, D. Roberts, V. Masson-Delmotte, and P. Zhai (Geneva: Intergovernmental Panel on Climate Change), 447–587.

Boyd, P., and Vivian, C. (2019). Should we fertilize oceans or seed clouds? no one knows. Nature 570, 155–157. doi: 10.1038/d41586-019-01790-7

Boysen, L., Lucht, W., and Gerten, D. (2017). Trade-offs for food production, nature conservation and climate limit the terrestrial carbon dioxide removal potential. *Glob. Change Biol.* 23, 4303–4317. doi: 10.1111/gcb.13745

Capron, M. E., Stewart, J. R., de Ramon N'Yeurt, A., Chambers, M. D., Kim, J. K., Yarish, C., et al. (2020). Restoring pre-industrial CO_2 levels while achieving sustainable development goals. *Energies* 13:4972. doi: 10.3390/en13184972

Ciais, P., Sabine, C., Bala, G., Bopp, L., Brovkin, V., Canadell, J., et al. (2013). "Carbon and other biogeochemical cycles," in *Climate Change 2013: The Physical Science Basis. Contribution of Working Group I to the Fifth Assessment Report of the Intergovernmental Panel on Climate Change*, eds T. Stocker, D. Qin, G. K. Plattner, M. Tignor, S. Allen, J. Boschung, A. Nauels, Y. Xia, V. Bex, and P. Midgley (Cambridge: Cambridge University Press), 465–570.

Duarte, C., Sintes, T., and Marba, N. (2013). Assessing the co|2| capture potential of seagrass restoration projects. *J. App. Ecol.* 50, 1341–1349. doi: 10.1111/1365-2664.12155

Dutreuil, S., Bopp, L., and Tagliabue, A. (2009). Impact of enhanced vertical mixing on marine biogeochemistry: lessons for geo-engineering and natural variability. *Biogeosciences* 6, 901–912. doi: 10.5194/bg-6-901-2009

Feng, E., Keller, D., Koeve, W., and Oschlies, A. (2016). Could artificial ocean alkalinization protect tropical coral ecosystems from ocean acidification? *Environ. Res. Lett.* 11:074008. doi: 10.1088/1748-9326/11/7/074008

Fennel, K. (2008). Widespread implementation of controlled upwelling in the north pacific subtropical gyre would counteract diazotrophic n_2 fixation. *Mar. Ecol. Prog. Ser.* 371, 301–303. doi: 10.3354/meps07772

Gallo, N., Victor, D., and Levin, L. (2017). Ocean commitments under the paris agreement. *Nat. Clim. Change* 7, 833–838. doi: 10.1038/nclimate3422

Gattuso, J.-P., Magnan, A., Bopp, L., Cheung, W., Duarte, C., Hinkel, J., et al. (2018). Ocean solutions to address climate change and its effects on marine ecosystems. *Front. Mar. Sci.* 5:337. doi: 10.3389/fmars.2018.00337

Gattuso, J.-P., Magnan, A. K., Gallo, N., Herr, D., Rochette, J., Vallejo, L., et al. (2019). *Opportunities for Increasing Ocean Action in Climate Strategies*. Iddri Policy Brief 02/19:1-4. Available online at: https://www.iddri.org/en/publications-and-events/policy-brief/opportunities-increasing-ocean-action-climate-strategies

GESAMP (2019). High level review of a wide range of proposed marine geoengineering techniques. *GESAMP Rep. Stud.* 98, 1–143.

Gonzalez, M., and Ilyina, T. (2016). Impacts of artificial ocean alkalinization on the carbon cycle and climate in earth system simulations. *Geophys. Res. Lett.* 43, 6493–6502. doi: 10.1002/2016GL068576

Hamilton, S., and Friess, D. (2018). Global carbon stocks and potential emissions due to mangrove deforestation from 2000 to 2012. *Nat. Clim. Change* 8, 240–244. doi: 10.1038/s41558-018-0090-4

Harrison, D. (2013). A method for estimating the cost to sequester carbon dioxide by delivering iron to the ocean. *Int. J. Glob. Warming* 5, 231–254. doi: 10.1504/IJGW.2013.055360

Harrison, D. (2017). Global negative emissions capacity of ocean macronutrient fertilization. *Environ. Res. Lett.* 12:035001. doi: 10.1088/1748-9326/aa5ef5

Harvey, L. (2008). Mitigating the atmospheric co|2| increase and ocean acidification by adding limestone powder to upwelling regions. *J. Geophys. Res.* 113:C04028. doi: 10.1029/2007JC004373

Hoegh-Guldberg, O., Caldeira, K., Chopin, T., Gaines, S., Haugan, P., Hemer, M., et al. (2019). *The Ocean as a Solution to Climate Change: Five Opportunities for Action*. World Resources Institute, Washington, DC.

Honegger, M., Michaelowa, A., and Roy, J. (2020). Potential implications of carbon dioxide removal for the sustainable development goals. Climate Policy. doi: 10.1080/14693062.2020.1843388

Howard, J., Hoyt, S., Isensee, K., Telszewski, M., and Pidgeon, E. (eds.). (2014). *Coastal Blue Carbon: Methods for Assessing Carbon Stocks and Emissions Factors in Mangroves, Tidal Salt Marshes, and Seagrasses*. Conservation International, Intergovernmental Oceanographic Commission of UNESCO, International Union for Conservation of Nature, Arlington, VA.

Howard, J., Sutton-Grier, A., Herr, D., Kleypas, J., Landis, E., McLeod, E., et al. (2017). Clarifying the role of coastal and marine systems in climate mitigation. *Front. Ecol. Environ.* 15, 42–50. doi: 10.1002/fee.1451

Ilyina, T., Wolf-Gladrow, D., Munhoven, G., and Heinze, C. (2013). Assessing the potential of calcium-based artificial ocean alkalinization to mitigate rising atmospheric co|2| and ocean acidification. *Geophys. Res. Lett*. 40, 5909–5914. doi: 10.1002/2013GL057981

IPCC (2018). "Summary for policymakers," in *Global warming of 1.5°C. An IPCC Special Report on the Impacts of Global Warming of 1.5°C Above Pre-Industrial Levels and Related Global Greenhouse Gas Emission Pathways, in the Context of Strengthening the Global Response to the Threat of Climate Change, Sustainable Development, and Efforts to Eradicate Poverty*, eds V. Masson-Delmotte, P. Zhai, H. O. Portner, D. Roberts, J. Skea, P. Shukla, A. Pirani, W. Moufouma-Okia, C. Pan, R. Pidcock, S. Connors, J. Matthews, Y. Chen, X. Zhou, M. Gomis, E. Lonnoy, T. Maycock, M. Tignor, and T. Waterfield (Geneva: Intergovernmental Panel on Climate Change), 32.

IPCC (2019). "Summary for policymakers," in *IPCC Special Report on the Ocean and Cryosphere in a Changing Climate*, eds H. O. Portner, D. Roberts, V. Masson-Delmotte, P. Zhai, E. Poloczanska, K. Mintenbeck, M. Nicolai, A. Okem, and J. Petzold (Geneva: Intergovernmental Panel on Climate Change), 3–35.

Jones, I. (2014). The cost of carbon management using ocean nourishment. *Int. J. Clim. Change Strat. Manag*. 6, 391–400. doi: 10.1108/IJCCSM-11-2012-0063

Karl, D., and Letelier, R. (2008). Nitrogen fixation-enhanced carbon sequestration in low nitrate, low chlorophyll seascapes. *Mar. Ecol. Prog. Ser*. 364, 257–268. doi: 10.3354/meps07547

Keller, D., Feng, E., and Oschlies, A. (2014). Potential climate engineering effectiveness and side effects during a high carbon dioxide-emission scenario. *Nat. Commun*. 5:3304. doi: 10.1038/ncomms4304

Köhler, P., Abrams, J., Völker, C., Hauck, J., and Wolf-Gladrow, D. (2013). Geoengineering impact of open ocean dissolution of olivine on atmospheric CO_2, surface ocean pH and marine biology. *Environ. Res. Lett*. 8:014009. doi: 10.1088/1748-9326/8/1/014009

Lenton, T. (2014). The global potential for carbon dioxide removal. *Iss. Environ. Sci. Technol*. 38, 52–79. doi: 10.1039/9781782621225-00052

Lovelock, J., and Rapley, C. (2007). Ocean pipes could help the earth to cure itself. *Nature* 449, 403–403. doi: 10.1038/449403a

Marbà, N., Arias-Ortiz, A., Masqué, P., Kendrick, G., Mazarrasa, I., Bastyan, G., et al. (2015). Impact of seagrass loss and subsequent revegetation on carbon sequestration and stocks. *J. Ecol*. 103, 296–302. doi: 10.1111/1365-2745.12370

McGee, J., Brent, K., and Burns, W. (2018). Geoengineering the oceans: an emerging frontier in international climate change governance. *Aust. J. of Marit. Ocean Affairs* 10, 67–80. doi: 10.1080/18366503.2017.1400899

McLeod, E., Chmura, G., Bouillon, S., Salm, R., Björk, M., Duarte, C., et al. (2011). A blueprint for blue carbon: toward an improved understanding of the role of vegetated coastal habitats in sequestering co|2|. *Front. Ecol. Environ*. 9, 552–560. doi: 10.1890/110004

Narayan, S., Beck, M., Wilson, P., Thomas, C., Guerrero, A., Shepard, C., et al. (2016). *Coastal Wetlands and Flood Damage Reduction: Using Risk Industry-Based Models to Assess Natural Defenses in the Northeastern USA*. Lloyd's Tercentenary Research Foundation, London.

National Academies of Sciences Engineering and Medicine (2018). *Negative Emissions Technologies and Reliable Sequestration*. The National Academies Press, Washington, DC.

Oschlies, A., Koeve, W., Rickels, W., and Rehdanz, K. (2010). Side effects and accounting aspects of hypothetical large-scale southern ocean iron fertilization. *Biogeosciences* 7, 4017–4035. doi: 10.5194/bg-7-4017-2010

Pan, Y., Fan, W., Zhang, D., Chen, J., Huang, H., Liu, S., et al. (2016). Research progress in artificial upwelling and its potential environmental effects. *Sci. China Earth Sci*. 59, 236–248. doi: 10.1007/s11430-015-5195-2

Pendleton, L., Donato, D., Murray, B., Crooks, S., Jenkins, W., Sifleet, S., et al. (2012). Estimating global "blue carbon" emissions from conversion and degradation of vegetated coastal ecosystems. *PLoS ONE* 7:e43542. doi: 10.1371/journal.pone.0043542

Renforth, P., and Henderson, G. (2017). Assessing ocean alkalinity for carbon sequestration. *Rev. Geophys*. 55, 636–674. doi: 10.1002/2016RG000533

Renforth, P., Jenkins, B., and Kruger, T. (2013). Engineering challenges of ocean liming. *Energy* 60, 442–452. doi: 10.1016/j.energy.2013.08.006

Reynolds, L., Waycott, M., McGlathery, K., and Orth, R. (2016). Ecosystem services returned through seagrass restoration. *Restor. Ecol*. 24, 583–588. doi: 10.1111/rec.12360

Rosentreter, J. A., and Williamson, P. (2020). Concerns and uncertainties relating to methane emissions synthesis for vegetated coastal ecosystems. *Glob. Change Biol*. 26, 5351–5352. doi: 10.1111/gcb.15201

Saderne, V., Geraldi, N., Macreadie, P., Maher, D., Middelburg, J., Serrano, O., et al. (2019). Role of carbonate burial in blue carbon budgets. *Nat. Commun*. 10:1106. doi: 10.1038/s41467-019-08842-6

Shepherd, J., Iglesias-Rodriguez, D., and Yool, A. (2007). Geo-engineering might cause, not cure, problems. *Nature* 449, 781–781. doi: 10.1038/449781a

Siikamaki, J., Sanchirico, J., and Jardine, S. (2012). Global economic potential for reducing carbon dioxide emissions from mangrove loss. *Proc. Nat. Acad. Sci. U.S.A*. 109, 14369–14374. doi: 10.1073/pnas.1200519109

Waycott, M., Duarte, C., Carruthers, T., Orth, R., Dennison, W., Olyarnik, S., et al. (2009). Accelerating loss of seagrasses across the globe threatens coastal ecosystems. *Proc. Nat. Acad. Sci. U.S.A*. 106:12377. doi: 10.1073/pnas.0905620106

Williamson, P., and Bodle, R. (2016). *Update on Climate Geoengineering in Relation to the Convention on Biological Diversity: Potential Impacts and Regulatory Framework*, CBD Tech. Ser. 84. Secretariat of the Convention on Biological Diversity, Montreal.

Williamson, P., Boyd, P., Harrison, D., Reynard, N., and Mashayekhi, A. (2021). "Biologically-based negative emissions in the open ocean and coastal seas," in *Negative Emission Technologies*, eds M. Bui and N. Mac Dowell (London: Royal Society of Chemistry).

Yool, A., Shepherd, J., Bryden, H., and Oschlies, A. (2009). Low efficiency of nutrient translocation for enhancing oceanic uptake of carbon dioxide. *J. Geophys. Res*. 114:C08009. doi: 10.1029/2008JC004792

Zeebe, R., and Archer, D. (2005). Feasibility of ocean fertilization and its impact on future atmospheric CO_2 levels. *Geophys. Res. Lett*. 32:L09703. doi: 10.1029/2005GL022449

Conflict of Interest: The authors declare that the research was conducted in the absence of any commercial or financial relationships that could be construed as a potential conflict of interest.

The reviewer CB declared a past co-authorship with one of the authors CD.

frontiers in Climate

PERSPECTIVE
published: 02 February 2021
doi: 10.3389/fclim.2021.576294

Casting a Wider Net on Ocean NETs

Emily Cox[1], Miranda Boettcher[2,3], Elspeth Spence[1] and Rob Bellamy[4]*

[1] School of Psychology, Cardiff University, Cardiff, United Kingdom, [2] Copernicus Institute of Sustainable Development, Utrecht University, Utrecht, Netherlands, [3] Institute for Advanced Sustainability Studies (IASS), Potsdam, Germany, [4] Department of Geography, The University of Manchester, Manchester, United Kingdom

Societal issues involving policies and publics are generally understudied in research on ocean-based Negative Emission Technologies (NETs), yet will be crucial if novel techniques are ever to function at scale. Public attitudes are vital for emerging technologies: publics influence political mandates, help determine the degree of uptake by market actors, and are key to realizing broader ambitions for robust decision-making and responsible incentivization. Discourses surrounding ocean NETs will also have fundamental effects on how governance for the techniques emerges, shaping how they are defined as an object of governance, who is assigned the authority to govern, and what instruments are deemed appropriate. This Perspective brings together key insights on the societal dimensions of ocean NETs, drawing on existing work on public acceptability, policy assessment, governance, and discourse. Ocean iron fertilization is the only ocean NET on which there exists considerable social science research thus far, and we show that much evidence points against its social desirability. Taken in conjunction with considerable natural science uncertainties, this leads us to question whether further research is actually necessary in order to rule out ocean iron fertilization as an option. For other ocean NETs, there is a need for further research into social dimensions, yet research on analogous technologies shows that ocean interventions will likely evoke strong risk perceptions, and evidence suggests that the majority of ocean NETs may face a greater public acceptability challenge than terrestrial NETs. Ocean NETs also raise complex challenges around governance, which pose questions well-beyond the remit of the natural sciences and engineering. Using a conceptual exploration of the ways in which different types of discourse may shape emerging ocean NETs governance, we show that the very idea of ocean NETs is likely to set the stage for a whole new range of contested futures.

Keywords: carbon dioxide removal, public perceptions, governance, policy assessment, discourse, negative emissions, climate change, marine geoengineering

OPEN ACCESS

Edited by:
Lennart Thomas Bach, University of Tasmania, Australia

Reviewed by:
Phillip Williamson, University of East Anglia, United Kingdom
Jonathan Symons, Macquarie University, Australia

****Correspondence:***
Emily Cox
CoxE3@cardiff.ac.uk

Specialty section:
This article was submitted to Negative Emission Technologies, a section of the journal Frontiers in Climate

Received: *25 June 2020*
Accepted: *07 January 2021*
Published: *02 February 2021*

Citation:
Cox E, Boettcher M, Spence E and Bellamy R (2021) Casting a Wider Net on Ocean NETs. Front. Clim. 3:576294. doi: 10.3389/fclim.2021.576294

INTRODUCTION

Given current atmospheric concentrations of greenhouse gases, it seems increasingly likely that both unprecedented emissions reductions and gigatonne-scale CO_2 removal will be required to keep global average temperature increase to "well below 2°C" (National Academies of Sciences, 2019). NET proposals are heterogeneous, with large uncertainties around their risks and benefits. As a hedge against unforeseen risks, including the risk of technology failure, some technical experts advise that it would be wise to explore a diverse range of NETs alongside ambitious efforts to reduce emissions (Lomax et al., 2015; Nemet et al., 2018).

The ocean has been posited by some as suitable for NETs because of its large available area, and the potential for CO_2 sequestration over extremely long timescales; yet the idea of intervening in complex marine ecosystems poses significant risks and societal concerns (GESAMP, 2019). Therefore, more research will be needed to assess which ocean NETs, where, at what scale, and under what societal conditions, might be considered as part of the climate response "toolbox." A wide variety of ocean NETs have been proposed, operating at different scales, including proposals for coastal waters (for example, restoring sea grasses and mangrove ecosystems), and proposals for international waters and the deep ocean (for example, ocean iron fertilization, direct injection of CO_2, or ocean upwelling/downwelling), as well as proposals ranging from utilization of existing biological systems to the development of highly novel engineering technologies. The technological characteristics of various ocean NETs proposals have been explored in more detail within the literature than the social science aspects; see GESAMP (2019) and National Academies of Sciences (2019) for an overview.

In this Perspective, we emphasize that assessments of the potential of ocean NETs must not be limited to technical, physical and economic questions. Research on negative emissions tends to focus on "supply-side" topics such as sequestration potential, resource availability, and cost (Nemet et al., 2018). Yet the demand side, including publics, policies and governance, will be just as important for assessing the "real world" potential of ocean NETs. Engaging with social science questions early on may help to anticipate potential pitfalls in technology development and inform the design of responsible governance mechanisms to avoid them. Engaging with wider society can additionally help to identify broader issues which experts might have missed, because they come into the topic "without blinkers on" (Cox et al., 2020a). It is also vital to assess policy options early in the innovation process, because most new technologies require the development of novel policy frameworks. Understanding the social science of ocean NETs also requires looking not only at the technologies and policies themselves, but also at the ways in which we talk about them. Understanding how discourses shape technology governance can help to avoid premature closure around solutions which may appear optimal according to particular types of knowledge, whilst simultaneously crowding out other options. This Perspective explores three fundamental aspects of the social science of ocean NETs: public perceptions, policy assessment, and the role of discourse in technology governance. The first three sections address these topics in turn, drawing on existing work on ocean NETs as well as analogous and related technologies and systems. We then identify common threads across these diverse bodies of literature, concluding with insights into the roles social science can play in the ethical and effective assessment of ocean NETs' potential as a climate response strategy.

PUBLIC PERCEPTIONS

There is little existing empirical work on public perceptions of ocean NETs. However, we can develop an idea of how perceptions are likely to emerge from research on public perceptions of the ocean, terrestrial NETs, and climate engineering (CE). Certain risk attributes have been shown to be important for a diverse range of technologies: these include the degree of control people have over the risk, its voluntariness, the possible severity of consequences, and the familiarity of the risk or system (Fischhoff et al., 1978; Slovic, 1987). In this respect, many ocean NETs proposals may be perceived as highly risky in the same way as nuclear power or Solar Radiation Management. One early UK study found lower support for ocean liming and ocean iron fertilization than for atmospheric sulfate injection, because of concerns about the riskiness, unpredictability and uncontrollability of the ocean environment (Ipsos Mori, 2010).

Previous work suggests that research carried out at small scale and under well-controlled conditions is likely to be generally acceptable (Cummings et al., 2017). However, in this respect the ocean presents challenges similar to atmospheric CE, because people may be skeptical of scientists' abilities to carry out controlled and accurate research in such an open, interconnected system (Pidgeon et al., 2013). A crucial determinant will be the extent to which ocean NETs are perceived to "tamper with nature" (Corner et al., 2013; Wolske et al., 2019). For example, when discussing oceanic disposal of CO_2, people in the United States expressed concerns about the impact this would have on marine organisms and saw it as "*…messing with some form of life…*" (Palmgren et al., 2004). The ocean is often perceived as fragile and pristine (Hawkins et al., 2016; Cox et al., 2020b), and research finds that ocean NETs might be seen as overstepping the limits of human ability to understand and control the environment (Macnaghten et al., 2015; Wibeck et al., 2017; Gannon and Hulme, 2018). Research in Scotland and Norway found that people felt changes in the deep sea would personally impact them and they were not confident in the abilities of management to protect the marine environment (Ankamah-Yeboah et al., 2020). The concern people express about the ocean is commonly linked to a positive emotional connection with it (McMahan and Estes, 2015), shown to be important for perceptions of ocean acidification (Spence et al., 2018). Despite low levels of prior awareness of ocean acidification, research in the US and UK demonstrates consistently high levels of public concern and strong emotional feelings (Capstick et al., 2016; Cooke and Kim, 2019). Importantly, NETs research suggests that emotional connection to the ocean manifests similarly in coastal and inland populations (Cox et al., 2020b).

That said, some ocean-based techniques may be perceived as more "natural" than others, for example restoration of coastal ecosystems such as mangroves, salt marshes or sea grass habitats which act as carbon sinks. Destruction of coastal ecosystems currently means that much of the carbon storage potential of these areas is being lost (Luisetti et al., 2019), and reversal of this could be perceived as a restoration of nature, rather than tampering. Similar terrestrial techniques such as peatland restoration are generally assumed to be unproblematic in terms of public perceptions (Royal Society and Royal Academy of Engineering, 2018), and work on terrestrial afforestation demonstrates that it is generally preferred (Wolske et al., 2019). However, perceptions of what constitutes

"natural" are fuzzy, dynamic, and contested, partly because even "pristine" landscapes are often the product of enormous human intervention (Corner et al., 2013). The specific context will be important: coastal restoration projects are not always without conflict, and can be socially or environmentally problematic (Myatt et al., 2003; Srivastava and Mehta, 2017). Work on terrestrial NETs also suggests that there may be trade-offs between the social and ethical impacts of a technique, and its scale of operation, which in turn affects its CO_2 sequestration potential (Cox et al., 2018); habitat restoration techniques may not benefit from the space afforded by transnational waters, and may be fundamentally constrained in their ability to sequester CO_2 over long timeframes (National Academies of Sciences, 2019).

Importantly, support or opposition for a particular project or research trial cannot be easily predicted, because it depends on when, where, and how it is implemented (Gough and Mander, 2019). Perceptions are neither fixed nor immutable, particularly in the early stages of technology scale-up; meaningful public engagement, drawing on lessons learned from other technologies, will be crucial (cf. Lockwood, 2017; Williams et al., 2017; Dwyer and Bidwell, 2019). Such flexibility early on means that views can be influenced by those with a platform, including the media, environmental organizations, and influential individuals such as celebrities or scientific advocates. For example, the first ocean iron fertilization projects encountered strong opposition from environmental organizations, which echoed people's feelings about the fragility, uncontrollability and inherent preciousness of the ocean (Fuentes-George, 2017). Such opposition was an important factor in the development of highly influential governance mechanisms which forbid the dumping of materials at sea (IMO, 2020). For lay publics, however, knowledge about novel ocean technologies is likely to be extremely low, meaning that at this stage perceptions may be mainly influenced by emotion and by risk attributes which cut across technology types (Macnaghten et al., 2015; Spence et al., 2018).

Views will also be constructed through contextually-specific local meanings (Mabon et al., 2014; Gannon and Hulme, 2018), and cultural differences will be important, such as the extent to which the ocean is perceived as an important food provider (Potts et al., 2016). Acceptance will also be highly conditional: for example, NETs are more likely to be supported as part of a package of emissions reduction policies, thus reassuring people that the "root cause" of climate change is being tackled (Cox et al., 2020b). Carbon capture and storage is widely seen as a "non-transition" (Butler et al., 2013; Mabon and Shackley, 2015), and any perception that ocean NETs are being used to continue business-as-usual may be damaging. Thus, rather than asking whether ocean NETs are publicly "acceptable, " it is more useful to identify the conditions under which a proposal might be perceived as reasonable by many people (Cox et al., 2018). Western and developing nations may also differ (Pidgeon et al., 2013; Carr and Yung, 2018), and in this respect we have precious little understanding of risk perceptions in non-western contexts. For example, a 2017 review of public perceptions research on climate engineering identified 23 studies, of which 19 included Western Europeans samples, 5 US/Canadian, and only one included a non-OECD nation. In more recent years, research on public perceptions has increased, yet the historical imbalance remains. A small number of studies find that risk perceptions in non-Western and non-affluent areas include several similar concerns regarding scale, unintended consequences, and irreversibility of techniques taking place in open environments (Winickoff et al., 2015; Carr and Yung, 2018). A study of Global South stakeholders on climate engineering found that even small experiments in open environments encountered concern regarding both physical and social risks (Winickoff et al., 2015).

POLICY ASSESSMENT

Publics—in combination with diverse experts and stakeholders—are also key to realizing broader ambitions for robust decision-making on ocean NETs. The early stage of technology development makes assessments particularly sensitive to framing effects, i.e., the conditioning of outcomes from the ways in which assessors choose to organize and communicate their assessments. Early assessments of ocean NETs have been criticized for adopting narrow framings that, among other things, employ reductive methods, exclude diverse forms of expertise, marginalize alternative options, disregard social criteria, and downplay uncertainties (Bellamy et al., 2012). Such framings have made certain technologies appear to be optimal courses of action; yet they only appear optimal under the narrow set of framings upon which their ostensible optimality is based. Accordingly, efforts are underway to broaden out and open up the framings going into assessments of ocean NETs, and to thereby render decision-making more robust. Such methods involve diverse participants, include alternative options, factor in social criteria, and are candid about uncertainties. The full range of ocean NETs are yet to be given this treatment; initial assessments of attitudes to ocean iron fertilization in Europe and Japan show it to be among the options for tackling climate change with the lowest level of public support (Bellamy et al., 2013, 2017; Amelung and Funke, 2015; Asayama et al., 2017; Jobin and Siegrist, 2020), but open policy assessment must also recognize the variety of ocean techniques, and as shown above, some may not experience the same issues as ocean iron fertilization.

These kinds of assessment are also key to growing calls for the responsible incentivization of research (Bellamy, 2018). Research into ocean NETs is undoubtedly needed, but this must be done responsibly, through broad societal participation in choosing which, if any, ocean NETs to incentivize in the first place, and continued participation in how to incentivize those NETs and ultimately in how to govern them. Building on cognate concepts of responsible innovation (Owen et al., 2013) and development (Waller et al., 2020), such a framework for incentivization encourages policy institutions and actors to go beyond technical considerations of policy design that would treat ocean NETs as though they were already fixed technologies or approaches. Instead, they are encouraged to engage with the diverse geographies of knowledge-making through which the pros and cons of ocean NETs will be negotiated in real-world contexts (Hulme, 2010). In this way, incentive and

governance regimes are not predefined for society, but defined through societal participation. So far, research is yet to gather social intelligence on what responsibly incentivized ocean NETs might look like. However, work on other NETs shows that incentives have so far been poorly aligned with societal values (Cox and Edwards, 2019) and that policy instrument choice can significantly affect public attitudes toward the technologies themselves (Bellamy et al., 2019).

More is known about preferences for governing ocean NETs. General principles drawn from the public include: (1) transparency of purposes, activities and reporting; (2) minimization and monitoring of environmental impacts; (3) independence from private interests, or at the very least sufficient oversight of them; (4) qualification of scales by perceived controllability; and (5) technology- and activity-specific governance protocols (Bellamy, 2018). Yet the dynamic and multi-faceted nature of public perceptions complicates matters, and experimental research has shown that views on what forms of governance should apply at different stages of research vary amongst people of differing underlying "worldviews" (Bellamy et al., 2017). Some have felt that self-regulation by scientists constitutes sufficient governance for small-scale or "contained" research, whereas others believe that only computational modeling should be left to self-regulation. However, people with various cultural worldviews often feel that international agreements will be necessary for large-scale, outdoors, or "uncontained" research.

THE ROLE OF DISCOURSE

Environmental and climate governance is shaped by discourse, therefore analyzing debates around emerging technologies can help us to understand how governance "truths" are produced (Leipold et al., 2019). Some work has investigated discourses on terrestrial NETs (Boettcher, 2020; Cox et al., 2020a; Low and Schäfer, 2020), but there has generally been little focus on ocean-based NETs apart from ocean iron fertilization. Most literature focuses on a run of highly controversial iron fertilization experiments between 2001 and 2012 (Buck, 2014; Fuentes-George, 2017; Horton, 2017; Gannon and Hulme, 2018), and the unique procedural dynamics of these experiments means that caution must be taken when extrapolating to other projects or technologies. However, they do provide useful lessons for other ocean NETs, in that controversy stemmed in part from divergent framings around the value of scientific uncertainty (Fuentes-George, 2017) and around mankind's relationship with nature (Gannon and Hulme, 2018).

A wider body of research on CE assesses how different types of discourse may be shaping the development of technology governance (Harnisch et al., 2015; Biermann and Möller, 2019; Boettcher, 2019; Low and Boettcher, 2020; Möller, 2020). This research has demonstrated how discussions on the feasibility and responsibility of various CE approaches have prioritized scientific and technical knowledge types (Matzner and Barben, 2018, 2020; Low and Schäfer, 2020). This is seen as particularly problematic in the Global South, where memories of broken promises mean that NETs may be seen as means for the Global North to avoid their responsibilities to reduce emissions (Cox et al., 2020a; Möller, 2020). Although the heterogeneous range of CE proposals raise differing governance challenges, a bounded range of expert knowledges have been shown to have both direct *de facto* governance effects on how the various techniques are being researched and developed, and indirect effects on how *de jure* governance (policy) is emerging (Boettcher, 2019; Gupta and Möller, 2019). Yet analyses have also shown that the idea of intervening into global systems—in particular the oceans—raises a plethora of governance questions which lie beyond the scope of purely scientific knowledge (Buck, 2014; Gannon and Hulme, 2018; McLaren, 2018). Given that ocean NETs research is still in its preliminary stages, there may be a greater opportunity to establish knowledge diversity before governance begins to emerge.

One promising analytical framework for exploring the link between discourse and ocean NETs governance is the Sociology-of-Knowledge Approach to Discourse (SKAD) (Keller, 2011; Boettcher, 2019). According to this approach, discourses are underpinning *systems of knowledge* which shape understandings of why governance is necessary, what is to be governed, by whom, and how. Therefore, discourses have a constitutive effect on what type of governance is "thinkable and practicable to both its practitioners and to those upon whom it is practiced" (Gordon, 1991, p. 3). If different systems of knowledge (discourses) become privileged in ocean NETs governance discussions, they will have varying implications for what types of governance become "thinkable and practicable." To illustrate this, **Table 1** contains a set of knowledge types which are present in the current ocean NETs debate, and a conceptual exploration of the different ways they may shape the why, what, who, and how of emerging ocean NETs governance. The table is based on a preliminary review of key literature on ocean NETs (IOC, 2010; Buck, 2014; Horton, 2017; Gannon and Hulme, 2018; Gattuso et al., 2018; Keller, 2018; Brent et al., 2019; GESAMP, 2019; McDonald et al., 2019), using a SKAD-based approach to map underpinning discourse types (see Boettcher, 2019, 2020). This thought experiment is not intended to be exhaustive or conclusive; yet it illustrates the varied, and potentially conflicting, implications that foregrounding legal, biogeochemical, economic, or cultural discourses in ocean NETs governance development may have.

DISCUSSION

This exploration of existing social science research on ocean NETs has, first and foremost, highlighted how limited the state of knowledge currently is. The only technique that has received a significant degree of attention so far is ocean iron fertilization, which has been roundly condemned in work on public perceptions and policy assessment (at least in OECD contexts), and has raised considerable concerns around prospective governance frameworks. Taken in conjunction with the exceptionally uncertain natural science of ocean iron fertilization (Strong et al., 2015), we might reasonably question whether further research is necessary in order to rule this out as an option.

In the absence of empirical research into the various other proposals for novel ocean NETs, reasonable inferences can be drawn from work on analogous techniques, including terrestrial

TABLE 1 | Shaping implications of different types of discourse for emerging Ocean NETS governance[a].

		Implications for emerging ocean NETs governance			
		Rationale (why)	**Object (what)**	**Actors (who)**	**Modes and instruments (how)**
Knowledge system/discourse	Legal	Governance of ocean NETs is needed because many ocean-based interventions would have trans-boundary effects (positive and negative), thereby contravening national jurisdictions and raising the risk of conflict	Ocean NETs approaches with trans-boundary effects. Scale of effects defining criterion	Legal experts, states, and international maritime bodies (LC/LP, UNCLOS, IOC, CBD)	Global/international, top-down. International laws, guidelines
	Bio-geochemical	Governance of ocean NETs is needed to prevent ecosystem damage, maintain marine biogeochemical systems, protect biological diversity	Ocean NETs approaches (regardless of scale) that have biogeochemical ecosystem effects. Environmental effects defining criterion	Marine biology, biogeochemical and biodiversity experts, NGOs, international maritime bodies (LC/LP, UNCLOS, IOC, CBD)	Global to local, top-down, monitoring, enforcing compliance with regulations
	Economic	Governance is needed to balance costs and (co-)benefits of ocean NETs approaches.	Cost-effective NETs approaches to be enabled, non-cost-effective to be restricted. Cost-effectiveness as defining criterion	Economic experts, assessment bodies, industrial, and commercial actors	Global to local, coordination/competition in flat hierarchies to allow the most cost-effective solutions to emerge
	Cultural	Governance is needed to preserve the cultural significance of the (natural) ocean	NETs approaches that are non-natural or invasive, that change the character of cultural (human) interactions with the ocean, alter human understandings of the natural Social acceptability within a given context as defining criterion	Cultural anthropology experts, local communities, NGOs, indigenous groups	Regional to local, bottom up, participatory engagement

[a] *LC/LP, London Convention/London Protocol on The Prevention of Marine Pollution by Dumping of Wastes and Other Matter; UNCLOS, United Nations Convention for the Law of the Sea; IOC, Intergovernmental Oceanographic Commission of UNESCO; CBD, Convention on Biological Diversity.*

NETs and climate engineering more broadly. These literatures have demonstrated that ocean interventions raise complex questions surrounding governance, which are not always within the scope of scientific/expert forms of knowledge. Discussions on the governance of ocean interventions seem likely to implicate an even wider range of discourses and types of knowledge than land-based NETs. Indeed, discussion over the emergent UNCLOS Global Ocean Treaty, which aims to protect biodiversity on the High Seas, reveals that different nations and people have very different understandings of the ocean, including whether it represents the "common heritage of mankind" (Silver et al., 2020). Similar differences concerning fundamental definitions and values were important in ocean iron fertilization controversies (Gannon and Hulme, 2018). Researchers working on ocean NETs would benefit from understanding how these diverse knowledge types may affect upstream governance of their work. They also raise tricky questions for public attitudes, because of the way in which the ocean is perceived as fragile, vital to human life, emotionally valuable, interconnected, and challenging to experiment on in an accurate and controllable manner. Evidence therefore suggests that the majority of ocean NETs will face a greater public acceptability challenge than terrestrial NETs. People will need to be assured that controlled, reversible and reliable testing can be carried out, and attempting to "communicate around" uncertainty or downplay risks is likely to backfire. That said, ocean NETs are highly diverse, and empirical research may reveal that some proposals encounter lower risk perceptions; our treatment of ocean NETs as a broad category in this short piece should not be taken to imply homogeneity. For example, some ocean NETs such as coastal habitat restoration do not claim to have trans-boundary effects, which means that they may not encounter the same governance challenges as NETs in the High Seas, and may not encounter public concerns about messing with nature. However, further research is needed, with no substitute for bespoke empirical testing. The remainder of this section sets out principles which can be used to guide responsible research and innovation in this field.

This paper has explored diverse bodies of literature on multiple social science topics, yet they all point toward the need for broad, participatory frameworks to address these issues. Engaging with a broader spectrum of actors early on can help to facilitate the development of techniques in an effective and ethical manner (Fiorino, 1990). The early stage of ocean NETs research creates unique opportunities in this regard, because the technologies and their governance are not yet "locked in." Therefore, participatory approaches could enable flexibility for establishing options for ocean NETs, including how the problems are defined, what methods are used, what criteria are selected, whose perspectives are included, and how uncertainties are conveyed (Stirling, 2007). However, previous participatory approaches have revealed challenges and constraints which will need addressing in social science research on ocean NETs. Firstly, there is the need to ensure that broader perspectives are actually integrated into the technology development, rather than as an add-on, an afterthought, or a legitimization exercise (Markusson et al., 2020). Secondly, more research is needed into frameworks for responsible incentivization, including policy mechanisms which might be able to incentivize ocean NETs even in absence of a high carbon price (Cox and Edwards, 2019). Such work needs to be better integrated into public attitudes research, that we might better understand the two-way relationship between public attitudes and policy: the ways in which publics generate the policy mandate for the incentivization of technologies, and the ways in which public attitudes depend on the policy frameworks used. Ocean NETs also raise challenges around the equitable distribution of risks and benefits, particularly for communities who are highly dependent on the ocean for their basic needs, and research is needed into the perspectives of coastal communities which may be among the most vulnerable to ocean impacts. Addressing the imbalance which currently exists in social science research on NETs, wherein the majority of information comes from Western and OECD samples, should be a priority.

There remains a lot to be done to explore the link between discursively (re)produced knowledge and ocean NETs governance development. Discursive mapping of the wider ocean NETs debate would help to identify which types of knowledge are being privileged or neglected, and what implications this may have for the emergence of ocean NETs governance. Furthermore, bringing these discourses to light may help to anticipate tensions between knowledge systems, mitigate potential conflict by integrating different knowledge types in NETs decision-making, and design deliberative processes to further "open up" discursive diversity in ocean NETs governance. The conceptual categorizations outlined in **Table 1** could provide the basis for several (complementary or competing) ocean NETs governance narratives for use in deliberative engagement. Discourse has been called "the source code with which contested futures are written" (Boettcher, 2019), and the idea of ocean NETs is likely to set the stage for a whole new range of contested futures. Further elucidating the shaping role of discourses underpinning the NETs debate is therefore key to anticipating and critically reflecting upon the emergence of ocean NETs governance.

Societal uncertainties are likely to play a key role in the emergence of NETs as a potential climate strategy. We therefore make a call for future research to "cast a wider net" on ocean NETs by taking societal and political "demand-side" dynamics seriously.

DATA AVAILABILITY STATEMENT

The original contributions presented in the study are included in the article/supplementary material, further inquiries can be directed to the corresponding author/s.

AUTHOR CONTRIBUTIONS

All authors contributed equally to the production of this paper.

FUNDING

EC and ES were funded by the Leverhulme Trust under project research grant RC-2015-029.

REFERENCES

Amelung, D., and Funke, J. (2015). Laypeople's risky decisions in the climate change context: climate engineering as a risk-defusing strategy? *Hum. Ecol. Risk Assess. Int. J.* 21, 533–559. doi: 10.1080/10807039.2014.932203

Ankamah-Yeboah, I., Xuan, B. B., Hynes, S., and Armstrong, C. W. (2020). Public perceptions of deep-sea environment: evidence from scotland and norway. *Front. Mar. Sci.* 7:137. doi: 10.3389/fmars.2020.00137

Asayama, S., Sugiyama, M., and Ishii, A. (2017). Ambivalent climate of opinions: Tensions and dilemmas in understanding geoengineering experimentation. *Geoforum* 80, 82–92. doi: 10.1016/j.geoforum.2017.01.012

Bellamy, R. (2018). Incentivize negative emissions responsibly. *Nat. Energy* 3, 532–534. doi: 10.1038/s41560-018-0156-6

Bellamy, R., Chilvers, J., Vaughan, N. E., and Lenton, T. M. (2012). A review of climate geoengineering appraisals. *Wiley Interdiscip. Rev. Clim. Change* 3, 597–615. doi: 10.1002/wcc.197

Bellamy, R., Chilvers, J., Vaughan, N. E., and Lenton, T. M. (2013). 'Opening up' geoengineering appraisal: multi-criteria mapping of options for tackling climate change. *Glob. Environ. Change* 23, 926–937. doi: 10.1016/j.gloenvcha.2013.07.011

Bellamy, R., Lezaun, J., and Palmer, J. (2017). Public perceptions of geoengineering research governance: an experimental deliberative approach. *Glob. Environ. Change* 45, 194–202. doi: 10.1016/j.gloenvcha.2017.06.004

Bellamy, R., Lezaun, J., and Palmer, J. (2019). Perceptions of bioenergy with carbon capture and storage in different policy scenarios. *Nat. Commun.* 10:743. doi: 10.1038/s41467-019-08592-5

Biermann, F., and Möller, I. (2019). Rich man's solution? Climate engineering discourses and the marginalization of the Global South. *Int. Environ. Agreem. Polit. Law Econ.* 19, 151–167. doi: 10.1007/s10784-019-09431-0

Boettcher, M. (2019). Cracking the code: how discursive structures shape climate engineering research governance. *Environ. Polit.* 29, 890–916. doi: 10.1080/09644016.2019.1670987

Boettcher, M. (2020). Coming to GRIPs with NETs discourse: implications of discursive structures for emerging governance of negative emissions technologies in the UK. *Front. Clim.* 2:595685. doi: 10.3389/fclim.2020.595685

Brent, K., Burns, W., and McGee, J. (2019). *Governance of Marine Geoengineering (Special Report)*. Waterloo, ON: Centre for International Governance Innovation.

Buck, H. J. (2014). "Village science meets global discourse : The Haida Salmon Restoration Corporation's ocean iron fertilisation experiment," in *Geoengineering Our Climate? Ethics, Politics, and Governance,* eds J. J. Blackstock and S. Low (Abingdon: Routledge), 107–112. doi: 10.4324/9780203485262-19

Butler, C., Parkhill, K., and Pidgeon, N. F. (2013). *Deliberating Energy System Transitions in the UK, Transforming the UK Energy System: Public Values, Attitudes and Acceptability*. London: UK Energy Research Centre.

Capstick, S. B., Pidgeon, N. F., Corner, A. J., Spence, E. M., and Pearson, P. N. (2016). Public understanding in Great Britain of ocean acidification. *Nat. Clim. Change* 6, 763–767. doi: 10.1038/nclimate3005

Carr, W. A., and Yung, L. (2018). Perceptions of climate engineering in the South Pacific, Sub-Saharan Africa, and North American Arctic. *Clim. Change* 147, 119–132. doi: 10.1007/s10584-018-2138-x

Cooke, S. L., and Kim, S. C. (2019). Exploring the "evil twin of global warming": public understanding of ocean acidification in the United States. *Sci. Commun.* 41, 66–89. doi: 10.1177/1075547018821434

Corner, A., Parkhill, K., Pidgeon, N., and Vaughan, N. E. (2013). Messing with nature? Exploring public perceptions of geoengineering in the UK. *Glob. Environ. Change* 23, 938–947. doi: 10.1016/j.gloenvcha.2013.06.002

Cox, E., and Edwards, N. R. (2019). Beyond carbon pricing: policy levers for negative emissions technologies. *Clim. Policy* 19, 1144–1156. doi: 10.1080/14693062.2019.1634509

Cox, E., Pidgeon, N., Spence, E., and Thomas, G. (2018). Blurred lines: the ethics and policy of greenhouse Gas Removal at scale. *Front. Environ.* Sci. 6:38. doi: 10.3389/fenvs.2018.00038

Cox, E., Spence, E., and Pidgeon, N. (2020a). Incumbency, trust and the monsanto effect: stakeholder discourses on greenhouse gas removal. *Environ. Values* 29, 197–220. doi: 10.3197/096327119X15678473650947

Cox, E., Spence, E., and Pidgeon, N. (2020b). Public perceptions of Carbon Dioxide Removal in the US and UK. *Nat. Clim. Change* 10, 744–749. doi: 10.1038/s41558-020-0823-z

Cummings, C., Lin, S., and Trump, B. (2017). Public perceptions of climate geoengineering: a systematic review of the literature. *Clim. Res.* 73, 247–264. doi: 10.3354/cr01475

Dwyer, J., and Bidwell, D. (2019). Chains of trust: Energy justice, public engagement, and the first offshore wind farm in the United States. *Energy Res. Soc. Sci.* 47, 166–176. doi: 10.1016/j.erss.2018.08.019

Fiorino, D. J. (1990). Citizen participation and environmental risk: a survey of institutional mechanisms. *Sci. Technol. Hum. Val.* 15, 226–243. doi: 10.1177/016224399001500204

Fischhoff, B., Slovic, P., Lichtenstein, S., Read, S., and Combs, B. (1978). How safe is safe enough? A psychometric study of attitudes towards technological risks and benefits. *Policy Sci.* 9, 127–152. doi: 10.1007/BF00143739

Fuentes-George, K. (2017). Consensus, certainty, and catastrophe: discourse, governance, and ocean iron fertilization. *Glob. Environ. Polit.* 17, 125–143. doi: 10.1162/GLEP_a_00404

Gannon, K. E., and Hulme, M. (2018). Geoengineering at the "Edge of the World": exploring perceptions of ocean fertilisation through the Haida Salmon Restoration Corporation. *Geo Geogr. Environ.* 5:e00054. doi: 10.1002/geo2.54

Gattuso, J.-P., Magnan, A. K., Bopp, L., Cheung, W. W. L., Duarte, C. M., Hinkel, J., et al. (2018). Ocean solutions to address climate change and its effects on marine ecosystems. *Front. Mar. Sci.* 5:337. doi: 10.3389/fmars.2018.00337

GESAMP (2019). *High Level Review of a Wide Range of Proposed Marine Geoengineering Techniques (Report of GESAMP Working Group 41 No. 98)*. London: International Maritime Organisation.

Gordon, C. (1991). "Governmental rationality: an introduction," in *The Foucault Effect: Studies in Governmentality,* eds G. Burchell, C. Gordon, and P. Miller (Chicago, IL: University of Chicago Press), 1–52.

Gough, C., and Mander, S. (2019). Beyond social acceptability: applying lessons from CCS social science to support deployment of BECCS. *Curr. Sustain. Energy Rep.* 6, 116–123. doi: 10.1007/s40518-019-0 0137-0

Gupta, A., and Möller, I. (2019). De facto governance: how authoritative assessments construct climate engineering as an object of governance. *Environ. Polit.* 28, 480–501. doi: 10.1080/09644016.2018.14 52373

Harnisch, S., Uther, S., and Boettcher, M. (2015). From "go slow" to "gung ho"? Climate engineering discourses in the UK, the US, and Germany. *Glob. Environ. Polit.* 15, 57–78. doi: 10.1162/GLEP_a_00298

Hawkins, J. P., O'Leary, B. C., Bassett, N., Peters, H., Rakowski, S., Reeve, G., et al. (2016). Public awareness and attitudes towards marine protection in the United Kingdom. *Mar. Pollut. Bull.* 111, 231–236. doi: 10.1016/j.marpolbul.2016.07.003

Horton, Z. (2017). Going rogue or becoming salmon? Geoengineering narratives in Haida Gwaii. *Cult. Crit.* 97, 128–166. doi: 10.5749/culturalcritique.97.2017.0128

Hulme, M. (2010). Problems with making and governing global kinds of knowledge. *Glob. Environ. Change* 20, 558–564. doi: 10.1016/j.gloenvcha.2010.07.005

IMO (2020). *Convention on the Prevention of Marine Pollution by Dumping of Wastes and Other Matter [WWW Document]*. Available online at: http://www.imo.org/en/OurWork/Environment/LCLP/Pages/default.aspx (accessed October 15, 2020).

IOC (2010). *Ocean Fertilization: A Scientific Summary for Policy Makers (No. IOC/BRO/2010/2)*. Paris: Intergovernmental Oceanographic Commission.

Ipsos Mori (2010). *Experiment Earth? Report on a Public Dialogue on Geoengineering*. Swindon: Natural Environment Research Council.

Jobin, M., and Siegrist, M. (2020). Support for the deployment of climate engineering: a comparison of ten different technologies. *Risk Anal.* 40, 1058–1078. doi: 10.1111/risa.13462

Keller, D. (2018). "Marine Climate-engineering," in *Handbook on Marine Environmental Protection: Science, Impacts and Sustainable Management*, eds M. Salomon and T. Markus (Cham: Springer International Publishing), 261–276. doi: 10.1007/978-3-319-60156-4

Keller, R. (2011). The sociology of knowledge approach to discourse (SKAD). *Hum. Stud.* 34, 43–65. doi: 10.1007/s10746-011-9175-z

Leipold, S., Feindt, P. H., Winkel, G., and Keller, R. (2019). Discourse analysis of environmental policy revisited: traditions, trends, perspectives. *J. Environ. Policy Plan*. 21, 445–463. doi: 10.1080/1523908X.2019.1660462

Lockwood, T. (2017). *Public Outreach Approaches for Carbon Capture and Storage Projects*. London: IEA Clean Coal Centre.

Lomax, G., Workman, M., Lenton, T., and Shah, N. (2015). Reframing the policy approach to greenhouse gas removal technologies. *Energy Policy* 78, 125–136. doi: 10.1016/j.enpol.2014.10.002

Low, S., and Boettcher, M. (2020). Delaying decarbonization: climate governmentalities and sociotechnical strategies from Copenhagen to Paris. *Earth Syst. Gov*. 5:100073. doi: 10.1016/j.esg.2020.100073

Low, S., and Schäfer, S. (2020). Is bio-energy carbon capture and storage (BECCS) feasible? The contested authority of integrated assessment modeling. *Energy Res. Soc. Sci*. 60:101326. doi: 10.1016/j.erss.2019.101326

Luisetti, T., Turner, R. K., Andrews, J. E., Jickells, T. D., Kröger, S., Diesing, M., et al. (2019). Quantifying and valuing carbon flows and stores in coastal and shelf ecosystems in the UK. *Ecosyst. Serv*. 35, 67–76. doi: 10.1016/j.ecoser.2018.10.013

Mabon, L., and Shackley, S. (2015). Meeting the targets or re-imagining society? An empirical study into the ethical landscape of carbon dioxide capture and storage in Scotland. *Environ. Val.* 24, 465–482. doi: 10.3197/096327115X14345368709907

Mabon, L., Shackley, S., and Bower-Bir, N. (2014). Perceptions of sub-seabed carbon dioxide storage in Scotland and implications for policy: a qualitative study. *Mar. Policy Compl.* 45, 9–15. doi: 10.1016/j.marpol.2013.11.011

Macnaghten, P., Davies, S. R., and Kearnes, M. (2015). Understanding public responses to emerging technologies: a narrative approach. *J. Environ. Policy Plan* 21, 504–518. doi: 10.1080/1523908X.2015.1053110

Markusson, N., Balta-Ozkan, N., Chilvers, J., Healey, P., Reiner, D., and McLaren, D. (2020). Social science sequestered. *Front. Clim.* 2:2. doi: 10.3389/fclim.2020.00002

Matzner, N., and Barben, D. (2018). "Verantwortungsvoll das Klima manipulieren? Unsicherheit und Verantwortung im Diskurs um Climate Engineering," in *Unsicherheit Als Herausforderung Für Die Wissenschaft*, eds N. Janich and L. Rhein (Berlin: Peter Lang), 143–178.

Matzner, N., and Barben, D. (2020). Climate engineering as a communication challenge: contested notions of responsibility across expert arenas of science and policy. *Sci. Commun*. 354, 182–183. doi: 10.1177/1075547019899408

McDonald, J., McGee, J., Brent, K., and Burns, W. (2019). Governing geoengineering research for the Great Barrier Reef. *Clim. Policy* 19, 801–811. doi: 10.1080/14693062.2019.1592742

McLaren, D. P. (2018). Whose climate and whose ethics? Conceptions of justice in solar geoengineering modelling. *Energy Res. Soc. Sci*. 44, 209–221. doi: 10.1016/j.erss.2018.05.021

McMahan, E. A., and Estes, D. (2015). The effect of contact with natural environments on positive and negative affect: a meta-analysis. *J. Posit. Psychol.* 10, 507–519. doi: 10.1080/17439760.2014.994224

Möller, I. (2020). Political perspectives on geoengineering: navigating problem definition and institutional fit. *Glob. Environ. Polit*. 20, 57–82. doi: 10.1162/glep_a_00547

Myatt, L. B., Scrimshaw, M. D., and Lester, J. N. (2003). Public perceptions and attitudes towards an established managed realignment scheme: Orplands, Essex, UK. *J. Environ. Manage*. 68, 173–181. doi: 10.1016/S0301-4797(03)00065-3

National Academies of Sciences, Engineering and Medicine (2019). *Negative Emissions Technologies and Reliable Sequestration: A Research Agenda.* Washington, DC: National Academies Press. doi: 10.17226/25259

Nemet, G. F., Callaghan, M. W., Creutzig, F., Fuss, S., Hartmann, J., Hilaire, J., et al. (2018). Negative emissions—Part 3: innovation and upscaling. *Environ. Res. Lett*. 13:063003. doi: 10.1088/1748-9326/aabff4

Owen, R., Bessant, J. R., and Heintz, M. (2013). *Responsible Innovation: Managing the Responsible Emergence of Science and Innovation in Society*. Chichester: John Wiley and Sons.

Palmgren, C. R., Morgan, M. G., De Bruin, W. B., and Keith, D. W. (2004). Initial public perceptions of deep geological and oceanic disposal of carbon dioxide. *Environ. Sci. Technol*. 38, 6441–6450. doi: 10.1021/es040400c

Pidgeon, N., Parkhill, K., Corner, A., and Vaughan, N. (2013). Deliberating stratospheric aerosols for climate geoengineering and the SPICE project. *Nat. Clim. Change* 3, 451–457. doi: 10.1038/nclimate1807

Potts, T., Pita, C., O'Higgins, T., and Mee, L. D. (2016). Who cares? European attitudes towards marine and coastal environments. *Mar. Policy* 72, 59–66. doi: 10.1016/j.marpol.2016.06.012

Royal Society and Royal Academy of Engineering (2018). *Greenhouse Gas Removal*. London: Royal Society and Royal Academy of Engineering.

Silver, J., Acton, L., Campbell, L., and Gray, N. (2020). *How a Global Ocean Treaty Could Protect Biodiversity in the High Seas*. The Conversation. Available online at: http://theconversation.com/how-a-global-ocean-treaty-could-protect-biodiversity-in-the-high-seas-139552 (accessed October 15, 2020).

Slovic, P. (1987). Perception of risk. *Science* 236, 280–285. doi: 10.1126/science.3563507

Spence, E., Pidgeon, N., and Pearson, P. (2018). UK public perceptions of ocean acidification – the importance of place and environmental identity. *Mar. Policy Mar.* 97, 287–293. doi: 10.1016/j.marpol.2018.04.006

Srivastava, S., and Mehta, L. (2017). *The Social Life of Mangroves - Resource Complexes and Contestations on the Industrial Coastline of Kutch, India* (STEPS Centre Working Paper). Falmer: Institute for Development Studies, University of Sussex.

Stirling, A. (2007). Risk, precaution and science: towards a more constructive policy debate. Talking point on the precautionary principle. *EMBO Rep*. 8, 309–315. doi: 10.1038/sj.embor.7400953

Strong, A., Cullen, J., and Chisholm, S. (2015). Ocean fertilization: science, policy, and commerce. *Oceanography* 22, 236–261. doi: 10.5670/oceanog.2009.83

Waller, L., Rayner, T., Chilvers, J., Gough, C. A., Lorenzoni, I., Jordan, A., et al. (2020). Contested framings of greenhouse gas removal and its feasibility: social and political dimensions. *WIREs Clim. Change* 11:e649. doi: 10.1002/wcc.649

Wibeck, V., Hansson, A., Anshelm, J., Asayama, S., Dilling, L., Feetham, P. M., et al. (2017). Making sense of climate engineering: a focus group study of lay publics in four countries. *Clim. Change* 145, 1–14. doi: 10.1007/s10584-017-2067-0

Williams, L., Macnaghten, P., Davies, R., and Curtis, S. (2017). Framing 'fracking': exploring public perceptions of hydraulic fracturing in the United Kingdom. *Public Underst. Sci*. 26, 89–104. doi: 10.1177/0963662515595159

Winickoff, D. E., Flegal, J. A., and Asrat, A. (2015). Engaging the Global South on climate engineering research. *Nat. Clim. Change* 5, 627–634. doi: 10.1038/nclimate2632

Wolske, K. S., Raimi, K. T., Campbell-Arvai, V., and Hart, P. S. (2019). Public support for carbon dioxide removal strategies: the role of tampering with nature perceptions. *Clim. Change* 152, 345–361. doi: 10.1007/s10584-019-02375-z

Conflict of Interest: The authors declare that the research was conducted in the absence of any commercial or financial relationships that could be construed as a potential conflict of interest.

frontiers FOR YOUNG MINDS

THE EARTH AND ITS RESOURCES
Published: 03 February 2021
doi: 10.3389/frym.2020.592018

CAPTURING AND REUSING CO_2 BY CONVERTING IT TO ROCKS

Caleb M. Woodall[1*], *Isabella Piccione*[1], *Michela Benazzi*[1] *and Jennifer Wilcox*[2]

[1] *Department of Chemical Engineering, Worcester Polytechnic Institute, Worcester, MA, United States*

[2] *Department of Chemical and Biomolecular Engineering, School of Engineering and Applied Science, University of Pennsylvania, Philadelphia, PA, United States*

YOUNG REVIEWER:

MARTA

AGE: 14

Within Earth's surface, there are billions of tons of rocks containing minerals that are reactive with CO_2, which is a greenhouse gas that has harmful effects on our planet's climate. Over thousands of years, these minerals interact with the CO_2 in the air, converting the gas into new carbonate minerals and permanently storing the CO_2 in a solid form. Today, as society develops solutions to combat the harmful effects of excess CO_2 in our atmosphere, the processes carried out by these reactive minerals could present a valuable opportunity. There is a challenge of speeding up the reactions so they happen within days (or even weeks), rather than thousands of years. Climate solutions like this are still new and will require more young and enthusiastic minds to advance their development so our climate is livable for generations to come!

WHY IS CO_2 HARMFUL, AND WHAT CAN BE DONE?

Since the late 1880s, we have used fossil fuels as our main source of energy. Fossil fuels include coal, petroleum, and natural gas. While they give us a lot of energy, they are also in limited supply, and they emit carbon dioxide (CO_2) when we burn them. Release of CO_2 into the atmosphere contributes to unfavorable changes in our planet's climate.

There are several ways to reduce the amount of CO_2 being emitted into Earth's atmosphere. One approach is replacing fossil fuel energy with **renewable energy**, like solar and wind, which do not emit CO_2. Another approach is to use energy-efficient technologies that require less energy, such as electric cars and LED bulbs. However, some CO_2 emissions cannot be avoided, and we call these "hard-to-avoid" emissions. These are most often found in industrial processes, like those that produce cement, iron, and steel. Because these products are necessary for building our roads, bridges, and buildings, it is important to find ways to avoid the emissions caused by their production. That is where **carbon capture** comes in to save the day!

Carbon capture works exactly as it sounds: technologies that "capture" CO_2 from emission sources. There are a lot of ways to go about capturing CO_2. One approach is called carbon mineralization, in which the CO_2 gas reacts with certain minerals to form new minerals, called **carbonates**.

RENEWABLE ENERGY

Energy that comes from a source that is in such abundance that it cannot be used up, such as wind or solar energies.

CARBON CAPTURE

A technology that captures CO_2 from emission sources (or directly from the air) to prevent the CO_2 from causing changes to Earth's climate.

CARBONATES

Solid minerals that are formed from interactions with CO_2 and water.

WHAT ARE CARBONATE MINERALS?

You have likely already seen lots of carbonate minerals since they are the building blocks of things like seashells, chalk, and concrete. These three examples all contain calcium carbonate ($CaCO_3$), which is also called limestone. The idea of carbon mineralization is based on a natural process called **mineral weathering**, in which certain minerals interact with CO_2 in the air, forming white carbonate minerals like those in the White Cliffs of Dover below (Figure 1). This process occurs over thousands of years, but if it could be sped up to take place over hours or days, we could use this approach to capture and store CO_2!

MINERAL WEATHERING

A natural process where rocks and minerals break down to form new rocks and minerals. Weathering can involve reactions with CO_2 from the atmosphere, leading to carbonate formation.

HOW DOES CARBON MINERALIZATION WORK?

The idea of a gas changing to a solid may seem strange, but it happens in other ways that you see every day. The orange rust you see on old metal objects like cars and bikes forms when iron gets wet and reacts with oxygen in the air. The frost you might see on your window in the winter is due to the water vapor in warm humid air touching the

Figure 1

You may have already seen carbonate minerals without realizing it. Calcium carbonate makes up seashells, chalk, and even the White Cliffs of Dover shown here. Carbonates can form from a variety of ways, all involving interactions with calcium and CO_2 that is dissolved in the water.

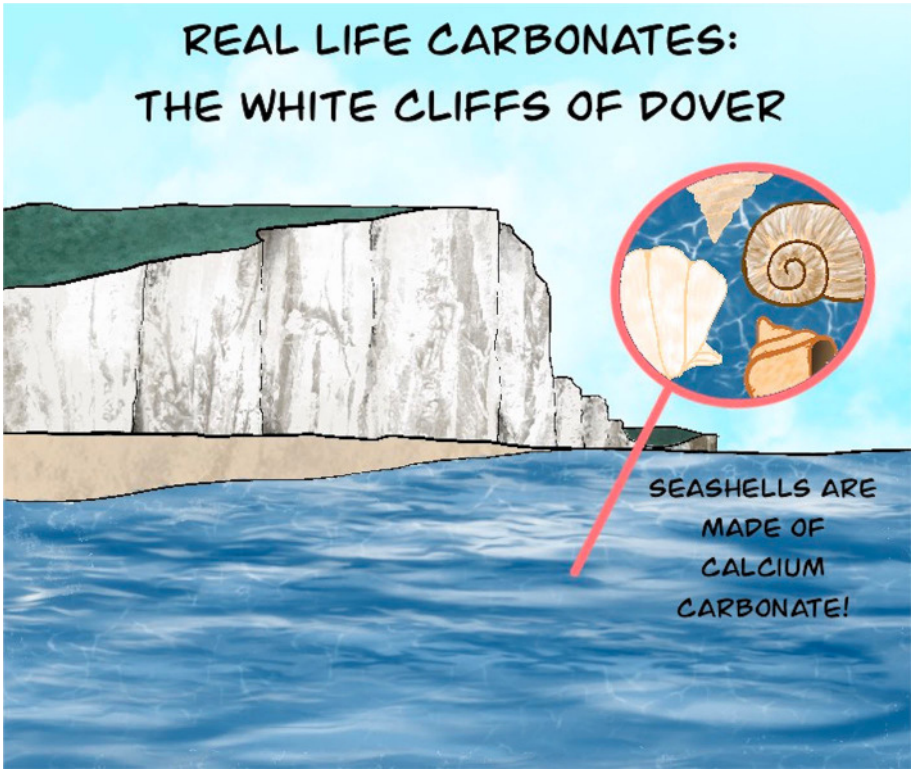

Figure 1

cold glass surface. In the case of carbon mineralization, when certain reactive minerals become wet and come into contact with CO_2, they react to form carbonates, permanently storing CO_2 and keeping it out of the atmosphere for thousands of years.

ULTRAMAFIC ROCK

Rocks with relatively large amounts of magnesium, making them ideal for carbon mineralization.

The reactive minerals used for carbon mineralization need to contain high amounts of calcium or magnesium. These can be found naturally in **ultramafic rocks**, which are found in the earth on a scale of up to hundreds of billions of tons (>100,000,000,000 tons). Reactive minerals can also be found in wastes from industrial and mining processes. When important materials are made (like iron, steel, or cement) or mined (like diamonds, nickel, or copper), waste is generated and placed in piles near the facility. Much of this waste is rich in calcium or magnesium.

It is important to remember that CO_2 is also a waste gas in our atmosphere. Ever since human civilization started using fossil fuels, this heat-trapping gas has been released into the air as a waste product of combustion. Using carbon mineralization, ultramafic rocks and industrial/mining waste could react with the waste CO_2 present in the air to form carbonate minerals, helping to remove CO_2 from the air and prevent it from accumulating to excessive amounts. This waste management process is illustrated in Figure 2.

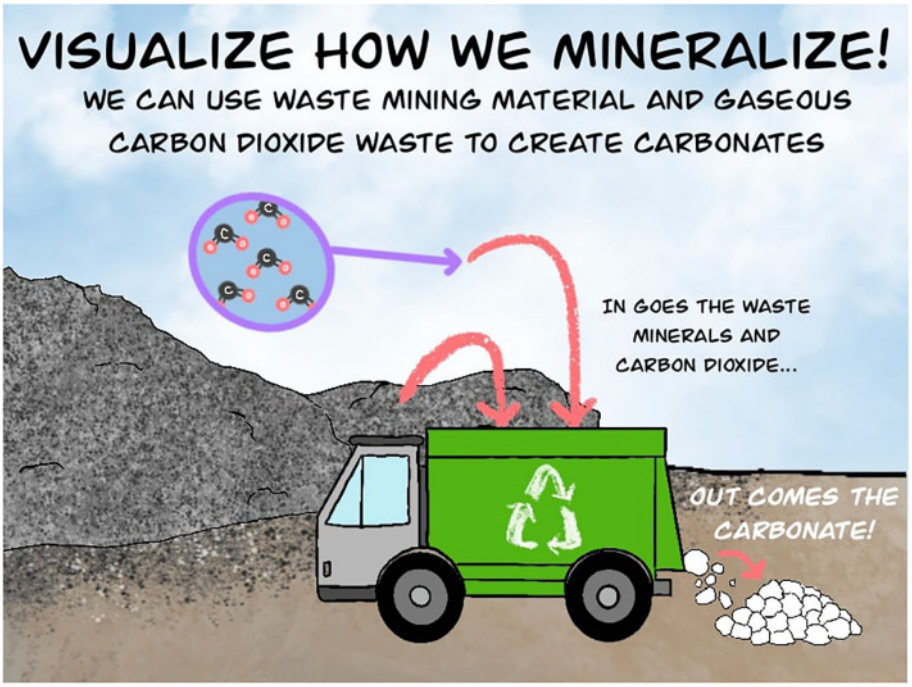

Figure 2

Carbon mineralization involves combining two forms of waste to make new carbonate products. When valuable materials are made (like iron, steel, and cement) or mined (like diamonds, nickel, and copper), solid wastes are also produced, which are often rich in calcium or magnesium. The same processes that produce or mine these valuable materials often also produce CO_2 as a waste that is emitted into the atmosphere. As shown in this figure, the waste CO_2 can be combined with the solid wastes to produce new carbonate minerals.

WHAT CAN WE DO WITH THE CARBONATE PRODUCTS?

The process of using the products produced from carbon mineralization is known as **CO_2 utilization**. Carbon mineralization can be expensive, so by selling the carbonate products, money can be made so that the process is more affordable. Also, if the carbonate products can be made into building materials, like concrete, these new building materials could replace current building materials that emit CO_2 when produced, so CO_2 utilization could potentially avoid tons of CO_2 emissions!

CO_2 UTILIZATION

The process of changing CO_2 into a new form and using it as a valuable product.

Let us look at concrete as an example. Concrete is made from a mixture of cement, **aggregates**, and water (Figure 3). Cement acts as the glue that binds the ingredients together. Various sizes of aggregates, such as gravel or sand, are used to provide volume and stability to the concrete. The water allows the concrete to be mixed well before it hardens.

AGGREGATES

Non-reactive materials that provide volume and stability to concrete, ranging from small sand particles to larger gravel rocks.

Cement production creates a lot of CO_2–it accounts for 8% of all of humanity's CO_2 emissions! Researchers are trying to find ways to reduce cement-related emissions by reducing the amount of cement used in concrete or by changing the way cement is produced. Successful changes in the cement industry could have a major impact on the amount of CO_2 being emitted into our atmosphere! Some companies are using carbonate minerals to create new aggregates for concrete that are more useful than normal aggregates. Some companies have figured out a way to inject CO_2 directly into wet concrete, where it reacts and causes the concrete to become even

Figure 3

Concrete is made up of cement, water, and aggregates. Aggregates are particles of various sizes, such as gravel or sand, and they provide volume and stability to the concrete. Cement acts as the glue that binds the aggregates together. Water is added to allow the concrete to mix well before it hardens.

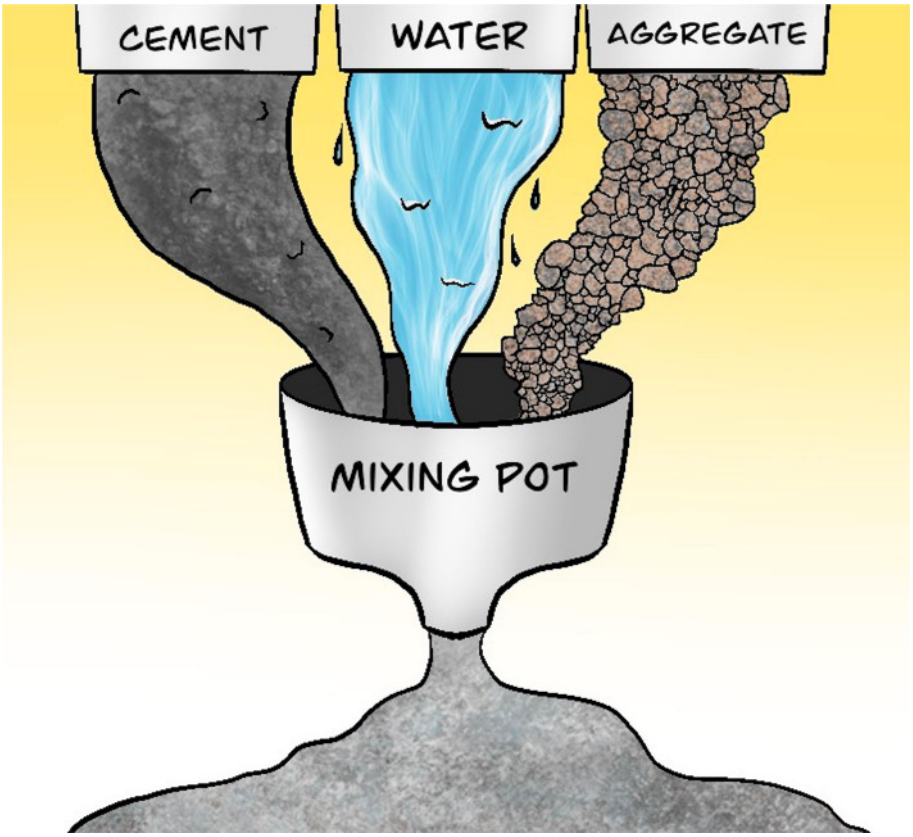

Figure 3

stronger once it dries. Other companies get creative by using different sources of calcium (like industrial wastes) as a new cement in their concrete.

There are already companies around the world that are using carbon mineralization to create new building products, but they are facing a difficult task. Most of the building materials we have today are cheap and relatively easy to use, so replacing them requires some creativity. It is not impossible to replace a cheap and useful product with a new one; take phones as an example. Before we had iPhones, we had basic flip phones that were simple, functional, and cheap. The iPhone became popular not because it was more affordable than a flip phone, but because it was a better product. Hence, new carbonate building materials must offer better features than materials that are currently available and release less CO_2 during their manufacture than current products do.

HOW DEVELOPED IS THIS TECHNOLOGY?

Building materials made from mineral carbonates have significant potential to decrease CO_2 emissions in the cement industry. However, for the technology to become popular, work still needs to be done in several areas:

- **Research:** The process to make carbonates with CO_2 is still expensive and complicated, and it needs to be improved. More research is also needed to prove that the new cement and concrete are better than the ones we have now.
- **Carbon incentives**: There are ways for the government to pay money to people who store CO_2 and prevent it from entering the air, "incentivizing" CO_2 storage and use. This would help carbon mineralization be more affordable.
- **Regulations**: There are strict regulations that dictate which materials can be used to make concrete for roads and buildings. Some of the regulations are old and could be updated to encourage the use of new carbonate materials. This would depend on whether the new materials are proven to perform well.

CARBON MINERALIZATION IN THE OCEAN

EQUILIBRIUM

A balance between opposite forces.

Just as CO_2 is floating in our air, it is also dissolved into our oceans. This is similar to how CO_2 is dissolved in your fizzy soft drinks. The CO_2 gas likes to be in **equilibrium** between the air and water. Because there is more CO_2 in a soda can than in the air around it, when you open a soda can, the CO_2 quickly leaves the can and enters the air so it can reach equilibrium.

Our oceans do not make bubbles like soda because the CO_2 is already in equilibrium between the ocean and the air. By adding calcium and magnesium to the ocean, the CO_2 dissolved in the ocean can mineralize and form carbonate minerals, reducing amount of CO_2 in the water and disturbing the equilibrium. This will cause more CO_2 to leave the air and enter the ocean. Scientists are researching safe ways to add calcium and magnesium to the oceans so that we can use the help of the oceans to remove CO_2 from the atmosphere! [1].

HOW CAN YOU GET INVOLVED?

Carbon mineralization is just one of the many solutions that are needed to stop Earth's climate from changing. All of the solutions will require help from all sorts of minds. For example, while scientists and engineers can help to develop carbon mineralization and other technologies, politicians and lawyers can help with government policies that encourage climate solutions, and journalists can communicate new technologies to the public. Additionally, we can all try to reduce our own carbon emissions by changing our everyday habits, such as by using less electricity or carpooling. Climate change will be a big problem for many years to come, but if everyone takes their own steps to help the fight, the problem could very well be solved!

REFERENCES

1. Renforth, P., and Henderson, G. 2017. Assessing ocean alkalinity for carbon sequestration. *Rev. Geophys.* 55:636–74. doi: 10.1002/2016RG000533

SUBMITTED: 06 August 2020; **ACCEPTED:** 21 December 2020;
PUBLISHED ONLINE: 03 February 2021.

EDITED BY: Kerryn Brent, University of Adelaide, Australia

CITATION: Woodall CM, Piccione I, Benazzi M and Wilcox J (2021) Capturing and Reusing CO_2 by Converting It To Rocks. Front. Young Minds 8:592018. doi: 10.3389/frym.2020.592018

CONFLICT OF INTEREST: The authors declare that the research was conducted in the absence of any commercial or financial relationships that could be construed as a potential conflict of interest.

YOUNG REVIEWER

MARTA, AGE: 14
My name is Marta, I am 14 years old and I live in Italy. I play volleyball. In my free time I like meeting my friends and reading. My favorite book is Harry Potter. I also like listening to music.

AUTHORS

CALEB M. WOODALL
I am a Ph.D. candidate in Chemical Engineering at Worcester Polytechnic Institute (WPI). My research works to advance carbon mineralization from several angles. In the lab, this includes developing and optimizing processes to react CO_2 with mine tailings, analyzing the economics of mineralization processes, and assessing the impact of utilizing the carbonate products. I am also particularly interested in broader communication and impact of mineralization technology, exhibited through youth outreach and work as a Policy Fellow at Clear Path. *cmwoodall@wpi.edu

ISABELLA PICCIONE

I am a third-year undergraduate researcher at Worcester Polytechnic Institute, studying Chemical Engineering. I am passionate about providing exciting and engaging STEM education content to young students. I was inspired to get into STEM by my teachers who made these complex topics fun and straightforward, and I want to be that for the new generation of scientists. In my spare time, I like to make jewelry and go to the beach!

MICHELA BENAZZI

I am an undergraduate researcher in Chemical Engineering at Worcester Polytechnic Institute. My work focuses primarily on climate mitigation technology and climate refugees. I am currently developing a laboratory curriculum inspired by the environmental assessment of Kivalina and by the climate mitigation techniques of Carbon Mineralization, Regenerative Ocean Farming, and the Artificial and Bionic Leaf. I have previously been the recipient of the Outstanding Performance Award at the International Symposium on STEM Education (University of Hong Kong, 2018).

JENNIFER WILCOX

I am the Presidential Distinguished Professor of Chemical Engineering and Energy Policy at the University of Pennsylvania and am also a Senior Fellow at the World Resources Institute. My research takes aim at the nexus of energy and the environment, developing both mitigation and adaptation strategies to minimize negative climate impacts associated with society's dependence on fossil fuels.

frontiers in Climate

ORIGINAL RESEARCH
published: 18 March 2021
doi: 10.3389/fclim.2021.614537

Alkalinization Scenarios in the Mediterranean Sea for Efficient Removal of Atmospheric CO_2 and the Mitigation of Ocean Acidification

Momme Butenschön[1]*, *Tomas Lovato*[1], *Simona Masina*[1], *Stefano Caserini*[2] and *Mario Grosso*[2]

[1] Ocean Modeling and Data Assimilation Division, Centro Euro-Mediterraneo sui Cambiamenti Climatici, Bologna, Italy,
[2] Dipartimento di Ingegneria Civile e Ambientale, Politecnico di Milano, Milan, Italy

It is now widely recognized that in order to reach the target of limiting global warming to well below 2°C above pre-industrial levels (as the objective of the Paris agreement), cutting the carbon emissions even at an unprecedented pace will not be sufficient, but there is the need for development and implementation of active Carbon Dioxide Removal (CDR) strategies. Among the CDR strategies that currently exist, relatively few studies have assessed the mitigation capacity of ocean-based Negative Emission Technologies (NET) and the feasibility of their implementation on a larger scale to support efficient implementation strategies of CDR. This study investigates the case of ocean alkalinization, which has the additional potential of contrasting the ongoing acidification resulting from increased uptake of atmospheric CO_2 by the seas. More specifically, we present an analysis of marine alkalinization applied to the Mediterranean Sea taking into consideration the regional characteristics of the basin. Rather than using idealized spatially homogenous scenarios of alkalinization as done in previous studies, which are practically hard to implement, we use a set of numerical simulations of alkalinization based on current shipping routes to quantitatively assess the alkalinization efficiency via a coupled physical-biogeochemical model (NEMO-BFM) for the Mediterranean Sea at 1/16° horizontal resolution (∼6 km) under an RCP4.5 scenario over the next decades. Simulations suggest the potential of nearly doubling the carbon-dioxide uptake rate of the Mediterranean Sea after 30 years of alkalinization, and of neutralizing the mean surface acidification trend of the baseline scenario without alkalinization over the same time span. These levels are achieved via two different alkalinization strategies that are technically feasible using the current network of cargo and tanker ships: a first approach applying annual discharge of 200 Mt $Ca(OH)_2$ constant over the alkalinization period and a second approach with gradually increasing discharge proportional to the surface pH trend of the baseline scenario, reaching similar amounts of annual discharge by the end of the alkalinization period. We demonstrate that the latter approach allows to stabilize the mean surface pH at present day values and substantially increase the potential to counteract acidification relative to the alkalinity added, while the carbon uptake efficiency (mole of CO_2 absorbed by the ocean per mole of alkalinity added) is only marginally

OPEN ACCESS

Edited by:
David Peter Keller, GEOMAR Helmholtz Center for Ocean Research Kiel, Germany

Reviewed by:
Peter Köhler, Alfred Wegener Institute Helmholtz Center for Polar and Marine Research, Germany
Friederike Fröb, Max Planck Society, Germany

***Correspondence:**
Momme Butenschön
momme.butenschon@cmcc.it

Specialty section:
This article was submitted to Negative Emission Technologies, a section of the journal Frontiers in Climate

Received: *06 October 2020*
Accepted: *12 February 2021*
Published: *18 March 2021*

Citation:
Butenschön M, Lovato T, Masina S, Caserini S and Grosso M (2021) Alkalinization Scenarios in the Mediterranean Sea for Efficient Removal of Atmospheric CO_2 and the Mitigation of Ocean Acidification. Front. Clim. 3:614537. doi: 10.3389/fclim.2021.614537

reduced. Nevertheless, significant local alterations of the surface pH persist, calling for an investigation of the physiological and ecological implications of the extent of these alterations to the carbonate system in the short to medium term in order to support a safe, sustainable application of this CDR implementation.

Keywords: climate change mitigation, ocean acidification, ocean alkalinization, Mediterranean sea, carbon dioxide removal, negative emission technologies, regional ocean model

1. INTRODUCTION

The Paris agreement of 2015 has set a cornerstone in international climate policy by defining the goal of limiting global warming to well below 2°C, a goal that is driven by the necessity to avoid irreversible change and to restrain intolerable risks to humanity, and supported by the feasibility to achieve this goal and by its simplicity as a tangible target bridging the communication gap between science and policy (Schellnhuber et al., 2016). It is widely accepted that to achieve this goal, it will not be sufficient to limit CO_2 emissions, but it will require the implementation of active CO_2 removal from the atmosphere (CDR) via negative emission technologies (NETs) (IPCC, 2018), as confirmed by the most recent generation of climate model projections within the CMIP6 initiative (Tokarska et al., 2020). Several candidates of NETs have been discussed in the past. Williamson (2016) has underlined that the requirement of the implementation of NETs to reach the goals of the Paris agreement calls for a broad assessment of the viability of CDR and demands urgent action. While some studies have emerged that assess NETs in theoretical, idealized experiments (e.g., Keller et al., 2014), high-level reports of various international bodies have identified the gap in current knowledge between these scientific intellectual exercises investigating the potential of a given NET and the feasibility of their practical implementation (Renforth and Wilcox, 2020). The ocean plays a particular role in the climate system acting as significant sink of atmospheric heat and CO_2 due to its greater heat capacity, solubility, and inertia. Recent estimates suggest that the ocean has taken up more than 90% of the excess heat in the climate system since 1970 and 20–30% of anthropogenic carbon since the 1980s (IPCC, 2019; von Schuckmann et al., 2020). This has caused the additional hazard of ocean acidification lowering the average pH of the ocean surface by approximately 0.017–0.027 units per decade. The pH alteration of ocean seawater since the pre-industrial period, that is unprecedented in the last 65 million years (Hoegh-Guldberg et al., 2018), has significant implications for marine organisms affecting their metabolic regulation and capability to form calcium carbonate (Kroeker et al., 2013), destabilizing the ecosystem and ultimately threatening vital ecosystem services (Gattuso et al., 2015).

Among the ocean-based NETs, artificial ocean alkalinization via the dissolution of $Ca(OH)_2$, known in short as ocean liming, has attracted attention due to its capability of contemporarily addressing two issues: global warming via increased uptake of CO_2 and ocean acidification. The principle behind ocean liming is based on the dissociation of calcium hydroxide and carbon-dioxide to calcium ions and bicarbonate:

$$Ca(OH)_2 + 2CO_2 \Longleftrightarrow Ca^{2+} + 2HCO_3^- \,. \qquad (1)$$

Hence, per mole of added slaked lime this reaction in principle consumes two moles of aqueous CO_2 increasing the alkalinity of the water body by two mole equivalents. It should be noted however, that this consumption of aqueous CO_2 does not correspond directly to a removal of atmospheric CO_2, which instead depends on the difference in partial pressure of CO_2 between sea and atmosphere at the water surface. The concentrations of dissolved inorganic carbon species within the carbonate system resulting from the reactions above adjust to a new equilibrium state depending on the environmental conditions in place (Zeebe and Wolf-Gladrow, 2001) and part of the added alkalinity is removed from the surface through advective, diffusive processes, and convection. The combination of these processes, along with the local temperature, salinity, and pressure, ultimately determine the partial pressure of CO_2 in the seawater and its pH. Furthermore, the production of slaked lime itself generates a considerable amount of CO_2 (Renforth et al., 2013). Even if the generated carbon-dioxide is generally of high purity and therefore feasible for geological storage, this underpins the requirement of CO_2 and cost-efficient technologies to provide slaked lime. In response to this challenge, Caserini et al. (2019) have proposed a combination of ocean liming, CO_2 storage and commercial industrial technologies producing H_2 as a by-product, that significantly improves the efficiency and reduces the cost of the overall process, but ultimately any full-scale implementation will need to be carefully balanced against the projected cost of CO_2 emissions.

Several studies have investigated the mitigation potential of ocean liming applications at the global scales via model projections of theoretical alkalinization scenarios following different strategies. Ilyina et al. (2013) used a global ocean biogeochemistry model to project a suite of scenarios with alkalinization levels applied homogeneously over areas of varying extend proportional to anthropogenic CO_2 emissions, corresponding to about 2.4 Pmol/y of alkalinity (approximately 89 Pg $Ca(OH)_2$/y) in the initial phase of the experiment, based on a scenario of rapid growth supported by intermediate use of fossil energy sources (SRES A1B). In their conclusions the authors indicate that a 2:1 molar ratio of added alkalinity per emitted CO_2 applied over a large area is required to fully counteract the decrease in mean global surface ocean pH, leading however to local conditions in the carbonate chemistry that exceed significantly from the range of natural variability. Keller

et al. (2014) projected in an Earth System Model a scenario of alkalinity discharge at 10 Pg $Ca(OH)_2$/y uniform in space and time corresponding roughly to the maximum carrying capacity of large cargo and tanker ships against an RCP8.5 baseline scenario, finding that even at this scale the potential in terms of mitigating atmospheric CO_2 levels and consequently global warming are marginal. Lenton et al. (2018) implemented a similar scenario with a global annual discharge of 0.25 Pmol/y (∼9.3 Pg $Ca(OH)_2$/y), but based on two opposing baselines of unmitigated (RCP8.5) vs. strongly mitigated (RCP2.6) climate change, revealing a significantly higher relative efficiency at lower emissions. In addition they showed a low sensitivity of the process when applied to large latitudinal bands or in different seasons with respect to a spatial and temporal homogeneous application of alkalinization. González and Ilyina (2016) constructed an alkalinization scenario based on a RCP8.5 with gradually increasing alkalinity additions calibrated to reach the atmospheric CO_2 levels of a corresponding RCP4.5 projection, concluding that 114 Pmol would be required to achieve the goal over the period from 2018 to 2100, at the price of unprecedented ocean biogeochemistry perturbations with unknown ecological consequences. None of these works however considered the practicalities of an actual large-scale implementation of ocean liming or investigated the relative efficiencies and sensitivities of different strategies with respect to the oceanic uptake of CO_2 and the mitigation of ocean acidification.

Here we propose a quantitative study of the potential of a practical, regional implementation of ocean liming to the Mediterranean Sea based on the existing network of tankers and cargo ships. The regional application of ocean liming to the Mediterranean Sea is supported by two factors: its wide coverage through existing shipping routes across the basin and its physical and biogeochemical characteristics. In fact, its strategic location enclosed by three continents and providing a short-cut connecting two ocean basins via the Suez channel results in a dense network of shipping traffic (see section 2). Such commercial routes provide an opportunity for the implementation of ocean liming using existing traffic as vehicle to distribute lime across the basin with very limited additional cost due to increased load ballast.

At the same time the physical characteristics of the semi-enclosed basin with only a small opening at the Gibraltar Straight strongly dominated by surface inflow, and with strong major currents leading to wide circulation patterns with small overturning cells at the Northern parts of the two sub-basins (Millot and Taupier-Letage, 2005; Pinardi et al., 2019) lead to an efficient distribution of discharged lime across the area limiting uncontrolled dispersal into confining waters. Moreover, the region represents an area of accumulation of anthropogenic carbon uptake (IPCC, 2013; Khatiwala et al., 2013; Palmiéri et al., 2015) and is generally recognized as a hotspot of climate change (Giorgi, 2006; UNEP/MAP, 2017) showing clear trends of warming and acidification across virtually the entire basin (MedSea, 2014; Lacoue-Labarthe et al., 2016; Soto-Navarro et al., 2020), which are nevertheless subject to high regional variability depending on physical (stratification, overturning) and biogeochemical features (productivity, alkalinity).

Alkalinization in the Mediterranean Sea is assessed in this study following two different approaches of lime discharge: a constant annual discharge and a time-varying approach based on the acidification trend of the basin without alkalinization. This strategy allows us to assess the evolution of the system for each individual approach and compare their respective potentials in mitigating the atmospheric CO_2 increases and the ocean acidification.

2. METHODS

The model simulations performed in this study are ocean-only experiments of a regional marine biogeochemical model system with concentration driven atmospheric boundary conditions of CO_2. It should be noted that this approach does not include feedback processes of the marine carbonate chemistry with the atmospheric concentrations, which is nevertheless justifiable in this context as the increase of the carbon sink due to alkalinization across the Mediterranean Sea emerging from this study is expected to be small compared to the global atmospheric carbon reservoir (approximately 800 GtC, Friedlingstein et al., 2019) and due to the swift adjustment of the atmospheric concentrations given the rapid mixing time scales of the atmospheric dynamics. It allows for simulations of multiple decades of different alkalinization scenarios required for the purpose of this work at resolutions that resolve the Mediterranean Sea dynamics, which would be unfeasible in a fully coupled system.

2.1. NEMO-BFM Model

The model used to simulate the marine physical and biogeochemical dynamics is composed by the general circulation ocean model NEMO (v3.4, Madec et al., 2013) and the Biogeochemical Flux Model (BFM v5.2, Vichi et al., 2020). Its application to the Mediterranean Sea relies on a spatial grid with a horizontal resolution of 1/16° degree (which corresponds to about 6.5 km) and a vertical z-coordinate discretization in 72 levels, with spacing ranging from 3 m in surface layer to 350 m at the bottom. The parameterizations and numerical schemes used to resolve the physical processes are thoroughly described in Oddo et al. (2009), therein referred to as MFS_V2.2 configuration. With respect to previous applications of the BFM (Lazzari et al., 2012; Cossarini et al., 2015; Visinelli et al., 2016), the ecosystem structure setup for the present work can be considered a light-weight implementation that accounts for two primary producers (Diatoms and Nanoflagellates) and two predator types (Micro- and Meso-zooplankton). A key difference is the representation of zooplankton and bacteria functional groups at fixed stoichiometric ratios. A total of 32 state variables are considered in the model, including dissolved inorganic constituents and dissolved and particulate organic matter. The parametrization of living and nonliving functional rates derives from Vichi et al. (2013). The carbonate system dynamics described by the prognostic evolution of Dissolved Inorganic Carbon (DIC) and Total Alkalinity (TA) and parameterizations for chemical dissociation rates and gas exchanges were set in agreement with the protocol described in Orr et al. (2017).

2.2. Reference Simulation

A reference experiment was designed to reproduce the physical and biogeochemical evolution of the Mediterranean Sea determined by the meteoclimatic forcing representative of present and future conditions under the RCP4.5 scenario (Moss et al., 2010), namely for the 2000–2050 period. In contrast to most previous works on ocean alkalinization that are based on scenarios with comparatively high levels of greenhouse gas concentrations (RCP8.5 or SRES A1B) we chose a scenario with an intermediate concentration pathway as baseline to recognize the fact that liming on its own is unlikely sufficient as a mitigation measure against global warming (e.g., Ilyina et al., 2013; Keller et al., 2014) and unlikely to be applied as a single strategy, but in combination with other mitigation strategies. In fact, a strong commitment to greenhouse gas emission reductions has been declared within the UNFCC process (UNFCCC, 2020) and net-zero emission targets have been declared by 823 cities, 101 regions, and 1541 companies (Data-Driven EnviroLab and NewClimate Institute, 2020).

Physical boundary conditions were extracted from the CMIP5 dataset of the atmosphere-ocean global circulation model CMCC-CM (Scoccimarro et al., 2011) and consist of 6-hourly atmospheric fields, daily fresh water discharges (rivers and Black Sea exchange), and monthly fields of temperature, salinity, and velocities prescribed at the open lateral boundaries in the neighboring parts of the Atlantic ocean (see Lovato et al., 2013 for technical details). The initial conditions for seawater temperature, salinity, dissolved oxygen, nitrate, phosphate, and silicate were derived from the SeaDataNet database (http://www.seadatanet.org/), while for DIC and TA two gridded datasets were blended in correspondence of the Gibraltar Strait: GLODAPv2 (Olsen et al., 2016) for the Atlantic region and the reconstructed fields of Lovato and Vichi (2015) for the Mediterranean sea. Biogeochemical properties at the lateral open boundaries were solved with a zero-gradient condition, as the Atlantic region included in the model is big enough to allow for internal adjustment of the ecosystem dynamics with minor drifts.

The terrestrial inputs of dissolved inorganic nutrients (nitrate, phosphate, and silicate) were prescribed using monthly climatologies corresponding to the median value over the period 1990–2009 of the estimates provided by Ludwig et al. (2010). As terrestrial inputs influencing the carbonate system are poorly constrained and only estimates at the subregional scale are available (see e.g., Regnier et al., 2013), a major effort was put in the compilation of an observational dataset of Dissolved Inorganic Carbon and Total Alkalinity concentrations for those Mediterranean rivers with a minimum annual water discharge of 1 km^3 as given in Ludwig et al. (2009). Reference concentration data for 66 rivers (see **Supplementary Table 1**) were combined with the respective annual freshwater flows to determine DIC and TA loads and missing concentrations were set equal to the average values computed over the 10 coastal sub-basins defined in Ludwig et al. (2010). Exchanges at Bosphorus Strait were set using constant values for DIC and TA as in Cossarini et al. (2015).

The coupled model components were spun up with a stepwise strategy by first running the physical component alone for 20 years and consequently using the last year to drive the biogeochemical process in a perpetual mode until the surface gas exchanges reached a stable condition, which occurred after 10 years. Afterwards, the reference experiment was performed using the time varying boundary conditions and forcing fields previously described. Alkalinization scenarios are started only 20 years within the reference experiment in order to allow for the system to return to a fully transitional, non-equilibrium state of air-sea fluxes. A brief comparison to reference data for present day conditions illustrating the feasibility of model results in the principle prognostic variables of this study is given in the **Supplementary Material** (section 3).

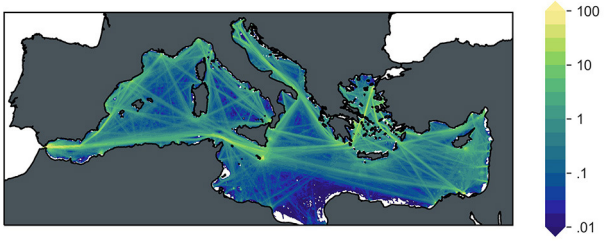

FIGURE 1 | Spatial distribution of annual slaked lime disposal over the Mediterranean basin for both alkalinization scenarios based on cargo and tanker shipping traffic. Discharge is given relative to the basin scale average, in a logarithmic scale.

2.3. Alkalinization Scenarios

This regional application of ocean liming to the Mediterranean Sea explores the potential of using the existing vessel traffic as a vehicle for lime disposal. Among the variety of vessels crossing the basin, bulk carriers, and container ships were identified as the best targets to perform liming operations due to their high load capacity and the wide spatial coverage of shipping routes (Caserini et al., 2021). The traffic associated with these two ship classes, taken from monthly data of traffic density in the year 2017 available from the EMODnet-Human Activities Project (EMODnet, 2019), was translated into a monthly climatological gridded dataset of vessel time suitable for lime disposal excluding any traffic closer than 5 km to the coastline and it represents the spatial driver of the following ocean liming scenarios that are implemented over a 30 year-long time period starting from 2020. The alkanization amounts per area and time unit are then computed from the gridded vessel time dataset by applying constant lime discharge rates of each vessel during navigation (see **Figure 1**).

Similar to previous studies (Keller et al., 2014; Lenton et al., 2018), a first scenario (CTS200) was implemented by considering a cumulative annual lime disposal of 200 Mtons over the entire basin, a technically feasible rate considering the amount of shipping traffic in the Mediterranean Sea and the typical capacity of cargo and tanker ships (Caserini et al., 2021). This rate was implemented in the model through the addition of 7.58 kg $Ca(OH)_2$/s to the surface TA for each ship,

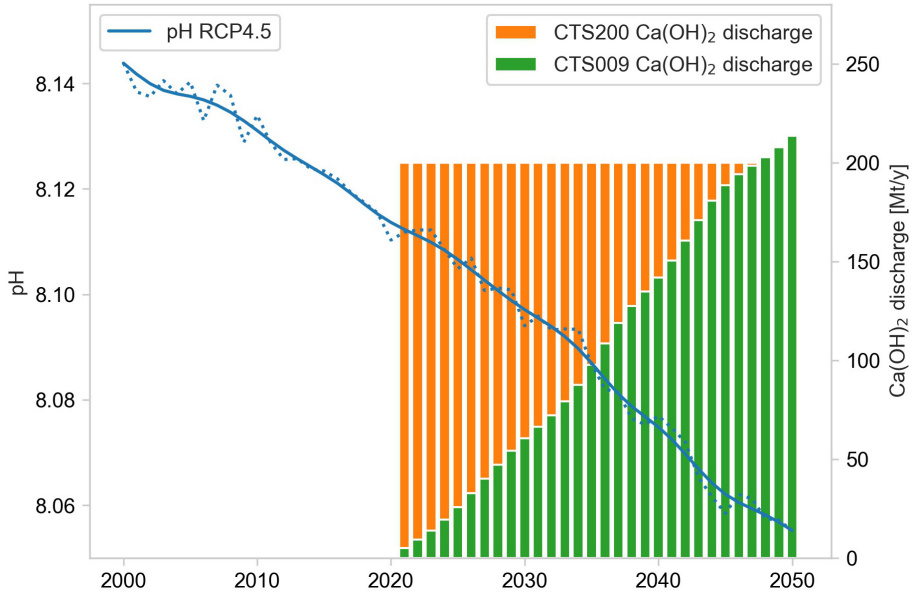

FIGURE 2 | Lime disposal over the Mediterranean basin for the CTS200 (orange) and CTS009 scenario (green) vs. mean surface pH trend of the RCP4.5 baseline scenario (blue; dotted: annual means, full line: smoothed trend).

which scaled by the time spent by vessels in a single gridpoint per month and integrated over space and time, leads to the cumulative target of 200 Mt/y and is significantly lower than the discharge of 1 t$Ca(OH)_2$/s hypothesized in other alkalinization scenarios (e.g., Renforth et al., 2013). The sedimentation of $Ca(OH)_2$ has been neglected here due to its short dissolution time scales compared to its sinking velocity (Caserini et al., 2021). This scenario primarily addresses the potential of a sudden intervention to sequestrate atmospheric CO_2 through alkalinization and evaluates the basin wide spatial changes occurring in the carbonate system.

A more adaptive strategy, somewhat similar to the approach adopted in Ilyina et al. (2013), was applied in a second simulation (CTS009) aiming to stabilize the mean surface pH at present day values. This scenario is based on the observation that the increase of surface pH through alkalinization is at first order proportional to the lime disposal increase emerging from a series of idealized one-dimensional perturbation experiments illustrated in **Supplementary Material** (section 4). We then assumed that this linear relationship would approximately transfer to the full scale experiment if stablization of present day pH conditions can be achieved at basin scale, an assumption ultimately to be confirmed by the result of this simulation. Hence, a time varying lime disposal was implemented with annual increments proportional to the smoothed mean surface pH trend of the baseline scenario (see **Figure 2**) leading to a cumulative discharge over the 2021-2050 period of approximately 3.2 Gt $Ca(OH)_2$ compared to the 6.0 Gt of the CTS200 scenario. We used the smoothed pH timeseries here in order to obtain a non-linear representation of the pH trend while maintaining the higher frequency interannual variability, which was achieved via the convolution of a Hann window function with a width of 11 years. The conversion factor used in this scenario to compute the alkalinization levels based on the pH trend was established empirically at 0.009 pH units per (mmol $Ca(OH)_2$ m^{-2} d^{-1}) of basin mean alkalinity addition via the adjustment of an initial guess in a brief sensitivity simulation and correcting it for the remaining pH trend.

A control simulation in perpetual mode representing the conditions of year 2000 was performed for the entire simulation period in order to identify any residual model drift ($\leq$2.5%), computed in the control simulation via Hann smoothing of the temporal evolution of the simulation (with the same 11 year width window used for the pH trend above) and removed from the scenario projections.

3. RESULTS

In this section we provide the results for the two alkalinization scenarios CTS200 and CTS009 investigated in this study compared to the baseline simulation RCP4.5 looking at the impact of the lime discharge on surface alkalinity and the two target indicators for the mitigation of greenhouse-gas increase and acidification, i.e., the air-sea flux of CO_2 representing the uptake of atmospheric CO_2 by the ocean and surface pH indicating the surface water acidity.

Figure 3 shows the mean surface alkalinity, pH and total air-sea flux of CO_2. The time-series for alkalinity (left) highlights a significantly different behavior for the two alkalinization strategies in terms of surface water alkalinity. Under the constant discharge scenario CTS200 (orange) it exhibits an abrupt increase in surface alkalinity by about 80 μmol kg^{-1} over the first few years and afterwards increases much more gradually and slower

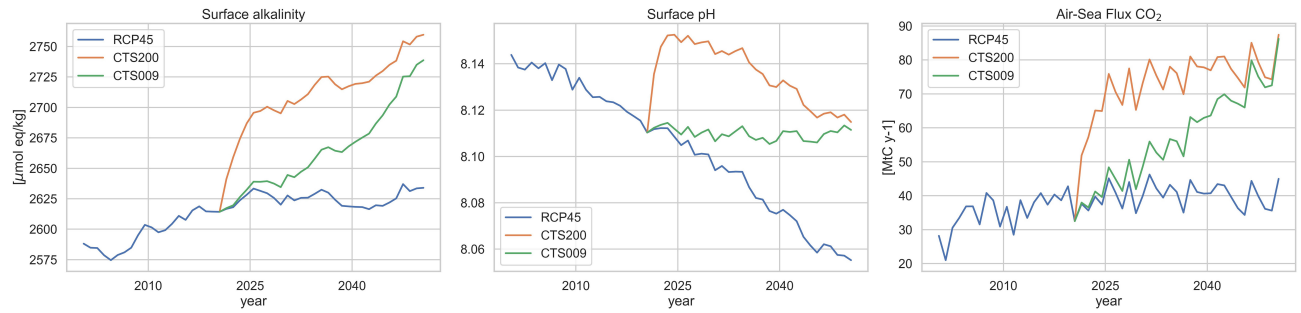

FIGURE 3 | Time series of annual mean surface alkalinity **(left)**, surface pH **(middle)**, and total annual air-sea flux **(right)** over the Mediterranean basin. Blue: RCP4.5 baseline projection, orange: CTS200 projection, green: CTS009 projection.

to reach about 2,760 μmol kg^{-1} by the end of the simulation, indicating significant fluxes of alkalinity from the surface to the deeper layers. For the CTS009 scenario (green) on the contrary surface alkalinity increases steadily over the entire period to reach a little lower surface average of 2,740 μmol kg^{-1} by 2050. Surface pH (center) exhibits under the constant discharge scenario CTS200 (orange) an abrupt increase of about 0.04 units over the first couple of years and afterwards resembles the trend of the baseline scenario (blue) maintaining the initial offset, while the variable discharge scenario CTS009 (green) fulfills its aim of stabilizing mean surface pH at the level of 2020 at the beginning of the alkalinization experiment. In case of the oceanic uptake of atmospheric CO_2, the CTS200 scenario rapidly doubles the carbon sink from little less than 40 Mt CO_2 y^{-1} to almost 80 Mt CO_2 y^{-1} and subsequently largely maintains this level showing only a minimal increase over the remaining years. The CTS009 scenario gradually increases the uptake over the alkalinization period, until reaching approximately the same level as the CTS200 scenario toward the end of the experiments. The values of CO_2 of air-sea exchange and the level of surface pH obtained are coherent with estimates from previous works on the Mediterranean basin (MedSea, 2014; Palmiéri et al., 2015).

The spatial distribution of the changes induced by the alkalinization scenarios is illustrated in **Figure 4** for surface alkalinity, **Figure 5** for surface pH and **Figure 6** for air-sea flux of CO_2. The mean present day conditions of surface alkalinity are, as to be expected, strongly correlated with surface salinity (**Supplementary Figure 1**) showing comparatively low values in the fresher waters of the Western Mediterranean along the North African coast gradually increasing toward the Levantine basin. An exception to this pattern is caused by large lateral inputs of alkalinity which lead to local extremes in surface alkalinity around the deltas of e.g., the Po and Rhone deltas and the Dardanelles. In areas of high alkalinity under present day conditions substantial increases can be observed under the RCP4.5 projected future conditions (mainly Adriatic and Aegean See, Northern Levantine Basin), while other areas remain comparatively stable. These changes are amplified under both alkalinization scenarios, leading to increase of alkalinity across the basin, even if at varying extent, with the exception of the Alboran Sea, the surface waters of which are mostly of Atlantic origin where no alkalinization was applied.

Acidification of the Mediterranean under the baseline scenario RCP4.5 occurs in general across the basin with stronger acidification levels of little less than 0.1 pH units in the Western Mediterranean gradually decreasing toward the Eastern Mediterranean where acidification levels vary between 0 and 0.05 pH units. A noteworthy exception to this general pattern is presented by the Adriatic Sea with particularly low pH decreases between 0 and 0.025 pH units and increasing levels of pH in the South Adriatic Gyre. Only along the shallow North-Eastern coast slightly higher levels of acidification are reached in this sub-basin. Other areas of low acidification levels are observed in coincidence with gyres and overturning cells in the Gulf of Lions, the Cretan Sea and west of Cyprus (Robinson and Golnaraghi, 1994; Pinardi et al., 2015, **Supplementary Figure 1**).

The relative geographic pattern is largely maintained in the alkalinization scenarios, but offset toward a pH neutral basin average as shown in **Figure 3**. Under the given discharge levels, the two scenarios lead to very similar changes in surface pH conditions at mid-century with marginally higher levels for the CTS200 simulation. For both alkalinization scenarios the highest increases in pH with respect to present day conditions are reached in the Northern Adriatic and Aegean Sea with increments up to approximately 0.2 and 0.1 pH units, respectively. Various local maxima of pH can be observed coincident with the circulation features previously mentioned for the baseline changes and in the vicinity of large ports where shipping traffic and hence discharge is particularly high, e.g., nearby Valencia, Marseille, Genova, Valletta, Piraeus.

Figure 6 illustrates the general characteristics of air-sea flux pattern of CO_2 of the Mediterranean Sea acting as strong sink over large parts of the Western Mediterranean, the Adriatic, and the Aegean Sea, while the Eastern Mediterranean acts as comparatively weak sink (top-left for average present-day conditions). Most noticeable changes under RCP4.5 for mid-century (top-right) are an increased influx of CO_2 in locations corresponding to the pH changes described in the previous paragraph, i.e., in the Adriatic Sea (particularly the South Adriatic gyre with maximum increases of around 50 mg C m^{-2} d^{-1}), the Aegean and Cretan Sea, the Gulf of Lions and west of Cyprus. The

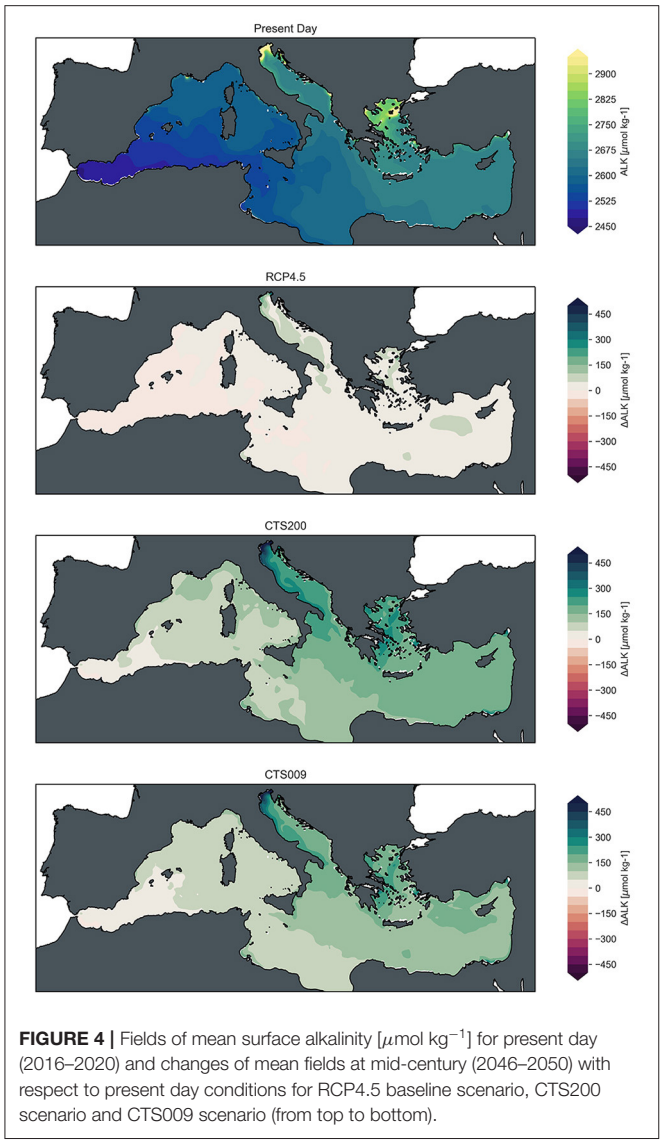

FIGURE 4 | Fields of mean surface alkalinity [μmol kg^{-1}] for present day (2016–2020) and changes of mean fields at mid-century (2046–2050) with respect to present day conditions for RCP4.5 baseline scenario, CTS200 scenario and CTS009 scenario (from top to bottom).

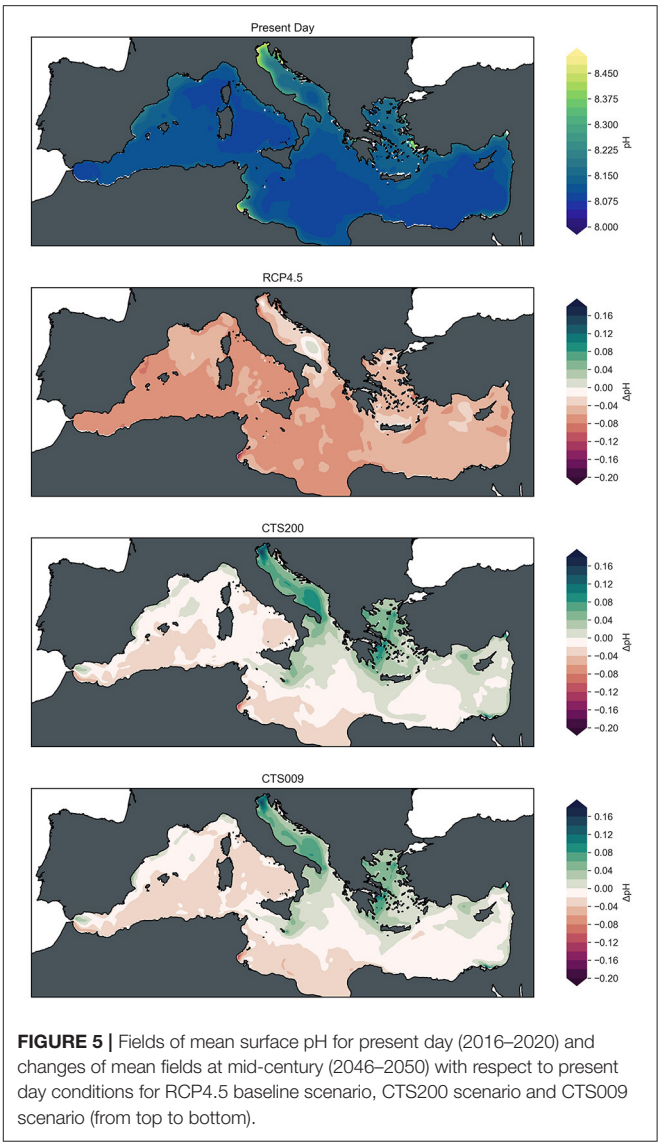

FIGURE 5 | Fields of mean surface pH for present day (2016–2020) and changes of mean fields at mid-century (2046–2050) with respect to present day conditions for RCP4.5 baseline scenario, CTS200 scenario and CTS009 scenario (from top to bottom).

maps of changes for the two alkalinization scenarios reflect this overall pattern elevating the CO_2 uptake to positive values across the entire basin which in the South Adriatic gyre and Aegean Sea reach levels in excess of 120 mg C m^{-2} d^{-1}, again with slightly stronger fluxes for the CTS200 scenario compared to the CTS009 scenario. In contrast to the pH fields, the high shipping traffic in the vicinity of ports does not seem to impact the air-sea flux pattern significantly.

Looking in more detail at these combined results some distinct features emerge in addition to these large scale patterns. In the two areas where increased shipping traffic (and therefore higher levels of alkalinization) coincides with significant lateral inputs of alkalinity and dissolved inorganic carbon and the topography of the area leads to accumulation of alkalinity, the patterns of the alkalinization scenarios diverge from those of the baseline scenario. The areas under direct influence of the lateral inputs are less sensitive to the artificial addition of alkalinity in terms of pH and air-sea flux response, while away from the lateral inputs toward the center of the basins alkalinization induces prominent features of pH and CO_2 uptake absent in the baseline scenario. Another interesting feature are the pronounced increases of CO_2 in the future scenarios at the locations of the cyclonic gyres in the South-Adriatic and North-West Mediterranean Sea, both subject to dense water formation and convection events in winter. In these locations the increase in air-sea flux is triggered by decreased levels of DIC originating from the intermediate layer that turns these locations into efficient carbon sinks, an effect that is further accentuated in the alkalinization scenarios.

4. DISCUSSIONS

The alkalinization strategies applied in this study to the Mediterranean Sea illustrate the potential of ocean liming to mitigate climate change by increasing the air-sea flux of CO_2

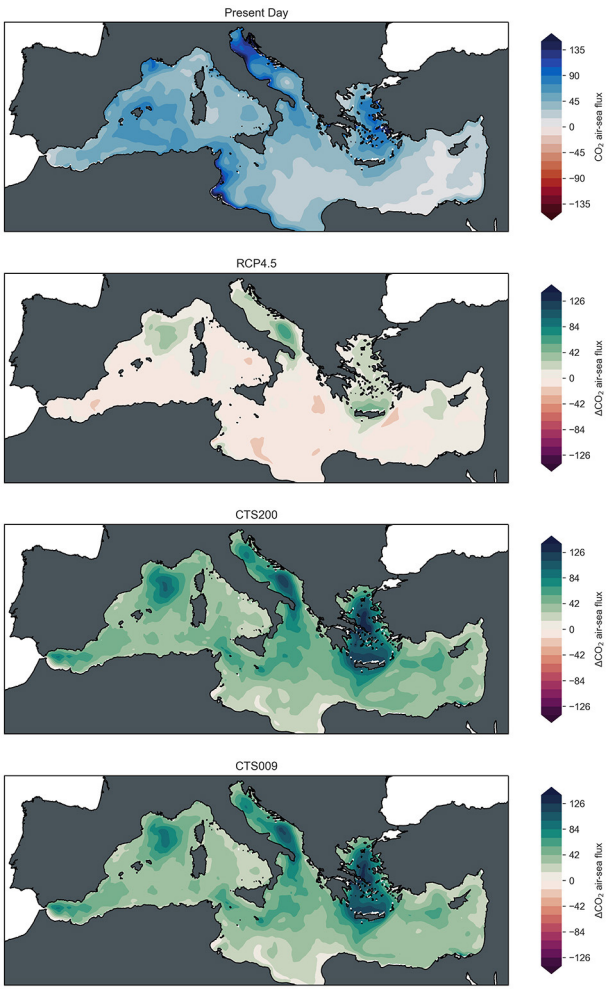

FIGURE 6 | Fields of mean CO_2 air-sea flux [mg m^{-2} d^{-1}] for present day (2016–2020) and changes of mean fields at mid-century (2046–2050) with respect to present day conditions for RCP4.5 baseline scenario, CTS200 scenario and CTS009 scenario (from top to bottom).

across the basin and counteracting acidification. In contrast to previous studies, the analyzed scenarios offer a clear pathway into practical implementation being based on realistic levels of lime discharge using the current network of cargo and tanker shipping routes across the Mediterranean Sea as described in more detail in the accompanying work of Caserini et al. (2021). Two different approaches of alkalinization scenarios have been explored: one (CTS200) with a constant annual discharge of lime over the entire scenario period and another with gradually increasing alkalinization levels (CTS009) proportional to the pH decreases in the baseline scenario RCP4.5. It should be noted that similar to previous works on the topic this study is based on a single model projection of a single baseline scenario. Consequently, the study provides a proof of concept of the feasibility of the approaches taken, while for a full, robust quantification taking into account the various sources of uncertainty involved (e.g., scenarios, model structure, and parametrization, internal variability) a larger set of ensemble simulations would be required.

Keeping this limitation in mind, we can state that both proposed approaches substantially increase the CO_2 sink of the Mediterranean Sea (doubling the uptake under present day conditions) and neutralize acidification in terms of the basin average pH by the end of the alkalinization period of 30 years. These conditions are achieved however on considerably different pathways. The CTS200 scenario of constant discharge provokes a rapid increase of surface pH and air-sea flux and resumes after this offset to follow the trends of the system under the baseline scenario with an annual uptake of around 70–80 MtC/y over the larger part of the simulation leading to a cumulative increase in CO_2 air-sea flux by 1.02 GtC achieved via the total discharge of 6.00 Gt $Ca(OH)_2$ over the full duration of the alkalinization scenario. The CTS009 scenario in contrast, gradually increases the air-sea flux toward a similar annual uptake of around 80 GtC/y at the end of the simulation, leading to a total of 0.53 GtC of air-sea flux increase discharging cumulatively 3.21 Gt $Ca(OH)_2$, but manages to stabilize the surface pH at present day levels. The difference between the two scenarios is particularly important with respect to the pH rise over the first couple of years in the CTS200 scenario, which exceeds twice the acidification rate occurring over a decade in the RCP4.5 scenario and hence strongly alters the alkaline environment of the Mediterranean Sea. While the ecological impacts of acidification of the ocean are subject to a wide field of research, comparatively little is known about the opposite process of alkalinization in order to appreciate the impacts of such changes on the Mediterranean Sea ecosystem. Among the side effects mentioned in literature are the potential of positive and negative feed-backs, affecting nutrient limitation of primary producers, causing physiological damage to marine organisms and altering their metabolic balance (Cripps et al., 2013; Bach et al., 2019), but more research is required on the topic in order to enable a quantified estimate of the resilience of marine ecosystems to alkalinization and an adequate risk assessment. This point is even more relevant when considering the spatial heterogeneity of alkalinization impacts illustrated in **Figure 5**, which shows that local extremes of pH variation may differ from the basin annual mean by more than 0.1 pH units. The location of pH maxima resulting from the map suggests the reduction of lime discharge in areas of high shipping traffic and reduced mixing with the surrounding water bodies like the Northern Adriatic and Aegean Sea. The same holds for the vicinity of large ports, where pH is strongly affected by alkalinization in contrast to areas of dense traffic but effective redistribution via ocean currents, e.g., Gibraltar and Alboran Sea in order to avoid damaging effects to the local ecosystems. Similarly, the results for the Agean and Adriatic Sea suggest, that it might be beneficial to reduce alkalinization in areas where other large sources of alkalinity seem to reduce the efficiency of the process. In contrast, while generally the increase of stratification across the basin reduces the carbon sink of the Mediterranean Sea, its cyclonic gyres that are associated with dense water formation appear increasingly efficient in absorbing atmospheric carbon, suggesting that increased alkalization in areas feeding into these gyres may be beneficial. Nevertheless, the present study does

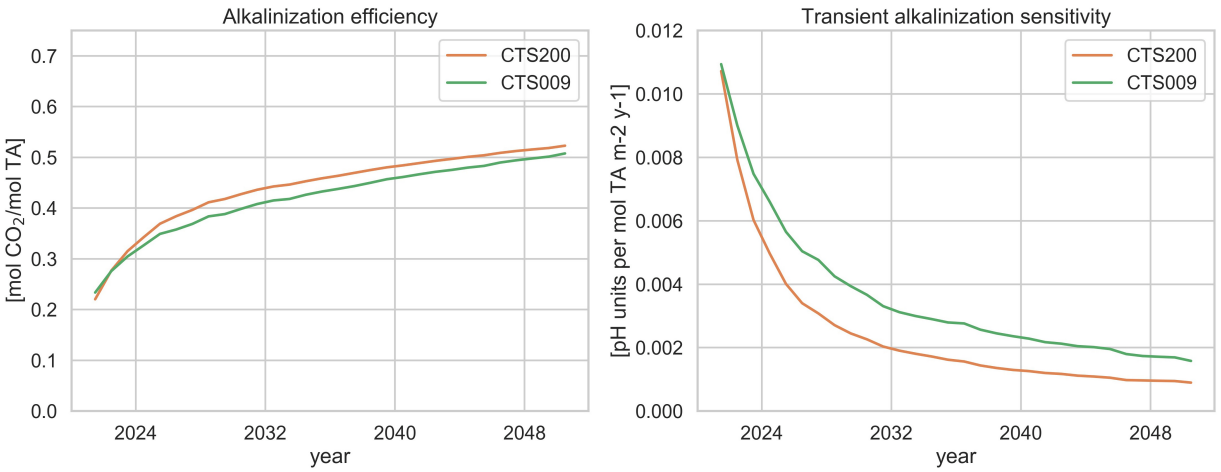

FIGURE 7 | Transient Alkalinization Efficiency **(left)**: CO_2 air-sea flux over alkalinization flux (cumulative); Transient Alkalinization Sensitivity **(right)**: pH change with respect to RCP4.5 baseline projection over cumulative alkalinization flux. Orange: CTS200 projection, green: CTS009 projection.

provide only a first indication toward the role of these features and their interaction with alkalinization strategies, more detailed and targeted studies are required for a more conclusive picture.

In order to fully appreciate the different potential of the two alkalinization pathways and given that the two scenarios apply different total amounts of lime and distribution of discharge over the alkalinization period even though reaching similar levels of air-sea flux and pH by the end of the scenarios, we put into relation lime discharge, air-sea flux and the pH changes with respect to the RCP4.5 baseline scenario. To this purpose we define two indicators: the transient alkalinization efficiency as the ratio of cumulative CO_2 air-sea flux increase over the cumulative added alkalinity and the transient alkalinization sensitivity as the ratio of change of mean surface pH with respect to the no alkalinization case over the cumulative added alkalinity.

Figure 7 shows the temporal evolution of these two indicators in the Mediterranean Sea over the alkalinization period for both liming scenarios. The transient alkalinization efficiency (left), which describes the CO_2 uptake potential of the alkalinization approach, starts at a value of little more than 0.2 mol CO_2 (mol TA)$^{-1}$ and reaches up to 0.5 mol CO_2 (mol TA)$^{-1}$ with slightly higher values (by about 3%) for the constant discharge scenario. These values are substantially lower than the upper bound of 1 mol CO_2 (mol TA)$^{-1}$ given by the consumption of aqueous CO_2 in Equation (1), due to two processes: the redistribution of inorganic dissolved carbon species toward a new equilibrium of the carbonate system and dynamic exchanges with the underlying water bodies further reducing the efficiency. They are also lower than the estimate of 0.8 mol CO_2 (mol TA)$^{-1}$ in Renforth et al. (2013), who however did not involve the latter process and the estimate of 0.7 mol CO_2 (mol TA)$^{-1}$ in Keller et al. (2014), but are consistent with the efficiency estimates given recently by Köhler (2020) for the near future in a multimillenial alkalinization experiment.

The transient alkalinization sensitivity (right), which describes the mean pH response of the system under alkalinization relative to the added alkalinity, is maximal at the beginning of the alkalinization period at about 0.11 pH units per mol TA m^{-2} y^{-1} and gradually decreasing to values of approximately 0.0016 and 0.0009 for the scenarios CTS009 and CTS2000, respectively. Hence, over the full alkalinization period, the gradually increasing approach reveals a substantially higher potential in counteracting ocean acidification than the constant discharge scenario whose cumulative sensitivity at the end of the period is about 44% lower. Note, that the sensitivities after the first year of the simulations CTS200 and CTS009 are nearly identical confirming that the sensitivity is independent of the alkalinization levels as long as the environmental conditions are not altered significantly, confirming the observation emerging from the idealized 1D experiments.

The substantially higher potential in counteracting acidification along with the avoidance of the abrupt changes in surface pH suggests that the approach of gradually increasing discharge following the acidification trend of the system without alkalinization is favorable in ecological and economic terms over the application of constant discharge rates, even if the latter appears slightly more efficient in terms of CO_2 uptake. It should be noted here that an actual implementation of any of these approaches should be preceded by a complete analysis of all costs and benefits taking into consideration the full chain of processes involved, including the production and transport of lime.

In conclusion, this study illustrates how technically feasible amounts of alkalinization allow to counteract the threat of ocean acidification and to remove CO_2 from the atmosphere, through a substantial increase in CO_2 uptake across the Mediterranean Sea. The preferred approach consists of gradually increasing lime discharge levels using the existing network of cargo and tanker ships, stabilizing the mean surface pH at present day values using the existing network of cargo and tanker ships. Ecological impacts and side-effects, particularly in local areas of high alkalinization levels due to denser ship

traffic and accumulation via ocean dynamics remain to be carefully assessed.

DATA AVAILABILITY STATEMENT

The datasets analyzed in this study can be found in the Zenodo repository (doi: 10.5281/zenodo.4068027). Additional data is available from the corresponding author on request.

AUTHOR CONTRIBUTIONS

MB developed the design of this study, performed the model simulations, and wrote the manuscript. TL assisted in the design of the study, in the preparation of the simulations, and in the writing of the manuscript and the supplements. SM, SC, and MG assisted in the design of the study and the writing of the manuscript. All authors contributed to the article and approved the submitted version.

FUNDING

The research was carried out within the Desarc-Maresanus project (www.desarc-maresanus.net), which received the financial support of Amundi SGR SpA.

SUPPLEMENTARY MATERIAL

The Supplementary Material for this article can be found online at: https://www.frontiersin.org/articles/10.3389/fclim.2021.614537/full#supplementary-material

REFERENCES

Bach, L. T., Gill, S. J., Rickaby, R. E. M., Gore, S., and Renforth, P. (2019). CO_2 removal with enhanced weathering and ocean alkalinity enhancement: potential risks and co-benefits for marine pelagic ecosystems. *Front. Clim*. 1:7. doi: 10.3389/fclim.2019.00007

Caserini, S., Barreto, B., Lanfredi, C., Cappello, G., Ross Morrey, D., and Grosso, M. (2019). Affordable CO_2 negative emission through hydrogen from biomass, ocean liming, and CO_2 storage. *Mitigat. Adapt. Strat. Glob. Change*. 24, 1231–1248. doi: 10.1007/s11027-018-9835-7

Caserini, S., Pagano, D., Campo, F., Abbá, A., De Marco, S., Righi, D., et al. (2021). Potential of maritime transport for ocean liming and atmospheric CO_2 removal. *Front. Clim.* 3. doi: 10.3389/fclim.2021.575900

Cossarini, G., Lazzari, P., and Solidoro, C. (2015). Spatiotemporal variability of alkalinity in the mediterranean sea. *Biogeosciences* 12, 1647–1658. doi: 10.5194/bg-12-1647-2015

Cripps, G., Widdicombe, S., Spicer, J. I., and Findlay, H. S. (2013). Biological impacts of enhanced alkalinity in carcinus maenas. *Mar. Pollut. Bull.* 71, 190–198. doi: 10.1016/j.marpolbul.2013.03.015

Data-Driven EnviroLab and NewClimate Institute (2020). *Accelerating Net Zero: Exploring Cities, Regions, and Companies' Pledges to Decarbonise*. Technical report, NewClimate Institute. Available online at: https://newclimate.org/wp-content/uploads/2020/09/NewClimate_Accelerating_Net_Zero_Sept2020.pdf

EMODnet (2019). *Shipping Density*. Available online at: https://www.emodnet-humanactivities.eu/view-data.php

Friedlingstein, P., Jones, M. W., O'Sullivan, M., Andrew, R. M., Hauck, J., Peters, G. P., et al. (2019). Global carbon budget 2019. *Earth Syst. Sci. Data* 11, 1783–1838. doi: 10.5194/essd-11-1783-2019

Gattuso, J.-P., Magnan, A., Billé, R., Cheung, W. W. L., Howes, E. L., Joos, F., et al. (2015). Contrasting futures for ocean and society from different anthropogenic CO_2 emissions scenarios. *Science* 349:aac4722. doi: 10.1126/science.aac4722

Giorgi, F. (2006). Climate change hot-spots. *Geophys. Res. Lett*. 33, 1–4. doi: 10.1029/2006GL025734

González, M. F., and Ilyina, T. (2016). Impacts of artificial ocean alkalinization on the carbon cycle and climate in earth system simulations. *Geophys. Res. Lett*. 43, 6493–6502. doi: 10.1002/2016GL068576

Hoegh-Guldberg, O., Jacob, D., Taylor, M., Bindi, M., Brown, S., Camilloni, I., et al. (2018). "Impacts of 1.5°C global warming on natural and human systems," in *Global Warming of 1.5°C. An IPCC Special Report on the Impacts of Global Warming of 1.5°C Above Pre-Industrial Levels and Related Global Greenhouse Gas Emission Pathways, in the Context of Strengthening the Global Response to the Threat of Climate Change, Sustainable Development, and Efforts to Eradicate Poverty. Intergovernmental Panel on Climate Change*. Available online at: https://www.ipcc.ch/sr15/chapter/chapter-3/

Ilyina, T., Wolf-Gladrow, D., Munhoven, G., and Heinze, C. (2013). Assessing the potential of calcium-based artificial ocean alkalinization to mitigate rising atmospheric CO_2 and ocean acidification. *Geophys. Res. Lett*. 40, 5909–5914. doi: 10.1002/2013GL057981

IPCC (2013). *Climate Change 2013: The Physical Science Basis. Contribution of Working Group I to the Fifth Assessment Report of the Intergovernmental Panel on Climate Change*. Cambridge University Press.

IPCC (2018). "Summary for policymakers," in *Global Warming of 1.5°C. An IPCC Special Report on the Impacts of Global Warming of 1.5°C Above Pre-Industrial Levels and Related Global Greenhouse Gas Emission Pathways, in the Context of Strengthening the Global Response to the Threat of Climate Change, Sustainable Development, and Efforts to Eradicate Poverty*, eds V. Masson-Delmotte, P. Zhai, H.-O. Pörtner, D. Roberts, J. Skea, P. Shukla, A. Pirani, W. Moufouma-Okia, C. Péan, R. Pidcock, S. Connors, J. Matthews, Y. Chen, X. Zhou, M. Gomis, E. Lonnoy, T. Maycock, M. Tignor, and T. Waterfield (World Meteorological Organization), 32. Available online at: https://www.ipcc.ch/sr15/chapter/spm/

IPCC (2019). "Summary for policymakers," in *IPCC Special Report on the Ocean and Cryosphere in a Changing Climate*, eds H. O. Pörtner, D. Roberts, V. Masson-Delmotte, M. T. Zhai, E. Poloczanska, K. Mintenbeck, A. Alegría, M. Nicolai, A. Okem, J. Petzold, B. Rama, and N. Weyer. Available online at: https://www.ipcc.ch/srocc/chapter/summary-for-policymakers/

Keller, D. P., Feng, E. Y., and Oschlies, A. (2014). Potential climate engineering effectiveness and side effects during a high carbon dioxide-emission scenario. *Nat. Commun*. 5, 1–11. doi: 10.1038/ncomms4304

Khatiwala, S., Tanhua, T., Mikaloff Fletcher, S., Gerber, M., Doney, S. C., Graven, H. D., et al. (2013). Global ocean storage of anthropogenic carbon. *Biogeosciences* 10, 2169–2191. doi: 10.5194/bg-10-2169-2013

Köhler, P. (2020). Anthropogenic CO_2 of high emission scenario compensated after 3500 years of ocean alkalinization with an annually constant dissolution of 5 Pg of olivine. *Front. Clim*. 2:575744. doi: 10.3389/fclim.2020.575744

Kroeker, K. J., Kordas, R. L., Crim, R., Hendriks, I. E., Ramajo, L., Singh, G. S., et al. (2013). Impacts of ocean acidification on marine organisms: quantifying sensitivities and interaction with warming. *Glob. Change Biol*. 19, 1884–1896. doi: 10.1111/gcb.12179

Lacoue-Labarthe, T., Nunes, P. A., Ziveri, P., Cinar, M., Gazeau, F., Hall-Spencer, J. M., et al. (2016). Impacts of ocean acidification in a warming Mediterranean Sea: an overview. *Region. Stud. Mar. Sci*. 5, 1–11. doi: 10.1016/j.rsma.2015.12.005

Lazzari, P., Solidoro, C., Ibello, V., Salon, S., Teruzzi, A., Béranger, K., et al. (2012). Seasonal and inter-annual variability of plankton chlorophyll and primary production in the Mediterranean Sea: a modelling approach. *Biogeosciences* 9, 217–233. doi: 10.5194/bg-9-217-2012

Lenton, A., Matear, R. J., Keller, D. P., Scott, V., and Vaughan, N. E. (2018). Assessing carbon dioxide removal through global and regional ocean alkalinization under high and low emission pathways. *Earth Syst. Dyn.* 9, 339–357. doi: 10.5194/esd-9-339-2018

Lovato, T., and Vichi, M. (2015). An objective reconstruction of the Mediterranean sea carbonate system. *Deep Sea Res. Part I Oceanogr. Res. Pap*. 98, 21–30. doi: 10.1016/j.dsr.2014.11.018

Lovato, T., Vichi, M., and Oddo, P. (2013). *High-Resolution Simulations of Mediterranean Sea Physical Oceanography Under Current and Scenario Climate Conditions: Model Description, Assessment and Scenario Analysis*. CMCC Research Paper. Available online at: https://www.cmcc.it/wp-content/uploads/2014/02/rp0207-ans-12-2013.pdf

Ludwig, W., Bouwman, A., Dumont, E., and Lespinas, F. (2010). Water and nutrient fluxes from major mediterranean and black sea rivers: past and future trends and their implications for the basin-scale budgets. *Glob. Biogeochem. Cycles* 24, 1–14. doi: 10.1029/2009GB003594

Ludwig, W., Dumont, E., Meybeck, M., and Heussner, S. (2009). River discharges of water and nutrients to the Mediterranean and Black Sea: major drivers for ecosystem changes during past and future decades? *Prog. Oceanogr*. 80, 199–217. doi: 10.1016/j.pocean.2009.02.001

Madec, G., Benshila, R., Bricaud, C., Coward, A., Dobricic, S., Furner, R., et al. (2013). *NEMO Ocean Engine. Note du Pole de Modélisation 27*, Institut Pierre-Simon Laplace (IPSL), France.

MedSea (2014). *Final Project Report*. Technical report, Mediterranean Sea Acidification in a changing climate,EU FP7 265103. Available online at: https://cordis.europa.eu/docs/results/265/265103/final1-project-final-report-lastdraft-3.pdf

Millot, C., and Taupier-Letage, I. (2005). "Circulation in the Mediterranean sea," in *The Mediterranean Sea, Handbook of Environmental Chemistry*, ed A. Saliot (Springer), 29–66. doi: 10.1007/b107143

Moss, R. H., Edmonds, J. A., Hibbard, K. A., Manning, M. R., Rose, S. K., Van Vuuren, D. P., et al. (2010). The next generation of scenarios for climate change research and assessment. *Nature* 463, 747–756. doi: 10.1038/nature 08823

Oddo, P., Adani, M., Pinardi, N., Fratianni, C., Tonani, M., Pettenuzzo, D., et al. (2009). A nested Atlantic-Mediterranean Sea general circulation model for operational forecasting. *Ocean Sci*. 5, 461–473. doi: 10.5194/os-5-46 1-2009

Olsen, A., Key, R. M., Van Heuven, S., Lauvset, S. K., Velo, A., Lin, X., et al. (2016). The global ocean data analysis project version 2 (GLODAPv2)-an internally consistent data product for the world ocean. *Earth Syst. Sci. Data* 8, 297–323. doi: 10.5194/essd-8-297-2016

Orr, J. C., Najjar, R. G., Aumont, O., Bopp, L., Bullister, J. L., Danabasoglu, G., et al. (2017). Biogeochemical protocols and diagnostics for the CMIP6 Ocean Model Intercomparison Project (OMIP). *Geosci. Model Dev*. 10, 2169–2199. doi: 10.5194/gmd-10-2169-2017

Palmiéri, J., Orr, J. C., Dutay, J.-C., Béranger, K., Schneider, A., Beuvier, J., et al. (2015). Simulated anthropogenic CO_2 storage and acidification of the Mediterranean Sea. *Biogeosciences* 12, 781–802. doi: 10.5194/bg-12-781-2015

Pinardi, N., Cessi, P., Borile, F., and Wolfe, C. L. P. (2019). The Mediterranean Sea overturning circulation. *J. Phys. Oceanogr*. 49, 1699–1721. doi: 10.1175/JPO-D-18-0254.1

Pinardi, N., Zavatarelli, M., Adani, M., Coppini, G., Fratianni, C., Oddo, P., et al. (2015). Mediterranean Sea large-scale low-frequency ocean variability and water mass formation rates from 1987 to 2007: a retrospective analysis. *Prog. Oceanogr*. 132, 318–332. doi: 10.1016/j.pocean.2013. 11.003

Regnier, P., Friedlingstein, P., Ciais, P., Mackenzie, F. T., Gruber, N., Janssens, I. A., et al. (2013). Anthropogenic perturbation of the carbon fluxes from land to ocean. *Nat. Geosci*. 6, 597–607. doi: 10.1038/ngeo1830

Renforth, P., Jenkins, B. G., and Kruger, T. (2013). Engineering challenges of ocean liming. *Energy* 60, 442–452. doi: 10.1016/j.energy.2013.08.006

Renforth, P., and Wilcox, J. (2020). Editorial: The role of negative emission technologies in addressing our climate goals. *Front. Clim*. 2:1. doi: 10.3389/fclim.2020.00001

Robinson, A. R., and Golnaraghi, M. (1994). *The Physical and Dynamical Oceanography of the Mediterranean Sea*. NATO ASI Series. Dortrecht: Springer Netherlands, 255–306. doi: 10.1007/978-94-011-0870-6_12

Schellnhuber, H. J., Rahmstorf, S., and Winkelmann, R. (2016). Why the right climate target was agreed in Paris. *Nat. Clim. Change* 6, 649–653. doi: 10.1038/nclimate3013

Scoccimarro, E., Gualdi, S., Bellucci, A., Sanna, A., Giuseppe Fogli, P., Manzini, E., et al. (2011). Effects of tropical cyclones on ocean heat transport in a high-resolution coupled general circulation model. *J. Clim*. 24, 4368–4384. doi: 10.1175/2011JCLI4104.1

Soto-Navarro, J., Jordá, G., Amores, A., Cabos, W., Somot, S., Sevault, F., et al. (2020). Evolution of Mediterranean Sea water properties under climate change scenarios in the Med-CORDEX ensemble. *Clim. Dyn*. 54, 2135–2165. doi: 10.1007/s00382-019-05105-4

Tokarska, K. B., Stolpe, M. B., Sippel, S., Fischer, E. M., Smith, C. J., Lehner, F., et al. (2020). Past warming trend constrains future warming in CMIP6 models. *Sci. Adv*. 6:eaaz9549. doi: 10.1126/sciadv.aaz9549

UNEP/MAP (2017). *Mediterranean Quality Status Report*. Technical report, United Nations Environment/Mediterranean Action Plan Barcelona Convention Secretariat. Available online at: https://www.medqsr.org/

UNFCCC (2020). *NDC Registry*. Available online at: https://www4.unfccc.int/sites/NDCStaging/Pages/LatestSubmissions.aspx (accessed September 30, 2020).

Vichi, M., Lovato, T., Butenschön, M., Tedesco, L., Lazzari, P., Cossarini, G., et al. (2020). *The Biogeochemical Flux Model (BFM): Equation Description and User Manual. BFM Version 5.2*. BFM Report Series 1, BFM Consortium. Bologna. Available online at: https://cmcc-foundation.github.io/www.bfm-community.eu/files/bfm-V5.2.0-manual_r1.2_202006.pdf

Vichi, M., Navarra, A., and Fogli, P. (2013). Adjustment of the natural ocean carbon cycle to negative emission rates. *Clim. Change* 118, 105–118. doi: 10.1007/s10584-012-0677-0

Visinelli, L., Masina, S., Vichi, M., Storto, A., and Lovato, T. (2016). Impacts of data assimilation on the global ocean carbonate system. *J. Mar. Syst*. 158, 106–119. doi: 10.1016/j.jmarsys.2016.02.011

von Schuckmann, K., Cheng, L., Palmer, M. D., Hansen, J., Tassone, C., Aich, V., et al. (2020). Heat stored in the earth system: where does the energy go? *Earth Syst. Sci. Data* 12, 2013–2041. doi: 10.5194/essd-12-2013-2020

Williamson, P. (2016). Emissions reduction: scrutinize CO_2 removal methods. *Nat. News* 530:153. doi: 10.1038/530153a

Zeebe, R. W., and Wolf-Gladrow, D. (2001). *CO_2 in Seawater: Equilibrium, Kinetics, Isotopes*. Elsevier Oceanography Series. Elsevier. Available online at: https://www.elsevier.com/books/co2-in-seawater-equilibrium-kinetics-isotopes/zeebe/978-0-444-50946-8

Conflict of Interest: The authors declare that the research was conducted in the absence of any commercial or financial relationships that could be construed as a potential conflict of interest.

frontiers in Climate

ORIGINAL RESEARCH
published: 08 April 2021
doi: 10.3389/fclim.2021.575900

Potential of Maritime Transport for Ocean Liming and Atmospheric CO_2 Removal

Stefano Caserini[1]*, *Dario Pagano*[1], *Francesco Campo*[1], *Antonella Abbà*[2], *Serena De Marco*[1], *Davide Righi*[1], *Phil Renforth*[3] and *Mario Grosso*[1]

[1] Dipartimento di Ingegneria Civile ed Ambientale, Politecnico di Milano, Milan, Italy, [2] Dipartimento di Scienze e Tecnologie Aerospaziali, Politecnico di Milano, Milan, Italy, [3] Research Centre for Carbon Solutions, School of Engineering and Physical Sciences, Heriot-Watt University, Edinburgh, United Kingdom

OPEN ACCESS

Edited by:
David Peter Keller,
GEOMAR Helmholtz Center for Ocean Research Kiel, Germany

Reviewed by:
Greg H. Rau,
University of California, Santa Cruz, United States
Chris Vivian,
Fisheries and Aquaculture Science (CEFAS), United Kingdom

***Correspondence:**
Stefano Caserini
stefano.caserini@polimi.it

Specialty section:
This article was submitted to Negative Emission Technologies, a section of the journal Frontiers in Climate

Received: 24 June 2020
Accepted: 10 March 2021
Published: 08 April 2021

Citation:
Caserini S, Pagano D, Campo F, Abbà A, De Marco S, Righi D, Renforth P and Grosso M (2021) Potential of Maritime Transport for Ocean Liming and Atmospheric CO_2 Removal. Front. Clim. 3:575900. doi: 10.3389/fclim.2021.575900

Proposals to increase ocean alkalinity may make an important contribution to meeting climate change net emission targets, while also helping to ameliorate the effects of ocean acidification. However, the practical feasibility of spreading large amounts of alkaline materials in the seawater is poorly understood. In this study, the potential of discharging calcium hydroxide (slaked lime, SL) using existing maritime transport is evaluated, at the global scale and for the Mediterranean Sea. The potential discharge of SL from existing vessels depends on many factors, mainly their number and load capacity, the distance traveled along the route, the frequency of reloading, and the discharge rate. The latter may be constrained by the localized pH increase in the wake of the ship, which could be detrimental for marine ecosystems. Based on maritime traffic data from the International Maritime Organization for bulk carriers and container ships, and assuming low discharge rates and 15% of the deadweight capacity dedicated for SL transport, the maximum SL potential discharge from all active vessels worldwide is estimated to be between 1.7 and 4.0 Gt/year. For the Mediterranean Sea, based on detailed maritime traffic data, a potential discharge of about 186 Mt/year is estimated. The discharge using a fleet of 1,000 new dedicated ships has also been discussed, with a potential distribution of 1.3 Gt/year. Using average literature values of CO_2 removal per unit of SL added to the sea, the global potential of CO_2 removal from SL discharge by existing or new ships is estimated at several Gt/year, depending on the discharge rate. Since the potential impacts of SL discharge on the marine environment in the ships' wake limits the rate at which SL can be applied, an overview of methodologies for the assessment of SL concentration in the wake of the ships is presented. A first assessment performed with a three-dimensional non-reactive and a one-dimensional reactive fluid dynamic model simulating the shrinking of particle radii, shows that low discharge rates of a SL slurry lead to pH variations of about 1 unit for a duration of just a few minutes.

Keywords: slaked lime, sea acidification, CO_2 removal, maritime traffic, ocean alkalinisation

INTRODUCTION

Purposefully increasing the alkalinity of the ocean is gaining mounting attention for the potential to mitigate ocean acidification, a major threat for some marine ecosystems, while simultaneously removing atmospheric CO_2. After Kheshgi (1995) first proposed to add alkaline materials to the ocean surface for removing atmospheric carbon and storing it in the seawater, some authors (Keller et al., 2014; Renforth and Henderson, 2017; Lenton et al., 2018; Rau et al., 2018) indicated a large potential for carbon removal by "ocean alkalinity enhancement," via spreading $Ca(OH)_2$ (commonly named slaked lime, SL) or NaOH in seawater, as well as for mitigating ocean acidification and enhancing the net calcification of reef (Albright et al., 2016).

However, technological challenges and potential side effects must be assessed, such as the impact on the ecological and biogeochemical functioning of the ocean. While chemical reactions of ocean alkalinity enhancement are theoretically known, and some processes to produce SL without CO_2 emissions into the atmosphere have been proposed (Renforth and Henderson, 2017; Caserini et al., 2019), less is known regarding the practical aspects of spreading large amounts of alkaline materials in the seawater for ocean alkalinity enhancement.

Many studies (i.e., IPCC, 2018; Nemet et al., 2018) shows that achieving the Paris Agreement goal of limiting warming to well below 2°C or even 1.5°C may require 10-20 gigatonnes (Gt) of CO_2 removed from the atmosphere per year by 2100, in addition to a rapid global economy-wide reduction in greenhouse gas emissions through "conventional" mitigation. The magnitude of the task and the rates required to achieve net carbon removal suggests that a portfolio of options should be implemented, and in the race to remove this tremendous amount of CO_2 research should be devoted not only to current frontrunners, i.e., bioenergy and carbon capture and storage, but also to approaches less formally evaluated in terms of cost, effectiveness, resource availability, and acceptability (Rau, 2019).

Previous research (Keller et al., 2014; Lenton et al., 2018) have simulated the spreading of 10 Gt/y (∼0.25 Pmol/y of alkalinity) in the period 2020–2100; this amount represents the total transport capacity of all large cargo ships and tankers assessed by Köhler et al. (2013), considering 0.33 Gt as the total deadweight tonnage (dwt) and an average of 32 ports called per ship per year.

Renforth et al. (2013) assessed the need of 101 dedicated 300,000 dwt bulk carriers to discharge 1 Gt/y of SL, assuming a discharge time of ∼3.5 days (at a discharge rate of 1 ton per second), within a discharge cycle length (including the loading and the time for reaching the open ocean and return) of ∼11 days. Harvey (2008) considered the addition of calcium carbonate to upwelling regions using smaller vessels, and suggested 750–3000 ships would be required to deliver 4 Gt of $CaCO_3$ per year. While the use of dedicated ships to spread SL offers greater control of the application area and distribution rates, the use of existing shipping capacity and routes would access a larger area and offer pathways to more rapid scalability.

In the present study, we have undertaken a detailed analysis of the potential of SL discharge for the Mediterranean Sea, a closed basin where maritime transport routes are denser than the global average, and precise data on navigation are available. Alternative scenarios that consider new dedicated ships, purchased or built for the purpose, and the use of ballast water tanks to carry and discharge the SL are also discussed. Conservative values of discharge rates of SL ($\leq$25 kg/s) have been considered, in order to minimize the risk of impacting the marine environment in the ships' wake.

The assessment of the localized impact produced by SL at the discharge point, due to a temporary increase of pH and alkalinity, is necessary to evaluate the environmental side effects of this practice. A pH increase (leading to a decrease in aqueous CO_2 and an increase in bicarbonate ion concentrations), as well as the co-dissolution of other elements, could have a detrimental impact on marine ecosystems (Bach et al., 2019). Pedersen and Hansen (2003) and Locke et al. (2009) demonstrate the low probability, for different kinds of organisms, to survive when exposed to high pH level, over several days or weeks. Cripps et al. (2013) point out to acid-base balance alterations in Carcinus maenas once again in response to acute exposure to $Ca(OH)_2$ concentrations. Bach et al. (2019), recognize how a pH increase, whilst leading to benefits such as the decrease in aqueous CO_2, the increase in bicarbonate ion concentrations, the co-dissolution of other elements, could, conversely, shift the current ecological equilibrium, with detrimental consequences for some organisms rather than others depending on the alkaline mineral used. Hence, a better understanding of the ecological implications of ocean liming requires additional dedicated experimental studies.

The local impact where SL is applied is related to the mineral composition (i.e., % of Mg) and to the technology of discharge chosen (Renforth and Henderson, 2017; Bach et al., 2019). The discharge of $CaCO_3$ in specific areas in the deep ocean (below 200 m) characterized by lower biodiversity (Costello and Chaudhary, 2017), favorable mixing conditions and upwelling currents, has been studied by Harvey (2008), and has the disadvantage that can only be applied in isolated upwelling regions of the world's ocean (Garcìa-Reyes et al., 2015) in order to impact climate. SL dispersion in the wake of a ship may be a more efficient technique since it allows it to dissolve quickly within the rapidly mixed wake while the ship is cruising. The dispersion is strongly dependent on the rate of dissolution within the mixed wake of the ship, influenced by vessel's waterline length, speed, and the discharge rate; accurate modeling and *ad hoc* experiments are needed to establish a relationship between the amount of SL discharged and the impact produced, i.e., to define application limits useful to avoid or minimize the environmental impact. An overview of modeling approaches for the assessment of SL concentration in the wake of the ships are presented here, and an initial assessment is performed with two modeling approaches: the first was a three-dimensional non-reactive computer fluid dynamics (CFD) model, where turbulent diffusion conditions have been applied to understand particles and concentrations behavior. Then, a one-dimensional reactive model was applied to provide an initial simplified method of incorporating chemical parameters into previous CFD modeling results.

MATERIALS AND METHODS

Potential Discharge at the Global Scale

Existing maritime vessels could be used for transporting SL and discharging it along the route. The equipment for SL loading and discharge could be easily designed, and a share of the capacity and loading space could be dedicated to the transport of pulverized SL; the latter could be discharged in the form of a slurry, also called "milk of lime," which can be prepared on board by mixing pulverized $Ca(OH)_2$ with water. The necessity of using milk of lime and not just limewater (the aqueous solution of calcium hydroxide) is due to the poor solubility of calcium hydroxide (1.73 kg/m^3 at 25°C), that would require a very relevant amount of seawater to dilute SL. Minimizing the volumes of water allows to speed up the discharge and to decrease the energy consumption for water management; the use of water from the engine cooling system could reduce the need of fresh seawater for mixing, reducing the interactions with seawater environment and saving energy for the pumping. The design of the solids handling system, and the optimum water content, is beyond the scope of this work.

The potential of SL discharge by existing maritime traffic depends on several factors, such as:

- fleet size and capacity;
- length of navigation at sea;
- fraction of the existing capacity that can be dedicated to SL transport;
- SL supply chain.

Existing Maritime Fleet Size and Capacity

Data regarding the number and use of the different types of ships, subdivided by type and size classes, are reported by the Greenhouse Gas Studies of the International Maritime Organization (IMO–International Maritime Organization, 2014), which refers to the year 2012, shown in **Supplementary Table 1**. Data on the number of vessels relate to both the total registered and the active ships circulating as detected by the AIS (Automatic Identification System); the latter is used to estimate the average sailing days, of interest for the discharge potential. The total equivalent hours of navigation per year could be calculated by multiplying the number of active ships by the number of average equivalent days at sea.

Table 1 shows the summary values for different categories of ships. The average values are calculated by weighting the different size classes based on the number of annual sailing days.

Figure 1 shows that 92% of the total active capacity, in terms of deadweight tonnage (the measure of how much weight a ship can carry), is related to two ship categories, cargo (bulk carrier, container, general cargo) and tanker (chemical tanker, oil tanker), although they represent only about 40% in terms of vessel number. Bulk carriers and container ships, directly suitable for SL discharge because of their structure and for logistic reasons (Panarello, 2020), have been considered for the assessment of SL discharge worldwide. They represent only 17% of the total commercial global fleet in terms of number, but 53% in terms of total active tonnage (**Table 1**).

Length of Navigation at Sea

Longer navigation at sea allows to either maximize or minimize the discharge rate of a fixed amount of SL. Container ships and bulk carriers have relevant average days of navigation (218 and 181 respectively), as well as about 70% of the total distance covered by vessels worldwide. A significant fraction of the registered fleet is not used, albeit this fraction is lower for bulk carriers and container ships. Although detailed data on the average distance traveled per typical sea-leg are not available, the average distance covered by commodities (6,278 km for dry bulk carriers, 8,938 km for Container ships, see **Supplementary Table 2**) was calculated using the ratio between the world seaborne trade in cargo in ton-miles and the total global trade (UNCTAD–United Nations Conference on Trade Development, 2018, 2019a).

Existing Ships Tonnage Dedicated to the Transport of Slaked Lime

The transportation of SL would obviously compete with the transportation of goods, and the convenience of SL transport could be increased by revenue that can be obtained from SL spreading (i.e., due to carbon credits for CO_2 removal generated). However, it must be considered that, for logistical reasons, ships dedicated to the transport of goods from the place of production to the place of consumption, are often sailing not fully loaded, in particular in the return trip (Narula, 2019). The space used for slaked lime storage and for all the equipment for making the slaked lime will be permanently not available for transporting goods, but will allow the discharge also during the return trip.

According to information gathered from a ship designer (Panarello, 2020), it may be assumed that some 10–20% of the net cargo capacity of the container ships could be used for carrying slaked lime, since in many routes containers ships can store SL in the hold. Although adding weigh on board would reduce the ship performances, and requires space permanently dedicated for SL storage in the hold, as well as pipes and pumps is subtracted for other uses, this option would not impair significantly the use of the ship and the intended operations. In this scenario, it would not be necessary to carry out extensive modifications to the ships as it would be just a matter of arranging dedicated tanks and suitable pumping and conveying systems, while much greater efforts would be required to install dedicated SL loading facilities at calling ports.

Bulk carriers could also be used for carrying SL during sea passages in ballast, i.e., trip with no cargo on board to get a ship in position for the next loading port or docking (see Use of Ballast Water Tanks of Existing Ships). SL should be more conveniently loaded in the ship as a powder and then mixed with water on board, so to produce a slurry, called "milk of lime," which is discharged in the sea. In order to limit the amount of water for SL dilution, it is assumed to use 2% of water dilution compared to saturation, equivalent to a SL concentration of 86.5 g/l (=1.73/0.02) or 11.6 liter per kilogram of SL discharged, which is typical for slurry management systems.

TABLE 1 | Main characteristics of the existing maritime fleet (Data source: IMO–International Maritime Organization, 2014).

Ship type	Total fleet size (IHSF data)	Active ships observed (AIS data)	Average days at sea	Total days of navigation (AIS data)	Average speed at sea	Distance covered		Average active capacity	Total active capacity	
			Days/year	Days/year	km/h	mkm/year	%	dwt	10^6 dwt	%
Bulk carrier	10,397	9,286	181	1,674,585	21.4	862	20%	75,752	703	40%
Container	5,132	4,855	218	1,046,903	27.4	688	16%	45,417	220	13%
General Cargo	16,486	9,433	165	1,554,792	18.1	675	15%	7,470	70	4%
Cargo	**32,015**	**23,574**	**184**	**4,276,280**	**21.7**	**2,224**	**51%**	**43,499**	**1,025**	**59%**
Chemical tanker	4,935	4,179	175	729,085	21.0	367	8.4%	20,883	87	5%
Oil tanker	7,395	5,165	178	891,817	20.0	429	10%	96,676	499	29%
Tanker	**12,330**	**9,344**	**177**	**1,620,902**	**20.5**	**796**	**18%**	**62,584**	**585**	**33%**
Ferry-pax only	3,152	1,197	184	219,503	25.6	135	3.1%	214	0.3	0.01%
Cruise	520	372	222	75,593	22.3	41	0.9%	6,104	2	0.1%
Ferry-RoPax	2,867	1,778	192	341,592	18.9	155	3.5%	2,110	4	0.2%
Passenger	**6,539**	**3,347**	**193**	**636,688**	**21.6**	**330**	**7.5%**	**1,931**	**6**	**0.4%**
Liquefied gas tankers	1,612	1,410	213	291,101	24.5	171	3.9%	35,294	50	3%
Other liquids tankers	149	39	116	4,530	15.4	2	0.0%	670	0	0.0%
Refrigerated bulk	1,090	763	173	132,076	21.5	68	1.6%	5,695	4	0.2%
Ro-Ro (Ferry)	1,745	909	89	157,428	10.1	38	0.9%	6,111	6	0.3%
Vehicle	837	776	255	196,410	24.4	115	2.6%	16,576	13	0.7%
Yacht	1,750	1,110	66	73,316	17.3	30	0.7%	171	0	0.0%
Service—tug	14,641	5,043	100	502,713	10.7	129	2.9%	119	1	0.0%
Miscellaneous—fishing	22,130	4,510	164	741,334	12.0	213	4.9%	181	1	0.0%
Offshore	6,480	5,082	106	538,228	12.8	166	3.8%	1,716	9	0.5%
Service–other	3,423	2,816	116	325,911	12.6	99	2.3%	2,319	7	0.4%
Miscellaneous–other	3,008	64	117	7,477	11.7	2	0.0%	59	0	0.0%
Other	**56,865**	**22,522**	**134**	**2,970,524**	**14.5**	**1,034**	**24%**	**5,768**	**130**	**7%**
Total	**107,749**	**58,787**	**170**	**9,504,393**	**19.2**	**4,383**	**100%**	**29,711**	**1,747**	**100%**

Slaked Lime Supply Chain

The possibility to transport the quantities of SL required does not only depend on the tonnage but also on the frequency of reload. If ships are loaded with SL only at the departure and arrival ports, the ships will discharge the load during the whole trip, thus the discharge rate will depend on the tonnage of the vessels and on the sea-leg length. The discharge potential increases if case reloading of SL is assumed during intermediate stops. Bulk carriers and container ships usually make several stops during their trips, when SL could be refilled during the standard loading and unloading operations in the ports. The analysis of several bulk carriers' routes via different platforms (Marinetraffic, 2019; Vesselfinder, 2019) shows that bulk carriers usually make one intermediate stop. For container ships, an average of four intermediate stops has been assessed by analyzing the main routes identified by UNCTAD–United Nations Conference on Trade Development (2019a), (Transpacific, Intra-regional, Europe-Asia, East-West, South-South, Europe-North America), and the data on routes lengths available in Marinetraffic (2019) considering the ports along the route (see **Supplementary Table 3** for details). Logistic constraints might limit the possibility of loading SL in each stop, for instance additional time required for loading or the lime manufacturing infrastructure.

Potential Discharge at the Local Scale—Mediterranean Sea

A more detailed assessment of the potential SL discharge is possible at the local scale, where maritime traffic data are available. Here a case study of the Mediterranean Sea is considered, where monthly data of traffic density in the year 2017 are available from the EMODnet-Human Activities Project (EMODnet, 2019a), as monthly hours of permanence in the cells of a 1 km x 1 km grid for the whole Mediterranean Sea (EMODnet, 2019b). Two vessel categories (cargo and tanker), have been considered. According to IMO–International

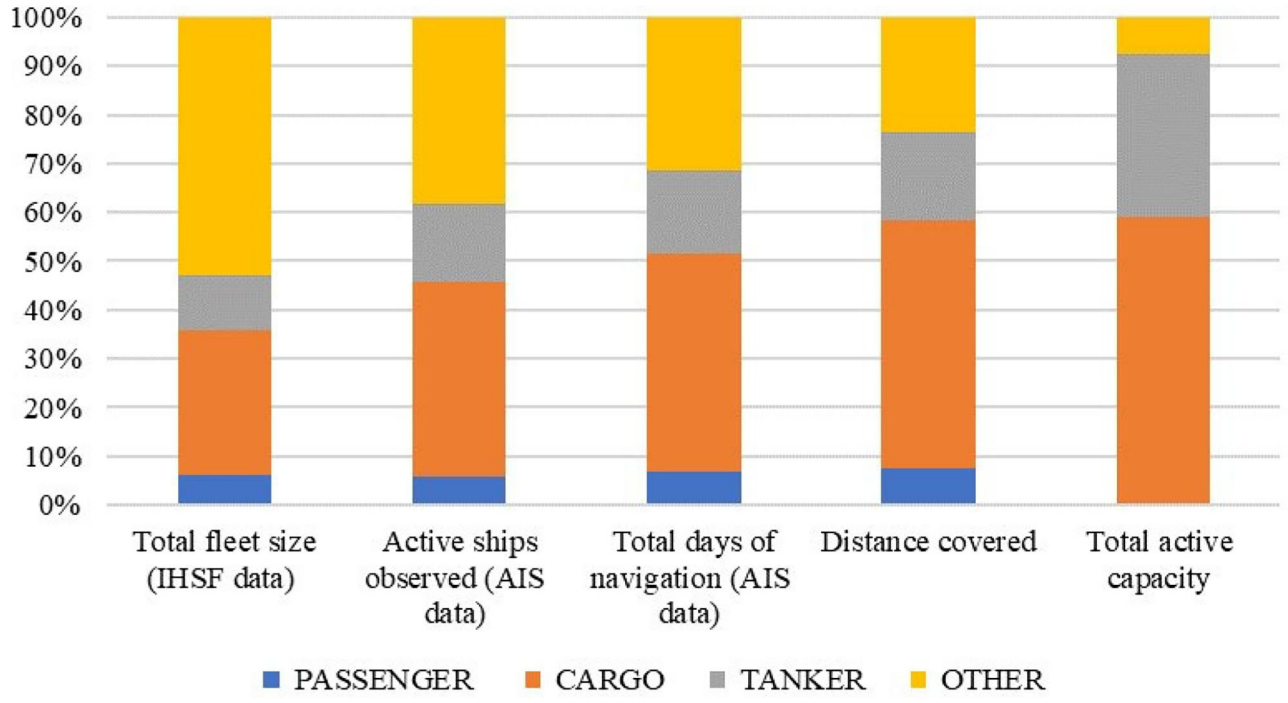

FIGURE 1 | Main characteristics of existing passenger, cargo and thanker ships (Data source: IMO–International Maritime Organization, 2014).

Maritime Organization (2014) they represent about 56% of all commercial vessels circulating in the world and 92% in terms of active tonnage. Other categories have limited navigation hours or operate near to the coast, thus they are less suitable for spreading SL.

EMODnet Data

EMODnet vessel traffic density data consider the hours when ships are at berth in the proximity of ports, which are clearly not of interest for the purpose of spreading SL. As an example, **Supplementary Figure 1** shows the detail of the original cargo and tanker traffic around Malta.

In order to exclude these data, the cumulative distribution of monthly hours of navigation for each cell and for each vessel category has been assessed; the maximum number of monthly hours in the cells has been limited to a threshold value of 10, thus assuming a limit value of 10 h/km^2/month for vessels density. The percentile of the distribution which corresponds to the threshold value 10 is quite similar for the two categories of vessels considered (99.3rd for the category Cargo, 99.7th for the category Tanker). The value chosen for the threshold, 10 h/month, is very close to the inflection point of the curves that represent the cumulative distribution of density values for the two categories of vessels (see **Supplementary Figure 2**). By means of visual comparison between the original traffic density maps and the maps after the application of the threshold, it has been verified that this choice of limitation to 10 h/month of the permanence of the ships in the cells, clearly identified as berth areas, did not substantially affect the cells in the routes of ships for the two categories of vessels.

Although the number of cells applicable is very low (<0.7% of the total cells of the grid) the application of the threshold leads to a drastic reduction of the total hours of navigation, respectively 51 and 53% for cargo and tanker ships. Monthly hours of navigation in the Mediterranean Sea before and after the application of the threshold are available in **Supplementary Table 4**.

Further processing has also been carried out to eliminate the cells of the EMODnet grid whose centroid is <5 km from the coast. The further reduction in the total hours of navigation, is−12.6 % for Cargo and−13.6% for Tanker. The total annual hours of navigation are shown in **Supplementary Table 5**.

The traffic density of cargo effectively exploitable for SL discharge is shown in **Figure 2**.

Comparison of Vessel Traffic in the Mediterranean Sea and Worldwide

A comparison between the annual hours of navigation in the Mediterranean Sea and the hours of navigation worldwide could be done considering for the IMO data reported in **Table 1**; it assesses the total equivalent navigation hours/year as the product of the number of vessels for the number of average equivalent days at sea (calculated by IMO considering the actual engine running hours and assuming 24 h per day). Results in **Table 2** show that the vessel traffic in the Mediterranean Sea accounts for 4.9% (cargo) and 5.8% (tanker) of the global traffic. This highlights that traffic density in the Mediterranean Sea is greater than the global average, since the surface of the Mediterranean

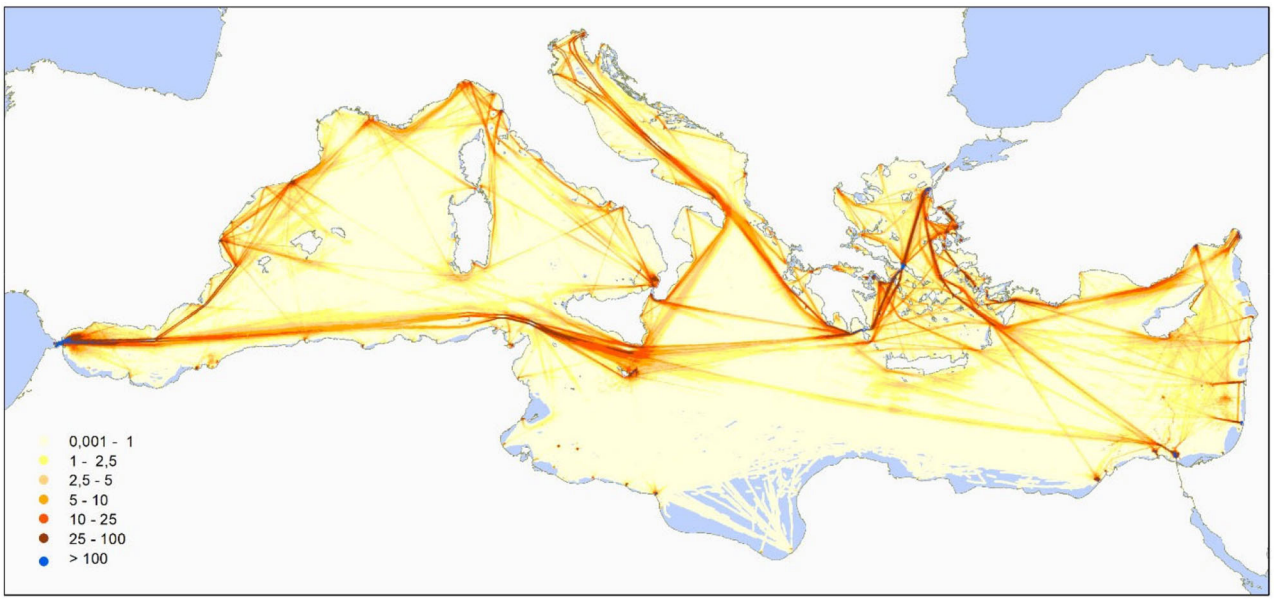

FIGURE 2 | Maritime traffic density (hours/year) for cargo exploitable for slaked lime discharge.

TABLE 2 | Hours of navigation in the Mediterranean Sea and worldwide.

		Cargo ships	Tankers
Navigation hours/year—Mediterranean Sea (EMODnet) (10^6)	a	5.2	2.3
Number of ships—World (IMO)	b	23,574	9,344
Equivalent average days/year of navigation—World (IMO)	c	184	177
Navigation hours/year—World (10^6)	$d = b \cdot c \cdot 24/10^6$	104	40
% Mediterranean Sea/World hours per year	% a/d	4.9%	5.8%

TABLE 3 | CO_2 LRIT signals of cargo and tanker maritime traffic in the Mediterranean Sea and worldwide (Source: EDGAR, 2018).

		Cargo ships	Tankers
LRIT signals—Mediterranean Sea	a	336,370	411,389
LRIT signals—World	b	14,085,525	14,085,146
% Mediterranean Sea/World	% a/b	2.4%	2.9%

Sea represents only 0.7% of the global ocean surface (2.51 Mkm^2 compared to 361 Mkm^2).

EDGAR Data

The Emission Database for Global Atmospheric Research (EDGAR) is a product of the Joint Research Center (JRC) and the PBL Netherlands Assessment Agency and contains inventories of global emissions of greenhouse gases and air pollutants (Wang et al., 2008; Alessandrini et al., 2017; EDGAR, 2018; Crippa et al., 2020). CO_2 emissions from maritime traffic for 2018 are shown in **Supplementary Figure 3**. EDGAR assesses emissions from ship traffic globally on the basis of the fuel consumption data used disaggregating them on a grid using LRIT (Long Range Identification and Tracking) data signals provided by the ships flying the flag of the European Union (EU) member states, Iceland, Norway and the overseas territories of the EU member states. Emissions downscaling is also carried out using LRIT signal density data by ship category, i.e., assuming the same emission factor worldwide for the same ship category. Focusing on the Mediterranean Sea, the percentage of LRIT signals in the Mediterranean Sea compared to the global total (that also represents the percentage of hours of navigation) of two categories of ships is shown in **Table 3**.

The percentages of maritime traffic in the Mediterranean Sea compared to global traffic (in terms of hours of navigation) estimated on the basis of EDGAR data for 2010 are substantially lower than those previously evaluated by EMODnet/IMO data for 2017/2012. This difference can only be partially due to the different years considered, since the average variation of CO_2 emissions from shipping traffic in the period 2012–2015 shows a very small increase (IMO–International Maritime Organization, 2014; ICCT–International Council on Clean Transportation, 2017); a more remarkable reason is that EDGAR's dataset covers ships flying the flag of States contributing to the EU LRIT

Cooperative Data Center (CDC), namely all EU Member States, Iceland, Norway, and Overseas Territories of EU Member States. Nominally, the LRIT vessel positions are refreshed every 6 h, while there is significant traffic in the Mediterranean Sea of ships flying the flags of non-European States.

As shown in **Table 4**, according to UNCTAD data (UNCTAD–United Nations Conference on Trade Development, 2019a), commercial ships flying the flag of a European state (including Norway) account for 14% of the world's commercial fleet in terms of numbers (21% in terms of gross tonnage); instead, ships belonging to shipping companies based in a European state (including the Principality of Monaco and the overseas territories of European states such as Bermuda Islands) account for 29% of the world's total commercial fleet (41% in terms of dead weight tonnage), 86% of which fly a foreign flag (i.e., a flag of a country other than that of the owner shipping company's headquarters). These numbers are congruent with numerous studies (e.g., Luo et al., 2013; European Commission, 2015; Deloitte, 2017) which have shown the relevance of the practice of "flagging out," where European shipping companies are using flags of convenience of non-European countries, such as Panama, Marshall Islands, Liberia, etc., in order to obtain tax benefits, reducing the costs of the crew and social security.

For example, the Mediterranean Shipping Company (MSC), Europe's leading CO_2 emissions company (Transport Environment, 2019), is reported to use the Panama flag for a large part of its fleet. As regards the countries, 52% of the ships belonging to shipping companies based in Greece, which make up about 9% of the world commercial fleet, fly the Liberian, Panamanian or Marshallese flag (UNCTAD–United Nations Conference on Trade Development, 2019b). In addition, a sample analysis of ships sailing in the Mediterranean Sea registered on marinetraffic.com (Marinetraffic, 2019) shows a significant proportion of ships flying the flags of non-European countries. It seems therefore very plausible that a significant part of the CO_2 emissions of ships is not represented by the EDGAR database, thus underestimating the maritime traffic in the Mediterranean Sea.

The Fluid Dynamics of Slaked Lime Discharge at Sea

The simulation of the behavior of SL particles after their release in the wake of a ship could be done with several methodologies and fluid dynamic modeling approaches.

Research on dilution rates in the wake of ships has initially considered the discharge of liquids (Delft, 1970; Delvigne, 1987; Byrne et al., 1988) and a model that describes the dependence of the dilution on the speed, dimensions and specific resistance coefficient of the ship has been proposed by Lewis (1985). A simplified formula (1), valid for the disposal of liquids, has been adopted in 1975 by the former International Maritime Consultative Organization, known today as International Maritime Organization (Renforth and Henderson, 2017).

$$D = \frac{c}{Q} \cdot U^{1.4} \cdot L^{1.6} \cdot t^{0.4} \quad (1)$$

where:

D: dilution factor
c: constant equivalent to 0.0030 for a single discharge orifice or 0.0045 for two discharge orifices
Q: volume discharge rate
U: vessel speed
L: waterline length
t: time after disposal

Further field testing (Byrne et al., 1988; Chou, 1996), however, showed that this formula underestimates the dispersal rate by 3 to 10 times. Other studies considered the dilution following discharges from large cruise ships (US-EPA, 2002; Loehr et al., 2006). Katz et al. (2003) simulated the dilution of pulped waste materials into the wake of a US Navy frigate, carrying out field measurements and computer modeling. Situ and Brown (2013) studied the fluctuations of surrogate pollutants concentrations released in the wake of an outboard motor within a small waterway, assessing experimentally the dispersion constant, aka the exponent of time t in formula (1). Chou (1996) identified three different behaviors of the flow within the ship wake development (**Figure 3**), considering the ratio between the distance from the ship (x) and the ship's width (B).

In the long-term diffusion region ($x/B>100$) and its influence on the dilution process of the lime, the flow motion is governed only by the ocean currents and the ambient turbulence. In the far wake ($7<x/B<100$) it is independent both on the geometry and configuration of the problem; as a consequence, the mean velocity profiles in the transversal direction present similar behavior at different distances from the ship, as theoretically proposed (Pope, 2000) and experimentally verified by numerous authors (Naudascher, 1965, Chen and Rodi, 1980). Moreover, in

TABLE 4 | Number of ships and total deadweight tonnage registered within the European Union and worldwide (Source: UNCTAD–United Nations Conference on Trade Development, 2019a).

Country or territory of ownership	Number of ships				Dead-weight tonnage (10^6 ton)			
	National flag	Foreign flag	Total	% foreign flag/total	National flag	Foreign flag	Total	% foreign flag/total
European Union (1)	3,251	12,500	15,219	82%	111	685	796	86%
World total	22,556	29,128	51,684	56%	542	1,420	1,963	72%
EU/World	14%	43%	29%		21%	48%	41%	

(1) Including the territory of Norway, Iceland, Monaco and overseas territories.

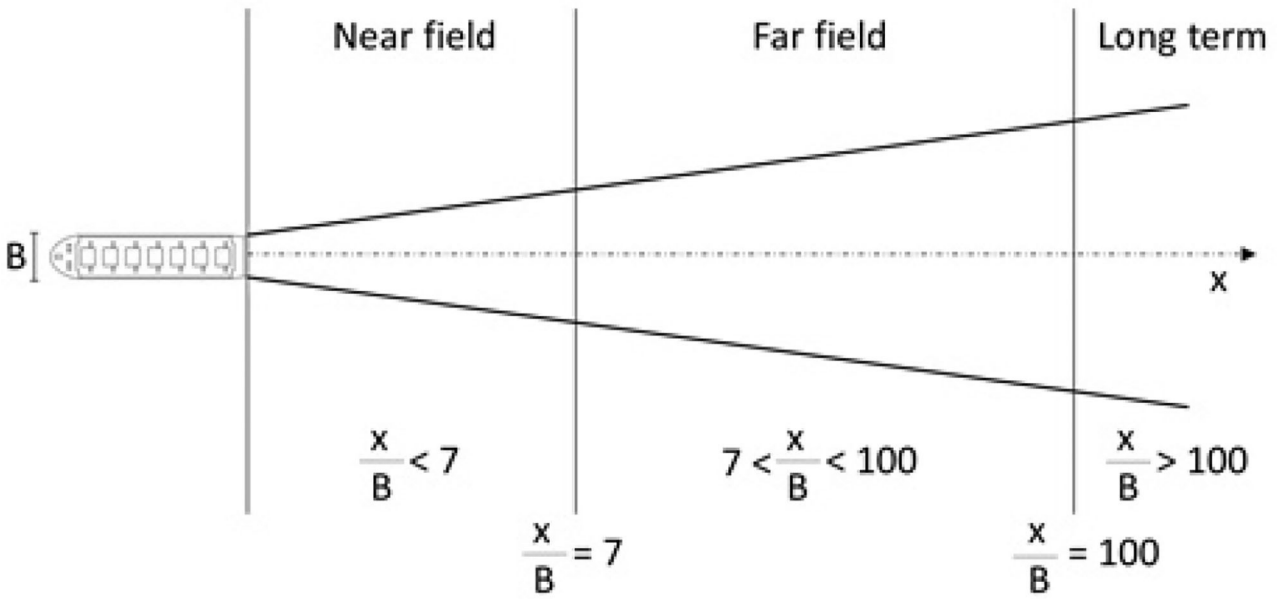

FIGURE 3 | Schematic subdivision of the ships' wake (adapted from Chou, 1996).

this region the dilution rate can be easily obtained, since non-reactive quantities, advected by the flow, behave similarly (Chou, 1996). The near wake (x/B < 7), wherein lower dilution rate and thus higher SL concentration in seawater could be expected, may not have a simple and universal solution. Indeed, in this region the flow strongly depends on the ship geometry and on the velocity induced by the propeller.

In recent years, thanks to the development of accurate numerical models and the improvements of computational resources, the Computational Fluid Dynamics (CFD) is frequently employed to investigate applicative problems of engineering interest. Especially for the naval and ocean research field, CFD has become a powerful tool because of the multiple difficulties that can be faced in producing experimental data both in the model and at the full scale. This is the case of the SL release, where a better understanding of SL dispersion in the near field of the wake of a ship could be derived from CFD.

Three-Dimensional Non-reactive CFD Model

A simulation of the flow behavior in the wake of a ship has been performed through a three-dimensional bi-phase CFD model, where SL discharged has been treated as a passive non-reactive substance (inertial article) advected by the flow. The aim is to attain a first assessment of how particles behave and what their dilution rate is. As the massive fluid stream is assumed to be found around the keel, all calculations have been made considering the wake raised by the ship in the region located in the back of the hull.

Numerical simulations have been performed using the free CFD Open-Source library called OpenFOAM (Open Field Operation and Manipulation) given the wide range of features that provides for the most various problems such as combustion, heat transfer, complex, and multi-phase flows. In the numerical code, the Unsteady Reynolds Averaged Navier-Stokes (URANS) equations are solved by using the transient *PimpleFoam* solver and the k-ω-SST turbulence model. Effects due to gravity (SL particle sinking) and the wave motion are considered negligible, with respect to the flow induced by the propeller in the wake. The propeller was modeled as an actuator disk (Hough and Ordway, 1964).

A Kriso container ship (KCS, Length 232.5 m; width 32 m; depth 19 m; speed 6 m/s or 21.6 km/h), one of the most widespread large ship model, has been chosen, being a valuable geometry for a real application of this process. A slurry of $Ca(OH)_2$ particles with 45 μm radius and initial concentration $C_0 = 86.5$ g/l is discharged by a circular nozzle, injected just above the screw where the velocity induced by the propeller is higher. Two flow rates, 10 kg/s and 100 kg/s have been considered, corresponding to nozzle diameters (d_0) of 0.27 and 0.86 m, respectively.

Although multiple injection points could be used to reduce the maximum load in the wake, a single injection point has been considered for the sake of simplicity. Mean velocity, relative to the ship reference frame, and the particle fields in the wake of the ship are shown in **Supplementary Figure 4**. Particle dispersion is mainly influenced by the advection of the mean flow. In this region, provided that particles are advected by the high velocity induced by the propeller, the flow can be described by a round jet model (Rajartnam, 1976) with axis aligned with the streamline of maximum velocity. This assumption is confirmed by the results of numerical simulations: the mean velocity of the flow is constantly equal to the value at the injection point (U_0), 10 m/s, as long as the distance, namely s, is <6 times d_0. From this distance on, the mean velocity varies well approximated by the

following equation (2) (Kundu et al., 2012), that considers the streamline starting at the center of the circular discharging area with maximum velocity and particles concentration:

$$U(s) = 6\,U_0\frac{d_0}{s}, \quad s \geq 6\,d_0 \tag{2}$$

where:

U(s): mean flow velocity along the axis of a turbulent round jet, with respect to the absolute reference frame [m/s];
U_0: flow velocity at the injection point, with respect to the absolute reference frame [m/s];
d_0: diameter of the circular area of discharge [m];
s: curvilinear abscissa along the streamline starting at the injection point [m].

As in round jets, diffusion and dilution begin for $s > 6d_0$, and thus particle concentration is constant until $s \approx 6d_0$. Furthermore, the particle concentration along the streamline starting at the injections point, obtained by the numerical simulations, is in good agreement with the jet model (Kundu et al., 2012) following the equation:

$$Cnr(s) = 5\,C_0 \cdot \frac{d_0}{s}, \quad s \geq 6\,d_0 \tag{3}$$

where:

C_{nr}: concentration of a non-reactive substance [g/l];
C_0: initial concentration [g/l].

One-Dimensional Reactive Model

A simplified one-dimensional reactive model for the dispersion of SL particles advected by the mean flow along the streamline starting at the injection point, is here formulated. The aim is now to assess SL particle radius and concentration along the wake, including dynamic chemical reaction between SL and the seawater. It is considered that particle settling velocity is not relevant compared to the velocity of the stream.

Fluid velocity is approximated by equation (2), and each calcium hydroxide particle is assumed to be solid and perfectly spherical. According to Tannenberger and Klein (2009), particle radius r_p is expected to shrink with the following expression:

$$r_p = \sqrt{r_{pI}^2 - 2\,\phi_0\,\sigma\,t} \tag{4}$$

where:

r_p: radius of the particle [μm];
r_{pI}: initial radius of the particle [μm];
ϕ_0: diffusion potential [-];
σ: seawater calcium ion diffusivity coefficient [m^2/s]
t: elapsed time [s].

As can be seen, radius particle is a function of a chemical parameter known as diffusion potential; it is a dimensionless number linked to two important chemical parameters, α and χ_0, as follows:

$$\phi_0 = \frac{\alpha \cdot \chi_0}{\rho_p} \tag{5}$$

where:

χ_0: difference between the saturation concentration of calcium at the particle surface and the calcium concentration in the bulk liquid [kg/m^3];

α: dimensionless ratio between mass transfer to the bulk and mass loss of the particle, known as a factor that should be taken into account for non-pure substances dissolution (Csanady, 1986).

The elapsed time from the injection of the particle located at s, is calculated integrating the reciprocal of the velocity given by Equation (2):

$$t(s) = \int_0^s \frac{1}{U(\xi)} d\xi \tag{6}$$

The rate of dissolution as expressed by Csanady (1986), depends on the mass flow M from the spherical particle to the water by this correlation:

$$\frac{d}{dt}\left(\frac{4}{3}\pi\rho_p r_p^3\right) = -\dot{M} \tag{7}$$

where:

$\dot{M}$: loss of mass of the particle [kg/s];
ρ_p: density of $Ca(OH)_2$ particle [kg/m^3].

Assuming that particle shrinking is mainly caused by the total mass transfer to the liquid phase, under diffusion and advection conditions, M can be modeled as proposed by Levich (1992):

$$\dot{M} = 6.33 \cdot \chi_0 \cdot \alpha \cdot \sigma \cdot r_p \cdot Pe^{1/3} \tag{8}$$

where:

Pe: dimensionless Peclet number which represents the ratio between convective and diffusive terms, assessed as:

$$Pe = \frac{2\,U(s)\,r_p}{\sigma} \tag{9}$$

Moreover, assuming that particles are advected by the fluid and drag effects are neglected, its velocity coincides with the fluid velocity, $U(s)$. Given the above, the relation held for particle concentration, in terms of time derivative, is calculated as the mass flow of a single particle, divided by the particle mass and multiplied by the local calcium hydroxide concentration. This leads to the following equation:

$$\frac{dC}{dt} = -\frac{\dot{M}C(s)}{\rho_p \frac{4\pi r_p^3}{3}} \tag{10}$$

where:

C(s): $Ca(OH)_2$ concentration along the streamline, as a function of the distance s [g/l].

Hence, provided that a time interval $dt = ds/U(s)$ corresponds to a fluid element displacement ds $[m]$ divided by the local fluid velocity, one can transform the equation (10) as follows:

$$\frac{dC}{ds} = -\frac{\dot{M} \cdot C(s)}{\rho_p \frac{4\pi r_p^3}{3} \cdot U(s)} \tag{11}$$

Finally, substituting $\dot{M}$ and the Peclet number in the equation (11) yields:

$$\frac{dC}{ds} = -\frac{7.54\ \phi_0\ C(s)}{\pi\ Pe^{2/3} r_p} \quad (12)$$

which can be integrated in space to obtain C as a function of the distance s.

While the concentration derivative is always negative, its absolute value increases with the particle radius reduction. Indeed, reducing the radius, the ratio between surface exchange and the mass of the particle increases, thereby accelerating the dilution process. Concentration reduction due to the particle size shrinking is thus applied to the concentration obtained by the advection of the fluid motion and by turbulent diffusion given by equation (2). Starting from the initial condition $C_{(0)} = 86$ g/l, equation (12) is integrated numerically using a four-step explicit Runge-Kutta scheme (Quarteroni et al., 2014), discretized on 2201 computational nodes equally distributed along the independent variable $0 \leq s \leq 1100$ m.

Parameters needed for the methodology presented here should derive from experimental works and be related to the local context where SL discharge happens. In this first analysis, all parameters have been taken from the literature, as reported in **Table 5**.

As diffusion potential appears to be an important parameter controlling the dilution rate of calcium hydroxide, since it combines the effect of α, χ_0 and ρ_p (see Equation 5), a preliminary analysis of its influence on the results has been performed by varying ϕ_0 within the range identified by Tannenberger and Klein (2009), from 0 to $2.09 \cdot 10^{-4}$.

pH Variation

Since the detailed evaluation of seawater pH increase due to $Ca(OH)_2$ dissolution requires chemical modeling which is outside the scope of this paper, a simplified approach has been used, based on a series of quadratic relationship between $Ca(OH)_2$ input and pH variation, assessed for different values of seawater pH through the software PHREEQC, developed by the U.S. Geological Survey to perform a wide variety of aqueous geochemical calculations (USGS, 2019).

A standard water composition (**Supplementary Table 6**, taken from Lyman and Fleming, 1940), with a pH of 8.12 (Butenschön et al., 2020) and a temperature of 20 °C has been considered. The continuous discharge has been divided into 50 meters steps, calculating input of dissolved $Ca(OH)_2$ in seawater in every step by the difference between $Ca(OH)_2$ particle concentration in seawater and the concentration of a non-reactive substance:

$$I_t = (Cnr_t - C_t) - (Cnr_{t-1} - C_{t-1}) \quad (13)$$

where:

I_t: input of dissolved $Ca(OH)_2$ at the step t [g/l];
Cnr_t: concentration of a non-reactive substance at the step t [g/l]—see Equation 3;
C_t: concentration of solid $Ca(OH)_2$ in seawater at the step t [g/l]—see Equation 12.

The pH increase in each step has been calculated with the quadratic relationship:

$$\Delta pH_t = a_t \cdot {I_t}^2 + b_t \cdot I_t + c \quad (14)$$

for different initial pH levels (**Supplementary Figure 5**); the fitting of the non-dimensional parameters a and b for the different pH initial levels proved the following equations (**Supplementary Figure 6**):

$$a = 0.000471 \cdot {pH_{t-1}}^2 + 0.00864 \cdot pH_{t-1} - 0.0397 \quad (15)$$

$$b = 0.0158 \cdot {pH_{t-1}}^2 - 0.294 \cdot pH_{t-1} + 1.36 \quad (16)$$

$$c = 0.0218 \cdot {pH_{t-1}}^2 - 0.401 \cdot pH_{t-1} + 1.86 \quad (17)$$

The final pH in every step is assessed by the following equation that considers the average pH due not only to the input of alkalinity, but also to the dilution in the wake (represented by Equation 2), that could be seen as an addition of "clean" water:

$$pH_t = -log_{10}\left(\frac{10^{-(pH_{t-1}+\Delta pH_t)} + 10^{-pH_0} \cdot D_t}{1 + D_t}\right) \quad (18)$$

where:

pH_0 = initial pH of seawater.

D_t = dilution during the step, calculated from the variation of a non-reactive substance along the streamline, $D_t = \frac{Cnr_{t-1}}{Cnr_t} - 1$. Considering Equation 3, it becomes $D_t = \frac{s_t}{s_{t-1}} - 1$, where s is the distance from the discharge calculated along the streamline.

The reaction of SL with CO_2 to produce calcium bicarbonate has not been considered since is the CO_2 uptake and hydration is potentially slower than the dissolution of SL. As such, this is a conservative assumption that predicts the largest impact on seawater pH since the reaction with CO_2 could reduce the pH spike.

Given that carbonate precipitation in natural seawater can take several dozens of minutes even at high pH (Chave and Suess, 1970; Pytkowicz, 1973), it was assumed that no $CaCO_3$ precipitation occurs in the ships' wake because of the rapid mixing time that leads to a short pH spike.

RESULTS

Potential Slaked Lime Discharge and CO_2 Removal Worldwide

Based on the existing global fleet size data and length of shipping route, the potential global discharge of SL has been assessed considering:

- The existing global fleet of bulk carriers and container ships;
- Fifteen percent of the ships' cargo capacity, resulting in the 13% of the average ships' tonnage, used for SL load;
- Ship discharge SL along existing routes, assuming an average distance of about 6,300 km for bulk carriers and 8,900 for container ships;
- Single load scenario, with SL loading at the departure; multiple loads scenario, with SL loading at one stop along the route for bulk carriers and two stops for container ships.

TABLE 5 | Constants quantities used in the one-dimensional bi-phase model.

Parameter		Value	u.m.	Source
r_{pI}	Initial radius of the particle	45	μm	Tannenberger and Klein, 2009
ρ_p	$Ca(OH)_2$ particle density	2240	kg m^{-3}	Tannenberger and Klein, 2009
ρ_l	Seawater density	1024.75	kg m^{-3}	Kaye and Laby, 1995
σ	Seawater calcium ions diffusivity	$6.32 \cdot 10^{-10}$	m^2 s^{-1}	Li and Gregory, 1974
η_l	Seawater dynamic viscosity	$1.08 \cdot 10^{-3}$	Pa s	Leyendekkers, 1979
α	Ratio between mass loss particle and mass transfer to bulk	0.54	-	Weast et al., 1989
χ_0	Chemical gradient for calcium ions dissolution	0.5781	kg m^{-3}	Pond et al., 1971; Csanady, 1986

- As shown in **Table 6**, the total potential SL discharge at a global scale is assessed between 1.7 Gt/year (load at departure), to 4.0 Gt/year assuming one intermediate reload for the bulk carriers and two for the container ships. It is worth noting that the discharge rate, estimated considering a uniform spreading of the load along the route, varies between 5 and 18 kg/s in the different cases analyzed.

Although atmospheric CO_2 removal should be evaluated by using biogeochemical cycle models through (particularly considering rebound effects from the ocean), it is possible to estimate the CO_2 removed from the atmosphere based on the amount of CO_2 absorbed per mole of $Ca(OH)_2$ added to seawater. The stoichiometric value suggests that 2 mol of CO_2 taken up per 1 mol of added $Ca(OH)_2$ (i.e., 2 mol of alkalinity neutralize 2 mol of carbonic acid, with 2 mol of atmospheric carbon dioxide dissolving into the ocean to reestablish the equilibrium). However, the reaction between a small proportion of the hydroxyl and bicarbonate ions to form carbonate and water, as well as vertical mixing of SL that could limit the actual availability of the alkaline water at the ocean's surface, reduce the efficiency of the uptake, thus a conservative value of 1.4 mol of carbon dioxide absorbed per each mole of $Ca(OH)_2$ added has been assessed by Keller et al. (2014). Considering this 1.4 mol/mol ratio, a range of total additional CO_2 uptake between 1.5 Gt/year and 3.3 Gt/year is assessed for single load and multiple loads.

Potential Slaked Lime Discharge in the Mediterranean Sea

The higher traffic density in the Mediterranean basin, compared to the global average, leads to a potential of SL discharge far higher than what requested for counteracting ocean acidification. Considering only the existing 5.15 million of hours of navigation of cargo ships, a low SL discharge rate of 10 kg/s leads to a total annual discharge of 186 Mt/year. Considering a conservative value of CO_2 absorbed per each mole of $Ca(OH)_2$, assessed as 1.1 mol/mol for the Mediterranean Sea (Butenschön et al., 2020), leads to a range of CO_2 additional uptake of about 122 $MtCO_2$/year, that is similar to the average annual baseline uptake of 120 $MtCO_2$/year assessed for the Mediterranean Sea in the period 2000–2019 by Butenschön et al. (2020). In other words, the discharge of SL by existing cargo ships along the Mediterranean route could provide a significant CO_2 removal and contrast to the ongoing seawater acidification trend.

Even a low discharge rate of 10 kg/s, the SL loaded in 15% of the ships' cargo capacity would be discharged in about 3300 km, without the need of any additional stops to reload along the majority of the routes in the Mediterranean Sea (See **Supplementary Table 7**). A discharge rate of 10 kg/s leads also to a volume of water of 416 m^3/h, that is similar to the water used for engine cooling in a 75,000 dwt bulk carrier ship, since main engines have a seawater flow rate of 0.06 m^3/h per kW of power (see **Supplementary Table 8** for details).

The same considerations apply for existing tanker ships, that also have a relevant discharge potential. The potential of passenger ships (i.e., cruise ship) is limited by their low capacity, as space use is already highly optimized. Assuming that 5% of dead weight cruise capacity is used for SL transport, SL would need to be reloaded daily if a discharge rate of only 1 kg/s is used. As such, the induced CO_2 removal by enhanced ocean alkalinization could only compensate no more than the CO_2 emitted by the vessel (see **Supplementary Table 7**).

Alternative Scenarios of Discharge

New Dedicated Ships

New dedicated ships built with the only purpose of spreading SL into seawater, with an average tonnage of 75,000 dwt, have been considered. Although this scenario allows flexibility in the choice of the discharge parameters (i.e., location and SL discharge rate), a discharge rate of 50 kg/s has been assumed. Since its discharge rate is five times higher than the one considered for existing ships in the Mediterranean Sea (see Alternative Scenarios of Discharge), specific works could be undertaken during the construction or renewal of the vessels in order to increase the points of discharge and to minimize the impact in the wake of the ship. The discharge rate is calculated assuming an average speed at sea of 25 km/h. Discharge is assumed to take place continuously throughout the route in the form of a slurry, using the power of additional engines and seawater for the mixing of the SL transported in pulverized form. The selection of the routes could be made in order to maximize the efficiency of CO_2 removal and the contrast to the ocean acidification, and avoiding areas where there could be eventual regulatory limitations for the discharge.

The total annual discharge by 1,000 new dedicated ships (assuming that 2.5 days are needed to load the ships in the ports, 15 days a year for maintenance stops and a discharge rate of 50 kg/s) assessed as shown in **Table 7**, amounts to 1.3 Gt/year.

TABLE 6 | Assessment of potential $Ca(OH)_2$ discharge from bulk carriers and container ships at the global scale.

		Bulk carriers		Container ships		
		Single load	Multiple load	Single load	Multiple load	
Average tonnage	dwt	75000		45000		See **Supplementary Table 1**
% dead weight cargo capacity (DWCC)	%	85%		85%		(See text)
% DWCC usable for $Ca(OH)_2$	%	15%		15%		(See text)
% Tonnage used for transporting $Ca(OH)_2$	%	13%		13%		(See text)
$Ca(OH)_2$ load on board	t	9563		5738		(See text)
Number of vessels per category	-	9286		4855		See **Supplementary Table 1**
Distance traveled of the maritime route	km	6300		8900		See **Supplementary Table 2**
Average cruising speed	km/h	21.4		27.4		IMO–International Maritime Organization, 2014
Average at sea days per annum	d/year	181		218		IMO–International Maritime Organization, 2014
Number of intermediate stops (with $Ca(OH)_2$ reload)	n°/year	0	1	0	2	(See text)
Average distance traveled per typical sea-leg	km	6,300	3,150	8,900	2,967	calc.
Navigation duration of the route	d	12.3	6.1	13.5	4.5	calc.
Average discharge rate along the route	kg/s	9.0	18.0	4.9	14.7	calc.
Number of exploitable yearly travels per vessel	n°/year	15	30	16	48	calc.
Total discharged $Ca(OH)_2$ per vessel	Mt/year	0.14	0.29	0.09	0.28	calc.
Total discharged $Ca(OH)_2$ by vessel category	Gt/year	1.3	2.7	0.4	1.3	calc.

Considering again a ratio of 1.4 mol of CO_2 absorbed per each mole of $Ca(OH)_2$ added (Keller et al., 2014) this correspond to a removal of 1.1 $GtCO_2$/year. Although the construction of 1,000 new ships, or in part the renewal of existing unused ships, is a monumental task, it should be taken into account that a quarter (about 8,000 ships) of the existing registered cargo fleet is not active (**Table 1**), and that United States built 2,710 Liberty ships in 4 years and a half during World War II (Davies, 2004). As such, the creation of ∼1000 dedicated ships over the coming decades appears plausible.

Use of Ballast Water Tanks of Existing Ships

Ballast water is carried in ships ballast tanks when the ships travel empty. It is filled or emptied when cargo is unloaded or loaded, or when a ship needs extra stability during critical weather conditions. A large number of bulk carriers are used only on a one-way trip for delivering cargo and are empty on their return trip. According to Brancaccio et al. (2018) 45% of bulk carriers travel without carrying any cargo on the return trip. Such trade asymmetries are larger for energy commodities and lower for commodities transported by containers (Narula, 2019).

Ballast water tanks could be used to contain and discharge SL into seawater, as proposed by Köhler et al. (2013). To discharge SL the installation of pumps for the purpose would not be necessary, since ballast pumps are designed for a rapid ballast water discharge. The use of ballast tanks to transport a slurry of SL could avoid the necessity of a dedicated cargo hold, and at the same time has the benefit of avoiding the treatment of ballast water (or at least reducing treatment costs), currently mandatory because ships are a major vector for the introduction of non-indigenous and harmful organisms (Johnson and McMahon, 1998; Sousa et al., 2008). pH increase through the addition of alkaline materials (one of which is calcium hydroxide) is an efficient and cheap ballast water treatment strategy (Starliper et al., 2015), since it kills the aquatic nuisance species that cause economic and ecological damages to oceans. International legislative constraints should be evaluated to understand the possibility of discharging SL slurry; ballast water treatment with SL is still not among the authorized treatment methods (IMO–International Maritime Organization, 2008).

Ballast water is about 36% of the deadweight tonnage of bulk carriers and container ships respectively (Globallast, 2017), thus the potential of SL discharge could be relevant, depending on discharge rate, sea-leg lengths and number of intermediate stops, as previously described. This option could be of great interest for some type of vessels (i.e., cruises) that have limitations in SL transport (see Slaked Lime Concentration and pH Variation in the Ships' Wake). Developments of carbon removal policy framework and CO_2 market recognizing revenue for SL discharge, therefore for enhanced ocean alkalinity, could generate potential revenues from ballast travels for the shipowners, thus making SL handling and transport more economically attractive. The main challenge connected to the use of ballast water for SL discharge is the prevention of $Ca(OH)_2$ precipitation in the slurry at the bottom of the tanks. This requires significant structural changes to the vessel to keep in suspension the SL in the

TABLE 7 | Assessment of the potential SL discharge from new dedicated ships.

	u.m.	Value	
Average single vessel tonnage	dwt	75,000	a
Percentage tonnage used for transporting $Ca(OH)_2$	%	85%	b
$Ca(OH)_2$ load (per ship)	t	63,750	c = a·b
Average cruising speed	km/h	25	d
Discharge rate	kg/s	50	e
Travel time of the sea leg	d	14.8	f = c/e·86.4
Average distance traveled per typical sea-leg	km	8,854	g = f·d/24
$Ca(OH)_2$ loading time at port	d	1.0	h
Number of yearly trips per vessel	-	21	i = 330/(f+h)
Average at sea days per annum	d	310	j = f·i
Total $Ca(OH)_2$ load discharged per vessel	Mt/year	1.3	$k = c \cdot i/10^6$
Number of vessels per category	-	1,000	l
Total potential $Ca(OH)_2$ discharge	Gt/year	1.3	$m = k \cdot l/10^3$

water, which should be further investigated before a more precise assessment of the discharge potential of this scenario.

Slaked Lime Concentration and pH Variation in the Ships' Wake

How the SL is added to the ocean will control the chemical changes in local seawater. The results of the modeling suggest that as in a round jet, the reduction of the concentration of a non-reactive substance with the distance is mainly related to the turbulent diffusion in the flow, besides to the diffusion of the mean velocity field due to entrainment of external flow. Velocity, particle concentration and relative dilution rate $D(s) = C_0/C(s)$ along the streamline are represented in **Figure 4** and **Supplementary Table 9** for discharge rates of 10 and 100 kg/s. Since the concentration is inversely proportional to the curvilinear abscissa (s), dilution grows linearly with the distance. With a discharge rate of 10 kg/s particle concentration is reduced by a factor 10 after 13 meters (about 2 s), and after 43 meters with a discharge of 100 kg/s. At the end of the near field of the wake (224 m), concentration is reduced 166 times and 52 times respectively for the lower and higher discharge rate evaluated.

This dilution considers only the dispersion of a non-reactant substance, thus in case of SL discharge, the dynamic of the chemical reaction between SL particle and seawater should be added in order to assess final SL concentration in the wake.

Results are reported in **Figure 5**, where the reduction of particle radius and its concentration are shown for 5 different values of the diffusion potential and 2 values of the discharge rate, as a function of the distance. The effect of the variation of the diffusion potential is evident since higher values cause a more rapid particle radius reduction as a consequence of dilution processes. The curve related to a null value of the diffusion potential reproduces exactly the behavior of the concentration under non-reacting conditions given by equation (3).

With 10 kg/s discharge rate, for distances lower than 250 m, particle radius remains >40 μm; afterward, concentration varies substantially depending on Φ_0. The lower the Φ_0, the slower the radius reduction and the lower the concentration decrease. A slower radius reduction entails a similar reduction in the divergence of concentration trends from that simulated in the first model. This implies that for all the near field and part of the a far field of the wake, the mass concentration reduction due to the particle size reduction is negligible with respect to the effect of the advection-diffusion related to the mean and the turbulent flow.

When the particle radius is reduced to smaller than 40 μm (after 400 m with a discharge rate of 100 kg/s), the effect of the chemical diffusion becomes dominant and the concentration diverges from the curve representing the pure diffusion derived by the fluid motion. Particle concentration becomes zero at a distance between 500 and 850 m (at the lower discharge rate) and after 900–1500 m (at the higher discharge rate). Dissolution of $Ca(OH)_2$ particle begins when particle concentration is about 0.4 g/l (discharge rate 10 kg/s) or 0.75 g/l (100 kg/s) thus a significant ionic load is provided to seawater within few minutes.

pH variations in the wake reach a maximum value of about in 1 unit, with minor differences (0.3 unit) between the two discharge rates. The high discharge rate (100 kg/s) moves the spike ahead, about 200–300 meters with higher diffusion potential and 500–700 m with lower, and increases the duration of higher pH value. With a 10 kg/s discharge rate, pH variation becomes lower than 0.2 units after 1400–1600 m from the discharge (230–330 s), while for 100 kg/s this happens 1700–3000 m (280–500 s) from the discharge (see **Supplementary Figure 7**). Eventually, this seawater would mix into the surrounding water.

These results could be refined considering the range of variation of other parameters listed in **Table 5**, which should be constrained through experimental studies or possible alternations to $Ca(OH)_2$ production. For example, decreasing the average particle radius in the slurry would decrease the time required for dissolution, thus increasing the rate of $Ca(OH)_2$ ionic load to seawater and thus maximum pH alteration.

DISCUSSION

A very high potential discharge of slaked lime in the sea can be achieved by using the existing global commercial fleet of bulk carriers and container ships and low discharge rates. This could reach several Gt/year of SL discharged if a significant share of the existing maritime traffic of dry bulk carriers and containers is used. In case between 20 and 40% of the existing fleet is involved in such operation of ocean liming, this would imply a potential of 1 Gt/y of CO_2 removal from the atmosphere.

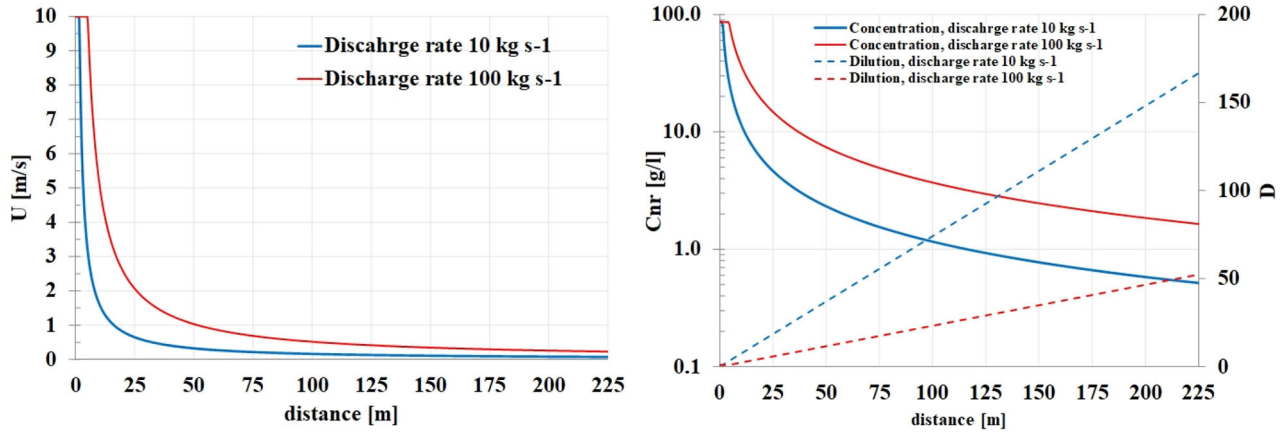

FIGURE 4 | Velocity of the flow (left plot), concentration of a non-reactive substance discharged in the wake (right plot, line) and dilution rate (right plot, dotted line), for two discharge rates.

For some closed basin, such as the Mediterranean Sea where traffic density is higher than the global average, the potential of SL discharge also with a low rate of 10 kg/s is far higher than what needed for counteracting ocean acidification (Butenschön et al., 2020).

Current global lime production is ∼360 Mt/year, which may increase to >500 Mt/year by 2100 and produces approximately an equivalent mass of CO_2 (Renforth, 2019). The proposal considered here would require the expansion of lime production to a scale equivalent to the global cement industry (4.5 Gt/year), with technologies that prevented the emission of the process CO_2 (e.g., Hanak et al., 2017). These facilities would need to located close to ports to avoid excessive overland travel, and additional loading facilities would be required. The design of an efficient logistic chain to increase the loading capacity of SL in ports is essential to the availability of SL for vessels at the departure or for the reload. High-capacity, zero-emissions hydroxide production could also be achieved via electrochemical water/salt/mineral splitting powered by non-fossil electricity (e.g., House et al., 2007; Rau et al., 2018).

Presently the addition of material to some areas of the ocean is restricted through national and international regulation. The responsible development of this approach requires that appropriate international governance mechanisms are considered and implemented before deployment (Lenton et al., 2019). While out of the scope of this study, it is important to consider how the research will be developed, including the development of laboratory-based experimentation, stakeholder engagement in experimental design, and the stage-gating of field trials.

However, important potential constraints should be considered, like the need of upscaling substantially the current levels of limestone mining and slaked lime production, the modification of existing ships, the implementation of loading facilities in the port or international and the national legislative restrictions that could limit the discharge in some areas. The definition of an efficient supply chain to increase the loading capacity of SL in ports is essential to the availability of SL for vessels at the departure or for the reload.

Using existing vessels has many advantages including lower substantial modifications of the ships for the purpose, lower capital and investment costs, low discharge rates due to the length of routes. However, a fleet of new dedicated ships could better manage SL storage and spreading. The use of ballast water tanks for carrying and discharging SL could be of great interest, but the risk of precipitation of $Ca(OH)_2$ or carbonate minerals (e.g., $CaCO_3$) in the slurry at the bottom of the containers would limit its application due to the long residence time in the ballast tanks.

The global potential of CO_2 removal from SL discharge by cargo and container ships (1.5-3.3 $GtCO_2$/year) or new ships (1.1 $GtCO_2$/y), assessed using average literature values of CO_2 removal per unit of SL added, could be limited by the actual availability of decarbonized SL as well as the maximum discharge rate that could avoid localized impacts of SL discharge on the marine environment.

Since a globally distributed alkalinity is responsible for a potentially small environmental local impact (Renforth and Henderson, 2017), low SL discharge rates in the ships' wake have been considered. SL dispersion on the wake of a ship, initially analyzed by representing the pure diffusion derived by the fluid motion, lead to two order of magnitude reduction of the initial SL concentration within the first 25 s in case of low discharge rates, and within the first 75 s with high discharge rates. The dissolution model added to the fluid dynamic analysis allows simulating the shrinking of particle radius, thus the dissolution of the ionic load to seawater. As much concentration diverges from the curve of the non-reactive diffusion, the higher the particle radius reduction, the dispersive phenomena would prevail over the advection. The pH variations are lower than 1.5 unit, and the duration of pH variation, higher than 1 unit, lasts just a few minutes for higher discharge rates. Diurnal fluctuations of 0.2 pH units

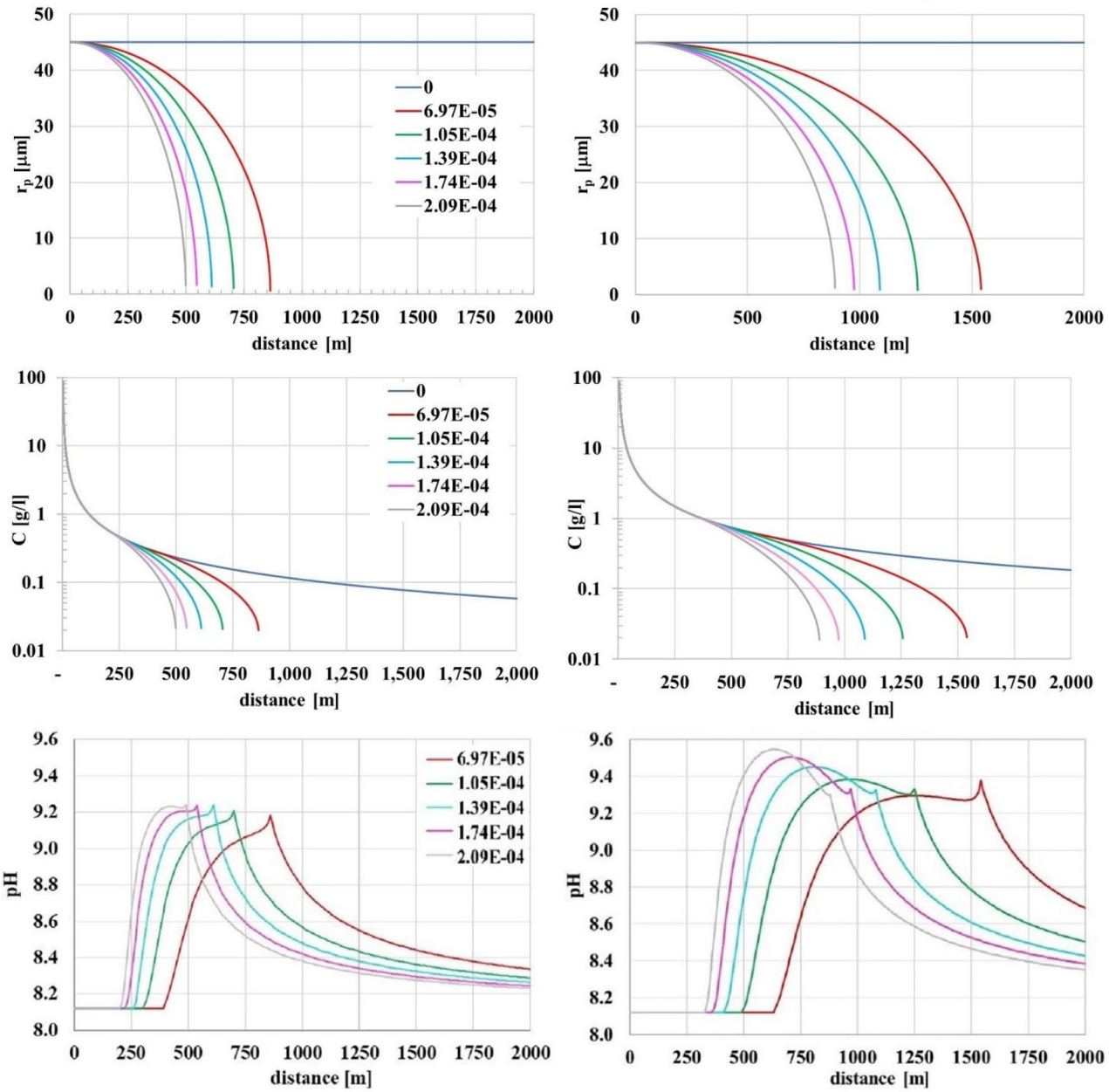

FIGURE 5 | Particle radius (top), $Ca(OH)_2$ concentration (middle) and pH variation (bottom) for different values of the diffusion potential ϕ_0 and two rate of discharge (left: 10 kg/s; right: 100 kg/s). Initial $Ca(OH)_2$ particle radius: 45 μm.

are not uncommon (Schulz and Riebesell, 2013), and diurnal changes of 1 pH unit is typical in coastal environments (Cornwall et al., 2013). While research that considers the impact of the changes in carbonate chemistry and ecosystem function due to ocean alkalinity enhancement is at an early stage (e.g., Gore et al., 2018), the results of this modeling work help to constrain the magnitude of the perturbation. Given that the effects described here would also be attenuated by CO_2 uptake, the impact is likely to be less than ∼1–1.5 pH units for several minutes.

The modeling approach discussed could be used to establish a relationship between SL addition rate and seawater pH increase, and thus threshold values for a safe SL discharge rate. Further investigations are needed to constrain the model parameters. Specifically, the diffusion and dissolution of calcium hydroxide. Future work should also include a more complex fluid dynamics model, taking into account all chemical parameters influencing particle motion, including SL particle radius, geometry, and porosity. Following this, relationships between physics and chemical simulations, and the local environmental changes

produced, must be established to assess the maximum SL quantity which can assure that the benefits from ocean liming are not hindered by localized impact of the discharge on marine life.

This paper has considered the use of SL as alkaline material to be added to seawater, because of the considerable worldwide availability of limestone and the industrial maturity of the calcination and slaking processes, although the storage of the large quantities CO_2 produced during calcination still represent a challenge (Bui et al., 2018). Anyway, other alternative alkalinity sources that have been proposed, such as $Mg(OH)_2$ (Renforth and Henderson, 2017), Na_2CO_3 (Kheshgi, 1995), NaOH (House et al., 2007), or electrogeochemical strategies (Rau et al., 2018) deserve attention and further research.

DATA AVAILABILITY STATEMENT

Publicly available datasets were analyzed in this study. This data can be found here: www.emodnet-humanactivities.eu/view-data.php.

AUTHOR CONTRIBUTIONS

SC conceptualized the research and with DP wrote the draft. DP performed the calculation on the SL discharge potential with the support of SC. AA performed the fluid dynamic analysis and wrote the draft of that session with support from SD and SC. SC, SD, and DR performed the analysis on pH variation. MG, PR, and FC critically revised and improved the draft. All authors approved the submitted version.

FUNDING

The research was carried out within the Desarc-Maresanus project (www.desarc-maresanus.net), which received the financial support of Amundi SGR SpA. Renforth is supported by the UKRI Greenhouse Gas Removal Programme (NE/P019730/2).

ACKNOWLEDGMENTS

Authors thank Andrea Panarello (Interprogetti Srl), Roberto Marras (Unicalce), Giovanni Cappello, and Dennis Ross Morrey (CO2APPS) for their useful suggestions, as well as Maria Ludovica Dall'Aglio for the support with the CFD modeling. Some of the results of this research were made possible by the computational resources made available at CINECA (Italy) by the high-performance computing projects ISCRA-C LWMITSW.

SUPPLEMENTARY MATERIAL

The Supplementary Material for this article can be found online at: https://www.frontiersin.org/articles/10.3389/fclim.2021.575900/full#supplementary-material

REFERENCES

Albright, R., Caldeira, L., Hosfelt, J., Kwiatkowski, L., and Maclaren, J. K. (2016). Reversal of ocean acidification enhances net coral reef calcification. *Nature* 531, 362–365. doi: 10.1038/nature17155

Alessandrini, A., Guizzardi, D., Janssens-Maenhout, G., Pisoni, E., Trombetti, M., and Vespe, M. (2017). Estimation of shipping emissions using vessel Long Range Identification and tracking data. *J. Maps* 13, 946–954. doi: 10.1080/17445647.2017.1411842

Bach, L. T., Gill, S. J., Rickaby, R. E. M., Gore, S., and Renforth, P. (2019). CO_2 removal with enhanced weathering and ocean alkalinity enhancement: potential risks and co-benefits for marine pelagic ecosystems. *Front. Clim.* 1:7. doi: 10.3389/fclim.2019.00007

Brancaccio, G., Kalouptsidi, M., and Papageorgiou, T. (2018). *Geography, Search Frictions and Endogenous Trade Costs*. NBER Working Paper No. 23581. Available online at: http://www.nber.org/papers/w23581

Bui, M., Adjman, C., Bardow, A., Anthony, E., Boston, A., Brown, S., et al. (2018). Carbon capture and storage (CCS): the way forward. *Ener. Environ. Sci.* 11, 1062–1176. doi: 10.1039/c7ee02342a

Butenschön, M., Lovato, T., Grosso, M., Masina, S., and Caserini, S. (2020). Alkalinisation scenarios in the Mediterranean Sea for efficient removal of atmospheric CO_2 and the mitigation of ocean acidification. *Front. Clim.* 3:6145537. doi: 10.3389/fclim.2021.614537

Byrne, C. D., Law, R. J., Hudson, P. M., Thain, J. E., and Fileman, T. W. (1988). Measurements of the dispersion of liquid industrial waste discharged into the wake of a dumping vessel. *Water Res.* 22, 1577–1584. doi: 10.1016/0043-1354(88)90171-6

Caserini, S., Barreto, B., Lanfredi, C., Cappello, G., Morrey, D. R., and Grosso, M. (2019). Affordable CO_2 negative emission through hydrogen from biomass, ocean liming, and CO_2 storage. *Mitig. Adap. Strat. Glob. Change* 24, 1231–1248. doi: 10.1007/s11027-018-9835-7

Chave, K. E., and Suess, E. (1970). Calcium carbonate saturation in seawater: effects of dissolved organic matter. *Limon. Oceanogr.* 15:633–37.

Chen, C. J., and Rodi, W. (1980). *Vertical Turbulent Buoyant Jets – A Review of Experimental Data*. Oxford: Pergamon Press

Chou, H.-T. (1996). On the dilution of liquid waste in ships' wakes. *J. Mar. Sci. Technol.* 1, 149–154. doi: 10.1007/BF02391175

Cornwall, C. E., Hepburn, C. D., McGraw, C. M., Currie, K. I., Pilditch, C. A., Hunter, K. A., et al. (2013). Diurnal fluctuations in seawater pH influence the response of a calcifying macroalga to ocean acidification. *Proc. R. Soc.* 280:1772. doi: 10.1098/rspb.2013.2201

Costello, M. J., and Chaudhary, C. (2017). Marine biodiversity, biogeography, deep-sea gradients, and conservation. *Curr. Biol.* 27, R511–R527. doi: 10.1016/j.cub.2017.04.060

Crippa, M., Solazzo, E., Huang, G., Guizzardi, D., Koffi, E., Muntean, M., et al. (2020). High resolution temporal profiles in the Emissions Database for Global Atmospheric Research. *Nat. Sci. Data* 7:121. doi: 10.1038/s41597-020-0462-2

Cripps, G., Widdicombe, S., Spicer, J. I., and Findlay, H. S. (2013). Biological impacts of enhanced alkalinity in *Carcinus maenas*. *Mar. Poll. Bull.* 71, 190–198. doi: 10.1016/j.marpolbul.2013.03.015

Csanady, G. T. (1986). Mass transfer to and from small particles in the sea. *Limnol. Oceanog.* 31, 237–248. doi: 10.4319/lo.1986.31.2.0237

Davies, J. (2004). *"Liberty" Cargo Ship*. Available online at: http://ww2ships.com/acrobat/us-os-001-f-r00.pdf

Delft (1970). *Studies on the Mixing of Dilute Acid With Seawater in the Propeller Slipstream of the Coaster "Kathe H."* Waterloopkundig Laboratory Delft M939.

Deloitte (2017). *EU Shipping Competitiveness Study*. London, UK: International Benchmark Analysis.

Delvigne, G. A. L. (1987). "Experiments on the dilution capacity of wakes from tankers dumping in the North Sea," in *Oceanic Processes in Marine Pollution Physicochemical Processes and Wastes in the Ocean,* O'Connor, T. P., Burt, W. V., Duedall, I. W., editors. (Malabar, FL: Krieger,), 11–19.

EDGAR (2018). *Emissions Database for Global Atmospheric Research*. Available online at: https://edgar.jrc.ec.europa.eu/gallery.php

EMODnet (2019a). *EMODnet-Human Activities Project–Shipping Density*. Available online at: www.emodnet-humanactivities.eu/view-data.php

EMODnet (2019b). *EU Vessel Density Map. Detailed Method*. Available online at: http://www.emodnet-humanactivities.eu/documents/Vessel%20density%20maps_method_v1.5.pdf

European Commission (2015). *Study on the Analysis and Evolution of International and EU Shipping*. Zoetermeer: Final Report.

Garcìa-Reyes, M., Sydeman, W. J., Schoeman, D. S., Rykaczewski, R. R., Black, B. A., et al. (2015). Under pressure: Climate change, upwelling, and eastern boundary upwelling ecosystems. *Front. Marine Sci.* 2:109. doi: 10.3389/fmars.2015.00109

Globallast (2017). Available online at: http://archive.iwlearn.net/globallast.imo.org/ballast-water-as-a-vector/index.html

Gore, S., Renforth, P., and Perkins, R. (2018). The potential environmental response to increasing ocean alkalinity for negative emissions. *Mitig. Adapt. Strat. Glob. Change*, 24, 1191–1211. doi: 10.1007/s11027-018-9830-z

Hanak, D. P., Jenkins, B., Kruger, T., and Manovic, V. (2017). High-efficiency negative-carbon emission power generation from integrated solid-oxide fuel cell and calciner. *Appl. Ener.* 205, 1189–1201. doi: 10.1029/j.apenergy.2017.08.090

Harvey, L. D. D. (2008). Mitigating the atmospheric CO_2 increase and ocean acidification by adding limestone powder to upwelling regions. *J. Geophys. Res.* 113:C04028. doi: 10.1029/2007JC004373

Hough, G. R., and Ordway, D. E. (1964). *The Generalized Actuator Disk*. Tech. Rep. Cameron Station, Alexandria, Virginia: TAR-TR 6401, Therm Advanced Research, Inc.

House, K. Z., House, C. H., Schrag, D. P., and Aziz, M. J. (2007). Electrochemical acceleration of chemical weathering as an energetically feasible approach to mitigating anthropogenic climate change. *Environ. Sci. Technol.* 41, 8464–8470. doi: 10.1021/es.0701816

ICCT–International Council on Clean Transportation (2017). *Greenhouse Gas Emissions From Global Shipping*, Washington DC, *2013–2015*.

IMO–International Maritime Organization (2008). *Resolution MEPC.174(58). Guidelines For Approval Of Ballast Water Management Systems* (G.8), London, UK.

International Maritime Organization (2014). Third IMO Greenhouse Gas Study 2014. Suffolk: Micropress Printers.

IPCC (2018). *Global Warming of 1.5°C: Summary for Policy Makers*. Available online at: http://report.ipcc.ch/sr15/pdf/sr15_spm_final.pdf

Johnson, P. D., and McMahon, R. G. (1998). Effects of temperature and chronic hypoxia on survivorship of zebra mussels (*Dreissena polymorpha*) and Asian clam (*Corbicula fluminea*). *Canad. J. Fish. Aqu. Sci.* 55, 1564–1572. doi: 10.1139/f98-030

Katz, C. N., Chadwick, D. B., Rohr, J., Hyman, M., and Ondercin, D. (2003). Field measurements and modeling of dilution in the wake of a US navy frigate. *Mar. Pollut. Bull.* 46, 991–1005. doi: 10.1016/S0025-326X(03)00117-6

Kaye, G. W. C., and Laby, T. H. (1995). *Tables of Physical and Chemical Constants*. Longman, 16th edition, London, UK.

Keller, D. P., Feng, E. Y., and Oschilies, A. (2014). Potential climate engineering effectiveness and side effects during a high carbon dioxide-emission scenario. *Nat. Communic.* 5:3304. doi: 10.1038/ncomms4304

Kheshgi, H. S. (1995), Sequestering atmospheric carbon dioxide by increasing ocean alkalinity. *Energy* 20, 915–922, doi: 10.1016/0360-5442(95)00035-F

Köhler, P., Abrams, J. F., Völker, C., Hauck, J., and Wolf-Gladrow, D. A. (2013). Geoengineering impact of open ocean dissolution of olivine onatmospheric CO_2, surface ocean pH and marine biology. *Environ. Res. Lett.* 8:014009. doi: 10.1088/1748-9326/8/1/014009

Kundu, P. K., Cohen, I. M., and Dowling, D. R. (2012). *Fluid Mechanics, 5th Edn*. Cambridge, MA: Elsevier.

Lenton, A., Boyd, P., Thatcher, M., and Emmerson, K. (2019). Foresight must guide geoengineering research and development. *Nat. Clim. Change* 9:342. doi: 10.1038/s41558-019-0467-z

Lenton, A., Matear, R. J., Keller, D. P., Scott, V., and Vaughan, N. E. (2018). Assessing carbon dioxide removal through global and regional ocean alkalinization under high and low emission pathways. *Earth Syst. Dynam.* 9, 339–357. doi: 10.5194/esd-9-339-2018

Levich, V. G. (1992). Physicochemical Hydrodynamics. Englewood Cliffs, NJ: Prentice Hall.

Lewis, R. E. (1985). The dilution of waste in the wake of a ship. *Water Res.* 19, 941–945. doi: 10.1016/0043-1354(85)90360-4

Leyendekkers, J. V. (1979). Prediction of the density and viscosity seawater, its concentrates and other multicomponent solution using the Tamman-Tait-Gibson model. *Desalination* 29, 263–274. doi: 10.1016/S0011-9164(00)82243-2

Li, Y.-H., and Gregory, S. (1974). Diffusion of ions in sea water and in deep-sea sediments. *Geochim Cosmochim Acta* 38, 703–714. doi: 10.1016/0016-7037(74)90145-8

Locke, A., Doe, K. G., Fairchild, W. L., Jackman, P. M., and Reese, E. J. (2009). Preliminary evaluation of effects of invasive tunicate management with acetic acid and calcium hydroxide on non-target marine organisms in Prince Edward Island, Canada. *Aqu Inv.* 4, 221–236. doi: 10.3391/ai.2009.4.1.23

Loehr, L. C., Beegle-Krause, C.-J., George, K., McGee, C. D., Mearns, A. J., and Atkinson, M. J. (2006). The significance of dilution in evaluating possible impacts of wastewater discharges from large cruise ships. *Mar. Poll. Bull.* 52, 681–688. doi: 10.1016/j.marpolbul.2005.10.021

Luo, M., Fan, L., and Li, K. X. (2013). Flag choice behaviour in the world merchant fleet. *Transportmetrica* 9, 429–450. doi: 10.1080/18128602.2011.594969

Lyman, J., and Fleming, R. H. (1940). Composition of sea water. *J. Mar. Res.* 3, 134–146.

Marinetraffic (2019). Available online at: https://www.marinetraffic.com

Narula, K. (2019). The maritime dimension of sustainable energy security. *Lect. Notes Ener* 9:68. doi: 10.1007/978-981-13-1589-3_9

Naudascher, E. (1965). Flow in the wake of self-propelled bodies and related sources of turbulence. *J. Fluid Mech.* 22, 625–656. doi: 10.1017/S0022112065001039

Nemet, G. F., Callaghan, M. W., Creutzig, F., Fuss, S., Hartmann, J., Jérôme, H., and et al. (2018). Negative emissions – part 3: innovation and upscaling. *Environ. Res. Lett.* 13:063002. doi: 10.1088/1748-9326/aabff4

Panarello, A. (2020). *Personal communication of Andrea Panarello, Interprogetti Srl*.

Pedersen, M. F., and Hansen, P. J. (2003). Effects of high pH on a natural marine planktonic community. *Mar. Ecol. Prog. Ser.* 260, 19–31. doi: 10.3354/meps260019

Pond, S., Pytkowicz, R. M., and Hawley, J. E. (1971). Particle dissolution during settling in the oceans. *Deep-Sea Res.* 18, 1135–1139. doi: 10.1016/0011-7471(71)90099-4

Pope, S. B. (2000). *Turbulent Flows*. London: Cambridge University Press.

Pytkowicz, R. M. (1973). Calcium carbonate retention in supersaturated seawater. *Am. J. Sci.* 273, 515–522.

Quarteroni, A., Sacco, R., Saleri, F., and Gervasio, P. (2014). *Matematica Numerica 4a edizione*. Milano: Springer.

Rajartnam, N. (1976). *Turbulent Jets*. Amsterdam: Elsevier.

Rau, G. (2019). The race to remove CO_2 needs more contestants. *Nat. Clim. Change* 9:256. doi: 10.1038/s41558-019-0445-5

Rau, G. H., Willauer, H. D., and Ren, Z. J. (2018). The global potential for converting renewable electricity to negative-CO2-emissions hydrogen. *Nature Clim. Change* 8, 621–625. doi: 10.1038/s41558-018-0203-0

Renforth, P. (2019). The negative emission potential of alkaline materials. *Nat. Comm.* 10:1401. doi: 10.1038/s41467-019-09475-5

Renforth, P., and Henderson, G. (2017). Assessing ocean alkalinity for carbon sequestration. *Rev. Geophy.* 55, 636–674. doi: 10.1002/2016RG000533

Renforth, P., Jenkins, B. G., and Kruger, T. (2013). Engineering challenges of ocean liming. *Energy* 60, 442–452. doi: 10.1016/j.energy.2013.08.006

Schulz, K. G., and Riebesell, U. (2013). Diurnal changes in seawater carbonate chemistry speciation at increasing atmospheric carbon dioxide. *Mar. Biol.* 160, 1889–1899. doi: 10.1007/s00227-012-1965-y

Situ, R., and Brown, R. (2013). Mixing and dispersion of pollutants emitted from an outboard motor. *Mar. Poll. Bull.* 69, 1-2, 19–27. doi: 10.1016/j.marpolbul.2012.12.015

Sousa, R., Antunes, C., and Guilhermino, L. (2008). Ecology of the invasive Asian clam *Corbicula fluminea* (Müller, 1774) in aquatic ecosystems: an overview. *Ann. Limnol.* 44, 85–94. doi: 10.1051/limn:2008017

Starliper, C. E., Watten, B. J., Iwanowicz, D., Green, P. A., Bassett, N. L., and Adams, C. R. (2015). Efficacy of pH elevation as a bactericidal strategy for treating ballast water of freight carriers. *J. Adv. Res.* 6, 501–509. doi: 10.1016/j.jare.2015.02.005

Tannenberger, M., and Klein, H. (2009). *Settling and Dissolution of Calcium Hydroxide Particles. Fakultätfür Maschinenwesen, Studiengang Chemieingenieurwesen*. Technischen Universität München.- München: Lehrstuhlfür Anlagen - und Prozesstechnik; Semesterarbeit

Transport and Environment (2019). *EU Shipping's Climate Record-Maritime CO_2 Emissions and Real-World Ship Efficiency Performance*. European Federation for Transport and Environment AISBL.

UNCTAD–United Nations Conference on Trade and Development (2019b). *Handbook of Statistics 2019* (Geneva).

United Nations Conference on Trade and Development (2018). *Review of Maritime Transport 2018* (Geneva).

United Nations Conference on Trade and Development (2019a). *Review of Maritime Transport 2019* (Geneva).

US-EPA (2002). *Cruise Ship Plume Tracking Survey Report. EPA 842-R-02-001, Office of Water,* Washington, DC. Available online at: https://www.epa.gov/sites/production/files/2015-11/documents/cruise_ship_plume_tracking_survey_report.pdf

USGS (2019). PHREEQC. *U.S. Geological Survey. vers. 3*. Available online at: http://www.usgs.gov/software/phreeqc-version-3

Vesselfinder (2019). Available online at: www.vesselfinder.com

Wang, C., Corbett, J. J., and Firestone, J. (2008). Improving spatial representation of global ship emissions inventories. *Env. Sci. Techn.* 42, 193–199. doi: 10.1021/es0700799

Weast, R. C., Lide, D. R., Astle, M. J. K., and Beyer, W. H. (1989). *Handbook of Chemistry and Physics*. Boca Raton: CRC Press, 70th edition.

Conflict of Interest: The authors declare that the research was conducted in the absence of any commercial or financial relationships that could be construed as a potential conflict of interest.

frontiers in Climate

ORIGINAL RESEARCH
published: 08 July 2021
doi: 10.3389/fclim.2021.624075

The Sensitivity of the Marine Carbonate System to Regional Ocean Alkalinity Enhancement

Daniel J. Burt[1,2]*, *Friederike Fröb*[1] *and Tatiana Ilyina*[1]

[1] *Max Planck Institute for Meteorology, The Ocean in the Earth System, Max Planck Society, Hamburg, Germany,*
[2] *International Max Planck Research School on Earth System Modelling, Max Planck Society, Hamburg, Germany*

Ocean Alkalinity Enhancement (OAE) simultaneously mitigates atmospheric concentrations of CO_2 and ocean acidification; however, no previous studies have investigated the response of the non-linear marine carbonate system sensitivity to alkalinity enhancement on regional scales. We hypothesise that regional implementations of OAE can sequester more atmospheric CO_2 than a global implementation. To address this, we investigate physical regimes and alkalinity sensitivity as drivers of the carbon-uptake potential response to global and different regional simulations of OAE. In this idealised ocean-only set-up, total alkalinity is enhanced at a rate of 0.25 Pmol a^{-1} in 75-year simulations using the Max Planck Institute Ocean Model coupled to the HAMburg Ocean Carbon Cycle model with pre-industrial atmospheric forcing. Alkalinity is enhanced globally and in eight regions: the Subpolar and Subtropical Atlantic and Pacific gyres, the Indian Ocean and the Southern Ocean. This study reveals that regional alkalinity enhancement has the capacity to exceed carbon uptake by global OAE. We find that 82–175 Pg more carbon is sequestered into the ocean when alkalinity is enhanced regionally and 156 PgC when enhanced globally, compared with the background-state. The Southern Ocean application is most efficient, sequestering 12% more carbon than the Global experiment despite OAE being applied across a surface area 40 times smaller. For the first time, we find that different carbon-uptake potentials are driven by the surface pattern of total alkalinity redistributed by physical regimes across areas of different carbon-uptake efficiencies. We also show that, while the marine carbonate system becomes less sensitive to alkalinity enhancement in all experiments globally, regional responses to enhanced alkalinity vary depending upon the background concentrations of dissolved inorganic carbon and total alkalinity. Furthermore, the Subpolar North Atlantic displays a previously unexpected alkalinity sensitivity increase in response to high total alkalinity concentrations.

Keywords: climate change mitigation, carbon cycle, ocean alkalinity enhancement, biogeochemical modelling, alkalinity sensitivity, carbonate system

OPEN ACCESS

Edited by:
Lennart Thomas Bach, University of Tasmania, Australia

Reviewed by:
Keith Lindsay, National Center for Atmospheric Research (UCAR), United States
Carolin Regina Löscher, University of Southern Denmark, Denmark

***Correspondence:**
Daniel J. Burt
daniel.burt@mpimet.mpg.de

Specialty section:
This article was submitted to Negative Emission Technologies, a section of the journal Frontiers in Climate

Received: *30 October 2020*
Accepted: *01 June 2021*
Published: *08 July 2021*

Citation:
Burt DJ, Fröb F and Ilyina T (2021) The Sensitivity of the Marine Carbonate System to Regional Ocean Alkalinity Enhancement. Front. Clim. 3:624075. doi: 10.3389/fclim.2021.624075

1. INTRODUCTION

Ocean Alkalinity Enhancement (OAE) is a strategy to remove CO_2 directly from the atmosphere by adding processed minerals [e.g., lime ($Ca(OH)_2$) or olivine (Mg_2SiO_4)] to marine areas. OAE increases the CO_2 buffering capacity of the ocean (de Coninck et al., 2018), which subsequently strengthens the oceanic CO_2 uptake (Köhler et al., 2010; Hartmann et al., 2013). The addition of

processed minerals is an acceleration of the natural delivery of weathered material that currently leads to the sequestration of ∼0.25 PgC a^{-1} (Taylor et al., 2016). Previous simulations of global alkalinity enhancement reveal spatially heterogeneous changes in the oceanic carbon inventories (Keller et al., 2014; González and Ilyina, 2016; Fröb et al., 2020), which indicates a regional sensitivity to alkalinity enhancement. Here, we investigate the drivers of these regional sensitivities and the response of the non-linear marine carbonate system to OAE.

The oceanic CO_2 uptake is strengthened by OAE because of the non-linearity of the marine carbonate system, which modulates the transfer of CO_2 between the atmosphere and ocean. Total Alkalinity (TA), defined as the weighted sum of charged ion concentrations in seawater (Dickson, 1981; Zeebe and Wolf-Gladrow, 2003), is added by dissolving alkaline minerals, which release proton acceptors that bind with free hydrogen ions and increase pH (Renforth and Henderson, 2017; Middelburg et al., 2020). The decreased hydrogen ion concentration shifts the dissolution equilibrium of CO_2, favouring the dissociation of aqueous CO_2 to bicarbonate (HCO_3^-) ions (Zeebe and Wolf-Gladrow, 2003; Renforth and Henderson, 2017). The establishment of this new balance of the carbonate system in seawater reduces the concentration of aqueous CO_2. Subsequently the partial pressure relative to the atmosphere decreases, which leads to a higher CO_2 solubility. While the dissociation equilibrium is dependent upon the partial pressure of CO_2, temperature and salinity (Renforth and Henderson, 2017; Middelburg et al., 2020), the magnitude of the enhanced CO_2 sequestration due to OAE depends on the initial state of the marine carbonate system (Köhler et al., 2010).

González and Ilyina (2016) propose that physical regimes, which influence temperature and salinity, and marine carbonate system states drive the regionally varying response to global OAE in their simulations. However, previous simulations of regionally deployed alkalinity enhancement reach seemingly contradictory conclusions. In a pioneering study to assess the potential of alkalinity enhancement to mitigate atmospheric CO_2 and ocean acidification, Ilyina et al. (2013b) conclude that the carbon-uptake potential of an OAE pulse depends on the dominant hydrodynamic regime. In contrast, a later study by Lenton et al. (2018) to determine CO_2 sequestration under different emission scenarios finds little sensitivity in the global response to OAE applied across different latitudinal bands. The comparability of these studies is limited primarily by their experimental designs, unlimited (Ilyina et al., 2013b) in contrast to limited (Lenton et al., 2018) alkalinity enhancement, and the use of models of varying complexity, ocean-only (Ilyina et al., 2013b) vs. Earth system (Lenton et al., 2018). As of now, it is still unknown what influence physical circulation and marine carbonate system states have on regional alkalinity enhancement and, subsequently, on the CO_2 buffering capacity and alkalinity sensitivity.

We evaluate the influence of physical circulation and marine carbonate system states on alkalinity enhancement in simulations of global and regional OAE using an idealised set-up of the ocean-only model, MPIOM-HAMOCC. To investigate the impact of OAE on the CO_2 buffering capacity, we quantify the impact of alkalinity enhancement globally and across eight selected regions on oceanic CO_2 sequestration. Furthermore, we analyse the response of alkalinity sensitivity with simulated deployments of global and regional OAE.

2. METHODOLOGY

2.1. Model Description

Our experiments are simulated using the physical and biogeochemical ocean model components of the Max Planck Institute for Meteorology Earth System Model version 1.2 (MPI-ESM1.2) as used in the 6th-phase of the Coupled Model Intercomparison Project (Mauritsen et al., 2019). The Max Planck Institute Ocean Model version 1.6 (MPIOM1.6) simulates the physical ocean and the oceanic components of the cryosphere (Marsland et al., 2003; Jungclaus et al., 2013; Mauritsen et al., 2019) and provides the 3-dimensional flow fields and turbulent mixing schemes required for the advection and mixing of biogeochemical tracers (Ilyina et al., 2013a; Mauritsen et al., 2019). The HAMburg Ocean Carbon Cycle version 6 (HAMOCC6) model simulates the transport and evolution of biogeochemical tracers at the air-sea interface and within the water column and surface sediment layers of the global ocean (Ilyina et al., 2013a).

The transport and evolution of biogeochemical tracers simulated by HAMOCC6 provides a limited representation of the ocean biogeochemistry response to OAE. Within HAMOCC6, the organic compartments are resolved through an extended Nutrient, Phytoplankton, Zooplankton and Detritus scheme (Six and Maier-Reimer, 1996) with prognostic parameterisations of bulk phytoplankton, cyanobacteria and zooplankton (Ilyina et al., 2013a; Paulsen et al., 2017). Inorganic carbon chemistry within the water column is resolved by HAMOCC6 through two prognostic tracers: Dissolved Inorganic Carbon (DIC) and TA (Ilyina et al., 2013a). DIC is computed as the sum of aqueous CO_2, carbonic acid (H_2CO_3), bicarbonate ions (HCO_3^-) and carbonate ions (CO_3^{2-}) (Orr et al., 2017):

$$[\mathrm{DIC}] = [\mathrm{CO_2}] + [\mathrm{H_2CO_3}] + [\mathrm{HCO_3^-}] + [\mathrm{CO_3^{2-}}] \quad (1)$$

Following Orr et al. (2017), TA explicitly considers contributions from carbonate, borate, sulphate, silicate, phosphate, fluoride and water and implicitly considers the influences of ammonia and sulphide:

$$\begin{aligned}[\mathrm{TA}] =& [\mathrm{HCO_3^-}] + 2[\mathrm{CO_3^{2-}}] + [\mathrm{B(OH)_4^-}] + [\mathrm{OH^-}] + [\mathrm{HPO_4^{2-}}] \\ &+ [\mathrm{PO_4^{3-}}] + [\mathrm{SiO(OH)_3^-}] - [\mathrm{H^+}] - [\mathrm{HSO_4^-}] \\ &- [\mathrm{HF}] - [\mathrm{H_3PO_4}]\end{aligned} \quad (2)$$

The solubility dependent uptake of atmospheric CO_2 increases DIC without changing TA. Biogeochemical processes such as organic matter production or remineralisation and calcium carbonate ($CaCO_3$) precipitation or dissolution influence both DIC and TA. Seawater TA is further modified by the external input of weathering fluxes, seawater-sediment interactions and changes in the physical seawater properties (Ilyina et al., 2013a).

2.2. Alkalinity Input Subroutine

The alkalinity input subroutine of González and Ilyina (2016) is modified for this study to implement a volumetric weighting scheme of the surface grid cells to account for variable layer thickness and different input areas. The default subroutine increases the prognostic TA tracer in the surface layer of the ocean as a product of an alkalinity correction ratio (González and Ilyina, 2016; González et al., 2018; Sonntag et al., 2018; Fröb et al., 2020). We define the alkalinity input region using a two-dimensional binary mask. The sum volume ($V_{sum}(k,j,i)$) of the cells within the masked regions (mask(j,i)) are computed from the layer thickness (D(k,j,i)) and cell area (A(k,j,i)), where the indices represent the vertical (k) and horizontal grid dimensions (j,i). In these experiments, TA is added only to the surface layer ($k = 1$):

$$V_{sum}(1,j,i) = \sum(D(1,j,i) \cdot A(1,j,i) \cdot \text{mask}(j,i)) \quad (3)$$

A spatially homogeneous input concentration of the TA tracer (ΔTA) is then determined at each time-step as the quotient of a TA input rate (δ TA) to the sum of the surface layer volume:

$$\Delta TA(j,i) = \frac{\delta TA}{V_{sum}(1,i,j)} \quad (4)$$

The input concentrations must be computed at each time-step to consider the variable surface layer volume produced by the free-surface implementation of the ocean primitive equations (Marsland et al., 2003). The input concentration is then added to the TA tracer computed by HAMOCC6.

2.3. Experimental Design

The coupled-ocean model is used in a standard MPIOM1.6 low-resolution grid configuration (GR1.5) (Jungclaus et al., 2013) and boundary conditions are prescribed using forcing datasets (Röske, 2005; Poli et al., 2016). The GR1.5 configuration is a rotated orthogonal curvilinear grid with a nominal horizontal resolution of 1.5° and 40 vertical levels arranged such that the first 20 levels are within the upper 700 m of the ocean (Jungclaus et al., 2013). The system is forced at each 30 min time-step by surface boundary conditions based on the European Centre for Medium-range Weather Forecasts (ECMWF) ERA-20C re-analysis dataset (Poli et al., 2016) with a reduced temporal resolution from 4- to 8-h. The forcing data is applied repetitively with a periodicity of 25 years using the years 1905–1930 as used to reproduce a pre-industrial ocean state in previous studies (DeVries et al., 2019; Liu et al., 2021). These data are combined with continental runoff forcing data for the Ocean Model Intercomparison Project (Röske, 2005).

Biological parameters in HAMOCC6 require tuning to account for grid resolution features and coupling or forcing frequencies (Mauritsen et al., 2019). Coupling or forcing frequencies which resolve diurnal variations in incoming solar radiation can produce a strong depletion of primary producer standing stocks due to high night-time mortality of primary producers in the model. The variables tuned in order to maintain the nitrogen and carbon source-sink dynamics under these conditions are: the maximum growth and mortality rates of cyanobacteria and the grazing rate on bulk phytoplankton (Paulsen et al., 2017). The maximum growth rate of cyanobacteria is increased from 0.2 to 0.3 d^{-1}, the cyanobacteria mortality rate is reduced from 0.1 d^{-1} to 0.07 d^{-1} and the grazing rate on bulk phytoplankton is reduced from 1 d^{-1} to 0.7 d^{-1}. This tuning produces a lower mean N_2 fixation rate (~68 Tg N a^{-1}) than the 82 Tg N a^{-1} which is reported for the MPI-ESM1.2-LR configuration (Mauritsen et al., 2019), and is lower than the range of observation-based estimates of 70–200 Tg N a^{-1} (Karl et al., 2002; Großkopf et al., 2012). The resulting carbon export (~7.1 Gt C a^{-1}) is greater than the 6.7 Gt C a^{-1} simulated in the MPI-ESM1.2-LR (Mauritsen et al., 2019) but within the reported range of export fluxes (3-20 Gt C a^{-1}) (Najjar et al., 2007).

Ocean-only experiments are simulated over 75 years for a pre-industrial control and for global and eight regional OAE deployments (section 2.4) each with a fixed atmospheric CO_2 mixing ratio of 280 ppm. The simulations are initialised from a quasi-stable model state, which has been spun-up under prescribed pre-industrial forcing (Röske, 2005; Poli et al., 2016); the initial condition is taken 600 years after the last change made during the model spin-up. This idealised set-up permits the investigation of short-term impacts on the marine carbonate system as a result of OAE for the mitigation of the atmospheric CO_2 mixing ratio. For comparability, the rate of alkalinity enhancement described by Lenton et al. (2018) is implemented; $\delta TA = 0.25\,\text{Pmol}\,a^{-1}$. While the surface areas of the defined global and eight regions are constant throughout the experiments, variations of surface wind speeds over time in the atmospheric forcing produce fluctuations of sea surface height, which lead to temporally varying volumes in the defined surface layer. The input concentration relative to the constant rate of alkalinity enhancement is modulated to account for these volume variations. The surface area and spatiotemporal mean input concentration deployed are presented in **Table 1**.

TABLE 1 | Alkalinity enhancement input regions as illustrated in **Figure 1**, region name abbreviation (code), region surface area and mean concentration of the alkalinity input over the simulation period.

Region	Code	Area (× 10^6 km^2)	Concentration (μmol m^{-3})
Global	GLOBAL	297.991	7.961
Subpolar N. Atlantic	SPNA	3.677	699.447
Subpolar N. Pacific	SPNP	9.251	278.584
Subtropical N. Atlantic	STNA	17.571	135.503
Subtropical N. Pacific	STNP	34.856	67.074
Indian Ocean	IND	19.354	118.351
Subtropical S. Atlantic	STSA	14.819	158.958
Subtropical S. Pacific	STSP	27.906	84.000
Southern Ocean	SO	7.561	354.020

2.4. Definition of Regions

To evaluate the efficiency of regional OAE, eight regions are defined based on a subset of physical conditions in order to

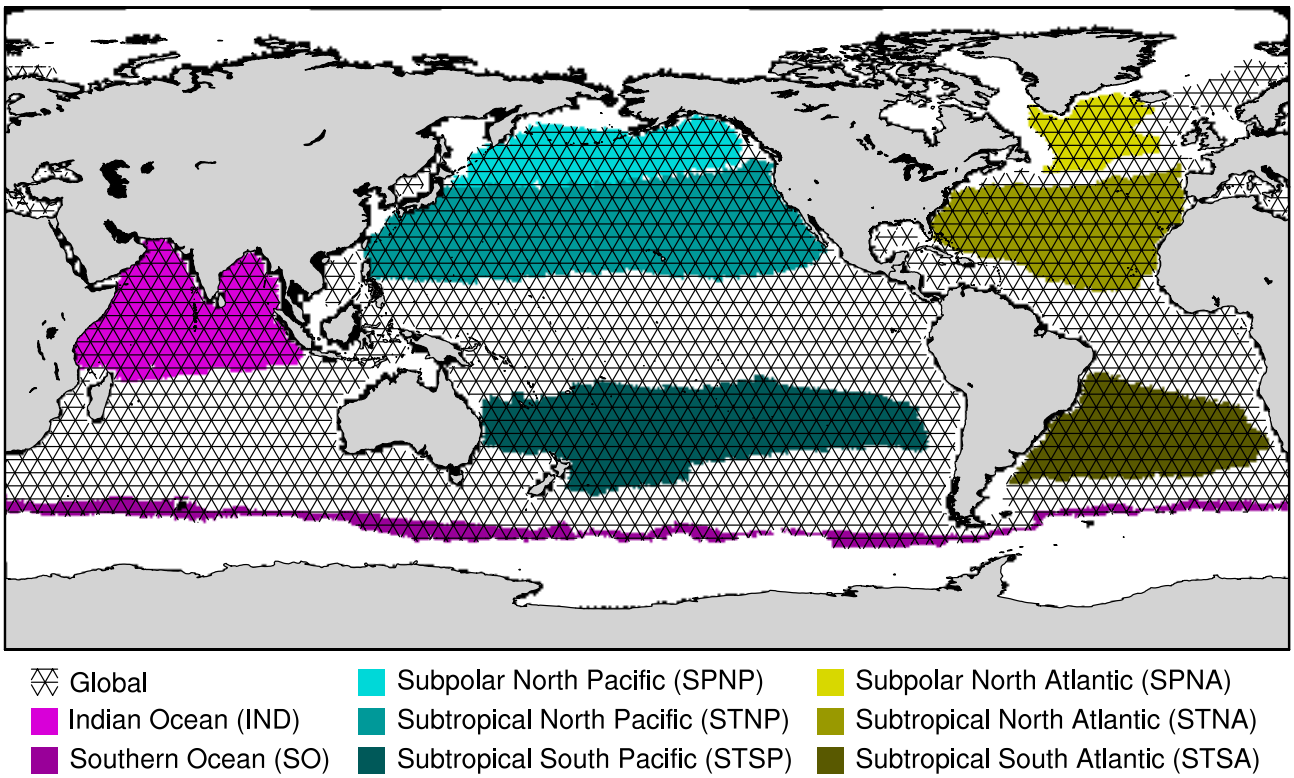

FIGURE 1 | Map of the selected regions: Subpolar North Atlantic - SPNA (light yellow); Subtropical North Atlantic - STNA (yellow); Subtropical South Atlantic - STSA (dark yellow); Subpolar North Pacific - SPNP (light cyan), Subtropical North Pacific - STNP (cyan); Subtropical South Pacific - STSP (dark cyan); Indian Ocean - IND (magenta); Southern Ocean - SO (dark magenta). The Global alkalinity enhancement region (GLOBAL) is indicated by the triangular mesh overlay. Only ice-free, open-ocean areas are included in the global and different regional definitions.

represent different hydrographic regimes in the global ocean. It should be noted that regions are not selected with consideration to real-world implementation. The eight selected regions are oriented with respect to persistent, large-scale gyre systems: the Subpolar and the Subtropical Atlantic and Pacific gyres; as well as the Indian Ocean and the Southern Ocean (**Figure 1**). We identify regions using the climatological (25-year) means of sea surface temperature (SST), salinity (SSS), elevation with respect to the geoid (SSH), the zonal and meridional velocity components, and the horizontal velocity vector from the pre-industrial control of the ocean-only MPIOM simulation. Subpolar and subtropical gyres rotate in opposing directions, producing variations in SSH due to Ekman transport, which can be used to indicate the boundaries between adjacent gyres (Knauss, 2005). We focus only on the open ocean and, therefore, exclude regions with a climatological maximum sea-ice concentration greater than 50% or areas shallower than 200 m.

We divide the Atlantic Ocean into three regions associated with major wind-driven gyres. A SSH anomaly of −0.7 m is used to indicate the division between the *Subpolar North Atlantic* (SPNA) and the Subtropical regions. The *Subtropical North Atlantic* (STNA) region is constrained with SSSs >35.8. The *Subtropical South Atlantic* (STSA) region is bound by the strong eastward South Atlantic and northwestward Benguela Current systems. A region of weaker currents, with horizontal velocity vector magnitudes <0.12 m s^{-1}, exists between these boundary currents and the South American continental landmass.

The *Southern Ocean* (SO) region is bound to the north by the Antarctic Polar Front, which is defined by a horizontal SST gradient of 0.01 K km^{-1} (Dong et al., 2006). This does not produce a contiguous boundary in the model SST climatological mean. Areas of 0.01 K km^{-1} occur along a contiguous 4 °C SST isotherm, which is substituted for the northern regional boundary.

As with the Atlantic, we separate the Pacific Ocean into three regions associated with major wind-driven gyres. We use the subtropical front between the Pacific Ocean and the Southern Ocean (SSS >34.6) as described by Chaigneau and Pizarro (2005) to define the southern extent of the *Subtropical South Pacific* (STSP) region. The Indo-Pacific Warm Pool as described by Wyrtki (1989) is not considered representative of the Subtropical South Pacific gyre, therefore SST >28 °C are excluded. Zonal (>-0.08 m s^{-1}) and meridional (>-0.09 m s^{-1}) velocity conditions are used to further constrain the STSP region. We define the *Subtropical North Pacific* (STNP) region with SSH >0.75 m as this provides a strong distinction in the western Pacific from tropical latitudes. In the eastern Pacific, we use SSTs of 12–25 °C to define a sector which agrees with the latitudinal extent of the STNP SSH region and continues to the North American

continental landmass as an eastern boundary. We characterise the *Subpolar North Pacific* (SPNP) region with a SSH threshold of <0.075 m. The Sea of Japan, South China Sea and Sea of Okhotsk are not included in the North Pacific regions as they are not representative of the open ocean.

The evaluation of climatological means precludes the evaluation of parameters characterised by the strong seasonal monsoon-cycle in the Northern Indian Ocean (Shetye et al., 1991; Schott et al., 2009; Vinayachandran et al., 2013). Therefore, the *Indian Ocean* (IND) region is defined as the region north of the strong, prevailing South Equatorial Current in the Indian Ocean where the Red Sea, Gulf of Aden and Gulf of Oman are excluded.

2.5. Model Evaluation

We qualitatively evaluate the 75-year mean states of TA, DIC (**Figure 2**) and alkalinity sensitivity (**Figure 3**) from the control experiment against mapped climatologies (Lauvset et al., 2016) based on the Global Ocean Data Analysis Project version 2 data product (GLODAPv2; Olsen et al., 2016). Due to differences in vertical resolution, the surface layer of the model (0–12 m) is compared to the vertical-mean of the topmost two layers (0 m, 10 m) of the mapped climatologies. Unit conversions are performed on model TA and DIC data using local seawater density approximations derived from surface potential temperature and practical salinity data using the Gibbs Seawater Oceanographic Toolbox (TEOS-10; McDougall and Barker, 2011). We evaluate the surface distributions of TA and DIC in the model (**Figure 2E**) as the magnitude of the carbon-uptake response to OAE is dependent on the background state of the simulated marine carbonate system (Köhler et al., 2010).

We find that the large-scale pattern of observed surface TA is well reproduced by the model (**Figures 2A,B**). However, TA is consistently underestimated in the pre-industrial control simulation, with a global annual mean of 2196±97 μmol kg^{-1}, compared to the mapped present-day surface climatology with a global mean of 2297±72 μmol kg^{-1}. The TA anomalies are heterogeneously distributed but uniformly negative across the global ocean (**Figure 2C**). The underestimation is the result of model tuning toward a net global CO_2 flux of 0 GtC a^{-1} between the ocean and atmosphere. However, the order of magnitude of TA anomalies in our experiments has been found acceptable in previous model studies (Keller et al., 2012; Ilyina et al., 2013a; Matear and Lenton, 2014). Note that the difference between present-day and pre-industrial surface TA is assumed to be minor (Sarmiento and Gruber, 2006; Middelburg et al., 2020). Typically, TA covaries with salinity (Middelburg et al., 2020), and the control (**Figure 2B**) successfully captures the pattern of high TA at subtropical latitudes, lower TA in equatorial, subpolar and polar regions and generally higher TA in the Atlantic than at similar latitudes in the Pacific. Larger positive and negative anomalies (**Figure 2C**) are displayed in regions associated with strong circulation regimes, marginal coastal and shelf sea regions and regions associated with strong freshwater fluxes, such as where the Arctic Ocean is influenced by Siberian river systems.

The model control (**Figure 2E**) also captures the large-scale distribution of surface DIC concentrations, while consistently underestimating the concentrations compared to the GLODAPv2 pre-industrial climatology (**Figure 2D**). The global mean surface DIC concentration of the model control is 1904±99 μmol kg^{-1}, in contrast to that of the mapped pre-industrial climatology, which is 1966±84 μmol kg^{-1}. The dominant drivers of the latitudinal surface DIC distribution of the GLODAPv2 climatology are temperature and vertical circulation regimes (Wu et al., 2019). The control simulation also exhibits a pattern of surface DIC with the highest concentrations in the Southern Ocean and the lowest concentrations in the coastal equatorial Pacific and eastern Indian Ocean (**Figure 2E**). The Arctic Ocean and Southern Ocean feature the largest anomalies. While the Arctic Ocean anomalies appear related to the surface TA anomalies, the surface DIC anomalies in the Southern Ocean may indicate poorly resolved vertical circulation in the Weddell Sea. However, the heterogeneity of the anomalies in the open ocean regions pertinent to this study (**Figure 2F**) indicate that these drivers are sufficiently resolved to reproduce the pattern of surface DIC concentrations.

Finally, we evaluate the alkalinity sensitivities derived from the model data (**Figure 3B**) against those derived from the GLODAPv2 climatology (**Figure 3A**). Alkalinity sensitivity describes the change in the seawater partial pressure of CO_2 to a molar increase of TA (Sarmiento and Gruber, 2006). Therefore, a smaller alkalinity sensitivity indicates a stronger reduction in the partial pressure and a greater sensitivity of the marine carbonate system to TA. We find that the model (**Figure 3B**) captures the large-scale pattern of alkalinity sensitivity derived from the observational climatology (**Figure 3A**), where the alkalinity sensitivity increases with latitude (Egleston et al., 2010). However, the model underestimates the alkalinity sensitivity of the marine carbonate system (0.6±0.7) and exhibits a weaker latitudinal gradient. The anomalies are spatially heterogeneous but are greatest in the Southern Ocean and Subpolar North Pacific and least in the equatorial Pacific and Atlantic (**Figure 3C**). The underestimation is acceptable for the purposes of this study but the weaker latitudinal gradient reduces the differences between the regional alkalinity sensitivity responses to OAE.

3. RESULTS

3.1. Global Carbon-Uptake Potential

The global and regional OAE experiments illustrate varying total ocean carbon uptakes in response to OAE. After 75 years, the total mean DIC inventories increase by 82–175 PgC (**Figure 4**). There is an initial non-linear increase in the rate of CO_2 sequestration and then near-linear inventory increases for the latter 65–70 years of the different experiments. Only the *Southern Ocean* (SO; 175 PgC) and *Subpolar North Pacific* (SPNP; 160 PgC) regional OAE simulations sequester more CO_2 than the Global OAE (157 PgC). In contrast, the *Subpolar North Atlantic* (SPNA) experiment displays the least carbon-uptake (82 PgC).

The same mass of alkalinity is added to each region; however, the actual impact of the alkalinity enhancement on surface TA concentrations depends on the area size of each region (**Table 1**). For example, the carbon uptake in the Global OAE experiment, which has the largest surface area and lowest input concentrations, is exceeded only by the SO and SPNP

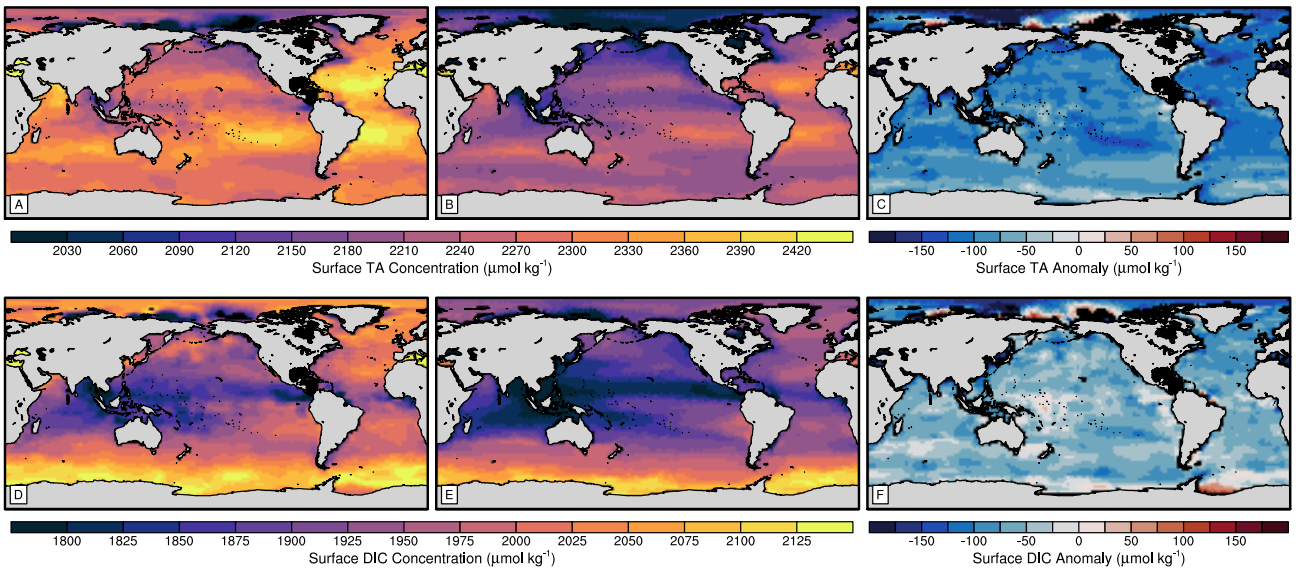

FIGURE 2 | Maps of total alkalinity **(A–C)** and dissolved inorganic carbon **(D–F)** of the **(A,D)** GLODAPv2 mapped climatology (Lauvset et al., 2016) surface vertical-mean, **(B,E)** 75-year mean surface model control state and **(C,F)** surface anomalies between the model control and the GLODAPv2 datasets.

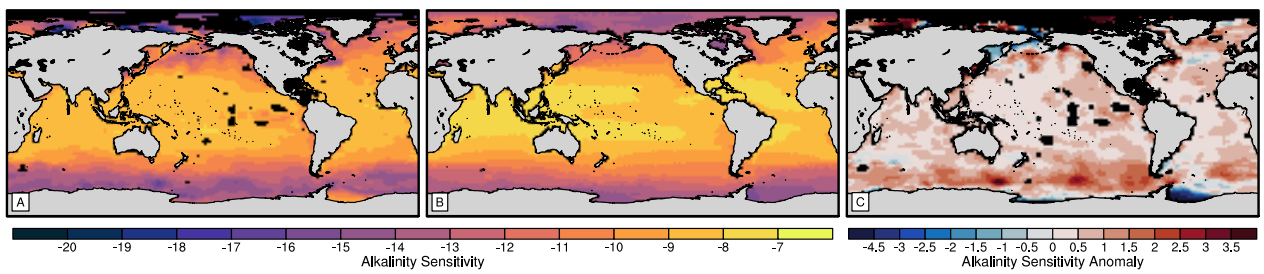

FIGURE 3 | Maps of alkalinity sensitivity derived from the **(A)** GLODAPv2 climatology surface vertical-mean and **(B)** 75-year mean surface model control state and **(C)** alkalinity sensitivity anomalies between the alkalinity sensitivities derived from the model control and GLODAPv2 datasets.

regional experiments, which have the second and third smallest surface areas and highest input concentrations of the regional experiments. However, the SPNA region, which has the smallest area and highest input concentration, sequesters the least CO_2 over the course of the experiment. Therefore, neither the surface area of the input region nor the subsequent input concentration directly regulates the carbon-uptake potentials between experiments.

The availability of the additional TA in the surface, where it influences the carbon-uptake potential, is controlled by the different hydrodynamic regimes between the selected regions. We refer to the total surface availability of enhanced alkalinity after vertical export as surface retention. The evolution of the total mean depth profile through time illustrates the influence of vertical export to surface retention (**Supplementary Figure 1**). The range of surface retention varies from the SPNP experiment, with the greatest total TA anomaly of 0.73 Pmol, to the SPNA, which exhibits the smallest total TA anomaly of 0.12 Pmol (**Figure 5A**). The increase of the total surface TA anomaly in each experiment is non-linear with a greater rate of increase initially, which decreases over the simulation period. The growth rates of the total surface TA anomaly for the *Subtropical North Pacific* (STNP) and *Subtropical South Pacific* (STSP) regional simulations are near-linear after an initial rate decrease. The *Indian Ocean* (IND), SPNP, STNP and STSP regions exhibit greater total surface TA anomalies after 75 years than the Global experiment, while only the SPNP and IND regions exceed the carbon-uptake in response to Global OAE. The surface retention of TA after 75 years of Global alkalinity enhancement (0.48 Pmol) also exceeds that of the SO experiment (0.34 Pmol). The total surface availability of TA, therefore, does not determine the carbon uptake response in our experiments.

Renforth and Henderson (2017, Equation 11) illustrate that carbon uptake is influenced by the mean ratio of ΔDIC to ΔTA, which we refer to as carbon-uptake efficiency. The carbon-uptake

efficiencies of the Global and regional OAE experiments decrease at different rates over time in response to alkalinity enhancement (**Figure 5B**). The SPNA region displays the largest decrease of –0.069 mol C mol^{-1} H^+ and the Global shows the least decrease of –0.007 mol C mol^{-1} H^+. The SO carbon-uptake efficiency remains greater than that of the Global experiment throughout the 75-year simulation. While the SPNP initially has a carbon-uptake efficiency greater than the Global, the carbon-uptake efficiency declines in the first 5–10 years to efficiencies comparable with those of the STNP and STSP regions for the remainder of the experiment. This initial rate of decrease within the first 5–10 year period is present in all of the regional OAE simulations. We find no correlation between the regional mean carbon-uptake efficiency (**Figure 5B**) and the total DIC inventory anomalies (**Figure 4**).

Neither the surface retention of TA nor the regional carbon-uptake efficiency are found to be predictors of the carbon uptake response to OAE. If the additional TA is retained in the input region then the total DIC inventory anomalies should be a function of the surface TA anomalies and the regional mean carbon-uptake efficiency. However, as this is not case, it indicates that there is horizontal export of additional TA from

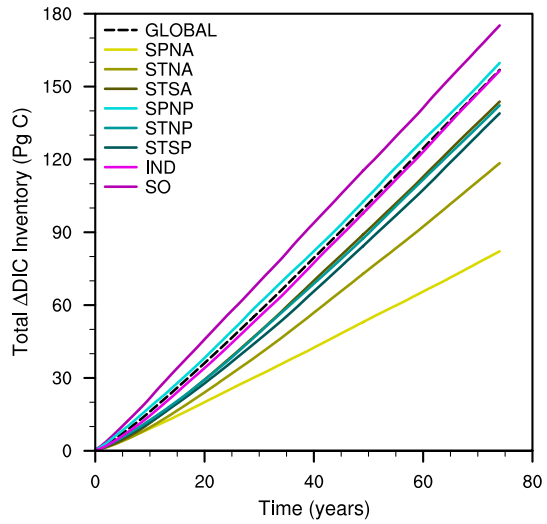

FIGURE 4 | Time series of total dissolved inorganic carbon inventory anomaly against time for the global (dashed) and different regional (solid) ocean alkalinity enhancement experiments.

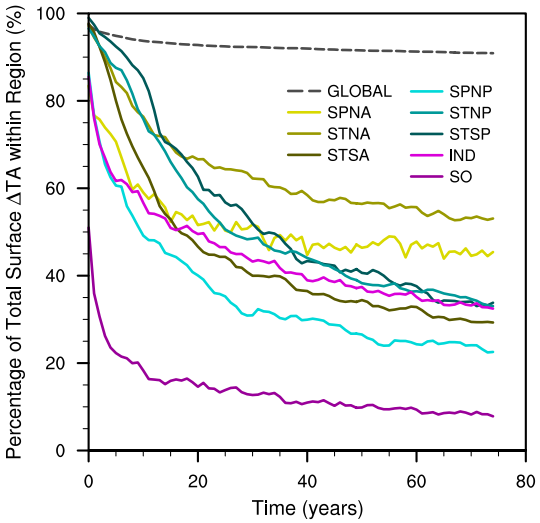

FIGURE 6 | Time series of the percentage of total surface total alkalinity anomalies within the defined region over time for the global and different regional ocean alkalinity enhancement experiments.

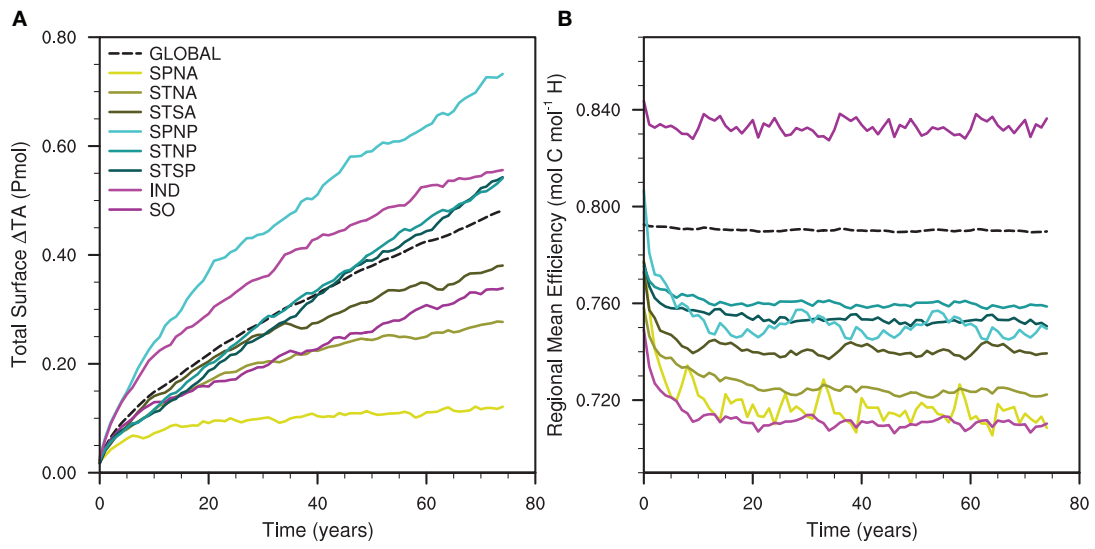

FIGURE 5 | Time series of **(A)** the total surface total alkalinity anomaly and **(B)** the carbon-uptake efficiency (Renforth and Henderson, 2017) over time for the global and regional artificial ocean alkalinity experiments.

the input region. Therefore, the surface TA anomalies are not confined to the input regions and the significance of the surface redistribution must be considered.

3.2. Influence of Total Alkalinity Surface Distribution on Carbon Uptake

The influence of the TA distribution in the surface ocean is evident when comparing the simulated (**Figure 4**) and predicted total DIC inventory changes, for example in the Global and *Southern Ocean* (SO) alkalinity enhancements. More carbon is sequestered over the course of the simulation in the SO than in the Global OAE experiment despite the SO having smaller surface TA anomalies (**Figure 5A**). While the Global region has a lower carbon-uptake efficiency (**Figure 5B**), this is insufficient to explain the response observed. If the surface TA anomalies (**Figure 5A**) are totally retained within the input regions and the input regions take up carbon at the regional mean carbon-uptake efficiencies (**Figure 5B**), then the Global experiment would be expected to sequester 213 PgC after the 75 years. In the same scenario, we would expect 162 PgC to be sequestered by the

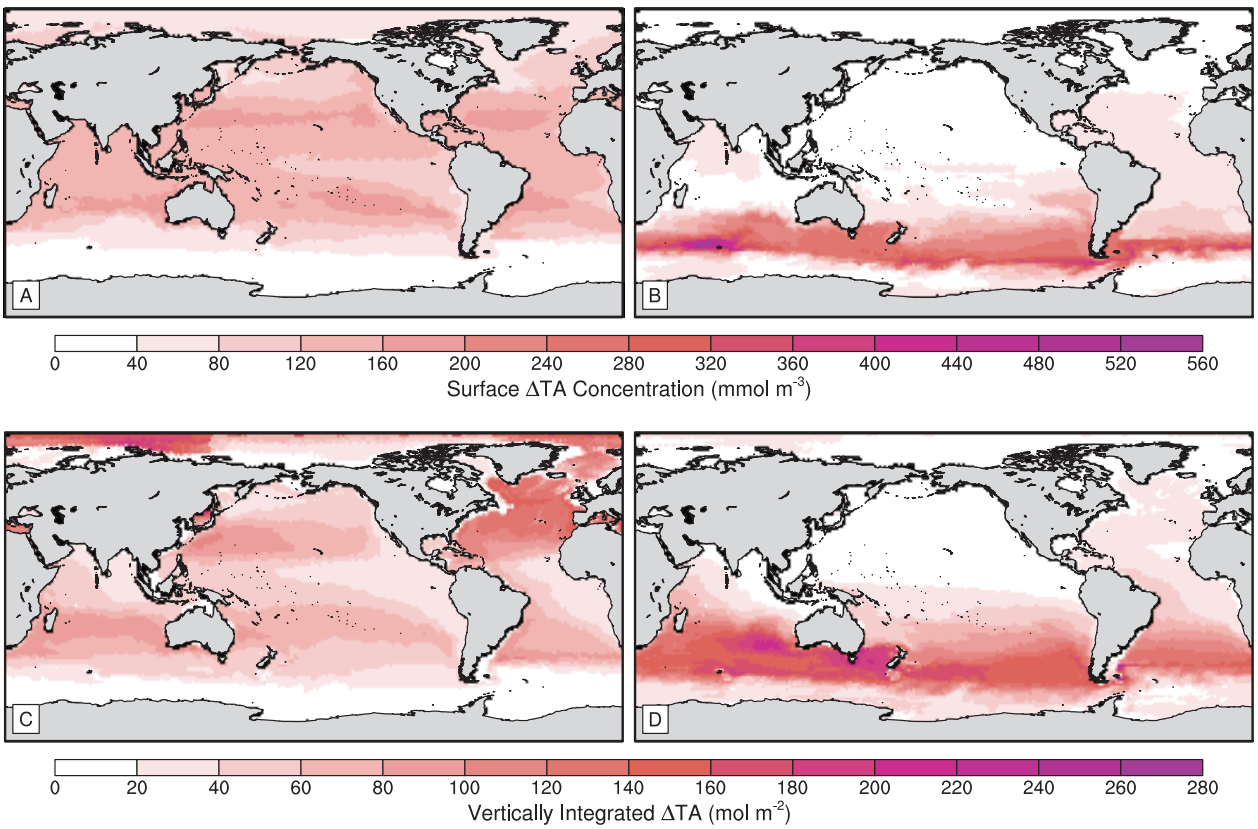

FIGURE 7 | Maps of **(A,B)** surface total alkalinity anomaly and **(C,D)** vertically-integrated total alkalinity anomaly for the **(A,C)** Global and **(B,D)** *Southern Ocean* ocean alkalinity enhancement experiments.

end of the SO experiment. Therefore, the simulated total DIC inventory changes for the Global experiment is less efficient than those predicted, while the SO experiment is more efficient (**Figure 4**); these divergences are attributed to the export of additional alkalinity from the input regions.

We illustrate this horizontal export of additional TA with the proportion of total surface TA anomalies which remain within the input region. The percentage of the total surface TA anomaly present within the input region for each experiment decreases non-linearly over time (**Figure 6**). The Global OAE simulation exhibits the greatest proportion of the total surface TA anomaly within the defined input region by the end of the experiment. However, within the first 2 years, the *Subtropical South Atlantic* (STSA) and *Subtropical South Pacific* (STSP) regions display greater proportions than the Global. The STSA and STSP also show the largest changes in proportion after 75 years, while the smallest change occurs in the *Subpolar North Atlantic* (SPNA) experiment. At the end of the simulation, the *Subtropical North Atlantic* (STNA) has the greatest proportion of total surface TA anomaly, while the SO is found to have the least out of the different regional OAE simulations. We find that the horizontal and vertical export of additional TA from the surface input region varies dependent upon the prevailing hydrodynamic regimes.

The patterns of surface and vertically-integrated TA anomalies from the Global experiment give insight into the mechanisms that distribute alkalinity across the surface ocean and to depth. The annual mean surface TA anomalies are heterogeneously distributed at the end of the 75 year Global OAE simulation, with higher concentrations at subtropical latitudes (**Figure 7A**). The smallest annual mean surface TA anomalies are found outside the input region, with greater invasion of TA to the Arctic Ocean than south of the seasonally ice-covered areas in the Southern Ocean. Smaller annual mean surface TA anomalies also occur in the eastern subtropical Atlantic and Pacific and in the eastern tropical Pacific. Similar annual mean surface TA anomaly features are present in the western subpolar Atlantic and Pacific. The vertically-integrated TA anomalies are also heterogeneously distributed, with the greatest anomalies occurring within the Arctic Ocean (**Figure 7C**). The vertically-integrated TA anomalies within the North Atlantic are greater than those of the other major ocean basins. There is an increasing east-west gradient in the vertically-integrated TA anomalies of the subtropical and equatorial regions, while the subpolar North Pacific has an inverse gradient, increasing west to east.

The distributions of surface and vertically-integrated TA anomalies differ considerably in the SO experiment compared with the Global. At the end of the 75 year simulation, the annual mean surface (**Figure 7B**) and vertically-integrated TA anomalies (**Figure 7D**) dominate the southern subpolar and subtropical latitudes with minor anomalies found in regions of the northern hemisphere. The greatest annual mean surface TA anomaly is found in the Indian Ocean sector of the SO region, while the greatest vertically-integrated anomaly is located in the South Atlantic. Surface TA anomalies are present in the northern Indian Ocean and North Atlantic, however the feature in the Indian ocean is not contiguous with other surface TA anomalies. The low surface TA anomalies displayed by the southern subtropical Indian Ocean appear to continue south around the African coastline to the South Atlantic. The disconnection of the northern Indian Ocean surface TA anomalies is not shared by the vertically-integrated TA anomalies. Large vertically-integrated TA anomalies occur in the southern subtropical Indian Ocean and Tasman Sea. The Arctic Ocean and the North Atlantic Ocean also display small vertically-integrated TA anomalies which are not apparent in the surface distribution of TA anomalies. There are no apparent east-west gradients of vertically-integrated TA anomalies across the southern subtropical regions in the SO OAE experiment such as those in the same regions of the Global.

TABLE 2 | Major oceans following International Hydrographic Organization region definitions, their mean carbon-uptake efficiency and the percentage of total surface total alkalinity anomaly and total alkalinity inventory anomaly within the region for the *Global* and *Southern Ocean* (SO) ocean alkalinity enhancement experiments.

	Efficiency	% of Surface TA		% of TA Inventory	
IHO Region	**(mol C mol^{-1} H)**	**Global**	**SO**	**Global**	**SO**
Arctic Ocean	0.869	2.5	0.5	3.2	0.5
N. Atlantic Ocean	0.813	13.9	7.0	18.0	5.3
S. Atlantic Ocean	0.823	10.4	17.2	10.0	15.9
Indian Ocean	0.821	19.3	28.1	19.9	33.3
N. Pacific Ocean	0.798	26.0	6.6	21.8	3.6
S. Pacific Ocean	0.811	24.1	35.2	23.9	37.0
Southern Ocean	0.893	0.4	4.4	0.5	4.1

The greater CO_2 sequestration exhibited by the SO compared to the Global OAE simulation is likely the result of the different surface TA anomaly distributions across regions of varying carbon-uptake efficiency. The patterns of annual mean surface and vertically-integrated TA anomalies for all of our experiments are illustrated in **Supplementary Figures 2, 3**. For comparability, we now consider the regional mean carbon-uptake efficiencies and patterns of surface TA anomalies and TA inventory anomalies with respect to the major ocean basins (**Table 2**) as defined by the International Hydrographic Organization (IHO; 1953). At the end of the SO simulation, there are greater proportions of the surface TA anomalies present in the South Atlantic and South Pacific, which exhibit greater regional mean carbon-uptake efficiencies than the North Atlantic and North Pacific. In contrast, the Global experiment displays greater proportions of surface TA anomalies in the less efficient North Atlantic and North Pacific (**Table 2**).

Carbon uptake is constrained by transport of added alkalinity through horizontal advection to regions which inhibit CO_2 uptake and by vertical convection away from the ocean surface. The Southern Ocean and Arctic Ocean display the greatest regional mean carbon-uptake efficiencies (**Table 2**). However, due to the influence of seasonal or permanent sea-ice cover, which is assumed in HAMOCC6 to prevent CO_2 uptake (Ilyina et al., 2013a), TA exported to the Southern Ocean and Arctic Ocean has a negligible influence on carbon uptake. The larger proportion of TA inventory relative to the surface TA present in the North Atlantic after 75 years in the Global simulation

(**Table 2**) illustrates the removal of TA from the surface by seasonal deep convection (Lazier et al., 2002; Sayol et al., 2019). The withdrawal of TA from the surface reduces how much additional TA is available to increase the buffering capacity and enhance the carbon-uptake potential in the North Atlantic. In the Global experiments, this presents a trap for the added alkalinity that has less impact in the SO alkalinity enhancement due to the pattern of surface TA (**Figure 7**).

3.3. Impact of Ocean Alkalinity Enhancement on Alkalinity Sensitivity

The total marine carbonate system becomes less sensitive to TA in all of our alkalinity enhancement experiments. The total mean alkalinity sensitivity increases non-linearly with respect to the total mean surface TA, where the rate of increase displays varying rates of decline between the different simulations (**Figure 8A**). The *Southern Ocean* (SO) OAE experiment has the lowest total annual mean alkalinity sensitivity which increases by 0.03 in the first year and increases at a slower rate in the following years. The greatest total mean alkalinity sensitivity (-8.51) occurs in the *Indian Ocean* (IND) simulation. The *Subpolar North Atlantic* (SPNA) and *Subtropical North Atlantic* (STNA) OAE experiments do not exhibit decreases in the alkalinity sensitivity growth rate within the range of surface TA simulated.

The marine carbonate system also becomes less sensitive regionally in all experiments except for the SPNA alkalinity enhancement, where sensitivity increases. The regional mean alkalinity sensitivities vary non-linearly with respect to the regional mean surface TA, where alkalinity sensitivity increases to a plateau in all of the OAE simulations, except for the SPNA and SO (**Figure 8B**). The SO exhibits the greatest increase of regional mean alkalinity sensitivity (+1.16) with the smallest range of regional mean surface TA (230 mmol m^{-3}) of the regional experiments. The IND, STNA and *Subtropical North Pacific* (STNP) OAE simulations exhibit similar increases of regional mean alkalinity sensitivity (0.58-0.60) at different magnitudes of alkalinity sensitivity. The STNA and STNP OAE simulations exhibit smaller increases of regional mean alkalinity than the *Subtropical South Atlantic* (STSA) or *Subtropical South Pacific* (STSP), respectively. The regional mean alkalinity sensitivity for the SPNA initially increases to a maximum of −6.90 with a regional annual mean surface TA of 2966 mmol m^{-3} before decreasing below the initial sensitivity to −7.24 at the end of the simulation.

4. DISCUSSION

4.1. Drivers of the Marine Carbonate System Response to Alkalinity Enhancement

The physical regimes within MPIOM, which drive the distribution of added alkalinity, represent real-world processes but are resolved with biases resulting from implementation, resolution and parameterisation choices (Jungclaus et al., 2013). The distribution of surface TA anomalies in the Global experiment (**Figure 7A**) is attributed to the pattern of prescribed freshwater fluxes (i.e., evaporation/ precipitation; Middelburg et al., 2020) and the resolved wind-driven circulation (Knauss, 2005). Surface TA is concentrated at subtropical latitudes by prevailing evaporation and anticyclonic gyre circulation (**Figure 7A**). Surface water is transported toward gyre cores, near the relative western boundaries, where it is forced downward by Ekman Pumping (Knauss, 2005); downward advection of added alkalinity produces the vertically-integrated TA anomalies in the western subtropics (**Figure 7C**). The downwelling circulation at subtropical latitudes is balanced by coastal upwelling, which raises deeper water (Knauss, 2005) without alkalinity enhancement to the surface, leading to the low anomalies displayed in **Figure 7A**. TA transported by surface currents into the Arctic Ocean (Karcher et al., 2012; Rudels, 2015) is trapped at depth by thermohaline convection, which leads to the contrast between the relatively large vertically-integrated TA anomalies and the relatively small surface TA anomalies. The divergence of upwelling water masses at the subpolar front of the Southern Ocean (van Heuven et al., 2011; Sévellec et al., 2017) inhibits the southward invasion of TA in the Global OAE simulation and produces the northward transport of TA exhibited by the *Southern Ocean* (SO) experiment. We show that the redistribution of additional TA is driven by physical circulation and ventilation and, therefore, is model dependent.

While the physical regimes drive the distribution of added alkalinity, the background state of the carbonate system drives the different local responses to OAE. Note that the increases visualised in **Figure 8** represent a decrease of the pCO_2 reduction per mole of TA added (Sarmiento and Gruber, 2006) and, subsequently, the system is less sensitive to further TA input. The increase of the total mean alkalinity sensitivity (**Figure 8A**) is attributed to the enhanced sequestration of CO_2 due to OAE, which dissociates to introduce further hydrogen ions. These counter the TA input and additional TA is then required to produce an equivalent change of the oceanic pCO_2. This effect, and the resulting change in sensitivity, is enhanced by the prescription of the atmospheric CO_2 mixing ratio. OAE reduces the atmospheric CO_2 growth rate in ESMs with interactive atmospheric CO_2 mixing ratios (Keller et al., 2014; González and Ilyina, 2016; Lenton et al., 2018), weakening the atmosphere-ocean concentration gradient. The decreased rate of change of the alkalinity sensitivity is related to the DIC:TA ratio. Egleston et al. (2010) illustrate that seawater buffer factors approach minima, where DIC:TA ratios approach one. The SO OAE simulation exhibits the highest DIC:TA ratio and the smallest change in total mean alkalinity sensitivity (**Figure 8A**). In contrast, the *Indian Ocean* (IND) experiment displays the lowest DIC:TA ratio and the greatest change in total mean alkalinity sensitivity. The wider implications of these responses suggest that when the rate of TA input exceeds the rate of carbon uptake, hydrogen ion concentrations become increasingly small. There are fewer hydrogen ions to be neutralised by additional alkalinity enhancement and, therefore, an increasingly weak impact on the atmosphere-ocean CO_2 concentration gradient (Zeebe and Wolf-Gladrow, 2003; Middelburg et al., 2020).

We show that physical regimes, which control patterns of TA and DIC, in combination with the non-linearity of buffer

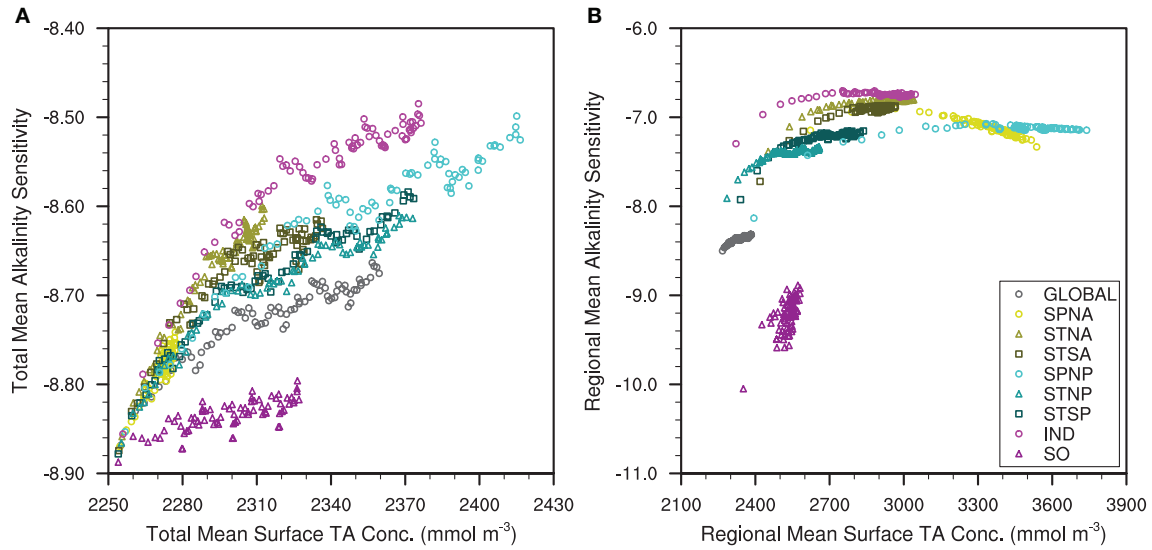

FIGURE 8 | (A) The total annual mean surface alkalinity sensitivity against the total annual mean surface total alkalinity and **(B)** the regional annual mean surface alkalinity sensitivity against the regional annual mean surface total alkalinity for the global and different regional ocean alkalinity enhancement experiments.

factors (Egleston et al., 2010) drive the regional alkalinity sensitivity response to OAE. The regional mean surface TA anomalies are inhibited in the SO region by the surface current connections to the Atlantic, Indian and Pacific Oceans. The *Subpolar North Atlantic* (SPNA) however, is constrained by land boundaries with limited connections to the Arctic Ocean and North Atlantic but experiences stronger seasonal vertical mixing/ diffusion due to wind stress than regions at lower latitudes (Kara et al., 2003). This seasonal vertical mixing/ diffusion drives the removal of TA and DIC from the surface ocean in the SPNA region (**Supplementary Figures 2C, 3C**). This permits the accumulation of the TA tracer and strong carbon uptake when the seasonal mixed-layer depth is shallow and the strong reduction of the surface signal with the seasonal deepening of the mixed-layer. The decreasing regional mean alkalinity sensitivity at high regional mean surface TA (**Figure 8B**) is likely due to the relatively low surface DIC concentrations. This occurs as the TA input rate is greater than the carbon uptake leading to lower DIC:TA ratios. In comparison, we consider that this does not occur in the *Subpolar North Pacific* (SPNP) region, which also exhibits high regional mean surface TA, because the SPNP experiences weaker vertical turbulent mixing/ diffusion. TA and DIC accumulate in the shallow surface mixed layer of the SPNP region, leading to a higher DIC:TA ratio (**Supplementary Figures 2B, 3B**). The surface concentrations of DIC and TA produce a lower regional mean alkalinity sensitivity in the SPNA than the SPNP (**Figure 8B**), despite the local DIC:TA ratios, due to the non-linear buffer factor responses (Egleston et al., 2010).

4.2. Comparisons of Modelled Regional Ocean Alkalinity Enhancement

The CO_2 sequestration of the Global OAE experiment is greater than expected from the results of Keller et al. (2014) or Lenton et al. (2018); this is likely due to the different representation of physical and biogeochemical processes in the different models. The total integrated DIC inventory change of the Global OAE experiment (+156.9 PgC; **Figure 4**) is greater than that of the global OAE simulation of Lenton et al. (2018) under the RCP2.6 scenario (+143.1 PgC). This is unexpected because Lenton et al. (2018) show that under the same OAE application, more CO_2 is sequestered at higher atmospheric CO_2 concentrations. Lenton et al. (2018) and Keller et al. (2014) find comparable total integrated DIC inventory changes under the RCP8.5 scenario, despite implementing different ESMs. The respective ESMs with their divergent process representations under transient climate scenarios are substantially different from the idealised ocean-only MPIOM-HAMOCC with prescribed pre-industrial climate. For instance, feedbacks between the ocean and other components of the climate system are absent in our set-up.

Beyond the variations of structure, formulation and resolution between models used in OAE studies, the physical and biogeochemical conditions of the pre-industrial climate-state are likely to be more sensitive to OAE than the present or predicted future climate-states. The pre-industrial climate-state (section 2.3) exhibits lower surface water temperatures and, respectively, greater CO_2 solubilities than the 21st century simulations conducted by Keller et al. (2014) and Lenton et al. (2018), which would be expected to enhance carbon uptake. Additionally, while wind-driven surface circulations have not changed significantly with climate change, enhanced ocean stratification is weakening vertical mixing (Bindoff et al., 2019); it is not clear to what extent these differences are resolved between the different models. Furthermore, the sensitivities of the marine carbonate system are expected to decrease with ongoing anthropogenic climate change (Egleston et al., 2010; Lenton et al., 2018), which increases the mass of TA required to produce the same response in the marine carbonate system.

The fixed atmospheric CO_2 mixing ratio in this study, in contrast to studies using ESMs with emission scenarios, limits the transferability of our findings to the real-world. We cannot directly assess growth rate changes in the atmospheric CO_2 mixing ratio in response to OAE, which is a topic of extensive study (Ilyina et al., 2013b; Köhler et al., 2013; Keller et al., 2014; González and Ilyina, 2016; Lenton et al., 2018; Sonntag et al., 2018; Fröb et al., 2020). Furthermore, the assumption of a constant atmospheric CO_2 mixing ratio is valid considering that the annual sequestration rates we describe (1.1-2.3 GtC a^{-1}) are lower than both the estimated range of the natural ocean carbon uptake (1.9–3.1 GtC a^{-1}) and anthropogenic emissions (8.9–9.9 GtC a^{-1}) in the present (Friedlingstein et al., 2020).

Previous studies on regional applications of OAE illustrate the sensitivity of carbon-uptake potential to application area and mass of TA added. We find that both the *Southern Ocean* (SO; +18 PgC) and *Subpolar North Pacific* (SPNP; +3 PgC) OAE simulations sequester more carbon than the Global, while the *Subpolar North Atlantic* (SPNA) sequesters less (–75 PgC; **Figure 4**). Lenton et al. (2018) implement the same TA input rate (section 2.3) but apply TA homogeneously in latitudinal bands without consideration for different physical regimes. Their experiments display similar changes in total integrated carbon uptake for global and regional OAE with little sensitivity to the OAE application region (Lenton et al., 2018). In contrast, Ilyina et al. (2013b) describe TA experiments designed to counter CO_2 emissions with a relative TA input rate. A CO_2 drawdown by regional OAE equivalent to a global application is illustrated, when TA is added to both the North Atlantic and North Pacific. Their results indicate a sensitivity to the OAE application region and also reveal a weaker CO_2 sequestration by regional OAE in the subpolar North Atlantic compared to the subpolar North Pacific or Southern Ocean (Ilyina et al., 2013b). The homogeneous distribution of TA in subpolar latitudes by Lenton et al. (2018) may have reduced the effectiveness of the regional application due to the weaker response of the SPNA compared with other subpolar regions described here and by Ilyina et al. (2013b).

4.3. Implications for Future Ocean Alkalinity Enhancement Studies

While HAMOCC6 resolves biological processes which influence TA (Ilyina et al., 2013a), there are no mechanisms by which the addition of the implemented conceptual TA tracer can directly affect the biological compartments. OAE influences environmental conditions such as increased calcite saturation states and pH (Feng et al., 2017; Renforth and Henderson, 2017; Gore et al., 2019) and indirectly impacts others, such as trace metal concentrations (Hartmann et al., 2013; Köhler et al., 2013) including iron. In some regions, elevated concentrations of iron in the surface ocean may have a fertilising effect on oceanic phytoplankton, which could subsequently enhance the biological carbon pump (Köhler et al., 2013; Bach et al., 2019). However, unlike anthropogenic ocean acidification, where the effects on biota, ecosystems and human communities are undergoing continual research (Doney et al., 2020), the consequences of alkalinity enhancement (Bach et al., 2019; Gore et al., 2019) are less frequently investigated. Therefore, due to sparse information, bulk phytoplankton, cyanobacteria and zooplankton are implemented within HAMOCC6 with constant mortality rates and cannot respond to extremes of biogeochemical variables (Ilyina et al., 2013a) such as those which occur in the subpolar regional OAE simulations.

In its present state, HAMOCC6 has only limited potential to explore biological feedbacks resulting from OAE. An explicit representation of alkalinity-enhancing minerals (e.g., olivine or lime) as tracers in the model would provide additional details related to the Earth system response to OAE. The implementation of bulk phytoplankton, cyanobacteria and zooplankton in HAMOCC6 cannot resolve community assemblage shifts in response to ocean acidification or alkalinity enhancement (Beszteri et al., 2018; Hoppe et al., 2018; Taucher et al., 2018); however, it can still be used to test the "white or green ocean hypothesis" described by Bach et al. (2019). This hypothesis suggests that lime-based OAE would benefit carbonaceous species (i.e., coccolithophores), leading to a whitening of the ocean-colour. In contrast, an olivine-based OAE scenario would benefit siliceous species (i.e., diatoms) and iron-limited but not nitrogen-limited production by cyanobacteria, leading to a greening (Bach et al., 2019). Furthermore, the representative tracers could be used to test their different carbon-uptake potentials with respect to a variable biological carbon pump beyond the previous works of Keller et al. (2014), González and Ilyina (2016), and Lenton et al. (2018).

The response of regional OAE is expected to evolve with changing climate due to physical feedbacks in the climate system. The weakening of buoyancy-loss driven overturning circulations predicted by ESM simulations (Bindoff et al., 2019) could reduce the strong seasonal surface removal in the *Subpolar North Atlantic* (SPNA) and enhance the effectiveness of OAE. Furthermore, with the assumption of sea-ice impermeability to gas exchange (Ilyina et al., 2013a), reduced sea-ice extents and concentrations due to climate change (Meredith et al., 2019) could enhance carbon uptake in high-latitude regions where the added TA is transported to current seasonally or permanently ice-covered regions. The dependence of the marine carbonate system on temperature and salinity, which evolve with climate (Bindoff et al., 2019), would also be expected to modify biogeochemical sensitivities to OAE over time.

The short duration of most OAE simulations does not illustrate the long-term climate system response, limited studies suggest an acceleration of anthropogenic climate change with the cessation of OAE. The relatively short simulation period (75 years) is comparable with previous regional and global OAE simulations (Ilyina et al., 2013a; Keller et al., 2014; González and Ilyina, 2016; Lenton et al., 2018; Sonntag et al., 2018). These durations are suitable for testing immediate mitigation of the atmospheric CO_2 mixing ratio but provide very limited information relating to the response of the ocean interior or long-term effects on the climate system. The sequestration of carbon to the deep ocean has the potential to trap the carbon on centennial-millennial timescales due to deep-ocean ventilation

times (Khatiwala et al., 2012). Previous studies of the long-term effects of alkalinity enhancement and the termination of alkalinity enhancement indicate a climate system response of accelerated warming and acidification (González et al., 2018). This suggests that the sequestered CO_2 is not contained within centennial-millennial reservoirs during such short-term alkalinity enhancement experiments.

5. SUMMARY AND CONCLUSIONS

The purposes of this study have been: first, to quantify the influence of regional, in contrast to global, deployments of OAE on CO_2 sequestration; and second, to analyse the impact of OAE on the alkalinity sensitivity in different global and regional experiments. We considered the regional variations with the underlying assumption that they are driven by differences between the dominant physical regimes and biogeochemical background states. Our analyses were based on experiments of OAE deployments, which were simulated for 75 years in the ocean-only MPIOM-HAMOCC model with a pre-industrial atmospheric forcing. Alkalinity was enhanced globally and in eight distinct regional experiments, which were selected to represent different hydrodynamic regimes.

Carbon uptake of regionally deployed OAE ranged between 82 and 175 PgC compared to the Global, where 157 PgC was sequestered; therefore, regional alkalinity enhancement has the potential to take up greater and lesser masses of carbon than when deployed globally. Between the different OAE experiments, the total mean alkalinity sensitivity increased by 0.09–0.37 with enhanced alkalinity. In contrast, the regional mean alkalinity sensitivities increased by 0.18–1.06 with increasing alkalinity in all experiments, except for the *Southern Ocean*, which was dominated by internal variability, and the *Subpolar North Atlantic*, which decreased by a maximum of 0.19 from its initial state. These regional differences are attributed to the prevailing physical circulation, driving the surface distribution of the added alkalinity, and the initial state of the marine carbonate system, as the alkalinity sensitivity is dependent upon the background DIC and TA.

In conclusion, enhancing alkalinity in smaller regions across the ocean's surface has the potential to exceed carbon uptake in response to global implementations, when hydrodynamic regimes are considered.

DATA AVAILABILITY STATEMENT

Primary data and code for this study are stored and made available through the Max Planck Society Publication Repository (https://pure.mpg.de/): http://hdl.handle.net/21.11116/0000-0008-ABCE-0 (Max Planck Society, Munich, 2021). The respective MPIOM and HAMOCC model code (SHA-1 ID: bb6936773b7e41fad177f8a400b7d0bc627663e6) is available on request after agreeing to the MPI-ESM license agreement and registering at the MPI-ESM Users Forum (https://mpimet.mpg.de/en/science/modeling-with-icon/code-availability, Max Planck Institute for Meteorology, Hamburg and Max Planck Society, Munich, 2021).

AUTHOR CONTRIBUTIONS

DJB provided the major contribution to the formal analysis, investigation, visualization, and writing. DJB, FF, and TI contributed equally toward concept design, methodology, review, editing, and further aspects of the development of this original research. All authors contributed to the article and approved the submitted version.

FUNDING

This work was funded by the German Science Foundation (DFG) within the Priority Program Climate Engineering: Risks, Challenges, Opportunities (SPP 1689). This project has received funding from the European Union's Horizon 2020 research and innovation programme under grant agreement No. 820989 (COMFORT) and under grant agreement No. 101003536 (ESM2025–Earth System Models for the Future). This work was also supported by the Research Unit TERSANE (FOR 2332: Temperature-related stressors as a unifying principle in ancient extinctions).

ACKNOWLEDGMENTS

All simulations were performed at the German Climate Computing Centre (DKRZ). We would like to thank Lennart Ramme for the internal review of this manuscript. The data presented in this study is also analyzed for a thesis (Burt, 2019) toward completion of the Masters of Integrated Climate System Science with the Universität Hamburg in association with the Max Planck Institute for Meteorology.

SUPPLEMENTARY MATERIAL

The Supplementary Material for this article can be found online at: https://www.frontiersin.org/articles/10.3389/fclim.2021.624075/full#supplementary-material

REFERENCES

Bach, L. T., Gill, S. J., Rickaby, R. E. M., Gore, S., and Renforth, P. (2019). CO_2 removal with enhanced weathering and ocean alkalinity enhancement: potential risks and co-benefits for marine pelagic ecosystems. *Front. Clim.* 1:21. doi: 10.3389/fclim.2019.00007

Beszteri, S., Thoms, S., Benes, V., Harms, L., and Trimborn, S. (2018). The response of three Southern Ocean phytoplankton species to ocean acidification and light availability: a transcriptomic study. *Protist* 169, 958–975. doi: 10.1016/j.protis.2018.08.003

Bindoff, N. L., Cheung, W. W. L., Kairo, J. G., Arístegui, J., Guinder, V. A., Hallberg, R., et al. (2019). "Changing ocean, marine ecosystems, and dependent communities," in *IPCC Special Report on the Ocean and Cryosphere in a Changing Climate*, eds H.-O. Pörtner, D. C. Roberts, V. Masson-Delmotte, P. Zhai, M. Tignor, E. Poloczanska, et al., Chapter 5 (Cambridge; New York, NY: Cambridge University Press), 447–587.

Burt, D. J. (2019). *The Sensitivity of the Marine Carbon Cycle to Regional Artificial Ocean Alkalinisation*. Master's thesis, School of Integrated Climate System Sciences, Universität Hamburg.

Chaigneau, A., and Pizarro, O. (2005). Surface circulation and fronts of the South Pacific Ocean, east of 120°W. *Geophys. Res. Lett.* 32:4. doi: 10.1029/2004GL022070

de Coninck, H., Revi, A., Babiker, M., Bertoldi, P., Buckeridge, M., Cartwright, A., et al. (2018). "Strengthening and implementing the global response," in *Global Warming of 1.5°C. An IPCC Special Report on the Impacts of Global Warming of 1.5$_0$C Above Pre-Industrial Levels and the Related Global Greenhouse Gas Emissionn Pathways, In The Context of Strengthening the Global Response to the Threat of Climate Change, Sustainable Development and Efforts to Eradicate Poverty*, eds V. Masson-Delmotte, P. Zhai, H.-O. Pörtner, D. Roberts, J. Skea, J., P. R. Shukla et al. Chapter 4 (Cambridge; New York, NY: Cambridge University Press), 313–444.

DeVries, T., Le Quéré, C., Andrews, O., Berthet, S., Hauck, J., Ilyina, T., et al. (2019). Decadal trends in the ocean carbon sink. *Proc. Natl. Acade. Sci. U.S.A.* 116, 11646–11651. doi: 10.1073/pnas.1900371116

Dickson, A. G. (1981). An exact definition of total alkalinity and a procedure for the estimation of alkalinity and total inorganic carbon from titration data. *Deep Sea Res. A Oceanogr. Res. Papers* 28A, 609–623. doi: 10.1016/0198-0149(81)90121-7

Doney, S. C., Busch, D. S., Cooley, S. R., and Kroeker, K. J. (2020). The impacts of ocean acidification on marine ecosystems and reliant human communities. *Annu. Rev. Environ. Resou.* 45, 83–112. doi: 10.1146/annurev-environ-012320-083019

Dong, S., Sprintall, J., and Gille, S. T. (2006). Location of the Antarctic Polar Front from AMSR-E satellite sea surface temperature measurements. *J. Phys. Oceanogr.* 36, 2075–2089. doi: 10.1175/JPO2973.1

Egleston, E. S., Sabine, C. L., and Morel, F. M. M. (2010). Revelle revisited: Buffer factors that quantify the response of the ocean chemistry to changes in DIC and alkalinity. *Glob. Biogeochem. Cycles*, 24:9. doi: 10.1029/2008GB003407

Feng, E. Y., Koeve, W., Keller, D. P., and Oschlies, A. (2017). Model-based assessment of the CO_2 sequestration potential of coastal ocean alkalization. *Earths Fut.* 5, 1252–1266. doi: 10.1002/2017EF000659

Friedlingstein, P., O'Sullivan, M., Jones, M., Andrew, R. M., Hauck, J., Olsen, A., et al. (2020). Global carbon budget 2020. *Earth Syst. Sci. Data* 12, 3269–3340. doi: 10.5194/essd-12-3269-2020

Fröb, F., Sonntag, S., Pongratz, J., Schmidt, H., and Ilyina, T. (2020). Detectability of artificial ocean alkalinization and stratospheric aerosol injection in MPI-ESM. *Earths Fut.* 8:18. doi: 10.1029/2020EF001634

González, M. F., and Ilyina, T. (2016). Impacts of artificial ocean alkalinization on the carbon cycle and climate in Earth system simulations. *Geophys. Res. Lett.* 43, 6493–6502. doi: 10.1002/2016GL068576

González, M. F., Ilyina, T., Sonntag, S., and Schmidt, H. (2018). Enhanced rates of regional warming and ocean acidification after termination of large-scale ocean alkalinization. *Geophys. Res. Lett.* 45, 7120–7129. doi: 10.1029/2018GL077847

Gore, S., Renforth, P., and Perkins, R. (2019). The potential environmental response to increasing ocean alkalinity for negative emissions. *Mitig. Adapt. Strat. Glob. Change* 24, 1191–1211. doi: 10.1007/s11027-018-9830-z

Großkopf, T., Mohr, W., Baustian, T., Schunck, H., Gill, D., Kuyprs, M. et al. (2012). Doubling of marine dinitrogen-fixation rates based on direct measurements. *Nature* 290, 361–364. doi: 10.1038/nature11338

Hartmann, J., West, A. J., Renforth, P., Köhler, P., De La Rocha, C. L., Wolf-Gladrow, D. A., et al. (2013). Enhanced chemical weathering as a geoengineering strategy to reduce atmospheric carbon dioxide, supply nutrients, and mitigate ocean acidification. *Rev. Geophys.* 51, 113–149. doi: 10.1002/rog.20004

Hoppe, C. J. M., Schuback, N., Semeniuk, D., Giesbrecht, K., Mol, J., Thomas, H., et al. (2018). Resistance of Arctic phytoplankton to ocean acidification and enhanced irradiance. *Polar Biol.* 41, 399–413. doi: 10.1007/s00300-017-2186-0

Ilyina, T., Six, K. D., Segschneider, J., Maier-Reimer, E., Li, H., and Núñez-Riboni, I. (2013a). Global ocean biogeochemistry model HAMOCC: Model architecture and performance as component of the MPI-Earth system model in different CMIP5 experimental realizations. *J. Adv. Model. Earth Syst.* 5, 287–315. doi: 10.1029/2012MS000178

Ilyina, T., Wolf-Gladrow, D., Munhoven, G., and Heinze, C. (2013b). Assessing the potential of calcium-based artificial ocean alkalinization to mitigate rising atmospheric CO_2 and ocean acidification. *Geophys. Res. Lett.* 40, 5909–5914. doi: 10.1002/2013GL057981

International Hydrographic Organization (1953). *Limits of Oceans and Seas*, Vol. 23 of *Special Edition*, 3rd Edn. Monte Carlo: International Hydrographic Organization.

Jungclaus, J. H., Fischer, N., Haak, H., Lohmann, K., Marotzke, J., Matei, D., et al. (2013). Characteristics of the ocean simulations in the Max Planck Institute Oceam Model (MPIOM) the ocean component of the MPI-Earth system model. *J. Adv. Model. Earth Syst.* 5, 422–446. doi: 10.1002/jame.20023

Kara, A. B., Rochford, P. A., and Hurlburt, H. E. (2003). Mixed layer depth variability over the global ocean. *J. Geophys. Res.* 108:15. doi: 10.1029/2000JC000736

Karcher, M., Smith, J. N., Kauker, F., Gerdes, R., and Smethie Jr., W. M. (2012). Recent changes in Arctic Ocean circulation revealed by iodine-129 observations and modeling. *J. Geophys. Res.* 117:17. doi: 10.1029/2011JC007513

Karl, D., Michaels, A., Bergman, B., Capone, D., Carpenter, E., Letelier, R., et al. (2002). "Dinitrogen fixation in the world's oceans," in *The Nitrogen Cycle at Regional to Global Scales*, eds E. Boyer and R. Howarth, Chapter 2 (Dordrecht: Springer), 47–98.

Keller, D. P., Feng, E. Y., and Oschlies, A. (2014). Potential climate engineering effectiveness and side effects during a high carbon dioxide-emission scenario. *Nat. Commun.* 5:11. doi: 10.1038/ncomms4304

Keller, D. P., Oschlies, A., and Eby, M. (2012). A new marine ecosystem model for the University of Victoria Earth System Climate Model. *Geosci. Model Dev.* 5, 1195–1220. doi: 10.5194/gmd-5-1195-2012

Khatiwala, S., Primeau, F., and Holzer, M. (2012). Ventilation of the deep ocean constrained with tracer observations and implications for radiocarbon estimates of ideal mean age. *Earth Planetary Sci. Lett.* 325-326, 116–125. doi: 10.1016/j.epsl.2012.01.038

Knauss, J. A. (2005). *Introduction to Physical Oceanography*. 2 Edn. Long Grove, IL: Wavland Press, Inc.

Köhler, P., Abrams, J. F., Völker, C., Hauck, J., and Wolf-Gladrow, D. A. (2013). Geoengineering impact of open ocean dissolution of olivine on atmospheric CO_2, surface ocean pH and marine biology. *Environ. Res. Lett.* 8:9. doi: 10.1088/1748-9326/8/1/014009

Köhler, P., Hartmann, J., and Wolf-Gladrow, D. A. (2010). Geoengineering potential of artificially enhanced silicate weathering of olivine. *Proc. Natl Acad. Sci. U.S.A.* 107, 20228–20233. doi: 10.1073/pnas.1000545107

Lauvset, S. K., Key, R. M., Olsen, A., van Heuven, S., Velo, A., Lin, X., et al. (2016). A new global interior ocean mapped climatology: the 1° x 1° GLODAP version 2. *Earth Syst. Sci. Data* 8, 325–340. doi: 10.5194/essd-8-325-2016

Lazier, J., Hendry, R., Clarke, A., Yashayaev, I., and Rhines, P. (2002). Convection and restratification in the Labrador Sea, 1990-2000. *Deep Sea Res.* 49, 1819–1835. doi: 10.1016/S0967-0637(02)00064-X

Lenton, A., Matear, R. J., Keller, D. P., Scott, V., and Vaughan, N. E. (2018). Assessing carbon dioxide removal through global and regional ocean alkalinization under high and low emission pathways. *Earth Syst. Dyn.* 9, 339–357. doi: 10.5194/esd-9-339-2018

Liu, B., Six, K. D., and Ilyina, T. (2021). Incorporating the stable carbon isotope ^{13}C in the ocean biogeochemical component of the Max Planck Institute Earth System Model. *Biogeosci. Discuss.* [Preprint]. doi: 10.5194/bg-2021-32

Marsland, S. J., Haak, H., Jungclaus, J. H., Latif, M., and Röske, F. (2003). The max-planck-institute global ocean/ sea ice model with orthogonal curvilinear coordinates. *Ocean Model.* 5, 91–127. doi: 10.1016/S1463-5003(02)00015-X

Matear, R. J., and Lenton, A. (2014). Quantifying the impact of ocean acidification on our future climate. *Biogeosciences* 11, 3965–3983. doi: 10.5194/bg-11-3965-2014

Mauritsen, T., Bader, J., Becker, T., Behrens, J., Bittner, M., Brokopf, R., et al. (2019). Developments in the MPI-M earth system model version 1.2 (MPI-ESM1.2) and its response to increasing CO_2. *J. Adv. Model. Earth Syst.* 11, 998–1038. doi: 10.1029/2018MS001400

McDougall, T. J., and Barker, P. (2011). *Getting started with TEOS-10 and the Gibbs Seawater (GSW) Oceanographic Toolbox*. Sydney, NSW: SCOR/IAPSO WG127.

Meredith, M., Sommerkorn, M., Cassotta, S., Derksen, C., Ekaykin, A., Hollowed, A., et al. (2019). "Chapter 3: Polar regions," in *IPCC Special Report on the Ocean and Cryosphere in a Changing Climate*, eds H.-O. Pörtner, D. C. Roberts, V. Masson-Delmotte, P. Zhai, M. Tignor, E. Poloczanska, et al. (Cambridge; New York, NY: Cambridge University Press), 203–320.

Middelburg, J. J., Soetaert, K., and Hagens, M. (2020). Ocean alkalinity, buffering and biogeochemical processes. *Rev. Geophys.* 58:28. doi: 10.1029/2019RG000681

Najjar, R. G., Jin, X., Louachni, F., Aumont, O., Caldeira, K., Doney, S. C., et al. (2007). Impact of circulation on export production, dissolved organic matter, and dissolved oxygen in the ocean: results from Phase II of the Ocean Carbon-cycle Model Intercomparison Project (OCMIP-2). *Glob. Biogeochem. Cycles*, 21:22. doi: 10.1029/2006GB002857

Olsen, A., Key, R. M., van Heuven, S., Lauvset, S. K., Velo, A., Lin, X., et al. (2016). The global ocean data analysis project version 2 (GLODAPv2) - an internally consistent data product for the world ocean. *Earth Sys. Sci. Data* 8, 297–323. doi: 10.5194/essd-8-297-2016

Orr, J. C., Najjar, R. G., Aumont, O., Bopp, L., Bullister, J. L., Danabasoglu, G., et al. (2017). Biogeochemical protocols and diagnostics for the CMIP6 Ocean Model Intercomparison Project (OMIP). *Geosci. Model Dev.* 10, 2169–2199. doi: 10.5194/gmd-10-2169-2017

Paulsen, H., Ilyina, I., Six, K. D., and Stemmler, I. (2017). Incorporating a prognostic representation of marine nitrogen fixers into the global ocean biogeochemical model HAMOCC. *J. Adv. Model. Earth Syst.* 9, 438–464. doi: 10.1002/2016MS000737

Poli, P., Hersbach, H., Dee, D. P., Berrisford, P., Simmons, A. J., Vitart, F., et al. (2016). ERA-20C: an atmospheric reanalysis of the twentieth century. *J. Clim.* 29, 4083–4097. doi: 10.1175/JCLI-D-15-0556.1

Renforth, P., and Henderson, G. (2017). Assessing ocean alkalinity for carbon sequestration. *Rev. Geophys.* 55, 636–674. doi: 10.1002/2016RG000533

Röske, F. (2005). *Global Oceanic Heat and Fresh Water Forcing Datasets Based on ERA-40 and ERA-15*. Reports on earth system science.

Rudels, B. (2015). Arctic Ocean circulation, processes and water masses: A description of observations and ideas with focus on the period prior to the International Polar Year 2007-2009. *Progr. Oceanogr.* 132, 22–67. doi: 10.1016/j.pocean.2013.11.006

Sarmiento, J. L., and Gruber, N. (2006). "Carbon cycle," in *Global Biogeochemical Dynamics*, Chapter 8 (Princeton, NJ: Princeton University Press).

Sayol, J.-M., Dijkstra, H., and Katsman, C. (2019). Seasonal and regional variations of sinking in the subpolar North Atlantic from a high-resolution ocean model. *Ocean Sci.* 15, 1033–1053. doi: 10.5194/os-15-1033-2019

Schott, F. A., Xie, S.-P., and McCreary Jr., J. P. (2009). Indian Ocean circulation and climate variability. *Rev. Geophys.* 47:46. doi: 10.1029/2007RG000245

Sévellec, F., de Verdiére, A. C., and Ollitrault, M. (2017). Evolution of intermediate water masses based on Argo Float displacements. *J. Phys. Oceanogr.* 47, 1569–1586. doi: 10.1175/JPO-D-16-0182.1

Shetye, S. R., Shenoi, S. S. C., Gouveia, A. D., Michael, G. S., Sundar, D., and Nampoothiri, G. (1991). Wind-driven coastal upwelling along the western boundary of the Bay of Bengal during the southwest monsoon. *Continental Shelf Res.* 11, 1397–1408. doi: 10.1016/0278-4343(91)90042-5

Six, K. D., and Maier-Reimer, E. (1996). Effects of plankton dynamics on seasonal carbon fluxes in an ocean general circulation model. *Glob. Biogeochem. Cycles* 10, 559–583. doi: 10.1029/96GB02561

Sonntag, S., Ferrer González, M., Ilyina, T., Kracher, D., Nabel, J. E. M. S., Niemeier, U., et al. (2018). Quantifying and comparing effects of climate engineering methods on the Earth system. *Earths Fut.* 6, 149–168. doi: 10.1002/2017EF000620

Taucher, J., Arístegui, J., Bach, L. T., Guan, W., Montero, M. F., Nauendorf, A., et al. (2018). Response of subtropical phytoplankton communities to ocean acidification under oligotrophic conditions and during nutrient fertilization. *Front. Marine Sci.* 5:14. doi: 10.3389/fmars.2018.00330

Taylor, L. L., Quirk, J., Thorley, R. M. S., Kharecha, P. A., Hansen, J., Ridgwell, A., et al. (2016). Enhanced weathering strategies for stabilizing climate and averting ocean acidification. *Nat. Clima. Change* 6, 402–406. doi: 10.1038/nclimate2882

van Heuven, S. M. A. C., Hoppema, M., Huhn, O., Slagter, H. A., and de Baar, H. J. W. (2011). Direct observation of increasing CO_2 in the Weddell Gyre along the Prime Meridian during 1973-2008. *Deep Sea Res. Part II Top. Stud. Oceanogr.* 58, 2613–2635. doi: 10.1016/j.dsr2.2011.08.007

Vinayachandran, P. N., Shankar, D., Vernekar, S., and Sandeep, K. K. (2013). A summer monsoon pump to keep the Bay of Bengal salty. *Geophysical Research Letters*, 40:1777–1782. doi: 10.1002/grl.50274

Wu, Y., Hain, M. P., Humphreys, M. P., Hartman, S., and Tyrrell, T. (2019). What drives the latitudinal gradient in open-ocean surface dissolved inorganic carbon concentration? *Biogeosciences* 16, 2661–2681. doi: 10.5194/bg-16-2661-2019

Wyrtki, K. (1989). "Some thoughts about the West Pacific warm pool," in *Proceedings of the West Pacific International Meeting and Workshop on TOGA COARE*, eds J. Picaut, R. Lukas, and T. Delcroix (Nouméa: Institut Français de Recherche Scientifique pour le Développement en Coopération), 99–109.

Zeebe, R. E., and Wolf-Gladrow, D. (2003). "Equilibrium," in *CO_2 in Seawater: Equilibrium, Kinetics, Isotopes*, Vol. 65 of *Elsevier Oceanography Series*, Chapter 1, 2nd Edn, eds R. E. Zeebe, D. Wolf-Gladrow and D. Halpern (Amsterdam: Elsevier Science B.V,).

Conflict of Interest: The authors declare that the research was conducted in the absence of any commercial or financial relationships that could be construed as a potential conflict of interest.

Advantages of publishing in Frontiers

OPEN ACCESS
Articles are free to read for greatest visibility and readership

FAST PUBLICATION
Around 90 days from submission to decision

HIGH QUALITY PEER-REVIEW
Rigorous, collaborative, and constructive peer-review

TRANSPARENT PEER-REVIEW
Editors and reviewers acknowledged by name on published articles

Frontiers
Avenue du Tribunal-Fédéral 34
1005 Lausanne | Switzerland

Visit us: www.frontiersin.org
Contact us: frontiersin.org/about/contact

REPRODUCIBILITY OF RESEARCH
Support open data and methods to enhance research reproducibility

DIGITAL PUBLISHING
Articles designed for optimal readership across devices

FOLLOW US
@frontiersin

IMPACT METRICS
Advanced article metrics track visibility across digital media

EXTENSIVE PROMOTION
Marketing and promotion of impactful research

LOOP RESEARCH NETWORK
Our network increases your article's readership